Concessionaria per la progettazione, realizzazione e gestione del collegamento stabile tra la Sicilia e il Continente Organismo di Diritto Pubblico
(Legge n° 1158 del 17 dicembre 1971, modificata dal D.Lgs. n°114 del 24 aprile 2003)

PONTE SULLO STRETTO DI MESSINA

PROGETTO DEFINITIVO

EUROLINK S.C.p.A.

IMPREGILO S.p.A. (MANDATARIA)
SOCIETÀ ITALIANA PER CONDOTTE D'ACQUA S.p.A. (MANDANTE)
COOPERATIVA MURATORI E CEMENTISTI - C.M.C. DI RAVENNA SOC. COOP. A.R.L. (MANDANTE)
SACYR S.A.U. (MANDANTE)
ISHIKAWAJIMA - HARIMA HEAVY INDUSTRIES CO. LTD (MANDANTE)
A.C.I. S.C.P.A. - CONSORZIO STABILE (MANDANTE)

IL PROGETTISTA	IL CONTRAENTE GENERALE	STRETTO DI MESSINA	STRETTODI MESSINA
Ing E.M.Veje COWI Dott. Ing. E. Pagani Ordine Ingegneri Milano n° 15408	PROJECT MANAGER (Ing. P.P. Marcheselli)	Direttore Generale e RUP Validazione (Ing. G. Fiammenghi)	Amministratore Delegato (Dott. P. Cucci)

PS0013_F0

Unità Funzionale	OPERA D'ATTRAVERSAMENTO
Tipo di sistema	SOVRASTRUTTURE
Raggruppamento di opere/attività	TORRI
Opera - tratto d'opera - parte d'opera	General
Titolo del documento	Specialist Technical Design Report, Annex

CODICE: C G 1 0 0 0 | P | R X | D | P | S V | T 4 | 0 0 | 0 0 | 0 0 | 0 0 | 0 1 | F0

REV	DATA	DESCRIZIONE	REDATTO	VERIFICATO	APPROVATO
F0	20-06-2011	EMISSIONE FINALE	CHSX	JJL	CHSX/LSJ

NOME DEL FILE: PS0013_F0

INDICE

1 Executive Summary

1.1 Introduction

This report describes the design of the following tower structural elements:

- Legs
- Cross Beams
- Base Anchorage

The design is based on that shown in the Tender Design.

In this project phase it was found advantageous to introduce the following changes to the tender design:

- The tower height was increased from 382.6 m to 399 m to compensate for the increase in deck weight;
- Flat plate longitudinal stiffeners replace T-shaped longitudinal stiffeners in the tower legs and cross beams;
- The tower leg transverse stiffener arrangement was revised to simplify fabrication and assembly of the tower leg segments;
- The tower leg transverse diaphragm arrangement was revised to eliminate unnecessary material;
- Braced frames replace the moment resisting frame transverse stiffening in the cross beams;
- Multi-strand post-tensioning tendons replace the anchor bolts in the tower base anchorage to simplify and reduce the reinforcing in the tower foundation; and
- Specifications of tuned mass dampers were modified based on the results of wind tunnel testing.

Calculations are typically based on the global IBDAS model version 3.3f.

1.2 Scope

This report describes the design of the structural elements of the two main towers, between the top of the concrete foundations (El. +18.06) and the underside of the main cable saddles (El. +384.415).

Design details for the non-structural tower components, such as maintenance/access systems and mechanical/electrical installations are described elsewhere.

The Specialist Technical Design Report focuses on summarizing the tower design, including the identification of load combinations governing the design of the tower components and the results of the component verifications.

1.3 Materials

Tower structural components are generally fabricated from Grade S460 ML structural steel with the exception of: the hot-rolled circular hollow sections comprising the cross beam internal bracing members, the tower base plate and the base anchorage stiffening plates, which are fabricated from Grade S355 ML structural steel. As an exception to the standard requirements of NTC08 and EN 10025-4 the mechanical properties of the steel shall not vary with material thickness for thicknesses up to 110 mm for S460ML steel and up to 150 mm for S355ML steel. The feasibility of the production of steel with the required properties has been confirmed.

High strength structural bolts of Grade 10.9, produced in accordance with EN ISO 898, are used for the tower leg construction joint splices.

All post-tensioning strands shall conform to the requirements of EN 10138-3 and shall have an ultimate strength of 1860 MPa.

1.4 Structural Analysis

The Messina Strait Bridge was modelled and analysed in the COWI proprietary analysis program IBDAS (Integrated Bridge Design and Analysis System). The tower design described in this report is based on Model 3.3f (version number) output.

The global model analysis was supplemented by the more detailed local analysis of selected components:

- Cross beam to tower leg connection;
- Tower leg transverse stiffeners and diaphragm plates;
- Tower leg longitudinal stiffener to transverse stiffener connections; and
- Sicilia Tower leg Segment 6 – analysed considering non-linear geometry and materials and including the effects of initial imperfections and residual stresses (used to verify design procedures).
- Calabria Tower leg Segment 17 – analysed considering non-linear geometry and materials and including the effects of initial imperfections and residual stresses (used to assess potential damage due to the force effects corresponding to the envelope of all time-history seismic analysis results).

1.5 General Description

The Messina Strait Bridge towers are approximately 381 m tall from the top of the concrete foundation to the main cable work point at the tower top. The towers comprise three main structural components: the legs, cross beams and base anchorage. The tower legs and cross beams comprise plated steel box shape cross sections that are stiffened longitudinally and transversally. The base anchorage comprises the base plate, post-tensioned anchorage tendons and tower leg anchorage stiffening.

The towers are painted on their outer and inner surfaces and the interior is further protected from deterioration by dehumidification.

The towers are provided with access systems comprising stairs, ladders, elevators, man lifts and movable gantries that allow all structural elements to be inspected and maintained.

1.6 Tower Legs

1.6.1 Longitudinal Plates and Stiffeners

The tower legs are steel box-sections comprising longitudinally and transversally stiffened panels. The tower leg cross section dimensions are constant over the full tower height from the top of the base plate to the underside of the main cable saddle, with a width perpendicular to the bridge axis of 12 m and a length parallel to the bridge axis of 20 m. A typical tower leg cross section is shown in Figure 1-1. The tower legs are shop fabricated in 21 full cross section segments, with lengths varying between 10.15 m and 20 m, and a maximum mass of approximately 1,525 tonnes, including tuned mass dampers. The tower leg segments are spliced at construction joints comprising high strength bolted connections that are slip critical at ULS for the longitudinal stiffeners and internal plates and full penetration welds for the skin plates. The two legs of each tower are sloped inwards at 1.929° with a centreline to centreline spacing that varies from 77.662 m at the base to 52.000 m at the main cable work point. The two tower legs are connected by transverse cross beams at approximately elevations +125 m, +250 m and +375 m. Each tower leg contains eight tuned-mass dampers between elevations 230 m and 260 m to control vortex shedding induced oscillations expected to occur at wind speeds of approximately 40 m/s and 65 m/s. In the reference dead load condition of the completed bridge, the tower legs lean towards the side spans by approximately 1.6 m at the tower top. The tower legs are fixed to the concrete foundations by post-tensioned anchorage tendons.

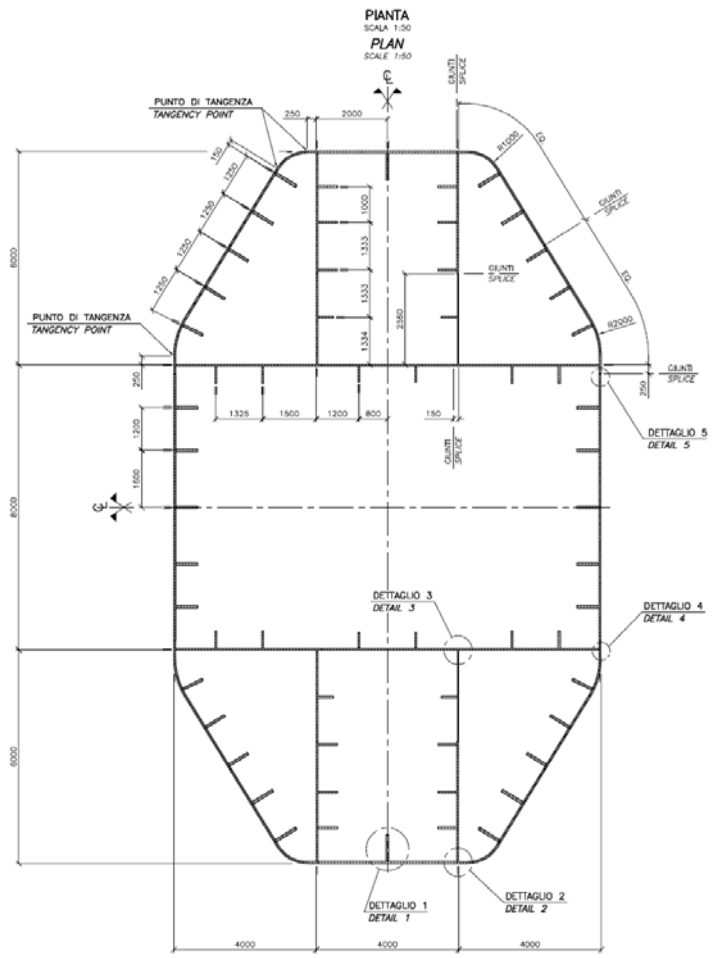

Figure 1-1: Tower leg cross section.

The towers are designed to be constructed vertical (without camber) and tied-back prior to main cable installation. The tie-back force, or rather displacement, that is introduced during construction is selected so as to leave the towers leaning slightly towards the side spans in the reference dead load condition after construction. The permanent lean of the tower legs is specified so as to better balance the maximum compressive stresses on the main and side span tower leg faces in the completed bridge.

The tower leg design is governed by the loads to which it is subjected in the completed bridge.

The longitudinal plates and stiffeners were proportioned using the equivalent width method specified in EN 1993-1-5 Sections 4.4 and 4.5, and as described further in the General Design Principles. The resulting plate thicknesses vary from 30 mm to 110 mm for both the Sicilia and

Calabria towers. The longitudinal stiffeners vary in spacing from 1,000 mm to 2,000 mm, and in size from 425x43 to 750x75.

Plate thicknesses and longitudinal stiffener spacing are selected to provide only the efficiency required to carry the maximum applied compressive stress at a particular point on the cross section. Efficiency is defined as the ratio of the compressive stress limit to the unfactored yield stress. Because the maximum design stresses are a combination of axial and flexural compression, the plates and stiffeners furthest from the cross-section centroid are subjected to the highest stresses, and therefore are proportioned to have the highest efficiency possible. Plates and stiffeners near the cross-section centroid are never subjected to the design yield stress and therefore can be more slender without affecting the overall cross-section capacity.

Tower leg axial forces are dominated by dead load effects. The unfactored dead load axial force is approximately four times the largest axial force from any other load components. Tower leg longitudinal moments are heavily dominated by seismic loads, with a maximum moment that is approximately four times the largest caused by other load components. Transverse moments are dominated by wind and seismic loading, with each producing governing values at some elevations. Wind loading typically produces the largest moments directly above and below each cross beam, and seismic loads typically produce the governing moments at mid-height between each cross beam because of the self response effect of the tower leg mass. In addition to the force effects described above, the tower legs experience additional forces resulting from global buckling of the tower (effect of equivalent imperfections). Global buckling moments contribute significantly to the total moment demands.

The tower leg design is based on the effects of all relevant load combinations. The utilization ratios for all points on the cross section are less than or equal to 1.0 for all load combinations. The tower legs are generally governed by ULS combination 7, which includes concurrent seismic and maximum live loading. ULS combination 6, comprising transverse wind, generally governs the plate C, D and H thicknesses and longitudinal stiffener sizes near the cross beams, where transverse moments are largest. Utilization ratios for all cross section points and tower leg segments for the governing load combinations are shown in Figure 1-2 and Figure 1-3, for the Sicilia and Calabria towers, respectively.

For all load combinations and tower segments, the governing stresses are generally located near the cross section corners, with the governing location being either the unstiffened corner or the longitudinal stiffener located adjacent to the corner. For these locations, the plate thickness and stiffener size were proportioned such that the maximum allowable compressive stress is as close to yield as possible (high efficiency). Governing utilization ratios are between 0.95 and 1.0 for all segments of both towers.

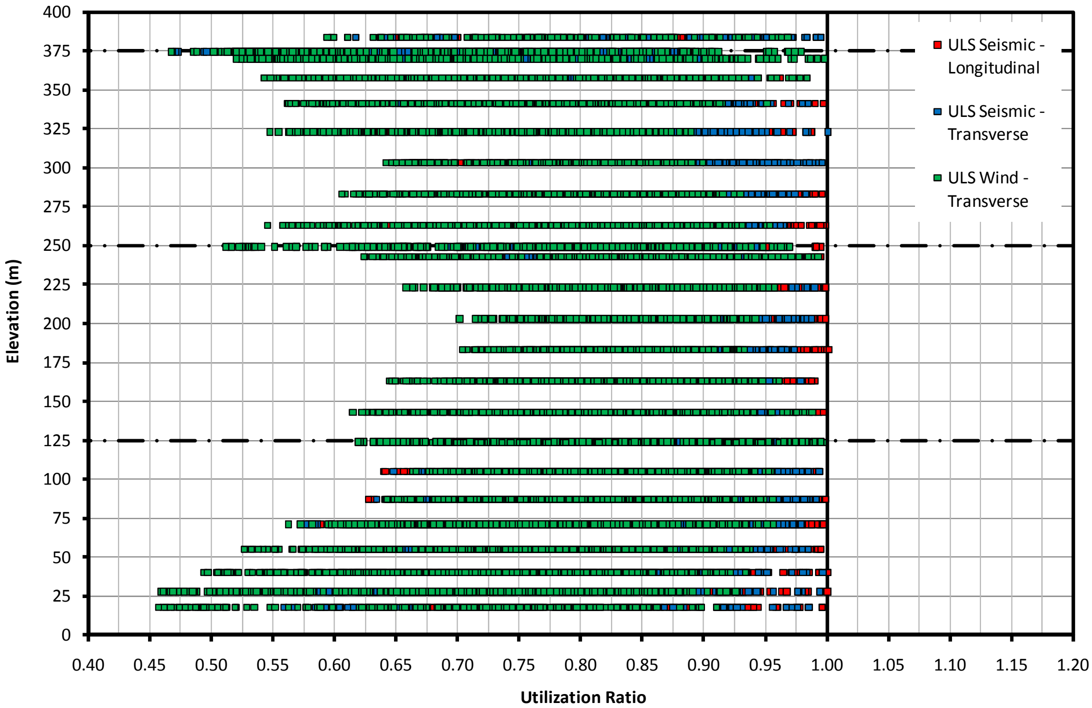

Figure 1-2: Sicilia tower leg governing utilization ratios.

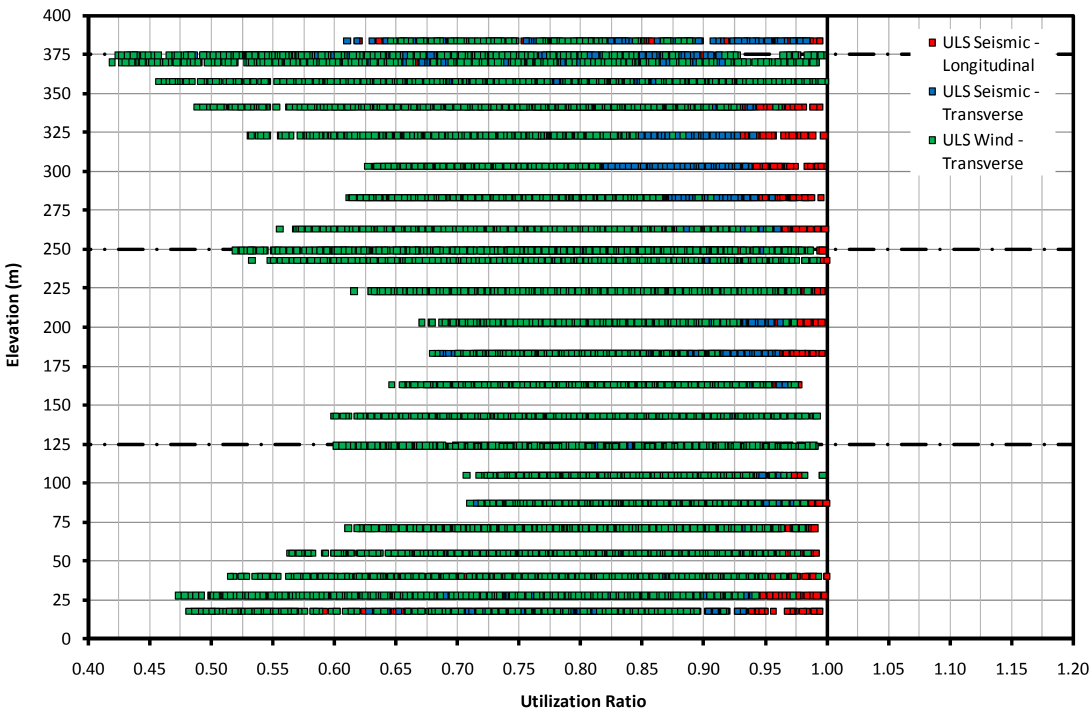

Figure 1-3: Calabria tower leg governing utilization ratios.

The tower leg design is heavily governed by axial and flexural compressive stresses. The cross section dimensions and plate thicknesses required to provide adequate resistance to these effects provide an excess of shear capacity. The interaction between longitudinal compressive stresses and transverse or longitudinal shear stresses does not have to be considered because the utilization ratios for shear forces acting concurrently with the maximum axial loads and moments are less than 0.5.

1.6.2 Transverse Field Splices

Tower leg field splices are made using a combination of full penetration welds on the skin plates and bolted splices on the longitudinal stiffeners and internal plates (longitudinal and transverse webs). In order to provide a similar stiffness to the welded skin plates, the bolted splices are slip critical at the ultimate limit state and all splice plates are proportioned to have an area greater than that of the smaller plate being spliced. The final tightening of all bolts in the splice shall be carried out only after the skin plate splice welds are completed. All bolts are to be M30 Grade 10.9.

1.6.3 Tower Leg Segment Detailed Finite Element Analysis

A finite element model was made of a complete leg segment to confirm the appropriateness of the resistances calculated using EN 1993-1-5 Section 4, which is the basis for the tower leg design verifications. The model considered the effects of non-linear geometry, non-linear material properties, initial geometric imperfections and residual stresses. The Sicilia tower leg segment 6 was modelled because it has thinner plates relative to the imposed axial load than other segments, and so might show greater sensitivity to buckling effects.

The detailed finite element analysis suggests an actual capacity that is 3% greater than that calculated by EN 1993-1-5 Section 4, but this might be slightly reduced in segments with higher ratios of moment to axial force. This, in general, confirms that the selected design methods result in a sufficiently safe and economical structure.

A second complete tower leg segment finite element model was made of Calabria tower leg segment 17 to assess the potential extent of damage that might be caused by the force effects corresponding to the envelope of all time-history analysis results (rather than the mean time-history analysis results that were used for design). This segment was selected for the detailed assessment because it was found to have the highest utilization ratio under the envelope of all seismic effects, considering all partial safety factors equal to 1.0. The detailed analysis confirmed that very limited plasticity would result in the critical-section with maximum compressive stresses being approximately equal to the nominal yield strength of the tower leg plate material and maximum compressive strains being less than approximately 0.00325, at which the material is not yet fully onto the yield plateau of the stress-strain relationship. The analysis predicted an actual cross section capacity approximately 11% larger than that predicted by the design verifications.

1.7 Cross Beams

Transverse cross beams connecting the two legs of each tower are located at approximately elevations +125 m, +250 m and +375 m. Each cross beam is 8 m wide and varies in depth from 11.5 m at the bridge centreline to approximately 22 m, 20 m and 18 m at the tower leg face, for cross beams 1, 2 and 3, respectively. The cross beams comprise longitudinally and transversally stiffened steel panels for the webs and flanges. Typical cross beam cross sections are shown in Figure 1-4. Each cross beam will be fully shop fabricated and erected as a complete unit.

The governing cross beam design loads are ULS wind (static + dynamic) acting transverse to the bridge axis for cross beams 1 and 2 and ULS seismic and wind for cross beam 3.The cross beams stabilize the tower leg from transverse buckling, and so global buckling of the tower (effect of equivalent imperfections) causes significant additional moments and shears in the cross beams. Utilization ratios for von Mises stresses at all cross section points for cross beams 1, 2 and 3 are shown in Figure 1-5, Figure 1-6 and Figure 1-7, respectively. Utilization ratios for ULS and SILS wind load combinations are represented by the red and blue markers, respectively, and utilization ratios for ULS seismic load combinations are represented by the green markers. The maximum utilization ratios in each cross beam are between 0.8 and 0.9.

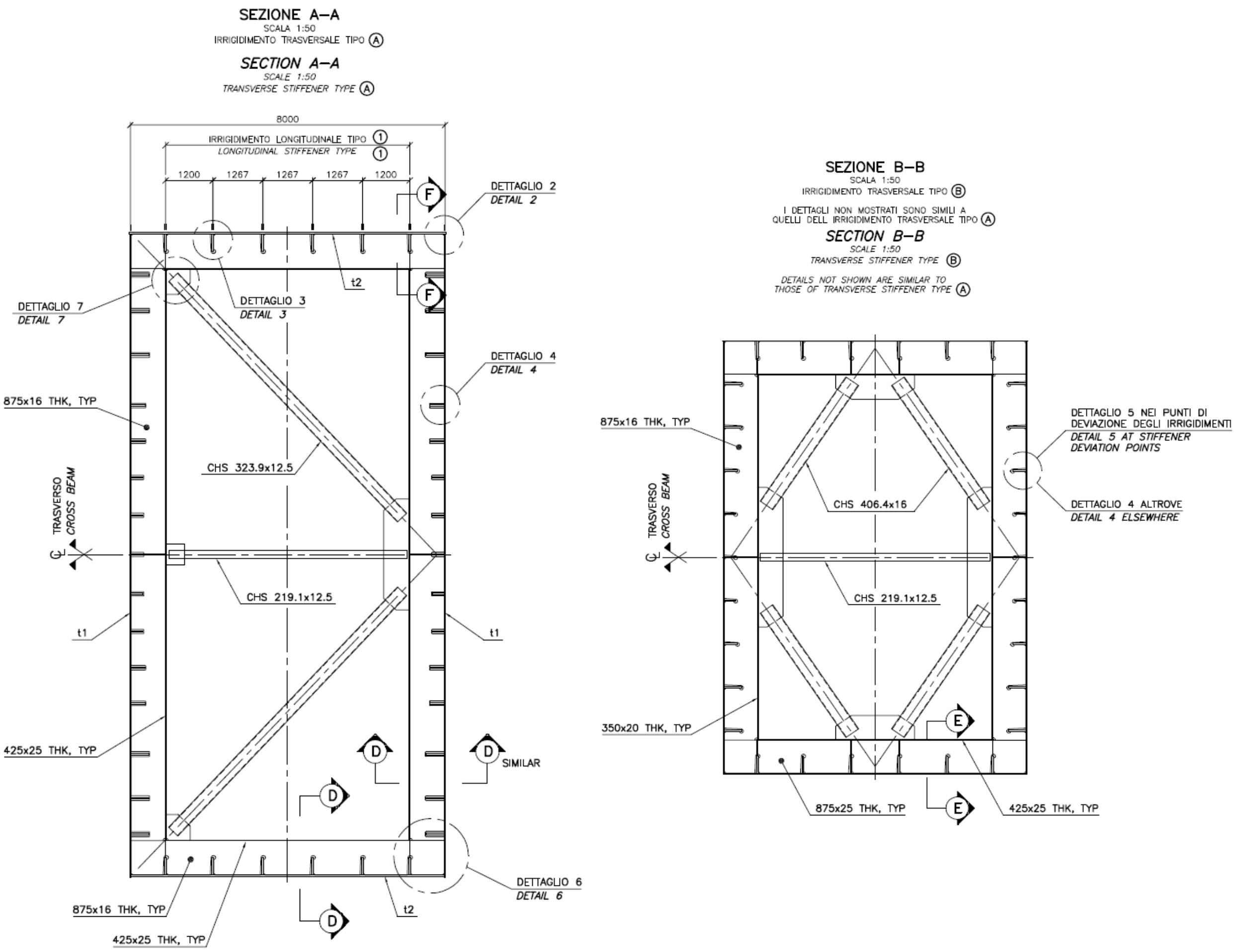

Figure 1-4: Typical cross beam cross sections.

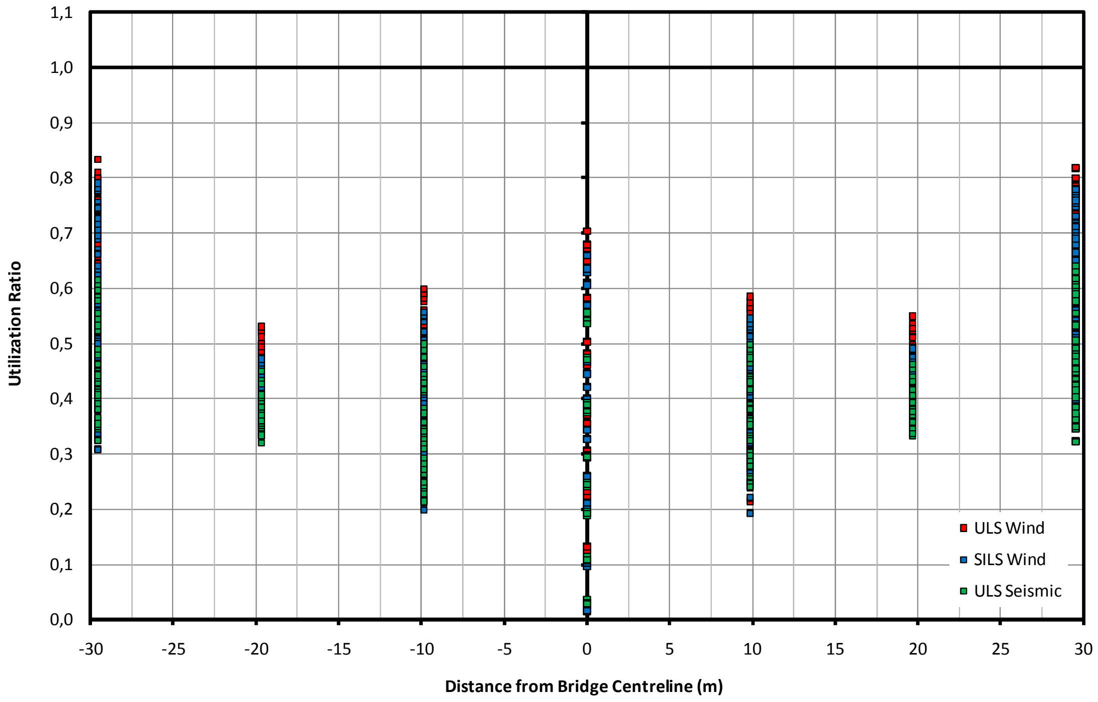

Figure 1-5: Sicilia tower cross beam 1 utilization ratios.

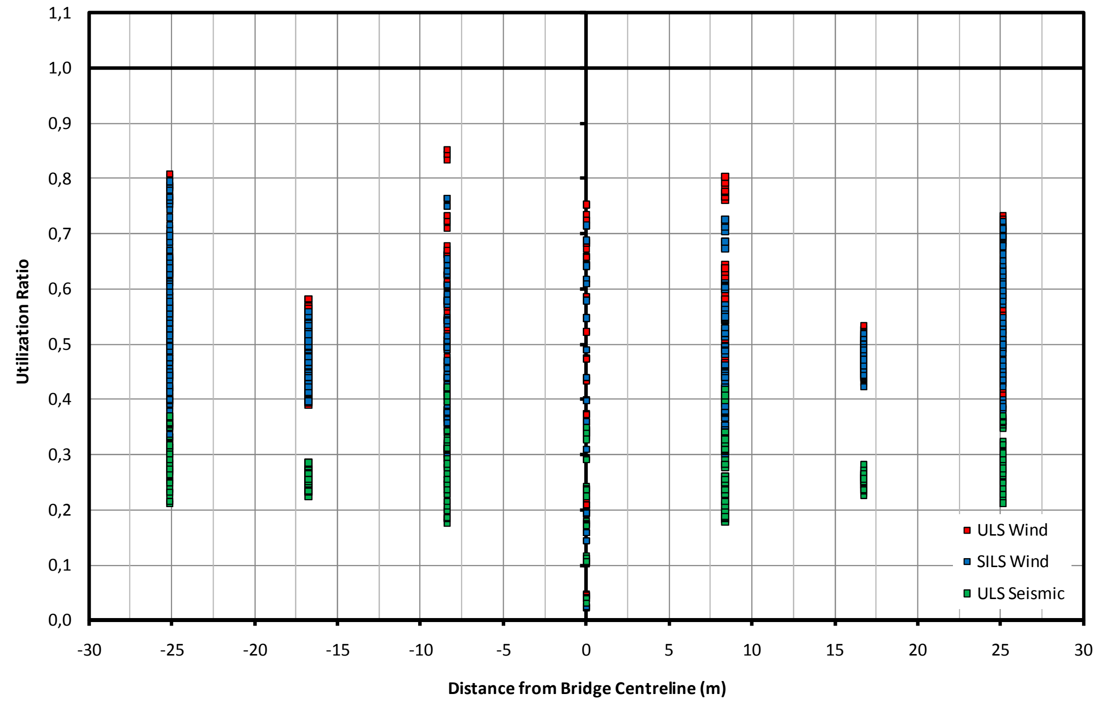

Figure 1-6: Sicilia tower cross beam 2 utilization ratios.

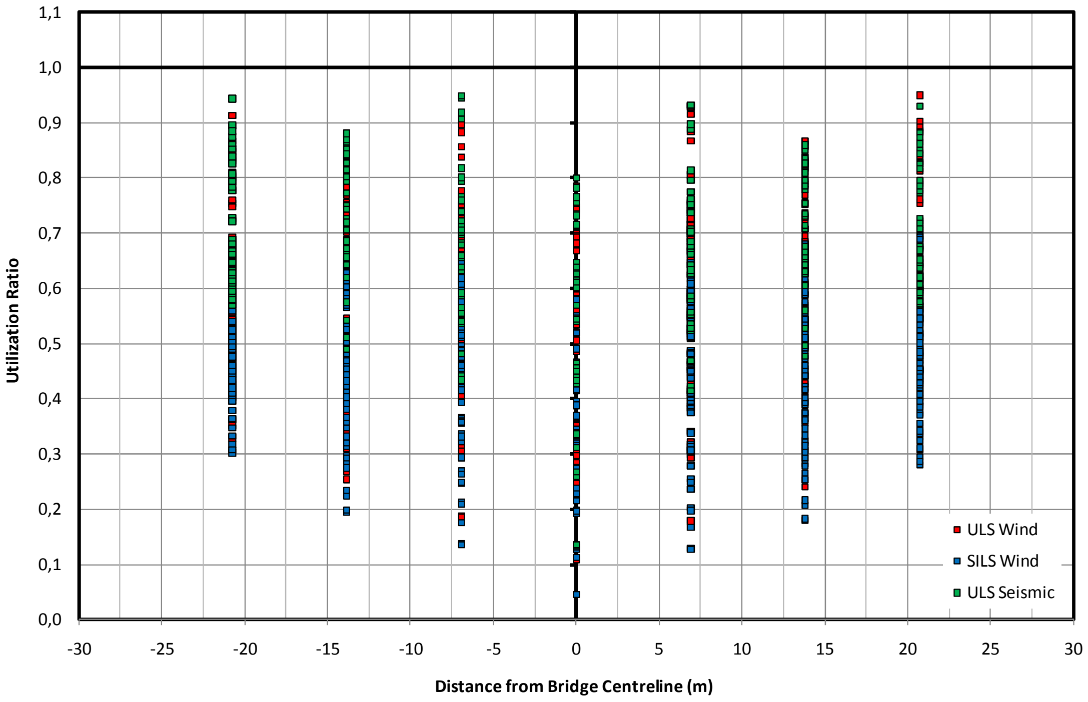

Figure 1-7: Sicilia tower cross beam 3 utilization ratios.

1.8 Base Anchorage

The tower base anchorage comprises multi-strand post-tensioned anchorage tendons, the base plate and the local tower leg stiffening. The current tower base anchorage is similar in concept to that developed in the tender design except that the anchor bolts have been replaced by post-tensioning tendons to reduce the quantity of foundation reinforcement. A plan view of the tower base showing the locations of the tendon anchorages is shown in Figure 1-8.

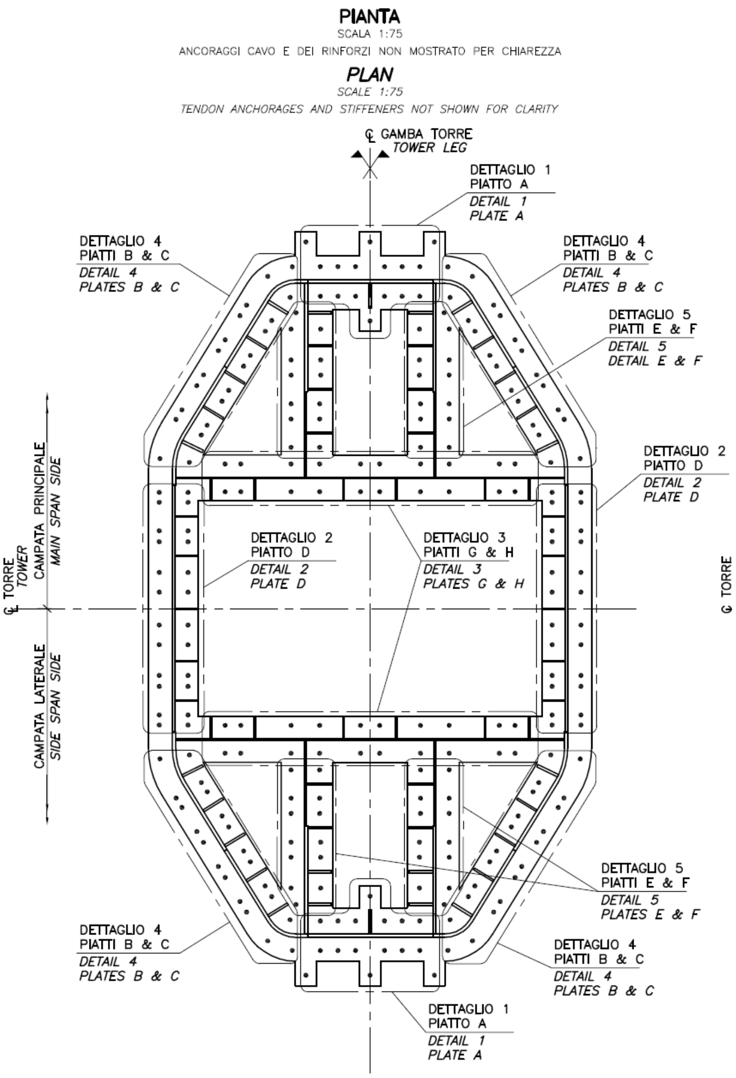

Figure 1-8: Tower base anchorage tendon arrangement.

All anchorage tendons are looped through the tower foundation such that both end anchorages resist tensile demands at some point on the tower base. Tendons anchoring plates A, E, F, G and H on the main span side of the tower leg loop to the corresponding anchor points on the side span side of the tower leg. Tendons anchoring plates B, C and D on the east side of the tower leg loop to the corresponding anchor points on the west side of the tower leg. The only exceptions to this arrangement are the tendons anchoring the corner regions at the intersections of plates A, B and E, which are anchored to plate B, but loop between the main and side span sides of the tower leg. A typical tendon anchorage plan view and cross section are shown in Figure 1-9.

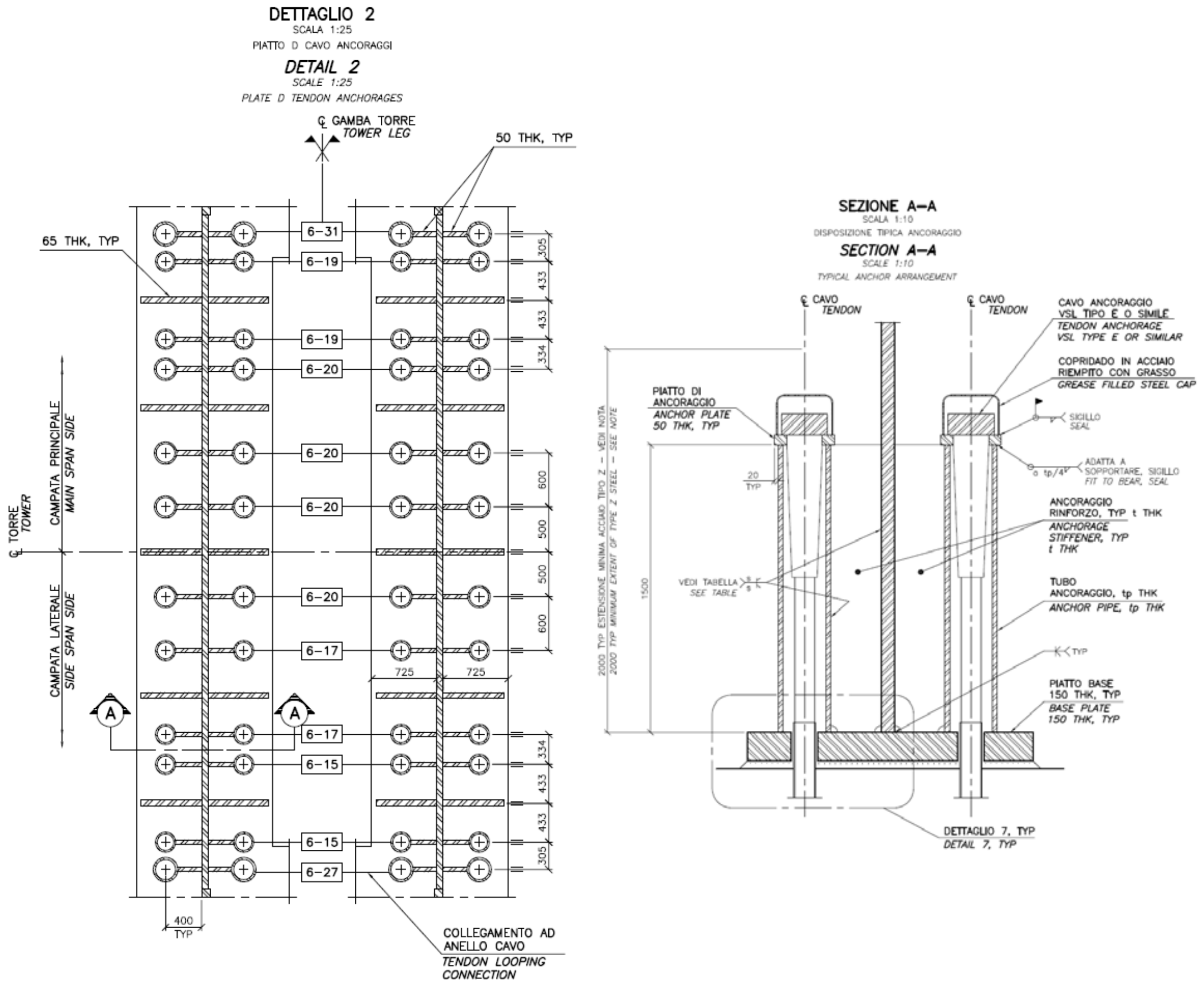

Figure 1-9: Plan view and cross section of plate D tendon anchorages.

The tendons comprise individually galvanized, greased and polyethylene sheathed strands, similar to those often used in parallel strand stay cables. The strands have an area of 150 mm^2 and an ultimate strength of 1860 MPa. The tendon ducts will be left ungrouted so that the tendons can be replaced. The strand anchors are contained in grease filled steel caps that are welded to the top of the anchor plate. This arrangement results in fully encapsulated tendon with multiple corrosion barriers. The tendons vary in size from 9 to 55 strands, with the largest tendons generally being concentrated along plates A, B and E, where the tensile forces are the largest.

The tendons are proportioned to prevent the tower base from decompressing under any of the ULS/SILS load combinations during construction or in the completed bridge. Tendons are proportioned based on an effective tensile stress after all losses of 0.65 f_{pk}, divided by an additional safety factor of 1.10. Tensile demands on the main span side of the tower leg are generally governed by the wind or seismic loads on the freestanding tower with tie-back; however, ULS seismic loads in the completed bridge govern the demands at the extreme longitudinal tower leg fibres on plates A, B and E and SILS wind loads in the completed bridge govern the demands on the extreme transverse tower leg fibres on plate D. Tensile demands on the side span side of the tower leg are generally governed by wind loads on the freestanding tower, except for the tensile demands on plate D, which are governed by SILS wind loads on the completed bridge.

The tower base plate stiffening comprises vertical base plate stiffeners and anchorage stiffeners. The plate stiffening elements are designed for combined shear and bending stresses in accordance with EN 1993-1-5 Section 10. The stiffeners are proportioned to carry only the tributary bearing pressures caused by externally applied loads. The anchorage stiffeners are also verified to have the shear capacity necessary to transmit the effective tensile force in the anchored tendon back to the tower leg plate.

The base plate is a 150 mm thick steel plate that distributes the compressive forces in all of the tower leg plates and longitudinal stiffeners, and the pre-tensioning forces in the anchorage tendons approximately uniformly to the underlying 40 mm thick grout pad, which spreads the load further to the underlying concrete tower foundation. The base plate plan geometry is selected to support all of the longitudinal stiffeners and limit the bearing stress at the top of the concrete foundation to approximately 60 MPa. The base anchorage shear capacity is provided by friction between the base plate and the underlying grout pad. The maximum tower base shear force is 158 MN and is caused by the SILS longitudinal seismic combination. The shear resistance of the tower base anchorage is 500 MN, resulting in a maximum utilization ratio of 0.32.

2 Introduction

This report describes the design of the following tower structural elements:

- Legs
- Cross Beams
- Base Anchorage

The design is based on that shown in the Tender Design.

In this project phase it was found advantageous to introduce the following changes to the tender design:

- The tower height was increased from 382.6 m to 399 m to compensate for the increase in deck weight;
- Flat plate longitudinal stiffeners replace T-shaped longitudinal stiffeners in the tower legs and cross beams;
- The tower leg transverse stiffener arrangement was revised to simplify fabrication and assembly of the tower leg segments;
- The tower leg transverse diaphragm arrangement was revised to eliminate unnecessary material;
- Braced frames replace the moment resisting frame transverse stiffening in the cross beams;
- Multi-strand post-tensioning tendons replace the anchor bolts in the tower base anchorage to simplify and reduce the reinforcing in the tower foundation; and
- Specifications of tuned mass dampers were modified based on the results of wind tunnel testing.

Calculations are typically based on the global IBDAS model version 3.3f.

A bridge elevation and plan are shown in Figure 2-1 and longitudinal and transverse tower elevations are shown in Figure 2-2.

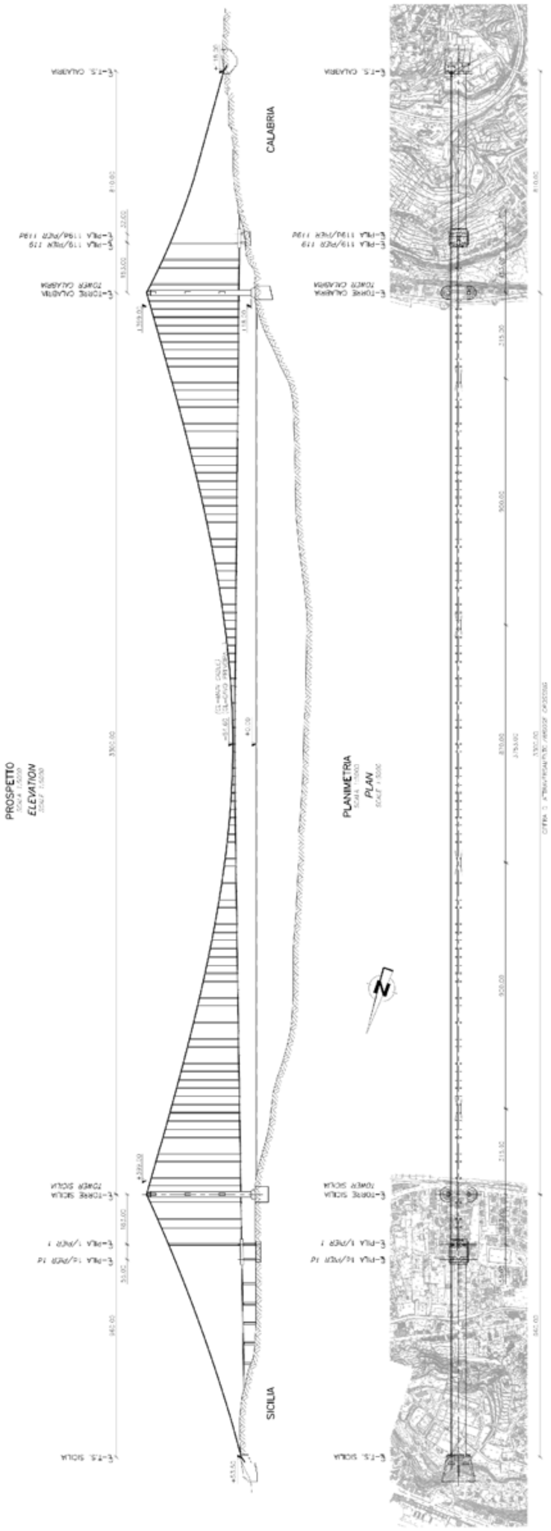

Figure 2-1: Bridge elevation and plan.

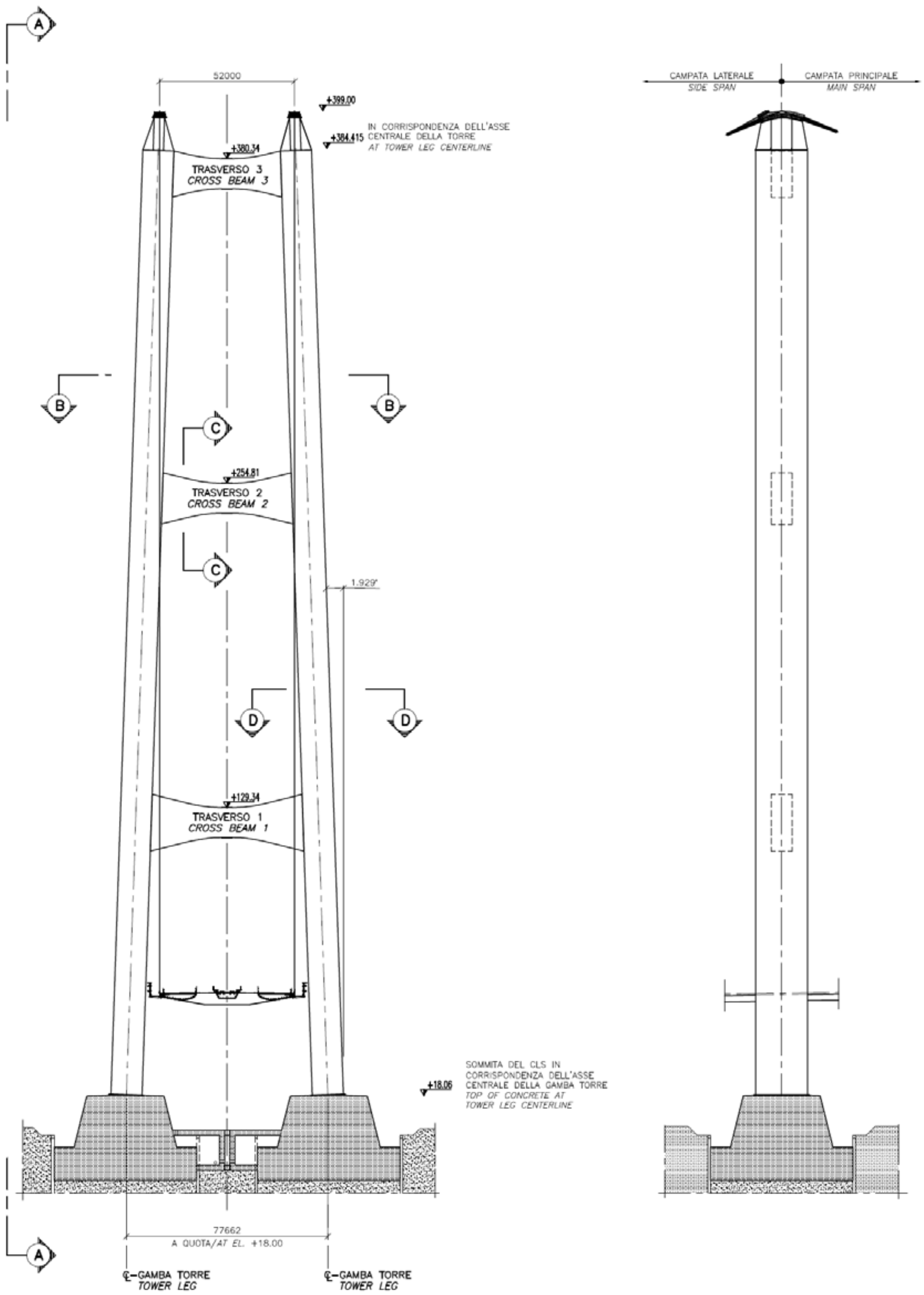

Figure 2-2: Tower elevations.

2.1 Scope

This report describes the design of the structural elements of the two main towers, between the top of the concrete foundations (El. +18.06) and the underside of the main cable saddles (El. +384.415).

Design details for the non-structural tower components, such as maintenance/access systems and mechanical/electrical installations are described elsewhere.

The Specialist Technical Design Report focuses on summarizing the tower design, including the identification of governing load combinations and the results of the component verifications.

2.2 Report Outline

This report is organized into the following sections:

- Section 1 includes an Executive Summary;
- Section 2 includes this introduction, provides a list of reference materials, including design specifications, design codes, material specifications, reference drawings and complementary reports;
- Section 3 provides definitions for terms that are commonly used in referencing particular tower components;
- Section 4 describes the four limit states that are considered in the tower design, serviceability, ultimate, fatigue and structural integrity;
- Section 5 provides descriptions of the materials that are used for each tower component;
- Section 6 provides brief descriptions of particular aspects of the structural analysis and tower modelling;
- Section 7 summarizes the design verifications that have been completed for the main structural components; and
- Section 8 presents a summary of the tower design.

2.3 References

2.3.1 Design Specifications

GCG.F.04.01 “Engineering – Definitive and Detailed Design: Basis of Design and Expected Performance Levels,” Stretto di Messina, 2004 October 27.

GCG.F.05.03 “Design Development – Requirements and Guidelines,” Stretto di Messina, 2004 October 22.

GCG.G.03.02 “Structural Steel Works and Protective Coatings,” Stretto di Messina, 2004 July 30.

CG.10.00-P-RG-D-P-GE-00-00-00-00-00-02 “Design Basis, Structural, Annex,” COWI (Current Revision).

2.3.2 Design Codes

“Norme tecniche per le costruzioni,” 2008 (NTC08).

EN 1991 Eurocode 1: Actions on Structures – Part 2: Traffic loads on bridges

EN 1993 Eurocode 3: Design of Steel Structures – Part 1-1: General rules and rules for buildings

EN 1993 Eurocode 3: Design of Steel Structures – Part 1-2: General rules – Structural fire design

EN 1993 Eurocode 3: Design of Steel Structures – Part 1-5: Plated structural elements

EN 1993 Eurocode 3: Design of Steel Structures – Part 1-8: Design of joints

EN 1993 Eurocode 3: Design of Steel Structures – Part 1-9: Fatigue

EN 1993 Eurocode 3: Design of Steel Structures – Part 1-10: Selection of steel for fracture toughness and through thickness properties

EN 1993 Eurocode 3: Design of Steel Structures – Part 2: Steel Bridges

EN 1998 Eurocode 8: Design of structures for earthquake resistance – Part 1: General rules, seismic actions and rules for buildings

EN 1998 Eurocode 8: Design of structures for earthquake resistance – Part 2: Bridges

Rete Ferroviaria Italia - Istruzione No. 44F “Verifiche a fatica dei ponti ferroviari”

2.3.3 Material Specifications

EN 10025-1:2004 Hot-rolled products of structural steels – Part 1: General delivery conditions.

EN 10025-2:2004 Hot-rolled products of structural steels – Part 2: Technical delivery conditions for non-alloy structural steels.

EN 10025-3:2004 Hot-rolled products of structural steels – Part 3: Technical delivery conditions for normalized / normalized weldable fine grain structural steels.

EN 10025-4:2004 Hot-rolled products of structural steels – Part 4: Technical delivery conditions for thermomechanical rolled weldable fine grain structural steels.

EN 10164:2004 Steel products with improved deformation properties perpendicular to the surface of the product – Technical delivery conditions.

EN ISO 898-1:2009 Mechanical properties of fasteners made of carbon steel and alloy steel – Part 1: Bolts, screws and studs.

EN 20898-2:1994 Mechanical properties of fasteners – Part 2: Nuts with special proof load values – coarse thread (ISO 898-2:1992).

UNI EN 14399:2005-3 High-strength structural bolting assemblies for preloading - Part 3: System HR - Hexagon bolt and nut assemblies

EN 10138-3:2006 Prestressing Steels. Strand

EN ISO 14555:1998 Welding-Arc stud welding of metallic materials. May 1995.

EN ISO 13918:1998 Welding-Studs for arc stud welding-January 1997.

2.3.4 Drawings

The reference tower design drawings for this report are listed in Table 2-1.

Drawing Title	Drawing Number
Tower Sicilia - General Arrangement	CG.10.00-P-AX-D-P-SV-T4-TS-00-00-00-01_0

Typical - Leg - Cross Section & Vertical Joints	CG.10.00-P-WX-D-P-SV-T4-TO-00-00-00-01_0
Tower Sicilia - Leg - Sections & Plate Thicknesses	CG.10.00-P-WX-D-P-SV-T4-TS-00-00-00-01_0
Typical - Leg - Cross Diaphragms	CG.10.00-P-AX-D-P-SV-T4-TO-00-D0-00-01_0
Typical - Leg - Cross Diaphragms, Details	CG.10.00-P-BX-D-P-SV-T4-TO-00-D0-00-01_0
Typical - Leg - Horizontal Joints	CG.10.00-P-AX-D-P-SV-T4-TO-00-00-00-01_0
Typical - Leg - Horizontal Joints, Details	CG.10.00-P-BX-D-P-SV-T4-TO-00-00-00-01_0
Typical - Cross Beam no. 1	CG.10.00-P-AX-D-P-SV-T4-TO-T0-00-00-01_0
Typical - Cross Beam no. 2	CG.10.00-P-AX-D-P-SV-T4-TO-T0-00-00-02_0
Typical - Cross Beam no. 3	CG.10.00-P-AX-D-P-SV-T4-TO-T0-00-00-03_0
Typical - Cross Beams - Details	CG.10.00-P-BX-D-P-SV-T4-TO-T0-00-00-01_0
Typical - Cross Beam Connection to Tower leg	CG.10.00-P-WX-D-P-SV-T4-TO-T0-00-00-02_0
Typical - Connection from Girder	CG.10.00-P-AX-D-P-SV-T4-TO-00-00-00-03_0
Typical - Base Section 1	CG.10.00-P-AX-D-P-SV-T4-TO-00-00-00-04_0
Typical - Base Section 2	CG.10.00-P-AX-D-P-SV-T4-TO-00-00-00-05_0
Typical - Base Section, Details	CG.10.00-P-BX-D-P-SV-T4-TO-00-00-00-02_0
Typical - Top Section	CG.10.00-P-AX-D-P-SV-T4-TO-00-00-00-06_0
Typical - Tuned Mass Dampers - Support Structure	CG.10.00-P-AX-D-P-SV-T4-TO-00-00-00-07_0
Typical - Tuned Mass Dampers	CG.10.00-P-AX-D-P-SV-T4-TO-00-00-00-08_0
Typical - Leg - Steelwork Modifications 1	CG.10.00-P-BX-D-P-SV-T4-TO-00-00-00-04_0
Typical - Leg - Steelwork Modifications 2	CG.10.00-P-BX-D-P-SV-T4-TO-00-00-00-05_0
Typical - Cross Beams - Steelwork Modifications	CG.10.00-P-BX-D-P-SV-T4-TO-T0-00-00-06_0
Tower Calabria - General Arrangement	CG.10.00-P-AX-D-P-SV-T4-TC-00-00-00-01_0
Tower Calabria - Leg - Sections & Plate Thicknesses	CG.10.00-P-WX-D-P-SV-T4-TC-00-00-00-01_0

Table 2-1: Reference tower drawings.

2.3.5 Complementary Reports

The tower design reports listed in Table 2-2 provide supplementary information about the tower design principles and verifications.

Report Title	Report Number
General Design Principles	CG.10.00-P-RG-D-P-SV-T4-00-00-00-00-01
Design Report - Tower Legs incl. Joints and Splices	CG.10.00-P-CL-D-P-SV-T4-00-00-00-00-01
Design Report - Cross Beams	CG.10.00-P-CL-D-P-SV-T4-00-00-00-00-02
Design Report - Tower Base	CG.10.00-P-CL-D-P-SV-T4-00-00-00-00-03

Table 2-2: Reference tower design reports.

3 Nomenclature

The section provides descriptions of terms commonly used throughout the report to refer to various tower components:

Legs – the vertical elements of the towers, extending from the tops of the concrete pedestals at elevation +18.06 to the undersides of the main cable saddles at elevation +384.415.

Cross Beams – the transverse beams connecting the tower legs at elevations +129.34 (Cross Beam 1), +254.81 (Cross Beam 2) and +380.34 (Cross Beam 3). The elevations provided are at the top of the cross beam at the bridge centreline.

Skin Plates – The plates around the perimeter of the tower legs or cross beams (Plates A, B, C and D of the tower legs and the webs and flanges of the cross beams).

Transverse Webs – the vertical transverse plates connecting the two sides of each tower leg; plates G and H. Also referred to more generically as internal plates.

Longitudinal Webs – the vertical longitudinal plates connecting the tower leg skin plates and transverse webs parallel to the bridge axis; plates F and E. Also referred to more generically as internal plates.

Longitudinal Stiffeners – the longitudinal plate elements used to stiffen the vertical tower leg plates and the flanges and webs of the cross beams.

Transverse Diaphragms – the transverse stiffening elements, typically located in each tower segment 1 m from the construction joint (Type 1), at the cross beam top and bottom flange connections to the tower legs (Type 2 or Type 3) and at the tuned mass damper elevations (Type 4).

Transverse Stiffeners – the intermediate transverse stiffening elements connected to all tower leg vertical plate elements and longitudinal cross beam plate elements, regularly spaced between the transverse diaphragms.

Construction Joints – the field connected joints between tower leg segments.

Base Anchorage – all components of the connection between the tower leg and the tower foundation, including stiffening plates, anchorage pipes, base plates and multi-strand post-tensioning tendons.

Cable Saddle – the steel weldment over which the main cables pass and which distributes the cable load to the top of the tower leg.

Tie-back – the longitudinal displacement of the towers towards the side spans in the reference dead load condition.

4 Limit States

The tower structural components are verified at Serviceability Limit States (1 and 2), Ultimate Limit States, Fatigue Limit States and Structural Integrity Limit States in accordance with the project design basis GCG.F.04.01 and NTC08. Detailed descriptions of the limit states considered in the tower design are provided in CG.10.00-P-RG-D-P-SV-T4-00-00-00-00-01 "General Design Principles."

5 Materials

Construction materials used in the tower structural components are summarized in this section. Detailed descriptions of material properties and partial factors considered in the tower design are provided in CG.10.00-P-RG-D-P-SV-T4-00-00-00-00-01 "General Design Principles."

5.1 Structural Steel

Tower structural components are generally fabricated from Grade S460 ML structural steel with the exception of: the hot-rolled circular hollow sections comprising the cross beam internal bracing members, the tower base plate and the base anchorage stiffening plates, which are fabricated from Grade S355 ML structural steel. As an exception to the standard requirements of NTC08 and EN 10025-4 the mechanical properties of the steel shall not vary with material thickness for thicknesses up to 110 mm for S460ML steel and up to 150 mm for S355ML steel. The feasibility of the production of steel with the required properties has been confirmed.

5.2 High Strength Bolts

High strength structural bolts of Grade 10.9, produced in accordance with EN ISO 898, are used for the tower leg construction joint splices.

5.3 Post-tensioning Strand

All post-tensioning strands shall conform to the requirements of EN 10138-3 and shall have an ultimate strength of 1860 MPa.

6 Structural Analysis

6.1 Global Modelling

The Messina Strait Bridge was modelled and analysed in the COWI proprietary analysis program IBDAS (Integrated Bridge Design and Analysis System). The bridge model and structural analysis, in general, are described in the report "CG.10.00-P-RG-D-P-SV-00-00-00-00-00-01 Global IBDAS Model, Description."

The tower design described in this report is typically based on Model 3.3f (version number) output.

The analysis model includes the tuned mass dampers provided to mitigate vortex shedding vibrations.

6.2 Local Modelling

The global model analysis was supplemented by the more detailed local analysis of selected components.

6.2.1 Cross Beam to Tower Leg Connection

A semi-local shell element model was integrated into the global IBDAS model to more clearly assess the flow of forces in this heavily stressed region. The model output was used to confirm the additional plate strengthening and stiffening that is required in the tower leg within the cross beam depth and which is not indicated by the global model output.

Details of the modelling, analysis and results are provided in CG.10.00-P-RG-D-P-SV-00-00-00-00-00-03 "Semi-local IBDAS Model, Towers."

6.2.2 Tower Leg Transverse Stiffener and Diaphragm Plate Buckling Analysis

A local shell element model of the typical tower leg transverse stiffening elements, an 8 m long T-shaped stiffener and a triangular plate diaphragm with a circular cut-out were created and analysed in SAP2000 to size the T-shaped stiffener flange and determine the required plate diaphragm thickness. The scope of the modelling work is summarized in CG.10.00-P-RG-D-P-SV-T4-00-00-00-00-01 "General Design Principles" and a detailed description of the modelling and results is provided in CG.10.00-P-CL-D-P-SV-T4-00-00-00-00-01 "Design Report - Tower Legs incl. Joints and Splices." The results of this analysis are summarized in Section 7.3.3.2 of this report.

6.2.3 Tower Leg Longitudinal Stiffener to Transverse Stiffener Connections

A local shell element model of the interface between the tower leg longitudinal stiffeners and transverse stiffeners was created and analysed in SAP2000 to confirm that the connections between the longitudinal and transverse stiffening elements are not required and to size the welds connecting the transverse stiffener web to the skin plate. The scope of the modelling work is summarized in CG.10.00-P-RG-D-P-SV-T4-00-00-00-00-01 "General Design Principles" and a detailed description of the modelling and results is provided in CG.10.00-P-CL-D-P-SV-T4-00-00-00-00-01 "Design Report - Tower Legs incl. Joints and Splices." The results of this analysis are summarized in Section 7.3.3.2 of this report.

6.2.4 Tower Leg Segment Model

A local shell element model of a full tower leg segment was created and analysed in ADINA to verify the appropriateness of the design methods used to proportion the tower leg plates and to confirm the computed capacities. A similar model was also created to assess the potential extent of damage that might result from imposing the force effects corresponding to the envelope of all time-history analysis results, rather than the mean time-history analysis results that were used for design. The models considered non-linear materials and geometry and included the effects of geometric imperfections and residual stresses. The scope of the modelling work is summarized in CG.10.00-P-RG-D-P-SV-T4-00-00-00-00-01 "General Design Principles" and a detailed description of the modelling and results is provided in CG.10.00-P-CL-D-P-SV-T4-00-00-00-00-01 "Design Report - Tower Legs incl. Joints and Splices." The results of this analysis are summarized in Section 7.3.3.3 of this report.

7 Tower Design Verifications

This section summarizes the governing load combinations and the design verifications that have been completed for the tower structural components. Design principles are described as necessary to clarify the effects of the governing load combinations and the verification results, however, the General Design Principles (CG.10.00-P-RG-D-P-SV-T4-00-00-00-00-01) should be consulted for more detailed descriptions and bases for the verification procedures.

7.1 General Description

The Messina Strait Bridge towers are approximately 381 m tall from the top of the concrete foundation to the main cable work point at the tower top. This report describes the design of all tower structural components between elevations +18.06 and +384.415, above which is located the main cable saddle, which is described elsewhere. The towers comprise three main structural components: the legs, cross beams and base anchorage. The tower legs and cross beams comprise plated steel box shape cross sections that are stiffened longitudinally and transversally. The base anchorage comprises the base plate, post-tensioned anchorage tendons and tower leg anchorage stiffening.

The towers are painted on their outer and inner surfaces and the interior is further protected from deterioration by dehumidification.

The towers are provided with access systems comprising stairs, ladders, elevators, man lifts and movable gantries that allow all structural elements to be inspected and maintained. This report describes the provision of access openings in the main structural steelwork, but the design of the access systems themselves is presented elsewhere.

7.2 Global Behaviour

The considerable length of the main span results in a significant proportion of the tower leg capacity being devoted to carrying the self weight of the bridge. At the tower base, approximately half of the governing design stresses in the legs are caused by axial loads and half are caused by combinations of transverse and longitudinal moments. At the tower top, almost all of the design stresses are caused by axial loads.

Longitudinally (parallel to the bridge), the tower behaves much like a propped cantilever, fixed to the stiff foundation by the base anchorage and pinned at the top by main cable, which because of the significant load that it carries is also very stiff. Transversally, the tower behaves as a moment resisting sway frame, although the behaviour is influenced by the transverse restraint that the main cables provide. Although, the main cables provide very little stiffness transversally in the undeformed position, they do provide a significant restoring force with any transverse displacement of the tower top.

7.2.1 Mode Shapes

The global mode shapes of the bridge can provide good insight into the structural behaviour and appropriateness of the modelling and are important inputs to the assessment of global buckling effects, seismic response spectrum analysis and dynamic wind buffeting analysis. The tower design considered both vibration modes and eigen-buckling modes for different aspects of the tower design.

7.2.1.1 Vibration Modes

The tower vibration modes were investigated in detail as part of the response spectrum seismic analysis and in considering the appropriate modes to use in developing the Rayleigh damping curve for the time-history seismic analysis. Based on the results of the response spectrum analysis, the contributions to the total governing longitudinal and transverse Sicilia tower leg moments from each vibration mode were ranked in descending order for several tower leg segments. Longitudinal tower leg moments are most strongly influenced by modes 101, 391, 995 and 347, shown in Figure 7-1, Figure 7-2, Figure 7-3 and Figure 7-4, respectively, in order of decreasing contribution. The four modes have periods between 0.4 s and 2.49 s. The total longitudinal moment at a particular cross section is typically dominated by only two or three modes, with the other modes producing insignificant contributions. The dominance of isolated modes in producing the total transverse moments is much less apparent and there is greater variation over the tower leg height in the mode that causes the maximum contribution. However, the three modes that most typically contribute most to the total transverse seismic moments are modes 395, 353 and 410, shown in Figure 7-5, Figure 7-6 and Figure 7-7, respectively. These three modes have periods between 0.74 s and 0.83 s.

Figure 7-1: Mode 101 - Period 2.49 s - Frequency 0.40 Hz.

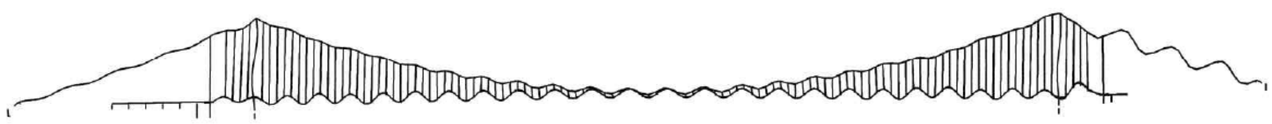

Figure 7-2: Mode 391 - Period 0.77 s - Frequency 1.30 Hz.

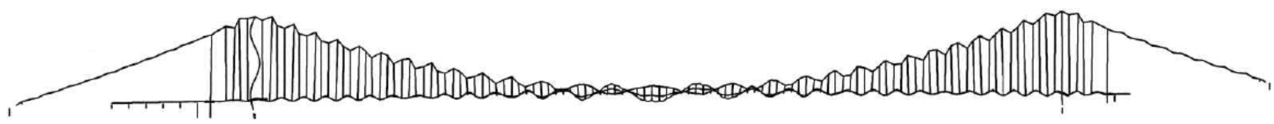

Figure 7-3: Mode 995 - Period 0.4 s - Frequency 2.58 Hz.

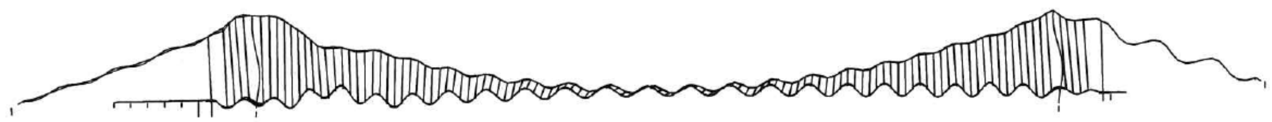

Figure 7-4: Mode 347 - Period 0.85 s - Frequency 1.18 Hz.

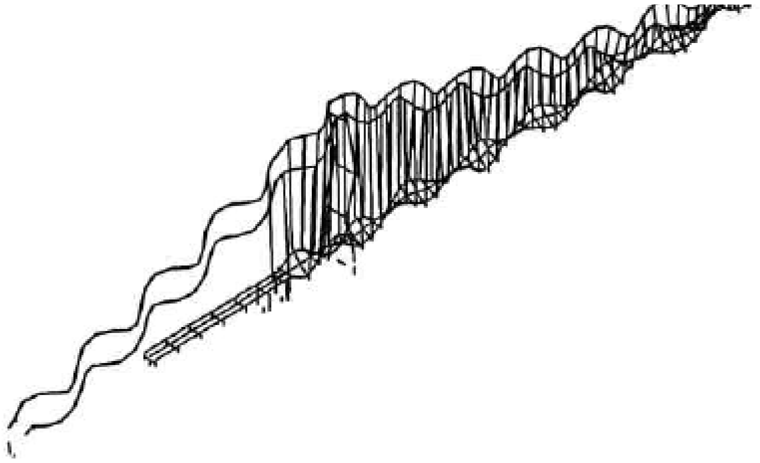

Figure 7-5: Mode 395 - Period 0.76 s - Frequency 1.31 Hz (Sicilia half of bridge shown).

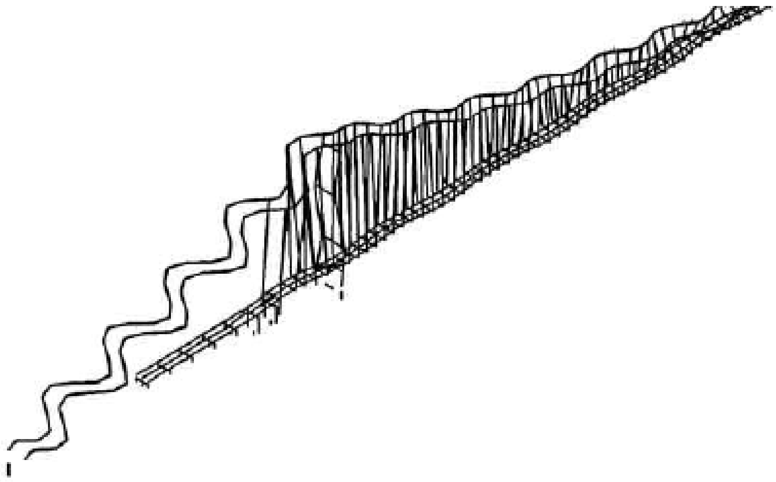

Figure 7-6: Mode 410 - Period 0.74 s - Frequency 1.35 Hz (Sicilia half of bridge shown).

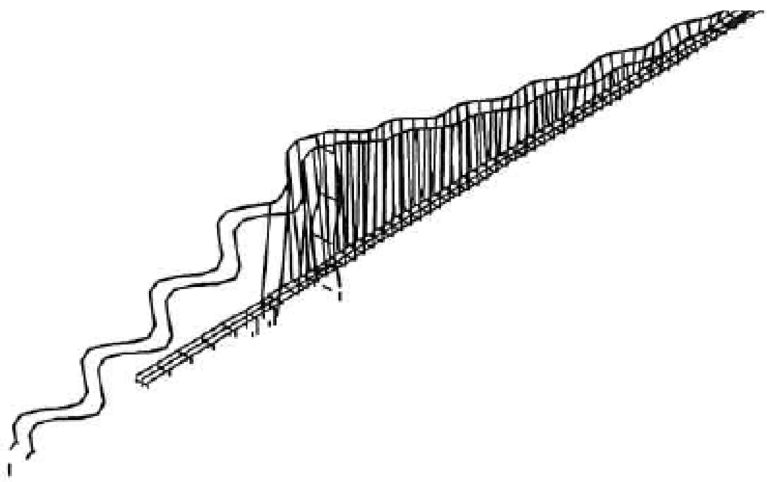

Figure 7-7: Mode 353 - Period 0.83 s - Frequency 1.20 Hz (Sicilia half of bridge shown).

7.2.1.2 Buckling Modes

The elastic buckling modes determined using an eigen-buckling analysis are the basis for the calculation of axial loads, moments and stresses due to equivalent imperfections, which account for the effects geometric tolerances and residual stresses in the global tower leg design. The equivalent imperfection stresses are based on the first longitudinal buckling mode, shown in Figure 7-8, and the first two transverse buckling modes, shown in Figure 7-9. The first longitudinal elastic buckling mode has a reference dead load axial force multiplier of 7.66, corresponding to an axial load at the base of one tower leg of 10,330 MN. The first transverse elastic buckling mode has a reference dead load axial force multiplier of 6.72, corresponding to an axial load at the base of one tower leg of 9,130 MN. The second transverse elastic buckling mode corresponds to a reference dead load axial force multiplier of 9.11, corresponding to an axial load at the base of one tower leg of 12,470 MN.

A detailed description of the methods used to calculate the effects of the equivalent imperfections is provided in the General Design Principles (CG.10.00-P-RG-D-P-SV-T4-00-00-00-00-01).

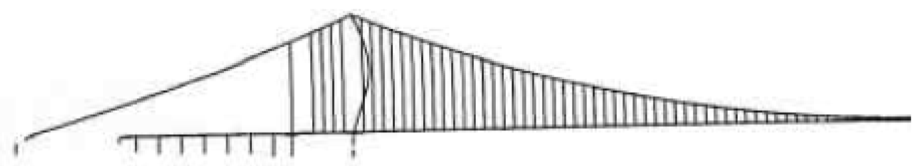

Figure 7-8: First longitudinal eigen-buckling mode for the Sicilia tower (Sicilia half of bridge shown).

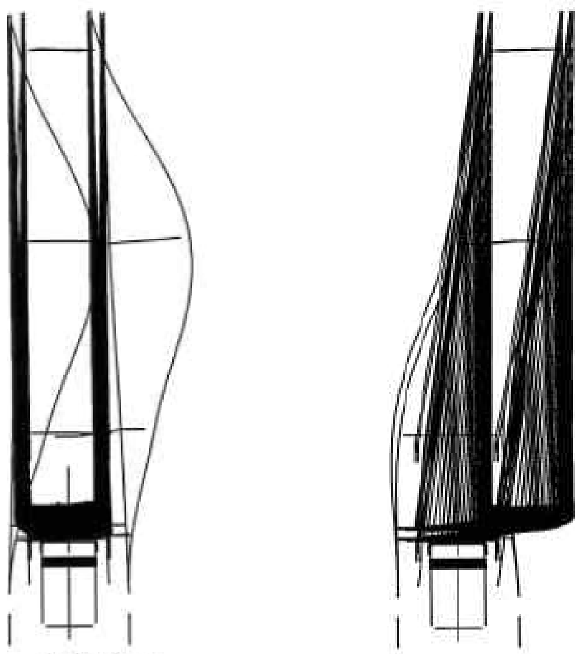

Figure 7-9: First and second transverse eigen-buckling modes for the Sicilia tower.

7.2.2 Maximum Displacements

The maximum longitudinal tower top displacements are caused by the ULS seismic load combination. The maximum transverse tower top displacements are caused by the SILS transverse wind loads. Maximum absolute and relative to dead load position tower top displacements are summarised in Table 7-1. In the reference dead load condition the Sicilia and Calabria tower tops are leaning towards the side spans by approximately 1.6 m.

The Sicilia tower moves slightly more longitudinally than the Calabria tower, both towards the side and main spans. Transverse tower top movements of both towers are similar.

Tower	Longitudinal				Transverse
	Absolute		Relative		
	Towards Side Span	Towards Main Span	Towards Side Span	Towards Main Span	
Sicilia	3.19	0.93	1.57	2.55	±1.98
Calabria	2.98	0.55	1.36	2.17	±1.92

Table 7-1: Maximum tower top displacements (m).

7.3 Tower Legs

The tower legs are steel box-sections comprising longitudinally and transversally stiffened panels. The tower leg cross section dimensions are constant over the full tower height from the top of the base plate to the underside of the main cable saddle, with a width perpendicular to the bridge axis of 12 m and a length parallel to the bridge axis of 20 m. A typical tower leg cross section and cross-section on which longitudinal stiffeners are designated are shown in Figure 7-10. The tower legs are shop fabricated in 21 full cross section segments, with lengths varying between 10.15 m and 20 m, and a maximum mass of approximately 1,525 tonnes, including tuned mass dampers. The two legs of each tower are sloped inwards at 1.929° with a centreline to centreline spacing that varies from 77.662 m at the base to 52.000 m at the main cable work point. The two tower legs are connected by transverse cross beams at approximately elevations +125 m, +250 m and +375 m. Each tower leg contains eight tuned-mass dampers between elevations 230 m and 260 m to control vortex shedding induced oscillations expected to occur at wind speeds of approximately 40 m/s and 65 m/s. In the reference dead load condition of the completed bridge, the tower legs lean towards the side spans by approximately 1.6 m at the tower top. The tower legs are fixed to the concrete foundations by post-tensioned anchorage tendons.

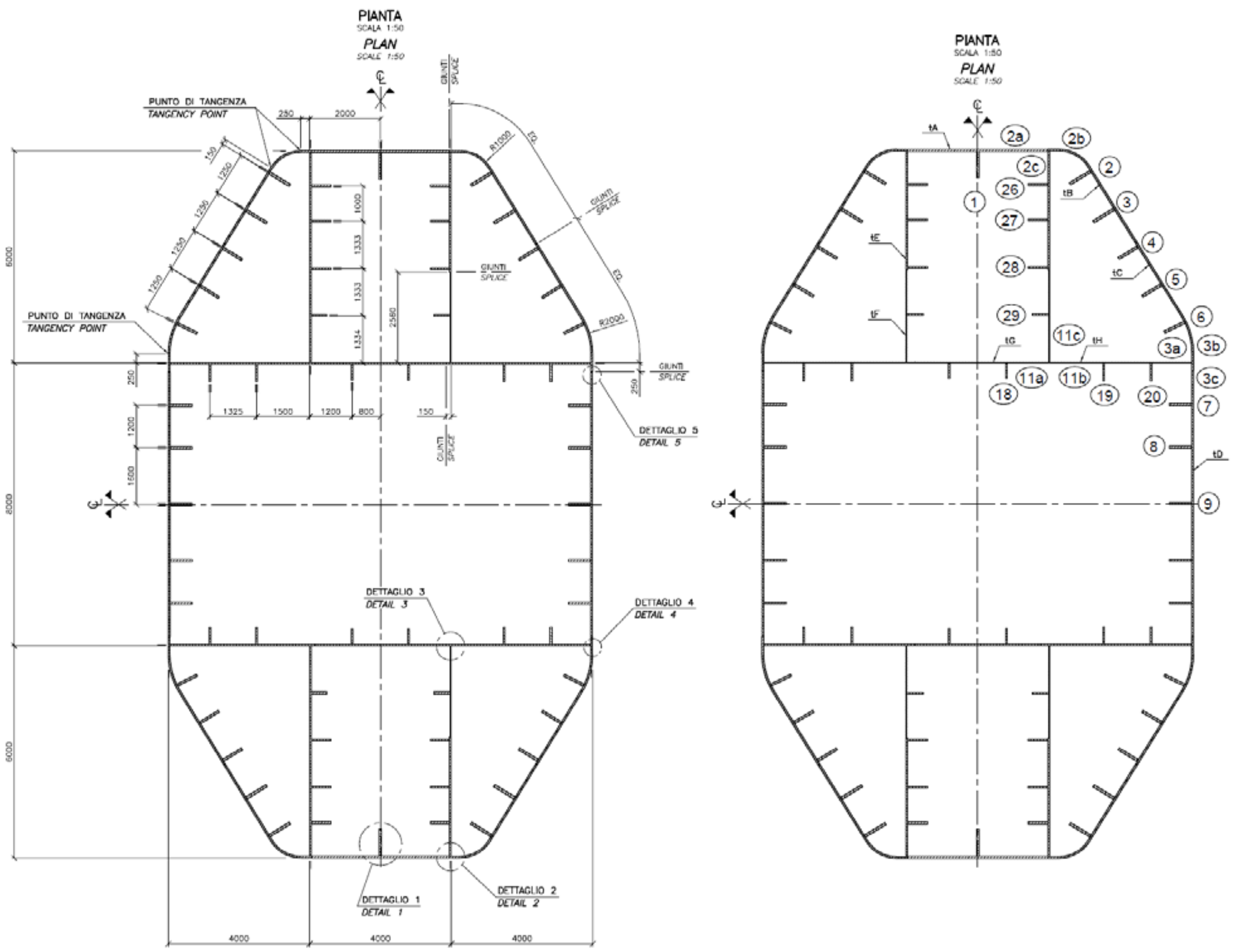

Figure 7-10: Tower leg cross section and plate/stiffener designations.

7.3.1 Freestanding Tower

Wind and seismic demands on the freestanding tower were considered in the tender phase and were shown not to govern the tower leg or cross beam design. Despite the tower height having increased since the tender design phase, the tower legs in the completed bridge are so dominated by axial compressive stresses that the minimal axial compression present in the freestanding tower ensures that this is not a governing condition. Therefore, no further investigations of the demands on the freestanding tower legs were completed in the Progetto Definitivo. However, the freestanding condition is considered for the base anchorage design, as described in Section 7.5.

7.3.2 Freestanding Tower with Tie-Back

The towers are designed to be constructed vertical (without camber) and tied-back prior to main cable installation. The tie-back force, or rather displacement, that is introduced during construction is selected so as to leave the towers leaning slightly towards the side spans in the reference dead load condition after construction. The permanent lean of the tower legs is specified so as to better balance the maximum compressive stresses on the main and side span tower leg faces in the completed bridge. In the completed bridge, maximum side span leaning moments in the tower legs are accompanied by minimum compressive loads (corresponding to minimum main span dead and live loads). The maximum main span leaning moments are of similar magnitude to the side span leaning moments, but are accompanied by maximum compressive loads (corresponding to maximum main span dead and live loads). This results in much higher maximum compressive stresses on the main span tower leg face unless the tower cross section is made asymmetric or the dead load stress state is adjusted by the construction sequence, as is proposed.

The longitudinal Sicilia tower leg displacement during construction is shown in Figure 7-11, with negative values indicating displacement towards the side span. After the tower is constructed, the first step of the tie-back process is the initial installation and stressing of the tie-back cables, which will connect the tower top and the main cable anchorage. The tie-back cable is then stressed to its maximum tension, pulling the tower top back to a displacement of approximately 3.8 m. After the main cables are installed the tie-back cables are removed, transferring the tie-back force into the main cables. During deck installation some of the sag is pulled out of the side span main cable, causing the tower top to move towards the main span by approximately 2.5 m. After construction the tower top leans towards the side span by approximately 1.6 m. The movements of the Calabria tower during construction are similar.

Sicilia tower leg longitudinal shear forces during construction are shown in Figure 7-12. The solid lines represent the shear forces directly output from the model, which are relative to the deformed member axis; the dashed lines represent the corresponding horizontal shear force computed based on the model output shear and the member axial load and inclination. As expected, because there are no longitudinal loads applied between the tower top and base, the horizontal shear force is constant over the tower height.

Sicilia tower leg longitudinal moments during construction are shown in Figure 7-13. The solid lines represent the total longitudinal moment on a section and the dashed lines represent the moment that is caused by the horizontal shear force. The increasing difference between the total moment and that caused by the horizontal shear force as construction proceeds indicates the increasing contribution of P-Delta moments to the total. At the end of construction, the tower leg has a side span leaning moment of approximately 2,000 MNm.

Although consideration of the freestanding tower with tie-back is important to the dead load stress state in the completed bridge, similar to the freestanding tower, it was shown in the tender design that the tower leg design is not governed by the construction condition because of the relative lack of axial compression; this was confirmed in the Progetto Definitivo. However, the freestanding tower with tie-back governs the design of the post-tensioning tendons in the base anchorage at some locations, as described in Section 7.5.

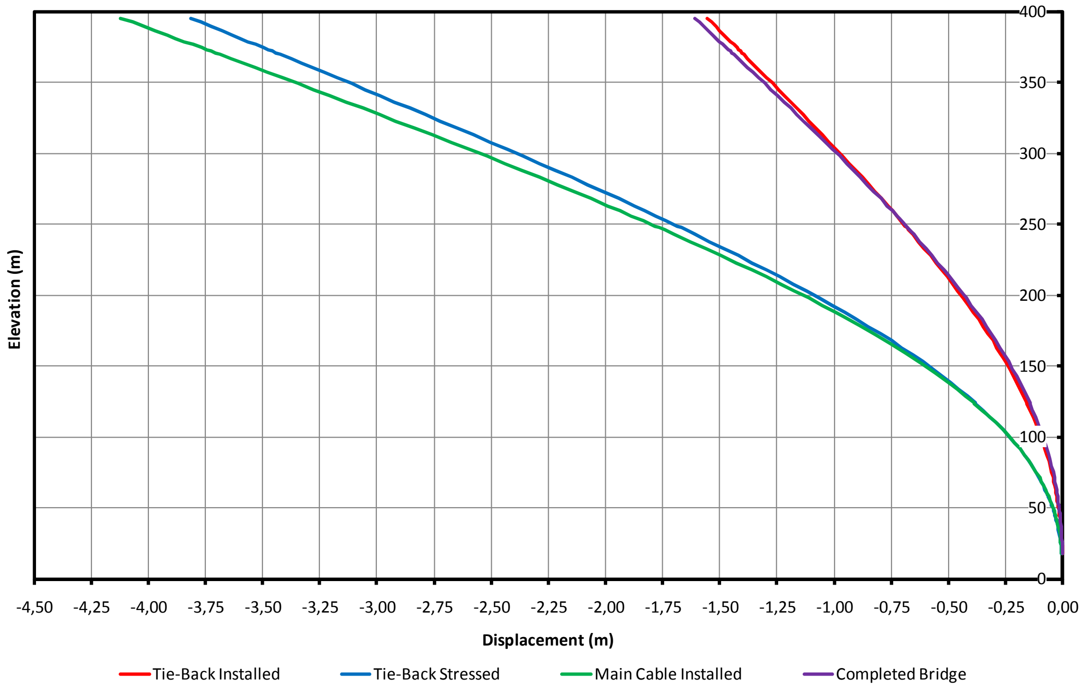

Figure 7-11: Sicilia tower leg longitudinal displacements during construction.

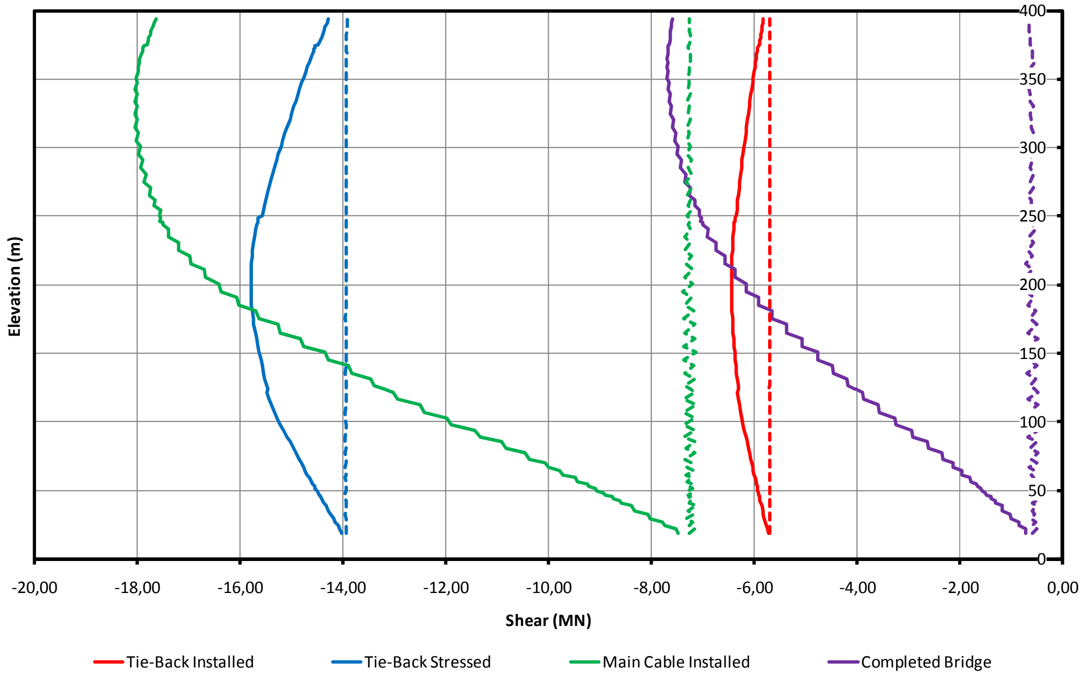

Figure 7-12: Sicilia tower leg longitudinal shear forces during construction (member shear forces - solid lines, corrected horizontal shear forces - dashed lines).

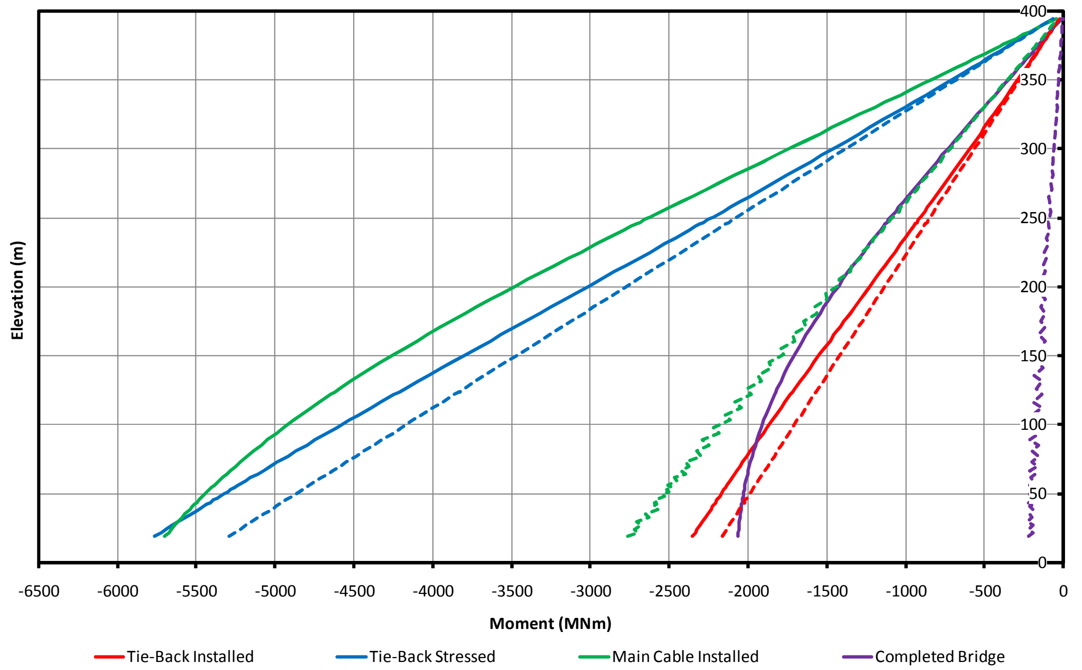

Figure 7-13: Sicilia tower leg longitudinal moments during construction (member moments - solid lines, moments based on horizontal shear forces - dashed lines).

7.3.3 Completed Bridge

7.3.3.1 Longitudinal Elements

The tower leg cross section comprises the perimeter skin plates, the internal longitudinal and transverse web plates, and the longitudinal stiffeners. The longitudinal stiffening arrangement differs from that presented in the tender design in that the previous T-shaped stiffeners have been replaced with flat plate stiffeners and the number of longitudinal stiffeners has been decreased from 64 to 60. The stiffener cross section was changed to simplify fabrication and the number of stiffeners was decreased to both simplify fabrication and achieve improved material economy. The tower leg segments are joined at transverse field splices comprising high strength bolted connections for the internal plates and longitudinal stiffeners, and full penetration welds for the skin plates. The design of the tower leg longitudinal plates, stiffeners and construction joint field splices is described in this section.

LONGITUDINAL PLATES AND STIFFENERS

The longitudinal plates and stiffeners were proportioned using the equivalent width method specified in EN 1993-1-5 Sections 4.4 and 4.5, and as described further in CG.10.00-P-RG-D-P-SV-T4-00-00-00-00-01 “General Design Principles.” The resulting plate thicknesses vary from 30 mm to 110 mm for both the Sicilia and Calabria towers, as shown in Table 7-2 and Table 7-3, respectively; the longitudinal stiffeners vary in spacing from 1,000 mm to 2,000 mm, as shown previously in Figure 7-10, and in size from 425x43 to 750x75, as shown Table 7-4 and Table 7-5 for the Sicilia and Calabria towers, respectively.

Segment	Plate Thickness (mm)							
	A	B	C	D	E	F	G	H
1	110	110	100	75	100	75	45	45
2	110	100	85	60	100	60	35	40
3	110	100	75	50	85	40	30	40
4	110	100	60	45	70	35	30	40
5	110	90	45	40	60	35	35	40
6	95	75	45	40	55	35	35	40
7	75	55	45	60	50	40	50	55
8	65	50	60	75	40	40	50	55
9	65	50	50	65	40	40	45	50
10	75	55	45	50	40	45	40	45
11	80	55	45	45	40	45	40	45
12	85	50	45	55	45	45	40	45
13	90	60	50	55	40	45	50	50
14	90	75	50	60	45	45	50	50
15	100	80	50	50	50	40	40	40
16	100	85	45	40	55	40	35	45
17	100	85	45	40	55	40	35	40
18	90	70	45	45	50	45	40	40
19	70	50	50	60	45	45	40	45
20	65	45	45	70	55	45	50	50
21	70	45	50	70	55	50	50	50

Table 7-2: Sicilia tower leg plate thicknesses.

Segment	Plate Thickness (mm)							
	A	B	C	D	E	F	G	H
1	110	105	80	80	85	50	35	40
2	110	100	70	65	80	40	30	40
3	105	90	65	55	70	35	30	40
4	100	80	60	50	60	35	30	40
5	95	70	45	45	50	40	35	40
6	80	50	45	50	45	35	40	45
7	65	45	50	60	45	40	50	55
8	60	55	60	75	45	35	50	55
9	70	50	50	65	40	35	40	45
10	75	55	45	50	45	40	40	40
11	80	60	40	40	50	40	40	40
12	80	60	40	50	45	40	40	40
13	80	55	45	60	45	40	50	50
14	90	55	50	60	45	40	50	50
15	100	60	45	50	50	40	35	40
16	105	60	45	40	50	40	35	40
17	95	60	40	40	50	40	40	40
18	85	55	40	45	45	40	40	40
19	65	50	45	55	40	35	40	45
20	60	45	45	65	40	45	50	50
21	65	45	45	60	50	50	50	50

Table 7-3: Calabria tower leg plate thicknesses.

Segment	Plate Thickness (mm)							
	A	B	C	D	E	F	G	H
1	750 x 75	700 x 70	700 x 70	650 x 65	725 x 73	600 x 60	475 x 48	475 x 48
2	750 x 75	700 x 70	700 x 70	650 x 65	725 x 73	575 x 58	450 x 45	450 x 45
3	750 x 75	700 x 70	700 x 70	625 x 63	725 x 73	550 x 55	450 x 45	450 x 45
4	750 x 75	700 x 70	675 x 68	625 x 63	700 x 70	525 x 53	450 x 45	450 x 45
5	750 x 75	675 x 68	625 x 63	600 x 60	675 x 68	500 x 50	450 x 45	450 x 45
6	750 x 75	675 x 68	625 x 63	625 x 63	650 x 65	500 x 50	475 x 48	475 x 48
7	750 x 75	675 x 68	650 x 65	650 x 65	625 x 63	475 x 48	475 x 48	550 x 55
8	750 x 75	650 x 65	675 x 68	675 x 68	625 x 63	475 x 48	475 x 48	550 x 55
9	750 x 75	675 x 68	650 x 65	675 x 68	600 x 60	475 x 48	475 x 48	525 x 53
10	750 x 75	675 x 68	625 x 63	650 x 65	575 x 58	475 x 48	450 x 45	500 x 50
11	750 x 75	675 x 68	600 x 60	625 x 63	575 x 58	475 x 48	450 x 45	500 x 50
12	750 x 75	650 x 65	600 x 60	650 x 65	575 x 58	475 x 48	450 x 45	525 x 53
13	750 x 75	675 x 68	625 x 63	675 x 68	550 x 55	450 x 45	475 x 48	550 x 55
14	750 x 75	700 x 70	600 x 60	675 x 68	550 x 55	450 x 45	475 x 48	550 x 55
15	750 x 75	700 x 70	600 x 60	650 x 65	575 x 58	475 x 48	475 x 48	475 x 48
16	750 x 75	700 x 70	550 x 55	600 x 60	575 x 58	450 x 45	450 x 45	450 x 45
17	750 x 75	700 x 70	550 x 55	575 x 58	575 x 58	450 x 45	450 x 45	450 x 45
18	750 x 75	700 x 70	550 x 55	575 x 58	575 x 58	475 x 48	450 x 45	475 x 48
19	750 x 75	650 x 65	575 x 58	600 x 60	550 x 55	500 x 50	475 x 48	550 x 55
20	750 x 75	650 x 65	575 x 58	625 x 63	575 x 58	500 x 50	500 x 50	550 x 55
21	750 x 75	650 x 65	575 x 58	625 x 63	600 x 60	550 x 55	550 x 55	550 x 55

Table 7-4: Sicilia tower leg longitudinal stiffener sizes.

Segment	Plate Thickness (mm)							
	A	B	C	D	E	F	G	H
1	750 x 75	700 x 70	675 x 68	675 x 68	650 x 65	500 x 50	450 x 45	475 x 48
2	750 x 75	700 x 70	650 x 65	650 x 65	600 x 60	500 x 50	450 x 45	450 x 45
3	750 x 75	675 x 68	625 x 63	625 x 63	600 x 60	475 x 48	450 x 45	450 x 45
4	750 x 75	675 x 68	625 x 63	600 x 60	600 x 60	475 x 48	450 x 45	450 x 45
5	750 x 75	675 x 68	625 x 63	600 x 60	600 x 60	475 x 48	450 x 45	450 x 45
6	750 x 75	650 x 65	600 x 60	600 x 60	575 x 58	475 x 48	450 x 45	475 x 48
7	750 x 75	625 x 63	625 x 63	625 x 63	575 x 58	475 x 48	475 x 48	550 x 55
8	750 x 75	625 x 63	650 x 65	650 x 65	550 x 55	475 x 48	475 x 48	550 x 55
9	750 x 75	625 x 63	650 x 65	650 x 65	550 x 55	475 x 48	425 x 43	525 x 53
10	750 x 75	650 x 65	625 x 63	625 x 63	550 x 55	475 x 48	425 x 43	500 x 50
11	750 x 75	675 x 68	625 x 63	600 x 60	575 x 58	475 x 48	425 x 43	500 x 50
12	750 x 75	675 x 68	600 x 60	650 x 65	600 x 60	475 x 48	425 x 43	500 x 50
13	750 x 75	675 x 68	600 x 60	650 x 65	600 x 60	475 x 48	475 x 48	550 x 55
14	750 x 75	675 x 68	625 x 63	650 x 65	600 x 60	475 x 48	475 x 48	550 x 55
15	750 x 75	700 x 70	625 x 63	625 x 63	600 x 60	475 x 48	425 x 43	475 x 48
16	750 x 75	700 x 70	600 x 60	625 x 63	600 x 60	475 x 48	425 x 43	475 x 48
17	750 x 75	675 x 68	575 x 58	575 x 58	600 x 60	475 x 48	425 x 43	475 x 48
18	750 x 75	675 x 68	600 x 60	600 x 60	575 x 58	475 x 48	425 x 43	450 x 45
19	750 x 75	625 x 63	600 x 60	625 x 63	550 x 55	475 x 48	425 x 43	475 x 48
20	750 x 75	600 x 60	600 x 60	650 x 65	575 x 58	500 x 50	500 x 50	550 x 55
21	750 x 75	600 x 60	600 x 60	625 x 63	600 x 60	550 x 55	550 x 55	550 x 55

Table 7-5: Calabria tower leg longitudinal stiffener sizes.

Plate thicknesses and longitudinal stiffener spacing are selected to provide only the efficiency required to carry the maximum applied compressive stress at a particular point on the cross section. Efficiency is defined as the ratio of the compressive stress limit to the unfactored yield stress. Because the maximum design stresses are a combination of axial and flexural compression, the plates and stiffeners furthest from the cross-section centroid are subjected to the highest stresses, and therefore are proportioned to have the highest efficiency possible. Plates and stiffeners near the cross-section centroid are never subjected to the design yield stress and therefore can be more slender without affecting the overall cross-section capacity. The efficiencies of the plates and longitudinal stiffeners are plotted in terms of the maximum allowable compressive stress for each tower segment for the Sicilia tower in Figure 7-14. In the plot for each plate, elevation is plotted on the vertical axis and maximum allowable stress in MPa is plotted on the horizontal axis. The stiffener numbers and corner designations are as shown previously in Figure 7-10. The stiffener comprises the stiffener itself and the associated tributary plate area. The corner comprises the plate area tributary to the intersection between two or more plates. The stiffeners and corners are distinguished by the fact that corner region effectiveness is not reduced for column/plate-like buckling. In each plot the cross beam elevations are represented by the black dashed lines.

The plotted tower leg plate efficiencies indicate a great deal about the tower leg behaviour, as they show the cross section elements that require the most strength at each elevation. The following observations can be made with respect to the plotted efficiencies:

- Plate A is located furthest from the cross-section centroid and is therefore subjected to the highest compressive stresses. As such, its thickness is selected so that it is typically fully effective and can reach yield.
- Plate B contributes significantly to the longitudinal moment resistance, however, only the plate end connecting to plate A will be subjected to the maximum cross-section stress and thus a slightly reduced efficiency, typically between 450 MPa and 460 MPa is acceptable.
- Plate C contributes to both the longitudinal and transverse moment resistances. Its efficiency generally increases towards the tower base and is typically between 440 MPa and 460 MPa.
- Plate D contributes most to the transverse moment resistance and it must therefore be efficient where the transverse moments are largest, in the regions above and below each cross beam. The shape of the efficiency lines for each stiffener mimic the shape of the

governing tower leg transverse moment diagram. The efficiencies of the stiffeners on plate D increase with their distance from the cross-section centroid, as they are subjected larger compressive stresses due to longitudinal moments. Efficiencies vary from approximately 390 MPa to 450 MPa, with the corner regions being able to reach 460 MPa.

- Plate E contributes to the longitudinal moment capacity. The stiffener efficiencies on plate E vary with their distance from the centroid. The portions of plate E closest to plate A are the most heavily stressed and so stiffener 26 is generally more efficient than stiffeners 27 and 28. Efficiencies vary from approximately 420 MPa to 460 MPa, near the tower base, with the corner region being able to reach 460 MPa.
- Plate F is relatively close to the cross section centroid and therefore efficiencies typically between 380 MPa and 420 MPa are acceptable.
- Plates G and H are typically the least stressed plates in the cross section because they are the closest to the centroid. Therefore, efficiencies as low as 360 MPa are acceptable at some elevations. However, at cross beam connections they are subjected to considerable in plane shear forces, requiring the plates to be thickened by approximately 15-20 mm relative to the thickness required just to carry the applied axial stresses.

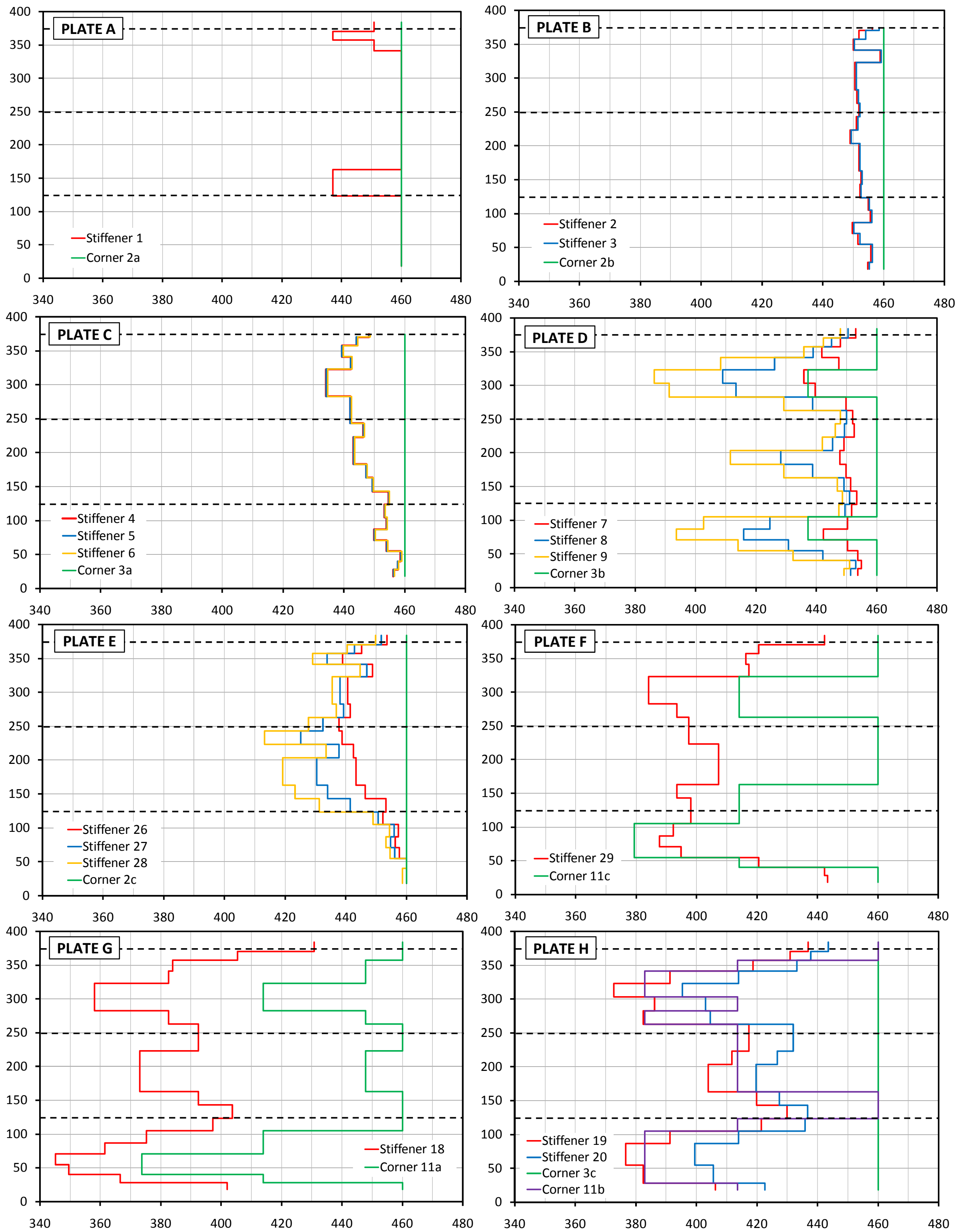

Figure 7-14: Sicilia tower leg plate/longitudinal stiffener unfactored allowable stresses.

GOVERNING FORCE EFFECTS AND UTILIZATION RATIOS

Axial and Flexural Compressive Stresses

Tower leg axial forces are dominated by dead load effects, as is shown in Figure 7-15, in which unfactored dead, wind, live and seismic load axial forces are plotted for a Sicilia tower leg. The seismic force effects used for the tower design are the mean force effect results of the eight input time-histories that were analysed. The output from the individual time-history analyses is presented in Appendix A and is compared to the results of the response spectrum seismic analysis. An additional investigation into the effects of the envelope of the time-history analysis results on the tower legs is described in Appendix C. The wind load forces are the maximum of either the dynamic wind response (static + dynamic wind loads) or vortex shedding response (static wind loads + vortex shedding induced oscillations). The cross beam elevations are represented by the black centrelines at elevations +125 m, +250 m and +375 m. Corresponding force effects for the Calabria tower are presented in Appendix B. The unfactored dead load axial force is approximately four times the largest axial force from any of the other load component.

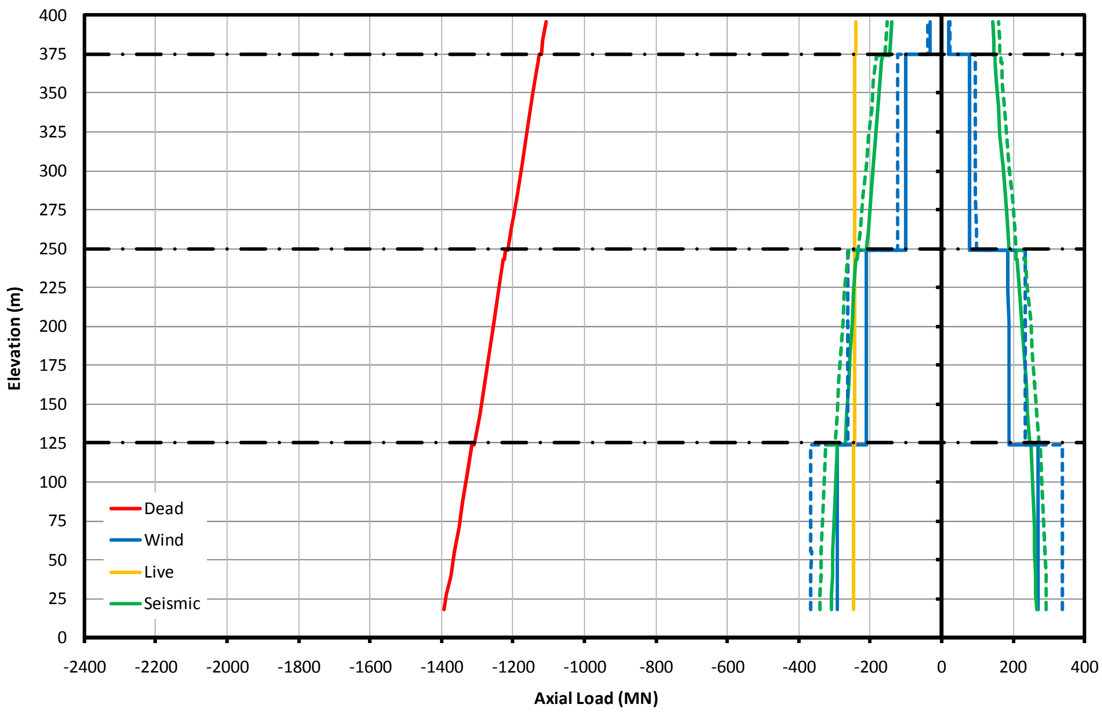

Figure 7-15: Sicilia tower leg axial forces (ULS - solid lines, SILS - dashed lines).

Unfactored tower leg longitudinal moments for the Sicilia tower are shown in Figure 7-16 for dead loads, wind loads, live loads and seismic loads. Negative moments cause the tower to lean towards the side span and positive moments cause the tower to lean towards the main span. The relative lack of a cable supported side span is apparent in the range of live load moments, which are almost entirely positive. Longitudinal wind load moments act with approximately equal positive and negative magnitudes, as do seismic moments. Tower leg longitudinal moments are heavily dominated by seismic loads, with a maximum moment that is approximately four times the largest caused by the other load components. Under seismic and wind loading the tower leg behaves as a propped cantilever with a maximum moment occurring at the fixed base and a minimum moment occurring at approximately 70% of the tower height. The inflection point in the longitudinal moment diagram is located at approximately the elevation of cross beam 1, +125.00, or about one-third of the tower height. Corresponding force effects for the Calabria tower are presented in Appendix A.

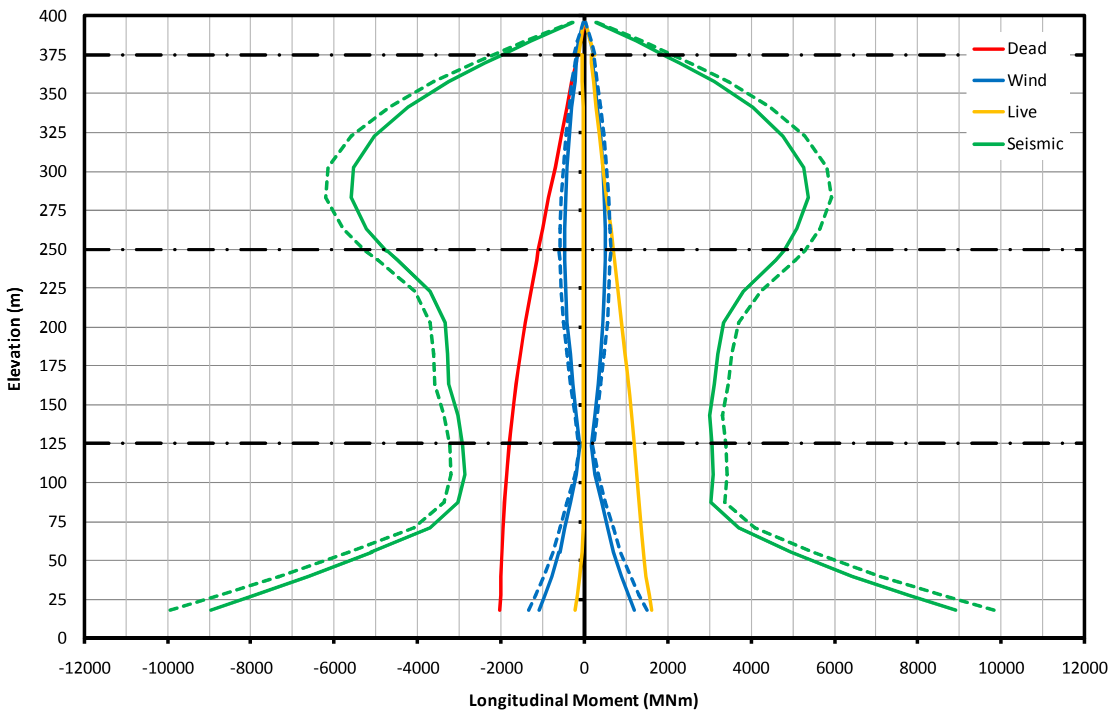

Figure 7-16: Sicilia tower leg longitudinal moments (ULS – solid lines, SILS – dashed lines).

Unfactored transverse tower leg moments for the Sicilia tower are shown in Figure 7-17 for dead loads, wind loads, live loads and seismic loads. Tower top main cable reactions cause transverse shear forces and moments because the cable saddle cantilevers above the top of cross beam 3 and because vertical cable reactions have a component that acts perpendicular to the inclined tower leg axis. Below elevation +300, dead and live load transverse moments are insignificant. Transverse moments are dominated by wind and seismic loading, with each producing governing values at some elevations. Seismic loads typically produce the largest moments at mid-height between each cross beam because of the self response effect of the tower leg mass, and wind loads typically produce the largest moments directly above and below each cross beam. The plotted wind load moments are the maximum of either dynamic wind response or vortex shedding response. It was found that the transverse wind load moments are governed by the dynamic wind response. Therefore, the force effects due to vortex shedding induced oscillations generally do not have an impact on the tower design. Corresponding force effects for the Calabria tower are presented in Appendix A.

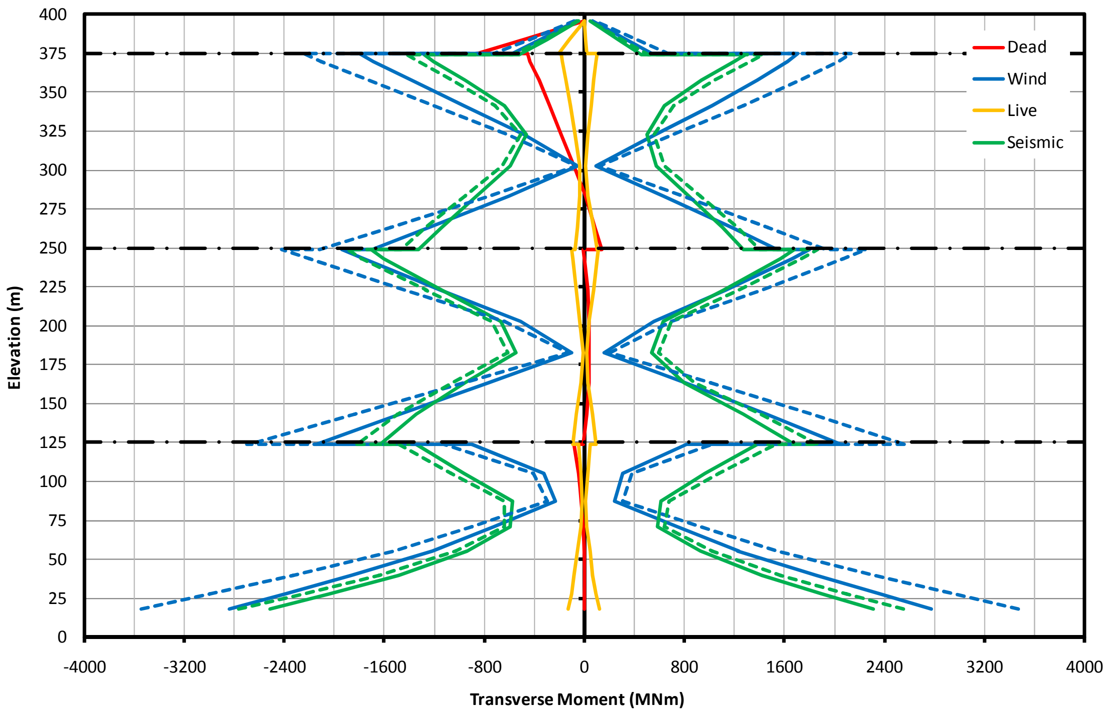

Figure 7-17: Sicilia tower leg transverse moments (ULS – solid lines, SILS – dashed lines).

In addition, to the applied force effects presented above, the tower legs experience additional forces resulting from global buckling (effect of equivalent imperfections). The method for determining the effects of global buckling is presented in CG.10.00-P-RG-D-P-SV-T4-00-00-00-00-01 "General Design Principles." The governing force effects resulting from the first longitudinal and first and second transverse global buckling modes are considered. The effects from multiple buckling modes need not be combined and the tower design considers only the worst effects of the three buckling modes at each cross section. As the global buckling can occur in any direction, all forces are taken as having equal positive and negative magnitudes. Longitudinal and transverse moments due to longitudinal and transverse buckling are shown in Figure 7-18 and Figure 7-19, respectively. The black centrelines in the figures represent the cross beam elevations. These force effects are added to the global model output, presented previously. Longitudinal buckling moments represent approximately the second largest contribution to the total factored longitudinal moment on the tower legs. Transverse buckling moments are approximately 30% to 50% of the maximum moments caused by the other load components. Although not shown, there is a small axial load in the tower legs that corresponds to transverse buckling, which is also considered in the design.

Figure 7-18 and Figure 7-19 show the buckling moments that occur for a single load combination. In reality, the global buckling effects are dependent on the axial force in the tower leg and change slightly for each load combination. This variation was considered in the tower design. However, the axial force is dominated by dead load and the variation between load combinations is small. Therefore, the buckling forces presented are indicative of the magnitude of the loads considered in the design.

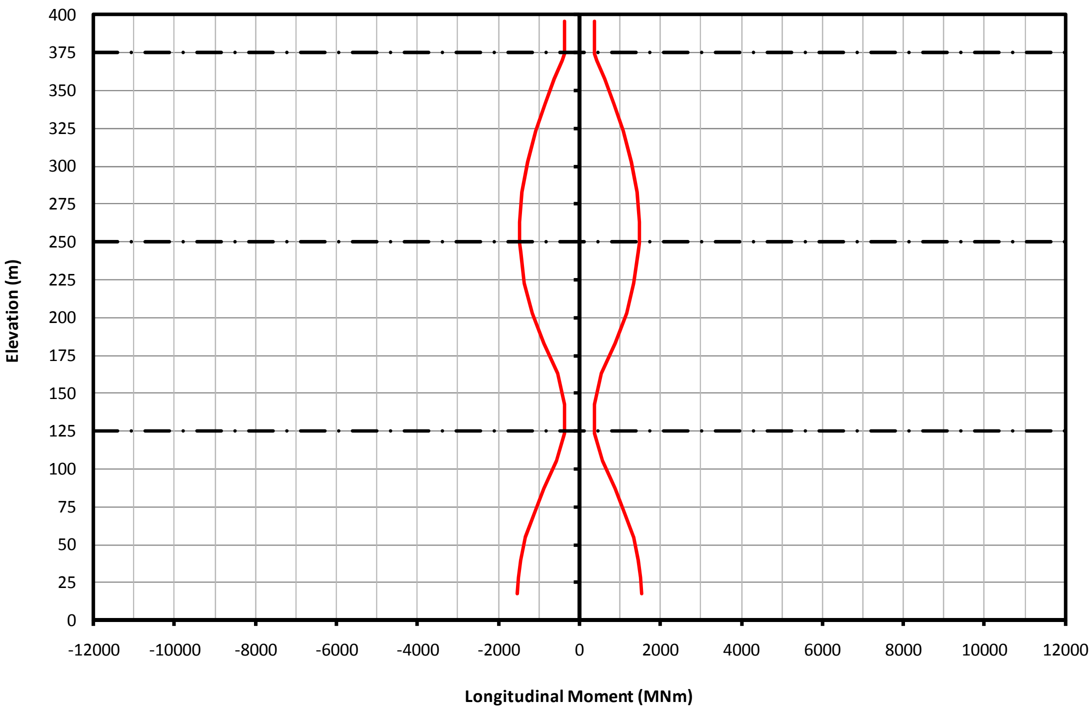

Figure 7-18: Longitudinal moments due to equivalent imperfections.

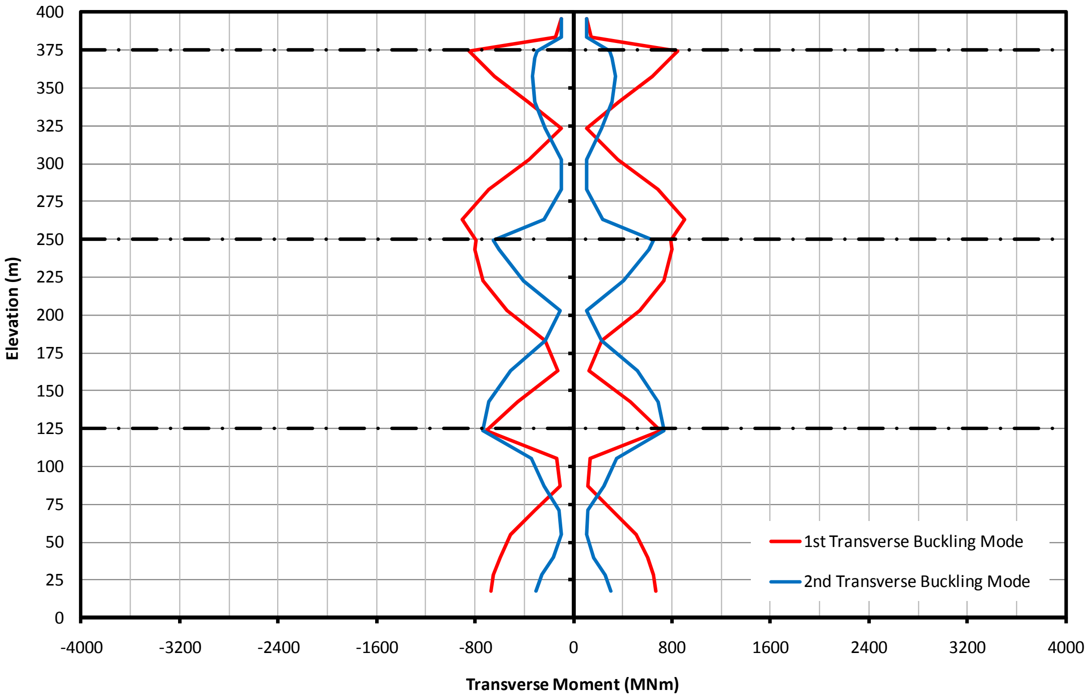

Figure 7-19: Transverse moment due to equivalent imperfections.

The tower leg design is based on the ULS and SILS load combinations specified in the design basis. Design force effect envelopes for the Sicilia tower, resulting from the combination of the individual load components presented previously, are shown in Figure 7-20 to Figure 7-24. The figures show the minimum and maximum envelopes of all relevant load combinations for ULS and SILS. These effects do not include forces from the global buckling of the tower shown previously. Corresponding force effects for the Calabria tower are presented in Appendix B.

The tower design is based on multiple load effects and considers only concurrent loads. The use of only minimum and maximum force effects would result in an overly conservative design as the maximum or minimum effects for each type of force effect rarely occur concurrently. Therefore, although the presented force effect envelopes show the maximum and minimum values of a particular effect, the governing stresses may not result from the maximum or minimum of any single effect. For instance, the governing stresses at the intersection of plates A and B may be caused by a combination including 90% of the maximum longitudinal moment and 90% of the maximum transverse moment. Tower leg stresses were evaluated for:

1 The maximum and minimum values of each load effect with concurrent values of the other load effects (e.g., maximum axial force with concurrent longitudinal and transverse moments); and

2 Linear combinations of effects, determined by IBDAS to find the loading pattern that produces the maximum and minimum stresses at the eight cross section corners based on the actual tower leg section properties.

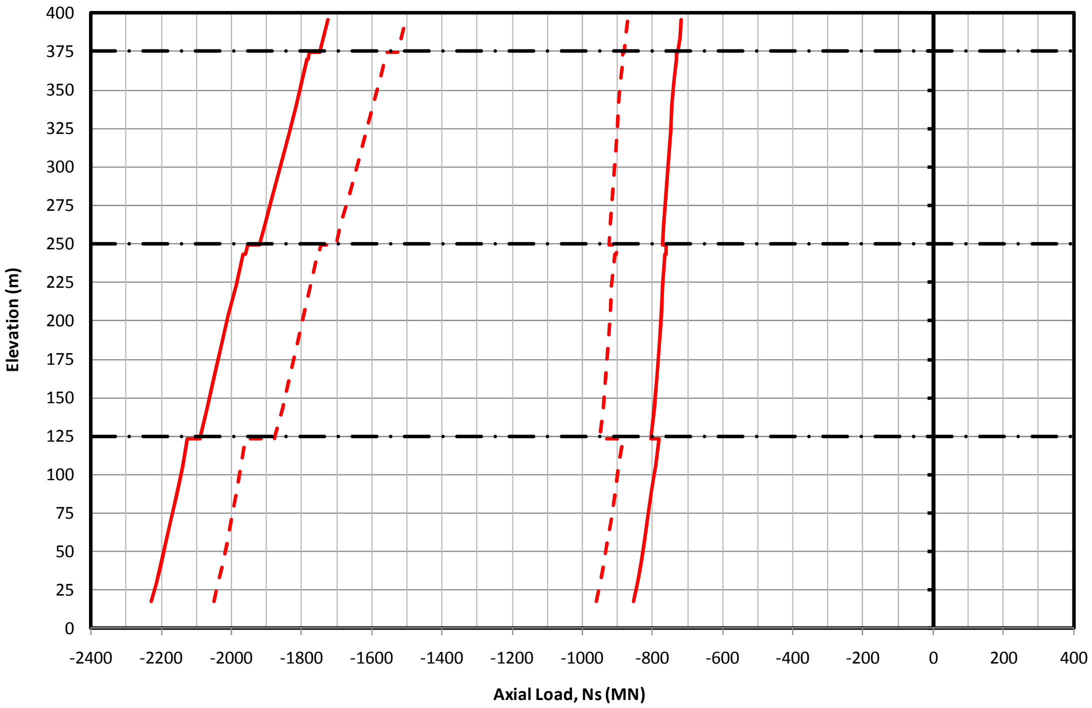

Figure 7-20: Sicilia tower leg factored axial load envelope (ULS – solid lines, SILS – dashed lines).

The governing combination for axial load is generally the seismic load as the seismic induced axial loads typically exceed those induced by wind. The axial load force effect envelope in Figure 7-20 shows that ULS load combinations produce larger axial loads than SILS load combinations. This is primarily a result of the reduced live load considered in the SILS combination, which uses the rarefied QR live load instead of the dense QA live load used in the ULS combinations. In addition, for the SILS load combination, the load factor for the non-structural components is taken as 1.0 instead of the 1.5 used in ULS combinations, resulting in a further reduction in factored axial load.

The longitudinal moment envelopes in Figure 7-21 are affected similarly, where in most cases the ULS moments are higher than the SILS moments. For the maximum moments, the reduced live load intensity and the reduced non-structural component dead load factor are responsible. ULS minimum moments are slightly larger in magnitude than SILS minimum moments because of the slightly lower, 0.9 instead of 1.0, non-structural component dead load factor. The maximum and minimum longitudinal moments for all locations are governed by load combinations with seismic loading as the moments greatly exceed the longitudinal moments from wind or live load.

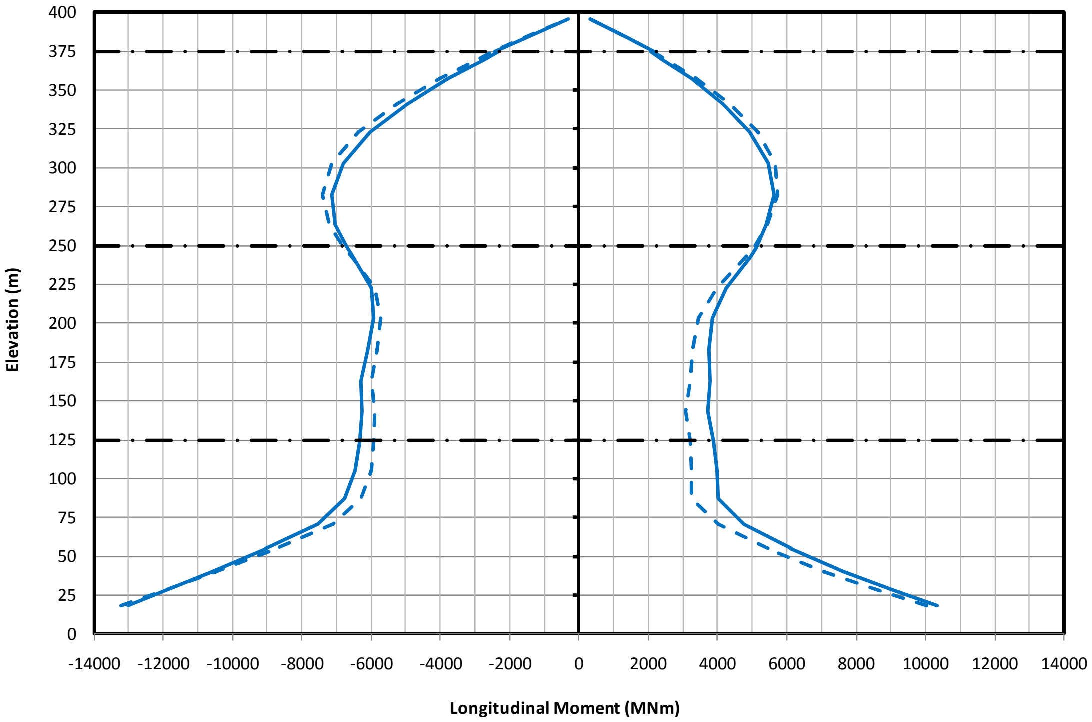

Figure 7-21: Sicilia tower leg factored longitudinal moment envelope (ULS – solid lines, SILS – dashed lines).

Transverse moment envelopes are governed by seismic and wind load and are not influenced significantly by dead or live loads. The only exception is at the tower top, where the transverse inclination of the tower legs relative to the main cable results in transverse bending moments. The minimum and maximum transverse moments are generally governed by wind loads as these slightly exceed the transverse moments due to seismic loading. Unlike axial forces and longitudinal moments, the transverse moments are greater for SILS load combinations than ULS load combinations. Because transverse moments are not significantly affected by dead and live loads, transverse moments increase proportionally to the increased wind loading.

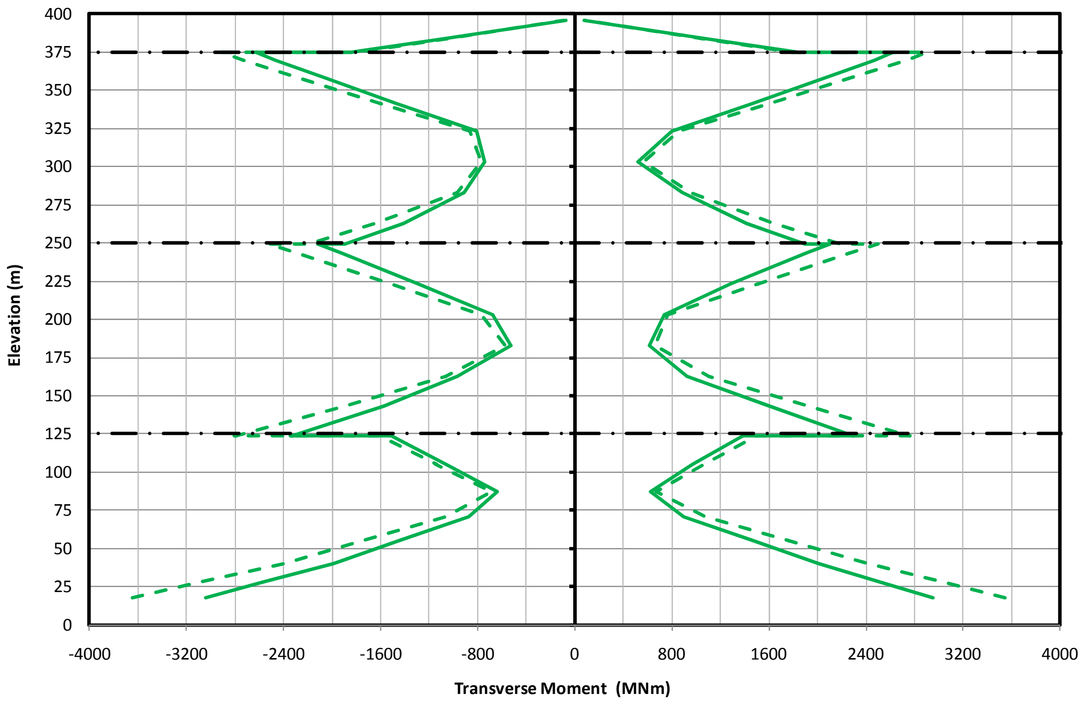

Figure 7-22: Sicilia tower leg factored transverse moment envelope (ULS – solid lines, SILS – dashed lines).

Longitudinal and transverse shear force envelopes are shown in Figure 7-23 and Figure 7-24, respectively. Longitudinal and transverse shear forces do not influence the tower leg design because the maximum shear stresses occurring concurrently with the governing longitudinal stresses are well below 50% of the shear capacity.

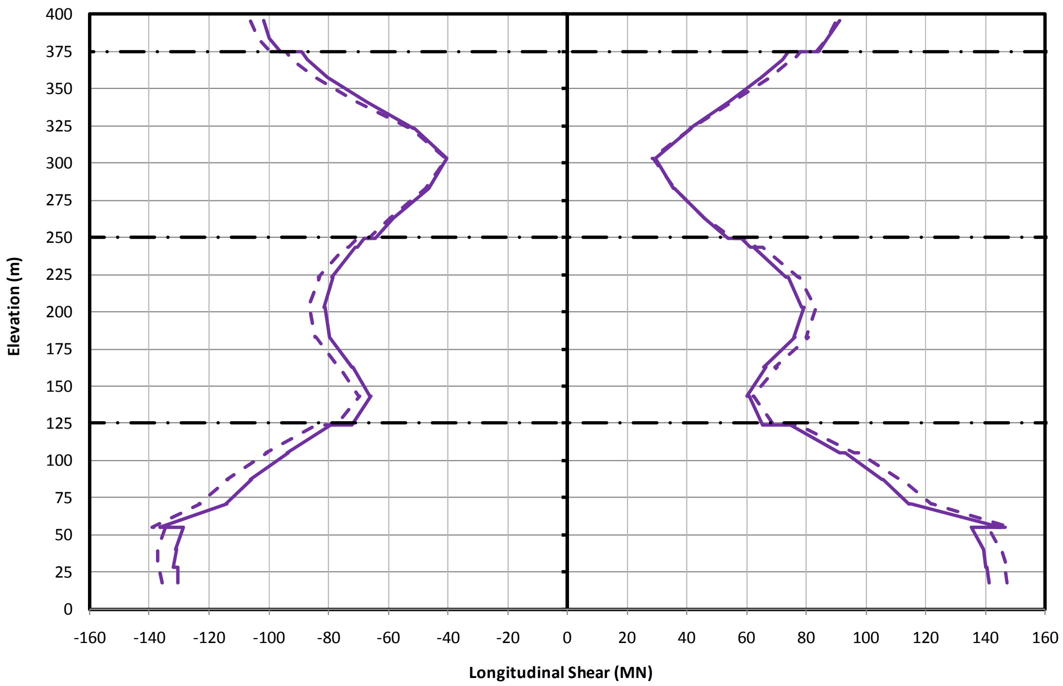

Figure 7-23: Sicilia tower leg factored longitudinal shear envelope (ULS – solid lines, SILS – dashed lines).

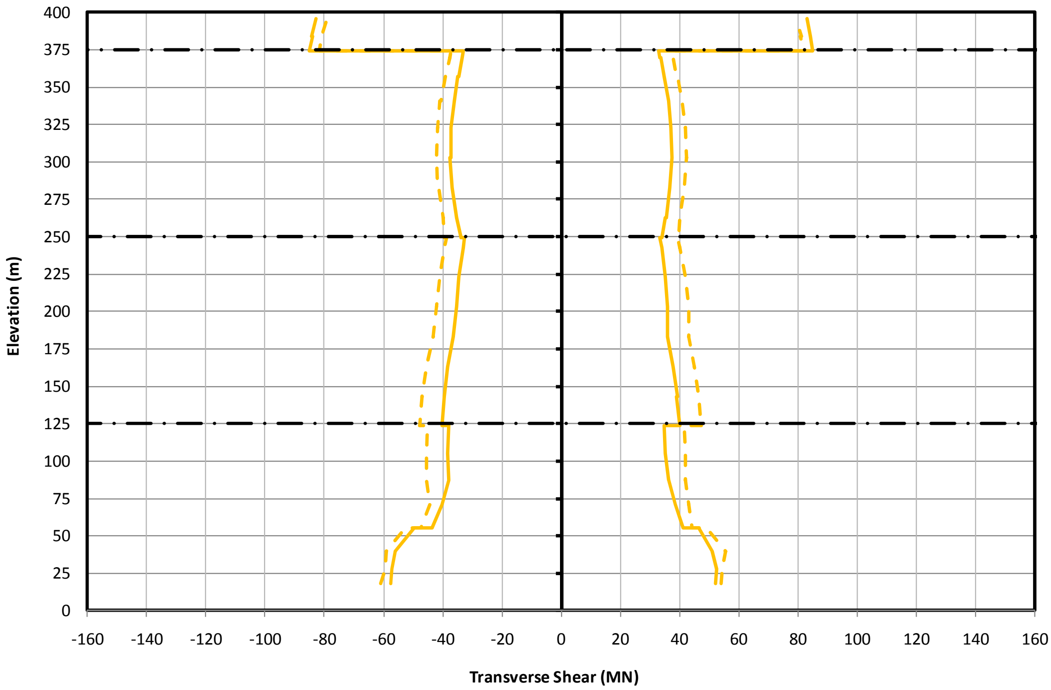

Figure 7-24: Sicilia tower leg factored transverse shear force envelope (ULS – solid lines, SILS – dashed lines).

The tower leg design is based on the effects of all relevant load combinations as described previously. For each load combination, a utilization ratio was obtained for each of the key cross section points identified in Figure 7-10 for each set of primary and concurrent effects and linear combinations of effects. The utilization ratios for all points on the cross section are less than or equal to 1.0 for all load combinations. The tower legs are generally governed by ULS combination 7, which includes concurrent seismic and maximum live loading. ULS combination 6, comprising transverse wind, governs the plate C, D and H thicknesses and longitudinal stiffener sizes near the cross beams, where transverse moments are largest. Utilization ratios for all cross section points and tower leg segments for the governing load combinations are shown in Figure 7-25 and Figure 7-26, for the Sicilia and Calabria towers, respectively.

For all load combinations and tower segments, the governing stresses are generally located near the cross section corners, with the governing location being either the unstiffened corner or the longitudinal stiffener located adjacent to the corner. For these locations, the plate thickness and stiffener size were proportioned such that the maximum allowable compressive stress is as close to yield as possible (high efficiency). Governing utilization ratios are between 0.95 and 1.0 for all segments of both towers.

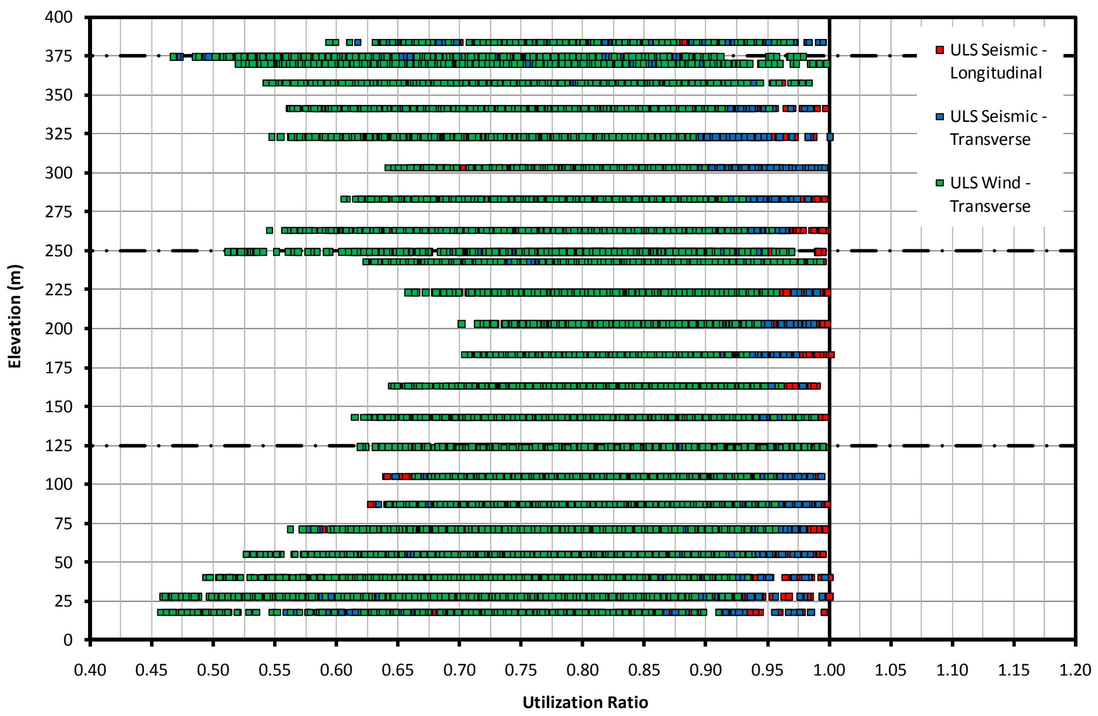

Figure 7-25: Sicilia tower leg governing utilization ratios.

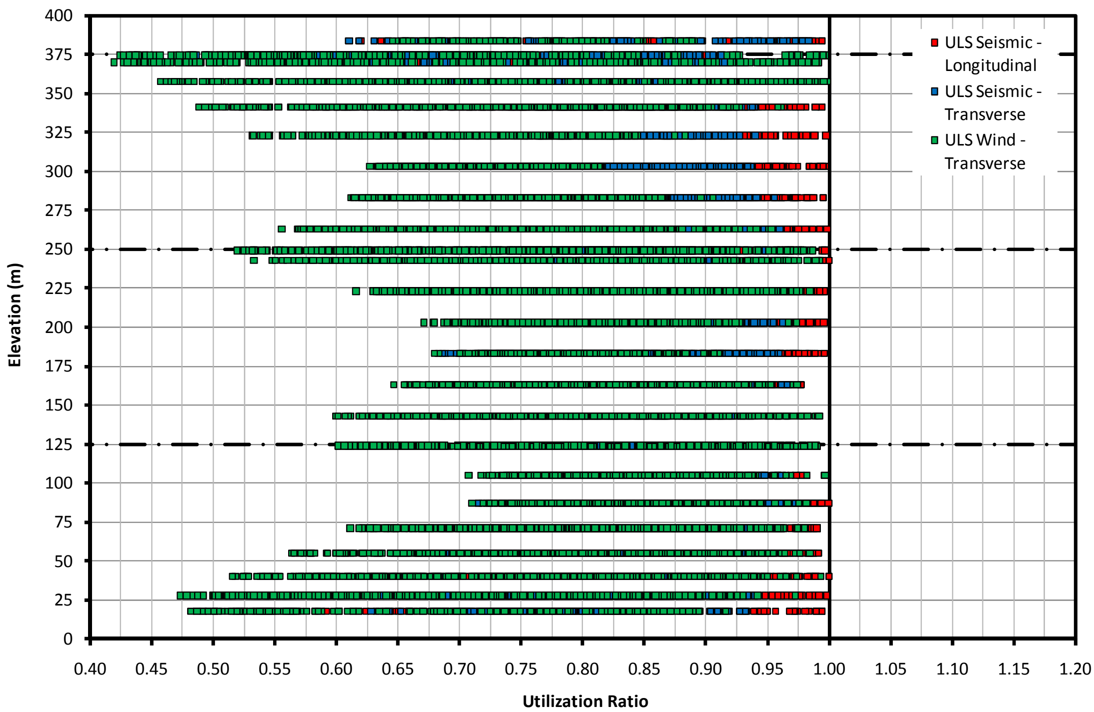

Figure 7-26: Calabria tower leg governing utilization ratios.

<u>Shear Stresses</u>

The tower leg design is heavily governed by axial and flexural compressive stresses. The cross section dimensions and plate thicknesses required to provide adequate resistance to these effects provide an excess of shear capacity. To confirm that the effects of shear do not need to be considered with longitudinal stresses, the maximum longitudinal and transverse average shear stresses that occur concurrently with the governing longitudinal stresses throughout the tower height were calculated. The stresses were then compared to the minimum shear capacity of the highest stressed resisting plate.

Plates A, B, C and D are assumed to contribute to the longitudinal shear capacity. Plates A, B, C, G and H are assumed to contribute the transverse shear capacity. The maximum computed longitudinal shear stress is 43.4 MPa and occurs near the tower top where the plates are relatively thin because of the small longitudinal moments. The maximum computed transverse shear stress is 33.8 MPa and it also occurs at the tower top.

The highest longitudinal shear stresses occur in plate D, which is also typically thinner than plates B and C. Because plate D is designed to be fully or almost fully effective for carrying the applied axial stresses, neither overall shear buckling of the panel nor buckling of the widest sub-panel occur, and so no reduction for shear buckling is required. Therefore, the shear capacity of the plate is equal to the design shear yield stress of 241 MPa, resulting in a shear utilization ratio of 0.18. In accordance with EN 1993-1-5 Section 7.1 (1), the interaction between longitudinal compressive stresses and transverse shear stresses does not have to be considered because the shear utilization ratio is less than 0.5.

The highest transverse shear stresses occur in plate G, which being located closest to the cross section centroid and with a minimum thickness of only 30 mm, is typically the least efficient plate in the cross section. EN 1993-1-5 Annex A3 indicates that the plate shear capacity is governed by overall buckling of the entire panel, for which a reduction factor of 0.72 applies. The shear capacity is therefore 0.72 x 241 = 174 MPa. Despite the panel shear buckling being relevant, the shear utilization ratio is still only 0.19 and the interaction between axial and shear effects does not require consideration. Because shear buckling is relevant for plate G, it is further confirmed in accordance with EN 1993-1-5 Section 9.3.3 (3) that the transverse stiffeners on plate G do not have to be designed for any axial force due to tension field action in the panel.

Given the magnitude of the shear utilization ratios noted above, shear forces generally do not influence the design of the tower leg longitudinal steel. Therefore, more detailed shear resistance calculations are generally unnecessary. However, at cross beam locations locally high shear stresses do influence the design of the longitudinal elements as described in Section 7.3.3.2.

CONSTRUCTION JOINT FIELD SPLICES

The 21 shop fabricated tower leg segments are connected by field splicing at transverse construction joints. The field splices are made using a combination of full penetration welds on the skin plates and bolted splices on the longitudinal stiffeners and internal plates (longitudinal and transverse webs). Elevations of typical bolted splices in a longitudinal stiffener and internal plate are shown in Figure 7-27 and Figure 7-28, respectively. At each transverse joint, the bolted splices must share load with the welded skin plates, and consequently these joints are classified as hybrid connections as per EN 1993-1-8 Section 3.9.3. This requires the bolted splices to be slip critical at the ultimate limit state.

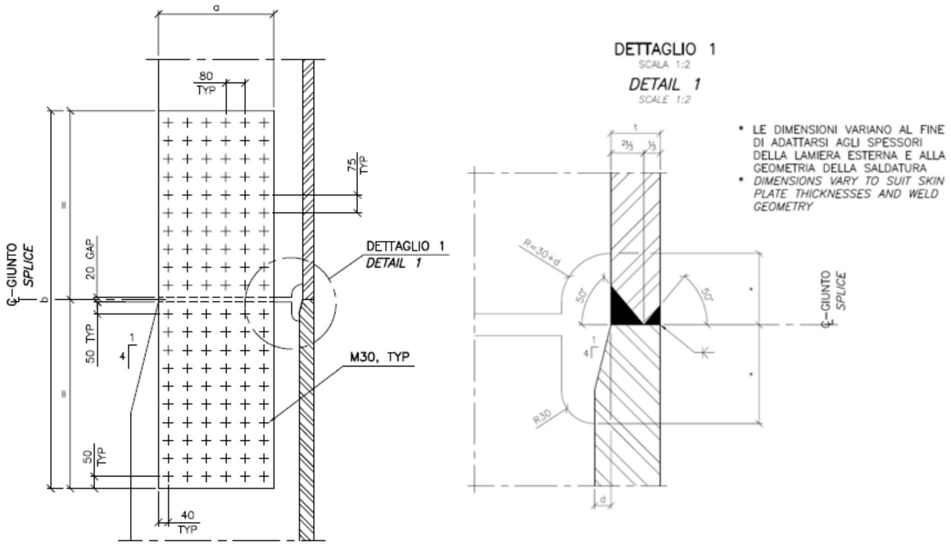

Figure 7-27: Skin plate longitudinal stiffener splice detail.

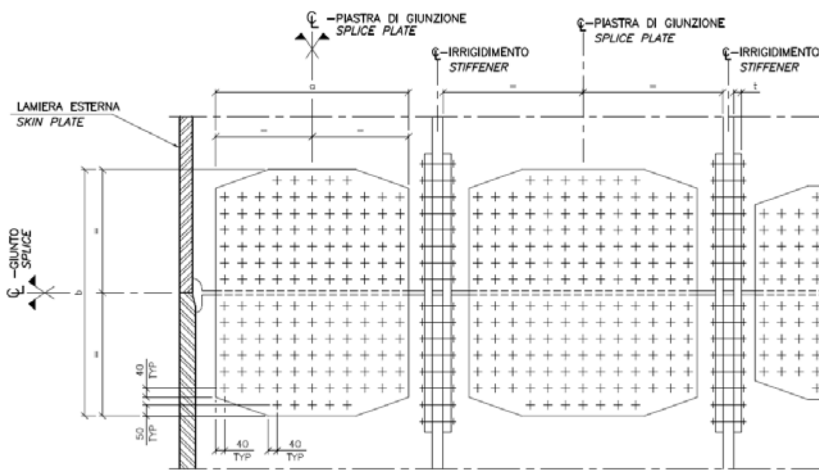

Figure 7-28: Typical internal plate splice detail.

To achieve their required capacity, the bolted splices require a preparation on all friction surfaces, including fill plates, to be such that a minimum slip factor (μ) of 0.45 is achieved. In addition, the final tightening of all bolts in the splice shall be carried out only after the skin plate splice welds are completed, as required by EN 1993-1-8 Section 3.9.3 for hybrid connections. All bolts are to be M30 Grade 10.9 preloaded bolts to the specifications of EN ISO 898.

The ULS seismic demands generally govern the design of the vertical tower leg steel, with most utilization ratios being very close to 1.0 in compression. Therefore, for a typical longitudinal stiffener splice, the number of bolts was chosen to develop the yield capacity of the stiffener being spliced. The bolt layout was designed to provide a simple and compact arrangement, while satisfying the spacing requirements of EN 1993-1-8 Section 3.5. Splice plates were sized to provide the axial compression capacity, axial stiffness and bending stiffness of the governing stiffener across the splice. Local buckling of the splice plates was checked at the longest spacing between bolts, and the tension capacity of the net section was checked against the maximum applied tension demand present in the section being spliced.

Bolted splices on the tower leg internal plates were designed to develop the yield capacity in compression of the internal plates being spliced, and to transfer the global shear demands present in the internal plates across the joint. The bolt group on each side of the horizontal centerline of a splice was thus proportioned to resist the combination of demands from both axial load and shear. This included the additional bolt demands required to resist the induced rotation of the splice plates generated by transfer of shear demand across the splice region. Similar to the longitudinal stiffener splices, bolt layout was chosen to provide a simple and compact arrangement in accordance with EN 1993-1-8 2005, Section 3.5. The splice plates were sized to resist the von Mises stresses from combined axial compression and shear demands. Local buckling of the splice plates between bolts was checked at the largest bolt spacing, and the tension capacity of the net section was checked against the maximum tension demand present in the internal plate section being spliced.

In general, splice plate widths and bolt placements have been checked to ensure adequate clearances for torque wrench access. The splice plate lengths provide adequate clearance to the transverse diaphragms located 1000 mm from the upper end of each tower leg segment, with the following exceptions: Sicilia tower leg plate E at joints between segments 1-2, 2-3 and 3-4, Calabria tower leg for plate E, at the joint between segments 1-2. These long splice plates are required due to the relatively thick plates being spliced. At these construction joints, the distance from the joint to the adjacent transverse type 1 diaphragm is increased to provide the required clearance.

The transverse splice at the tower top between segment 21 and the main cable saddle was designed similarly to the other transverse splices; however, because skin plates B and C terminate at the top of cross beam 3, plates E, F and H become skin plates above this point, and so only plate G is considered to be an internal plate. Plates E, F and H at this joint are connected with full penetration welds in the same manner as plates A and D. The longitudinal stiffener splice plates are inclined to match the angle of the saddle segment skin plates, and the bolts have an inclined and slightly more dense arrangement to accommodate the tighter clearances while still satisfying EN 1993-1-8 Section 3.5.

7.3.3.2 Transverse Elements

The tower leg transverse elements comprise the transverse stiffeners and diaphragm types 1, 2, 3 and 4. The typical transverse stiffener elements are spaced at 3 m to 3.5 m in each tower leg segment. Type 1 diaphragms are typically located 1 m below the transverse field splice in each tower leg segment. Type 2 diaphragms are located at the connections of the cross beam top and bottom flanges to the tower legs; resulting in five per tower leg. Type 3 diaphragms are located at the connection of the cross beam 3 top flange to the tower leg. Type 4 diaphragms are located at tuned mass dampers elevations.

TRANSVERSE STIFFENERS AND TYPE 1 DIAPHRAGMS

The tender design transverse stiffener arrangement was changed in this phase to reduce fabrication costs by allowing for a simplified cross-section assembly procedure and reducing the number of transverse stiffening elements through which the longitudinal stiffeners pass. Plate A was thickened so that regular transverse stiffeners are not required and the transverse stiffeners to plates B, C, E, F and H were replaced by a triangular diaphragm plate, which is more efficient, and requires cut-outs for the longitudinal stiffeners only along plates B and C.

The revised typical transverse stiffener section comprises the following structural elements:

- The 4 m long T-shaped stiffener on plate G;
- The 8 m long T-shaped stiffener on plate D; and
- The plate diaphragms in the triangular cells bounded by plates B, C, E, F and H.

The arrangement of the type 1 diaphragms is similar to the transverse stiffeners, but is distinguished by a heavier T-shaped stiffener on plate D and an additional 4 m long T-shaped stiffener on plate A. It was found in this phase that the typical full plate diaphragm proposed in the tender design is not required, and that sufficient robustness and rigidity can be provided with the noted modifications to the typical transverse stiffeners. The arrangement of the transverse stiffener and type 1 diaphragm elements is shown in Figure 7-29.

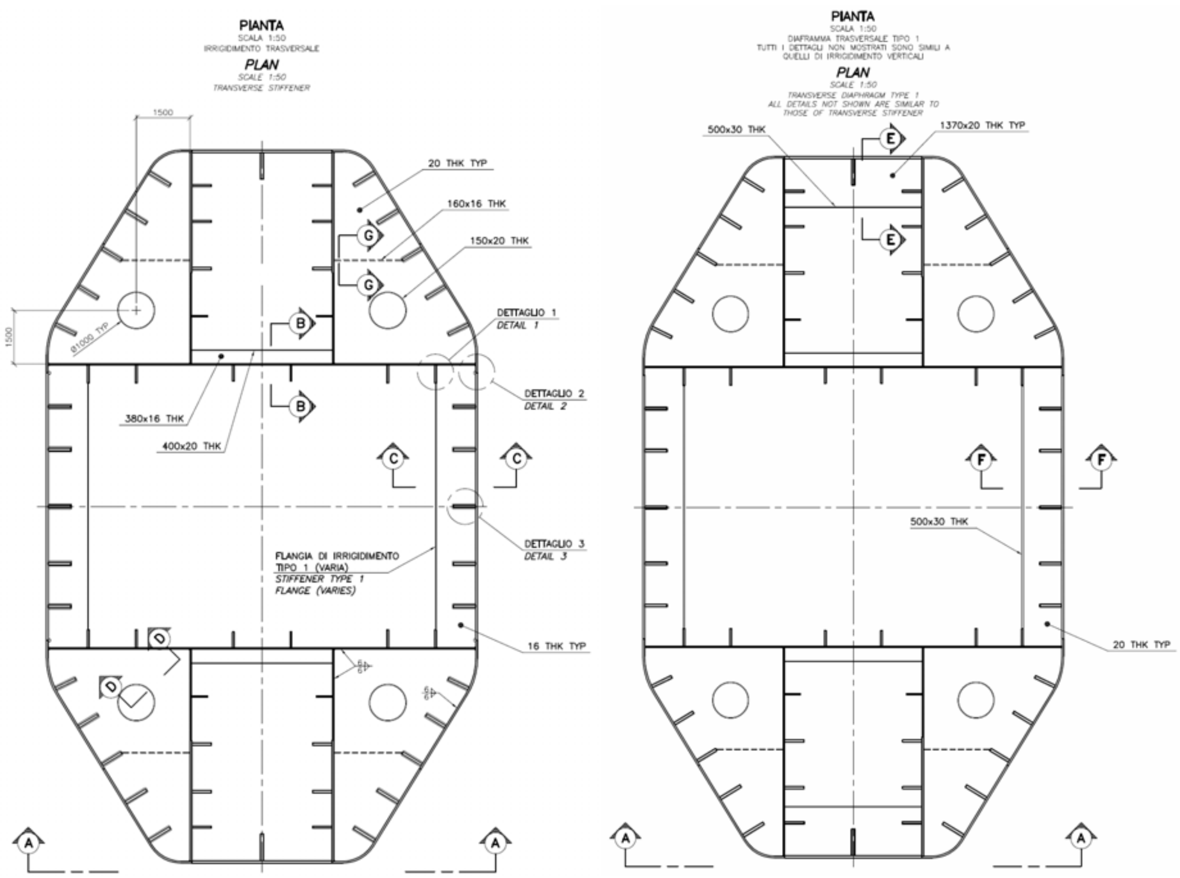

Figure 7-29: Tower leg transverse stiffeners and Type 1 diaphragms.

In the general concept submission, the plate D transverse stiffener flange was braced to the longitudinal stiffeners to prevent torsional buckling and all longitudinal stiffeners were connected to the transverse stiffening elements by tab plates. The tab plates were provided to:

- To transfer deviation forces ("kick" forces from buckling of the adjacent compressed panels) from the longitudinal stiffener to the transverse stiffener; and
- To improve the lateral torsional stability of the transverse stiffener flange;

Both of these connections between the transverse and longitudinal stiffeners are fabrication intensive and therefore undesirable. The removal of similar connections between the longitudinal and transverse stiffening systems was proven acceptable on Akashi Kaikyo Bridge towers using both experimental and analytical investigations. Therefore, to reduce fabrications costs, additional detailed finite element analysis of the interface between the transverse and longitudinal stiffeners has been completed to:

1 Determine the required transverse stiffener flange size to prevent lateral torsional buckling; and

2 Determine the required weld size for connecting the transverse stiffener web to the skin plate.

The same shell element model was used to investigate the removal of both connections as each has an effect on the other. The model comprised the following:

- a transverse stiffener spanning 8.0 metres between plates H with cut-outs to allow the longitudinal stiffeners to pass;
- the skin-plate extending 3.5 metres above and below the transverse stiffener;
- the longitudinal stiffeners extending 3.5 metres above and below;
- the adjoining plate H extending 3.5 metres above and below (the presence of the longitudinal stiffeners on plate H is ignored because they cannot be relied upon to provide stability as the loading on the leg approaches the ultimate limit state and they are fully stressed from longitudinal loads); and
- a row of elements of extremely low flexural stiffness along the transverse stiffener web at the interface with the skin plate; required to respect the requirement of EN 1993-1-5 Section 9.2.1(9) “not considering rotational restraint from the plate”.

The model was loaded with the second-order loading calculated in accordance with EN 1993-1-5 Section 9.2.1, applied laterally to the outside face of the skin plate at the transverse stiffener elevation. Parametric analysis was completed to assess the effect of the plate D area on the required stiffener flange size and the weld size.

The finite element analysis showed that double sided 5 mm fillet welds connecting the transverse stiffener web to the skin plate allow for removal of the tab plate connections for all panel areas, provided the panels are straight (i.e., there no angle change along the panel length) and subjected only to the restraint forces considered (i.e., no externally applied out-of-plane loads). Transverse stiffener web shear and direct stress demands are shown for the out-of-plane loading from an 85 mm thick plate D in Figure 7-30 and Figure 7-31, respectively. This thickness is larger than any actual thickness used for plate D in either tower and therefore results in a conservative estimate of the maximum weld demands. The stress demands are reported in kN/mm. The figures show a plan view of the transverse stiffener web, with cut-outs for the passage of the longitudinal stiffeners.

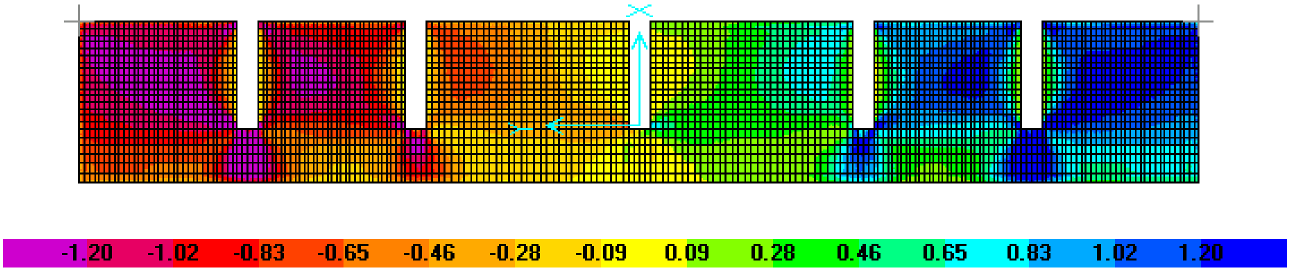

Figure 7-30: Transverse stiffener web shear stress contours.

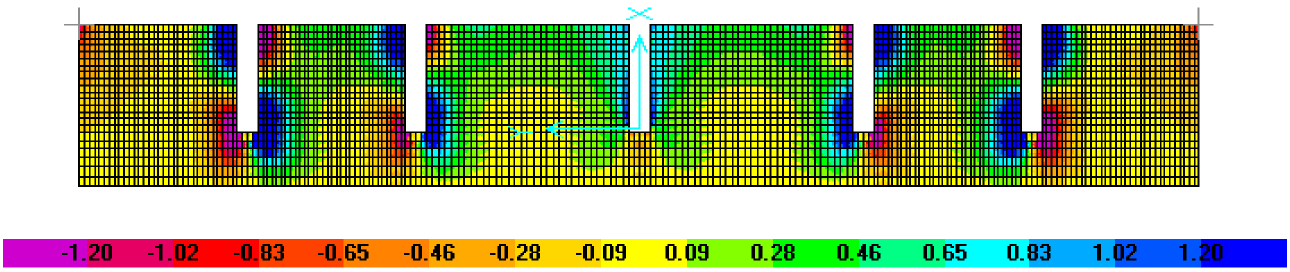

Figure 7-31: Transverse stiffener web direct stress contours.

The finite element analysis was also used to determine the elastic critical buckling stress of the transverse stiffener. The finite element analysis accounts for the variation of bending stress along the stiffener, producing greater economy than is conveniently possible with hand calculations. The analysis showed that a transverse stiffener flange size of 360x20 could be used for most tower leg segments and a 420x25 flange could be used for tower leg segments 1, 8 and 9. The first buckling mode for a transverse stiffener with a 420x25 flange is shown in Figure 7-32. The out-of-plane loading (perpendicular to plate D) on the transverse stiffener is that caused by an 85 mm thick plate D with 700x70 mm longitudinal stiffeners, which as described above, results in a conservative estimate of the stiffener demands.

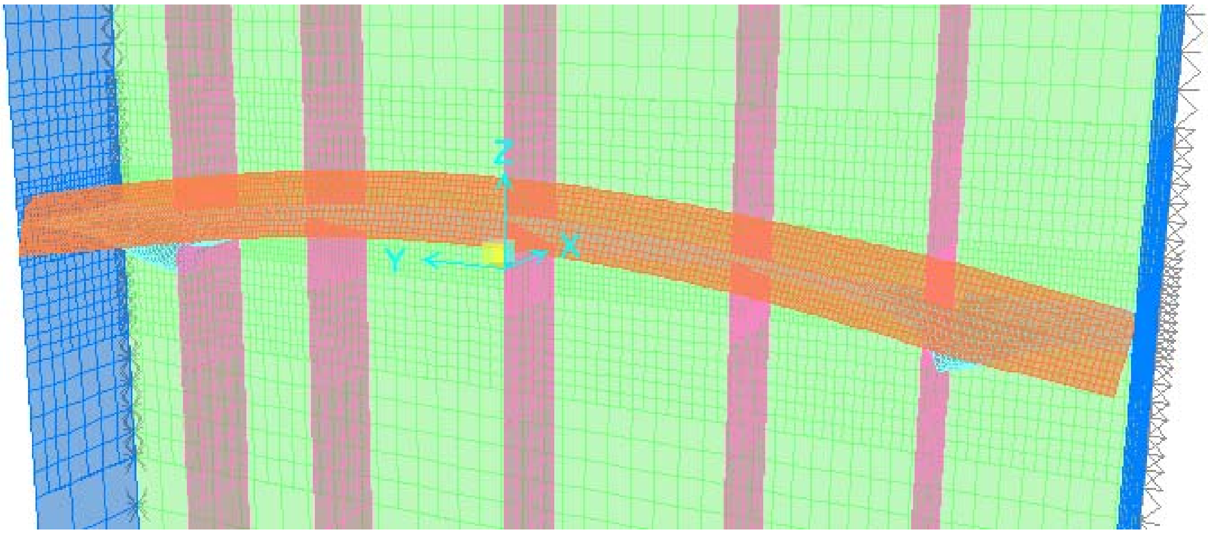

Figure 7-32: Buckled shape of transverse stiffener with 420x25 flange.

The plate D transverse stiffener web depth was selected to meet the requirements of EN 1993-1-5 Section 9.2.4 (4) and to provide the required shear capacity. The 16 mm thick web is adequate for all plate D areas.

The plate G transverse stiffener was proportioned initially using the standard Eurocode provisions as described in CG.10.00-P-RG-D-P-SV-T4-00-00-00-00-01 "General Design Principles." Because of the short stiffener span and the relatively small plate G thicknesses, this sizing indicated plate thicknesses of 8 mm to 10 mm would be adequate for the webs and flanges. Such small thicknesses are not considered appropriate for a structural component on a structure of this size and so the web thickness was increased to 16 mm and the flange thickness was increase to 20 mm to improve the less quantifiable robustness and rigidity of the cross section.

The triangular plate diaphragms were proportioned using EN 1993-1-5 Section 10 and Annex B.1. A detailed finite element analysis was completed to determine the elastic buckling and ultimate factors. The finite element analysis model comprised:

- a flat plate diaphragm with cut-outs to allow the longitudinal stiffeners to pass through and a circular hole;
- the skin-plate extending 3.5 metres above and below the diaphragm;
- the longitudinal stiffeners extending 3.5 metres above and below; and

- the adjoining plates B, C, E, F and H extending 3.5 metres above and below.

The loading for both the buckling and ultimate analyses was the second-order in-plane loading calculated from EN 1993-1-5 Section 9.2.1, but assuming no growth of imperfection because of the stiffness of the diaphragm.

The critical buckling mode for the plate diaphragm is shown in Figure 7-33 (plates E, F and H are not shown for clarity). The critical buckling mode is caused by plates B, C, E, F and H all buckling inwards on the diaphragm.

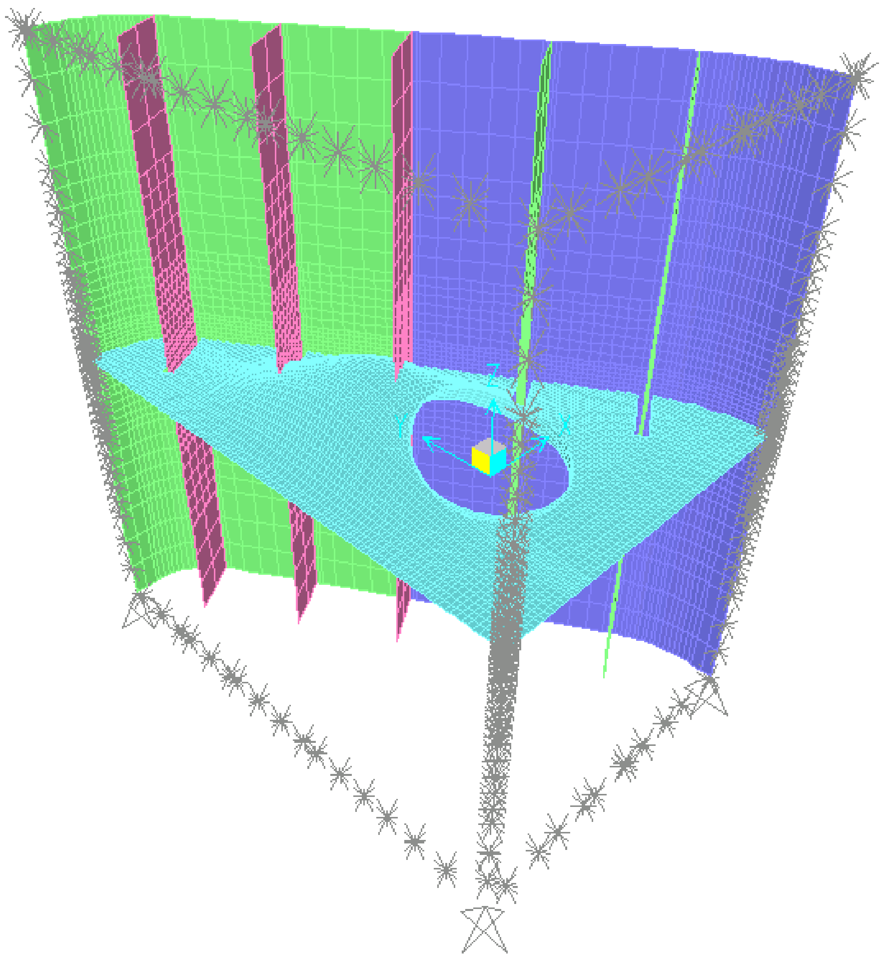

Figure 7-33: Triangular plate diaphragm critical buckling mode.

The above calculation gives a utilization ratio of 0.97 for a plate thickness of 20 mm considering the heaviest possible applied in-plane loading. The effects of potential vertical loading on the diaphragm are accounted for by adding the ring stiffener around the hole and the transverse 160x16 stiffener under the diaphragm.

More detailed descriptions of the modelling and analysis can be found CG.10.00-P-RG-D-P-SV-T4-00-00-00-00-01 “General Design Principles” and in CG.10.00-P-CL-D-P-SV-T4-00-00-00-00-01 “Design Report - Tower Legs incl. Joints and Splices.”

Cross Beam to Tower Leg Connections - Type 2 and 3 Diaphragms

Type 2 diaphragms are located at the elevations where the cross beam 1 and 2 top and bottom flanges, and the cross beam 3 bottom flange only, meet the tower leg. The type 2 diaphragms distribute the cross beam flange forces through the tower leg cross section and into the tower leg longitudinal plates and stiffeners. Type 3 diaphragms are located at the tower top where the cross beam 3 top flange meets the tower leg and in addition to distributing the top flange force to the tower leg, must also resist the outwards thrusts being applied to the diaphragm by the inclined main cable saddle plates. Type 2 diaphragms comprise a 40 mm thick plate in the central tower leg cell, with a 6 m x 2.2 m cut-out for the access staircase, and 60 mm thick plates in the triangular cells, with 1 m diameter cut-outs for the access ladders, as shown in Figure 7-34. The diaphragm plate in the central cell is stiffened parallel to and transverse to the bridge axis. The diaphragm plates in the triangular cells are unstiffened. The type 3 diaphragms comprise a 70 mm thick plate in the central cell, with small 0.6 m x 0.8 m cut-outs for accessing the cable saddle, and thin 20 mm thick plates in the triangular cells, as shown in Figure 7-35. The diaphragm plate in the central cell is stiffened similarly to the type 2 diaphragm. The type 3 diaphragm plates in the triangular cells also form the top surface of the tower leg, as the skin plates B and C are not part of the main cable saddle. As such these plates are inclined at 5% to allow for drainage.

The proportioning of the type 2 and 3 diaphragms and the additional stiffening required in the tower legs at the cross beam connections is described in this section.

The forces due to bending in the cross beam top and bottom flanges flow directly into the type 2 diaphragms at the top and bottom of the cross-beam. The forces due to bending in the cross beam webs flow directly into the transverse webs, plates H (inner), G and H (outer). Transverse equilibrium in the tower legs is maintained by shears, primarily a large shear between the cross beam top and bottom flanges, but also by the smaller shears above and below the cross beam. The large shear within the cross beam depth is shared between two systems of plates, the transverse webs directly in line with the cross beam webs and skin plates A, B and C on either side of the cross beam. The shear force in plates A, B and C is transmitted mostly by the type 2 diaphragms but some forces are transferred by the diaphragms/transverse stiffeners above and below the cross beam.

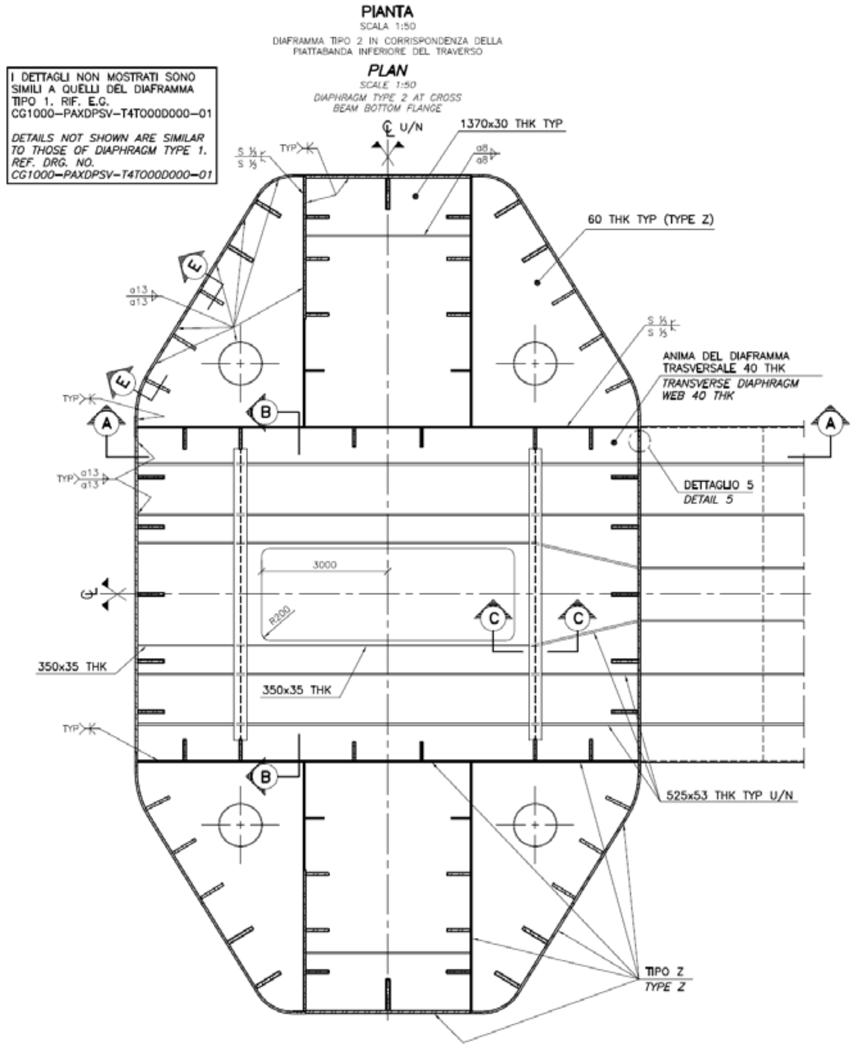

Figure 7-34: Type 2 diaphragm plan view.

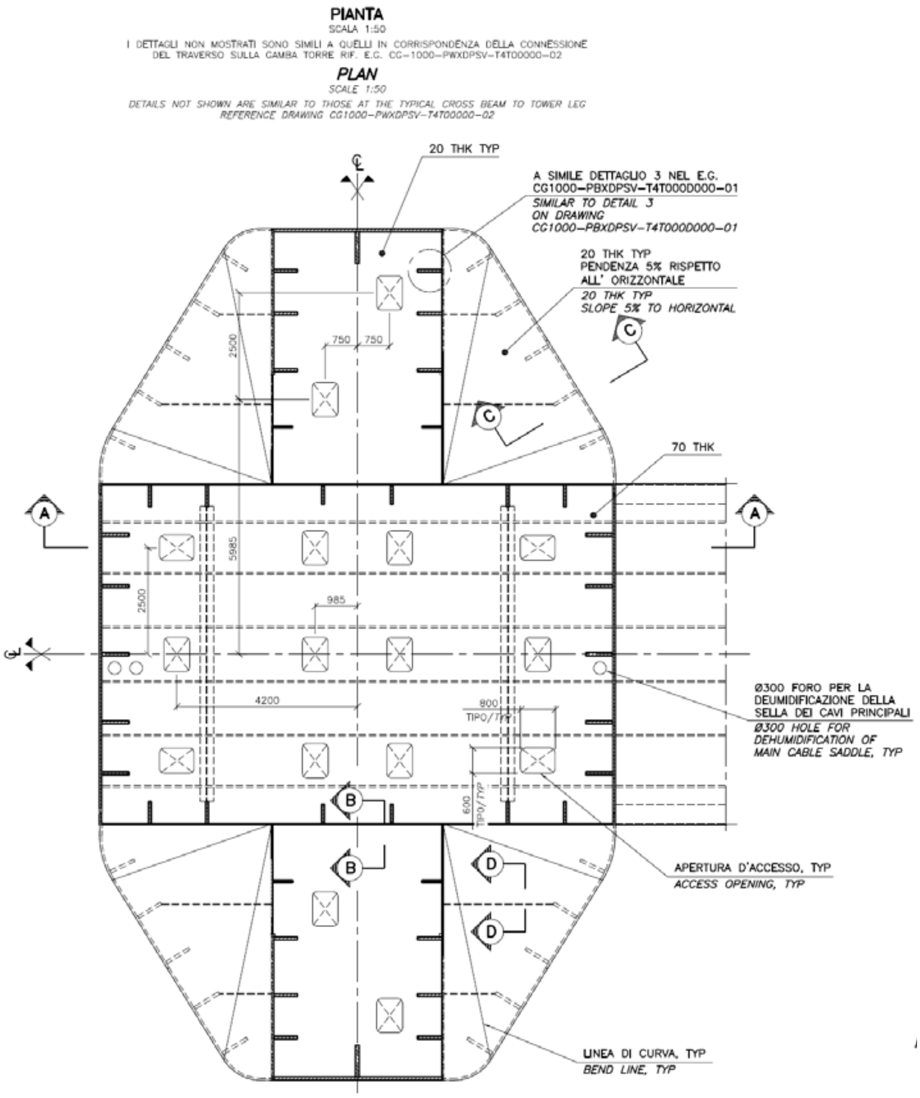

Figure 7-35: Type 3 diaphragm plan view.

The tower leg transverse webs resist:

1 Longitudinal forces in the legs;

2 Shear from the cross beam end moments; and

3 Transverse forces form the bending stresses in the cross beam webs.

This combination of direct forces and shears gives very high stress and buckling demands. Therefore, the cross beam web stiffeners are continued into the legs along plate H. In the middle and outer thirds of the tower leg transverse webs, plates G and H (outer), the transverse stresses are reduced, and so the stiffeners are terminated for maximum economy of fabrication. They are terminated after crossing plate F, so that they have adequate lateral restraint at their ends. In the middle and outer thirds of the transverse webs, the longitudinal stiffeners alone provide stability for the combination of direct forces and shears.

The cross beam connections are proportioned using a combination of both classical methods using EN 1993-1-1 and EN 1993-1-5, and the output from the semi-local shell element model that was incorporated in the global IBDAS model (reference CG.10.00-P-RG-D-P-SV-00-00-00-00-00-03 “Semi-local IBDAS Model, Towers”). The model output included direct stresses, shear stresses and von Mises stresses. The calculations were completed for the most severely loaded connection, which is at cross beam 2. The design of the cross beam 2 connection was used to proportion the other cross beam connections with appropriate modifications for each cross beam location.

Plate H (inner) Design Verifications

Plate H is stiffened longitudinally by the main tower leg stiffeners and transversely by the continuation of the cross beam web stiffeners. The plate is thicker than would be required for the longitudinal forces alone because of the higher coexistent shear and transverse stresses. The plate is checked for both yield (using the von Mises criterion in accordance with EN 1993-1-1 Section 6.2.1) for coexistent shear, longitudinal compression and transverse tension, and for buckling (to EN 1993-1-5 Section 10) for coexistent shear and direct stresses.

Plate G Design Verifications

Plate G is stiffened only longitudinally (vertically), so buckling resistance of the plate between the stiffeners is verified for curvature in one direction (similar to strut buckling) using EN 1993-1-5 Section 4.4 and for curvature in two directions (alternate dishing) using EN 1993-1-5 Section 10. The longitudinal stiffener stability is verified using EN 1993-1-5 Section 9.2.1, accounting for (i) the action as “transverse stiffeners” for the horizontal direct stresses in plate G (from the cross beam web flexural stresses) and (ii) the vertical compression from the tower leg vertical forces. In the calculation of the stresses in these stiffeners, the initial imperfection applied to the axial compression was taken as b/300 (which is more onerous than the requirement of EN 1993-1-5 Section 9.2.1 of s/300) because the loading is dominated by axial compression and the stability equation relies on elastic stiffness.

Plate H (outer) Design Verifications

The transverse stresses in plate H on the tower leg side opposite the cross beam are much less than in plate G. The verifications for outer plate H are similar to the verifications for plate G, except that the initial imperfection applied to the axial compression was taken as the mean of b/300 and the imperfection corresponding to the buckling resistance of EN 1993-1-5 Section 4.5.4 based on first-yield (which is still more onerous than the requirement of EN 1993-1-5 Section 9.2.1 of s/300). This was done in recognition that the transverse stresses are lower in outer plate H and that as the transverse stresses approach zero, the resistance should agree with EN 1993-1-5 Section 4.5.4.

Type 2 Diaphragm Verifications

Type 2 diaphragms comprise three zones, the two cantilever zones in the triangular cells outside the inner transverse webs and the central zone in the cell between the transverse webs. The diaphragm resists in-plane shear and in-plane bending, both overall bending from the shears in plates C/B/A/B/C and local bending from the shears in plates C/B/A/B/C being carried by Vierendeel action across the elevator opening. Generally, the tower leg skin plate assists in resisting these bending moments, relieving the bending stresses that would otherwise be generated in the diaphragm plate. However, at the curved portions of the plate C, close to plates D and H, the skin plate effective stiffness is reduced by the curvature, so there are high bending stresses on the same section as the maximum shear. The diaphragm plate thickness in the triangular cells is determined by the stresses at this section.

The central cell diaphragm plate is verified for resistance to the force from the cross beam flange. The capacity accounts for a reduced effectiveness due to shear lag across the 8 m cell width. The cross beam flange longitudinal stiffeners are continued onto the central diaphragm plate so that the flange axial forces can be spread through the plate to the vertical tower leg plates. Two T-shaped “transverse” stiffeners parallel to the bridge axis span between the transverse web to stabilize the diaphragm plate and allow the horizontal direct forces to be framed around the staircase opening.

Type 3 Diaphragm Verifications

Type 3 diaphragms are verified using similar methods as described for the type 2 diaphragms; however, additional consideration is given to the transverse thrusts being applied by the inclined main cable saddle plates, which add to the tension from the cross-beam top flange. This results in a thicker central cell plate than in the type 2 diaphragm. The elevator and ladders do not extend through this level, and so an additional diaphragm plate is added in the cell bounded by plates A, E, F and G and there is no opening in the triangular cell diaphragm plates. This eliminates the local moments caused by the Vierendeel action around the large openings, and allows thinner plates than required for the type 2 diaphragm.

TYPE 4 DIAPHRAGMS

Type 4 diaphragms are provided at tuned mass damper elevations and serve the dual purposes of providing a transverse stiffening element for the tower leg plates and providing a support for the tuned mass dampers. Type 4 diaphragms are similar to the type 1 diaphragm, except that the plate D transverse stiffener is deepened to support the tuned mass damper, as shown in Figure 7-36. The deepened plate D transverse stiffener also comprises two T-beams spanning between the plates H to transfer the tuned mass damper weight and the horizontal loads generated when it is active into the tower structure.

TUNED MASS DAMPERS

Eight tuned mass dampers are provided in each tower leg of both towers, centred approximately at the cross beam 2 elevation. Each damper unit has a mass of 35 tonnes, a frequency of 0.466 Hz and 11% modal damping. The tuned mass dampers comprise a steel mass suspended from a steel support frame by four pendulums. The steel mass is also connected to the support frame by two diagonal springs and two horizontal dampers, as shown in Figure 7-37.

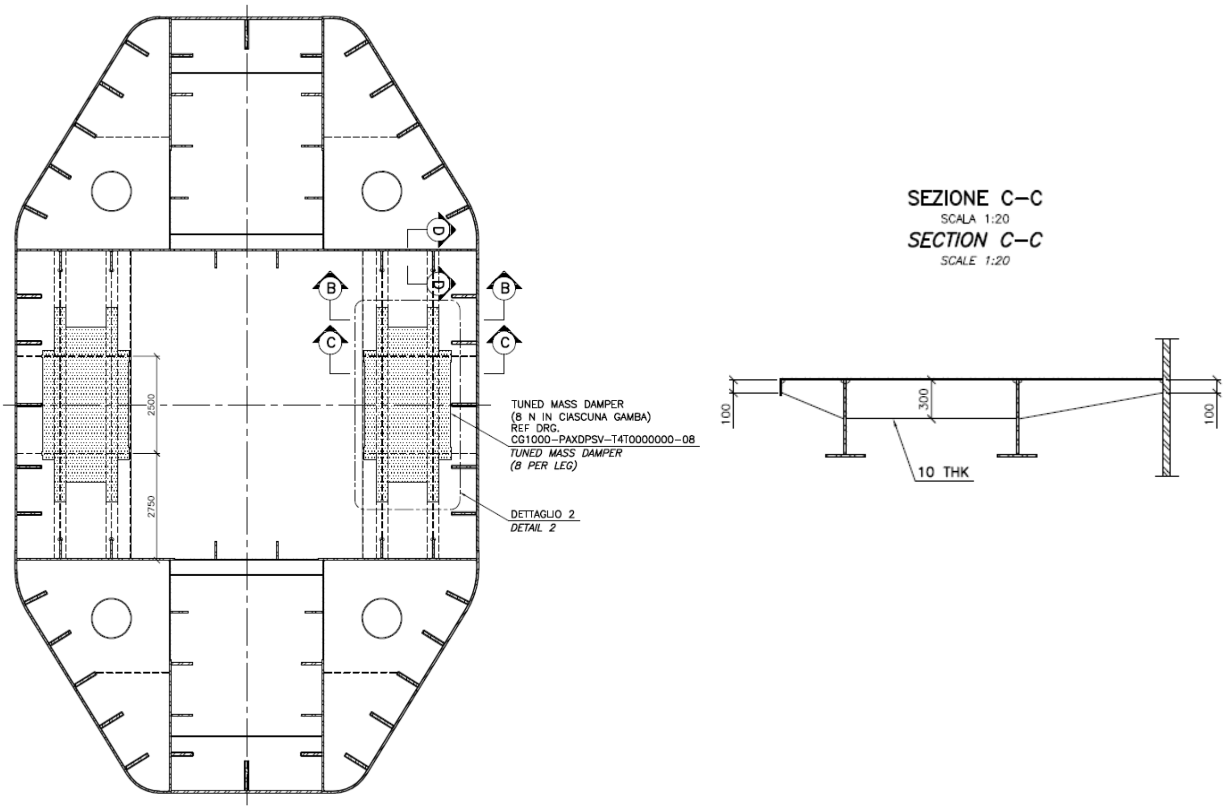

Figure 7-36: Type 4 diaphragm plan view and section through plate D transverse stiffener.

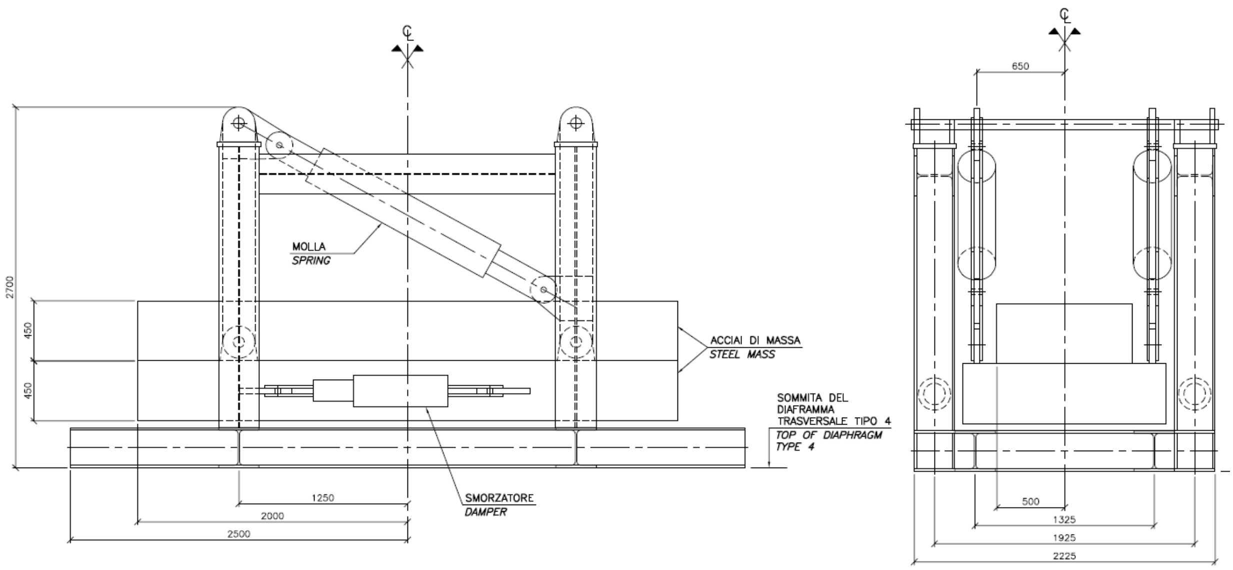

Figure 7-37: Tuned mass damper elevation and end views.

DECK BUFFER CONNECTIONS

The suspended deck is restrained longitudinally and transversally by hydraulic buffers at both towers. Four longitudinal buffers are pin-connected to both tower legs and two transverse buffers are pin-connected to only the north-east tower leg. The buffers have a bi-linear load deformation response and act to control deformations and absorb energy under seismic loading. The buffer connections to the tower legs comprise thick pin plates outside of the tower leg cross section and load transfer box beams spanning between the longitudinal webs for the longitudinal buffers and between transverse webs for the transverse buffers. The longitudinal buffer transfer beam width (perpendicular to load) is 3 m and the depth (parallel to load), which is limited by the clearance envelope required for the elevator, is 1,500 mm. The transverse buffer transfer beam is 2,000 mm deep and 1,550 mm wide. Plan views and cross sections through the buffer connections are shown in Figure 7-38.

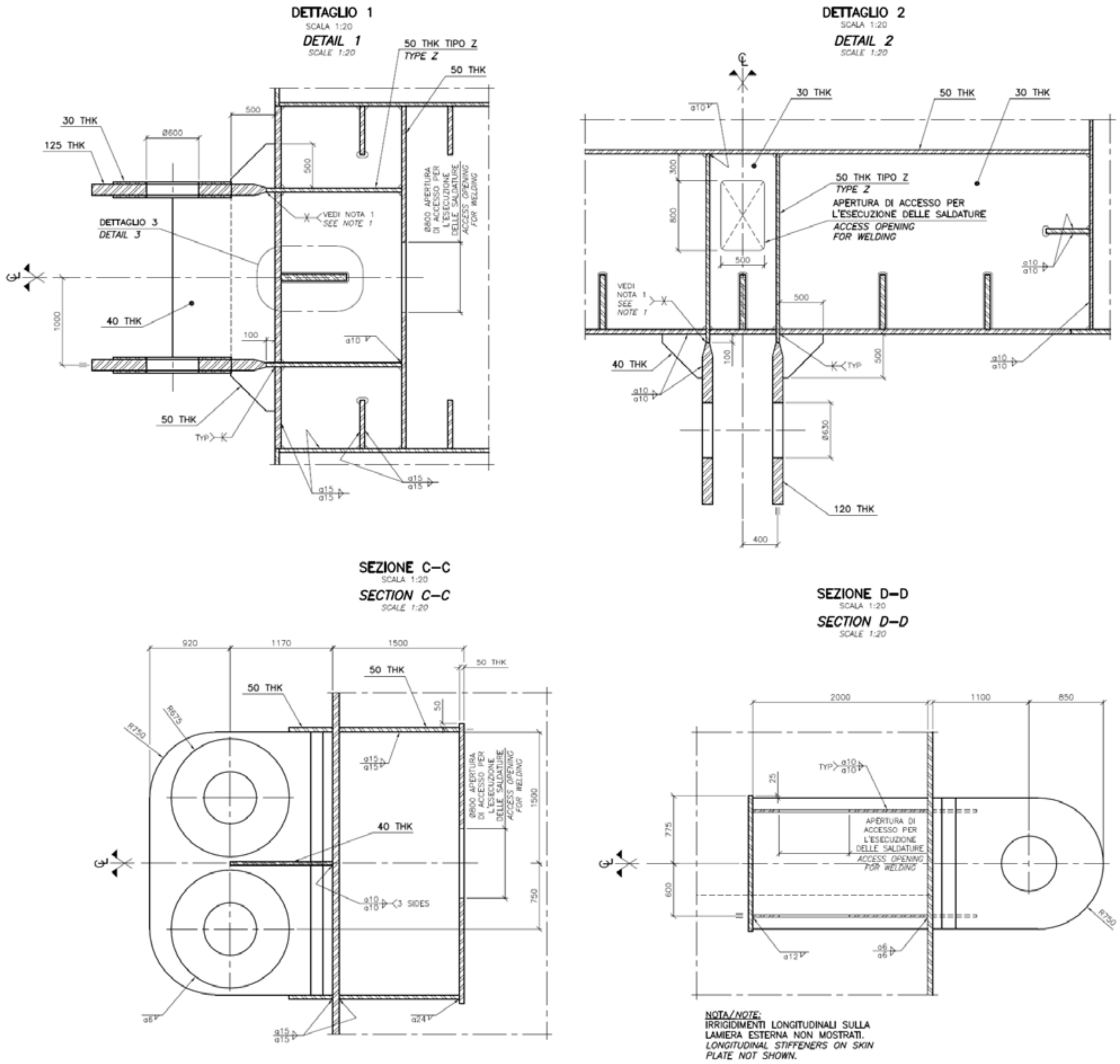

Figure 7-38: Deck buffer connection details.

The buffer connections were proportioned for the 10 MN maximum load that each buffer is designed to carry, rather than the loads resulting from the analysis. This results in maximum total design loads of 40 MN and 20 MN on the longitudinal and transverse buffer connections, respectively. Concurrent effects of the applied axial loads and deck displacement, which cause vertical or horizontal shears across the connection face, were considered by assuming the maximum axial loads could be applied at a 5% slope in the vertical plane or 2% slope in the horizontal plane, relative to the tower leg face. In a subsequent design phase the actual concurrent deck displacements and buffer forces should be considered to refine the design.

7.3.3.3 Tower Leg Segment Detailed Finite Element Analysis

APPROACH

As indicated in Section 6.2.4, a finite element model was made of a complete leg segment to confirm the appropriateness of the resistances calculated using EN 1993-1-5 Section 4, which is the basis for the tower leg design verifications. The model considered the effects of non-linear geometry, non-linear material properties, residual stresses and initial geometric imperfections, subtle yet important factors in the tower leg behaviour that are considered only implicitly in the simplified design provisions of EN 1993-1-5 Section 4.

The Sicilia tower leg segment 6 was modelled because it has thinner plates relative to the imposed axial load than other segments, and so might show greater sensitivity to buckling effects. The modelled plate thicknesses and longitudinal stiffener dimensions differ slightly from those listed in Table 7-2 and Table 7-4, respectively, because the analysis was completed for a previous iteration of the tower leg design. The analysis model differed from the final tower configuration as shown in Table 7-6. In all cases the analysis model comprised more slender elements than are present in the final configuration and so final configuration will be no more sensitive to buckling effects.

Parameter	Modelled	Current
Plate A thickness	85 mm	95 mm
Plate B thickness	70 mm	75 mm
Plate G longitudinal stiffener	450 x 45 mm	475 x 48 mm

Table 7-6: Difference between analysis model and final tower confirguration.

The model is 18 metres high and comprises six 3 m spans of longitudinal stiffeners. Both the plates and the longitudinal stiffeners are modelled with shell elements. Bar elements are used to model the horizontal stiffeners and to represent the restraint provided by triangular diaphragms. Bar elements simplify the model and are sufficient. Moments and forces are applied to the top and bottom of the model through a “spider” of rigid elements. Plan and isometric views of the model are shown in Figure 7-39.

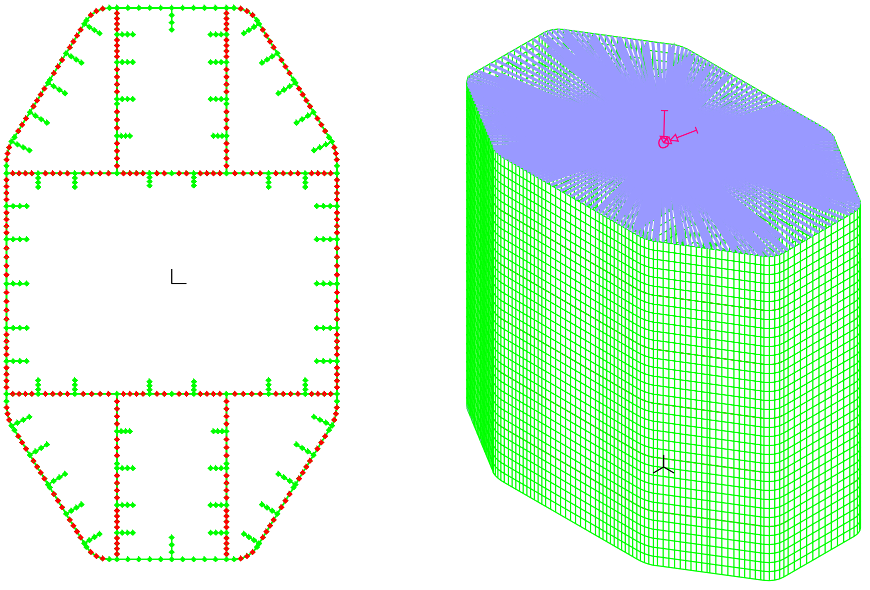

Figure 7-39: Plan and isometric views of tower leg segment finite element model.

It was originally planned to include the effects of imperfections by modelling the plates and stiffeners with the equivalent imperfections specified in EN 1993-1-5 Annex C, using the geometrical form of the elastic buckling modes of the panels as the basis. Several issues were encountered with this approach:

- The 1:400 "equivalent imperfection" specified for longitudinal stiffeners in EN 1993-1-5 Table C.2 is no greater than the manufacturing tolerance allowed in EN 1090-2 Table D.1.6. This means that if the tower leg panels were manufactured to the allowable tolerances, the analysis would have been made with no allowance for residual stresses and therefore might be unconservative;
- The "equivalent imperfections" specified for a plate between stiffeners in Table C.2 will cause a reduction in the resistance of the plate, whereas EN 1993-1-5 Section 4 gives no reduction for the plate slenderness for the width-to-thickness ratios used in the majority of panels in the tower legs;
- It is very difficult to find the most onerous arrangement of "equivalent imperfections" for stiffener twist because there are so many different combinations possible; and

- There is no single buckling mode in the panels that gives magnitudes of out-of-plane panel deformations similar to those specified in EN 1993-1-5 Table C.2, so an alternative method of generating suitable initial imperfections was required.

It was concluded that the most realistic resistance assessment would be provided by:

- Using out-of-plane geometrical imperfections along the longitudinal stiffeners in the form that occurs when applying equal line loads along each stiffener and accepting the resulting plate between stiffener and stiffener twist imperfections as the appropriate values for those initial imperfections; and
- Account for residual stresses directly (not by equivalent imperfections) using an appropriate stress-strain curve.

The maximum geometric imperfection in each panel was taken as the allowable stiffener fabrication tolerance of 1:400 as specified in EN 1090-2 Table D.1.6. The residual stresses were incorporated by a modifying the stress-strain curve from bi-linear elastic/plastic to multi-linear, so as to represent the average stress-strain response of steel with residual stresses, and including the 0.2% proof strain that is expected with higher strength steels such as S460ML.

UNCERTAINTIES

- As with all modelling and analysis tasks, assumptions had to be made regarding some inputs because of a lack of readily available information. These uncertainties may have some effect on the specific analysis results; however, they are unlikely to alter the overall conclusions of the work. The residual stresses from the manufacture of the Grade S460ML plates used in the tower are not known and the residual stress pattern that was used is from a higher strength steel. The maximum residual compressive stress was 26% of yield. Because of the uncertainty of the residual stress pattern appropriate for the Grade S460ML plates, the additional stresses from welding and cutting were not included. During the analysis of the results, it was observed that the imperfections from EN 1993-1-1 Section 5.3.2(11) that were used in the design are larger than those derived from analysis results. This suggests that the Eurocode expects higher residual stresses and may indicate that the residual stresses used in this analysis are too small. Higher residual stresses would reduce the cross section capacity. It is recommended that the actual residual stress patterns in the S460ML plates to be used for the tower be investigated prior to a subsequent design phase, so that the effects can be more accurately considered in the analysis.

- Realistic twist imperfections in the longitudinal stiffeners were not modelled. However, for the width-to-thickness ratios of the stiffeners and plate thicknesses to which they are welded, realistic twist angles are unlikely to significantly affect the capacity.

RESULTS

The most dramatic result of the analysis is the reduction of the section stiffness, and in particular the rotational stiffness, as the load increases. Because the leg is a tall compression member, the member stiffness has significant influence on the structure's capacity. Therefore, the segment stiffness must be considered together with the capacity to obtain a reliable assessment of the overall effect on the tower capacity.

The highest utilization ratio and the greatest stiffness loss occur for the minimum linear combination L002 seismic load combination. The load deformation response of the model for the governing load combination is shown in Figure 7-40, in which the fraction of the specified load is plotted on the vertical axis and the fraction of the elastic strain (shortening and rotation) under the specified loads is plotted on the horizontal axis. The load deformation response up to failure for axial forces (N), longitudinal moments (My) and transverse moments (Mz) are represented by the blue, pink and green lines, respectively. The specified loads at the top of the segment, those corresponding to load factors of 1.0, considered in this analysis are N = 2119 MN compression, My = 4382 MNm and Mz = 404 MNm. The section resistance should be at least γ_{M1} (partial factor considering buckling) times the demand to comply with the Eurocode requirements for compression members. This is confirmed by the use of γ_{M1} in EN 1993-1-1 Sections 6.3 and 5.3.2(11), and EN 1993-1-5 Section 10, which is intended for use with the output from computer models. Figure 7-40 has a horizontal line at 1.1 on the vertical axis (load factor) indicating the load factor that must be achieved. There is considerable non-linearity of response for all three force effects, as indicated by the flattening of the curves at a load factor of approximately 1.0. While part of this is due to geometric non-linearity, which is reversible, the rest is due to irreversible plasticity, which will absorb significant energy for seismic loads approaching the section capacity.

At a load factor of 1.1, the flexural secant stiffness has decreased by a factor of approximately 1.5, which increases the second-order effects and therefore increases the bending moments above the design values. At failure, the secant stiffness has decreased by a factor of 2.17 (i.e., the secant stiffness has reduced to 46% of the elastic value).

The maximum cross-sectional resistance reaches 1.197/1.1 = 1.09 times the required resistance based on the design values of forces and moments. However, at this loading the secant stiffness has dropped so much that the actual moments would be greater than the design values, and so the effective strength increase is less. The increased total moments were calculated by separating them into moments that are increased by a lower secant stiffness (buckling loads) and loads that are reduced by a lower secant stiffness (moments from restraint of the tower top by the cables). These moments were then factored to allow for the reduced secant modulus, which gave a modest increase in the total moment.

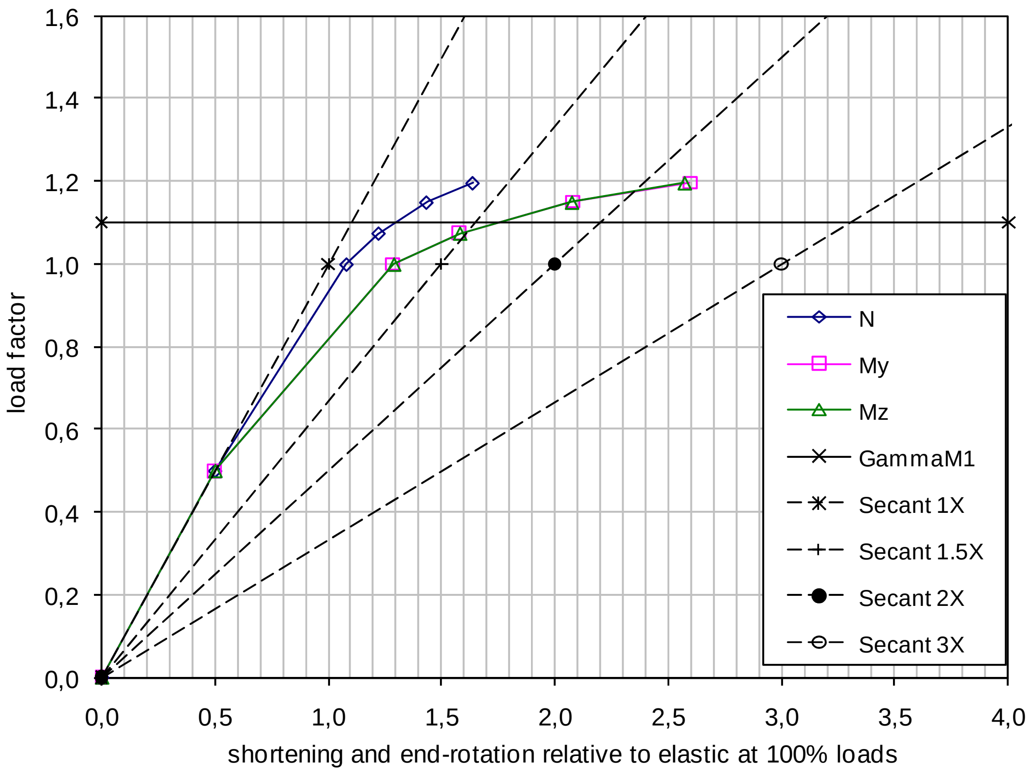

Figure 7-40: Model shortening and end rotation relative to elastic at 100% of the applied loads.

The section resistance with these greater moments was calculated using the average strain on the plate A centre-line as the governing criterion. The average strain was calculated as:

$$\frac{\left[\text{shortening} + \left(\text{end rotation} \times \text{distance from centroid to plate A}\right)\right]}{\text{height}}$$

At the maximum load sustained by the model, this strain was -3.75×10^{-3}. The strain arising from the increased moments (due to reduced secant stiffness) was calculated from the ratio of the increased moments to the moments applied to the model at each load factor. These increased strains are shown in the Figure 7-41. The maximum average strain reaches the limiting value at a load factor of about 1.17. Therefore, the maximum design resistance = 1.17/1.1 = 1.064 times the required resistance, based on the design values of forces and moments, giving a utilization ratio of 0.94.

Using EN 1993-1-5 Section 4, the legs were designed for utilization ratios between 0.98 and 1.0. Taking the median value of 0.98, the model predicts a resistance of 0.99/0.94 = 1.05 times that predicted by EN 1993-1-5 Section 4, a resistance increase of only 5%. This should be expected to be slightly lower in segments in which the bending moment is higher (for example at the base or in the region near elevation 250 m) because the bending moments at these locations require a higher proportion of the total resistance, and it is the bending moment that is increased by the reduced secant stiffness.

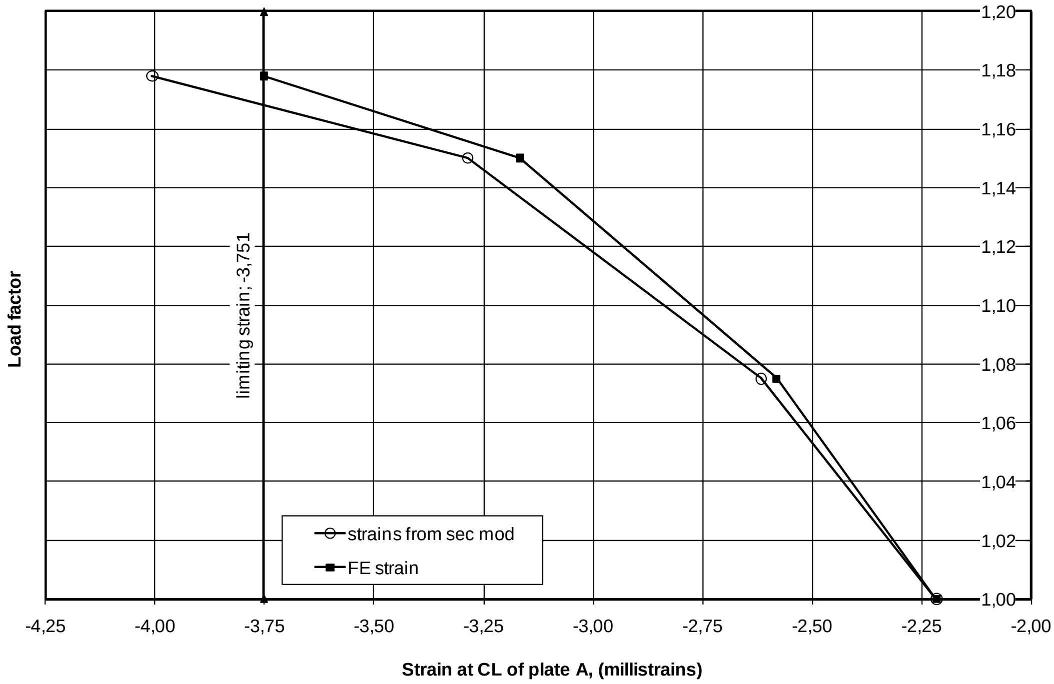

Figure 7-41: Strain the centreline of plate A as a function of load factor.

EFFECT OF RESIDUAL STRESSES

To assess the magnitude of the residual stresses, the three cases of maximum axial force with coexistent moments, and maximum moments with coexistent axial force and moment were also analyzed using bi-linear elastic/plastic material properties. These analyses were performed using a model based on a previous iteration of the tower leg design, for which the plate thicknesses were slightly different from those indicated in Table 7-2; however, the conclusions of the analyses are still valid. The differences between the final plate thicknesses and those for which these analyses were run are indicated in Table 7-7. In general, the plate thicknesses in the model used for these analyses are thinner than the final plate thicknesses. The analyses showed resistances only slightly higher than achieved considering residual stresses, with 2% greater resistance for the load combination with maximum longitudinal moment and 4% greater resistance for the load combination with maximum axial compression. However, the rotations were of the order of 50% less than in the analyses using residual stresses, indicating the marked effect that residual stresses have on stiffness.

Plate	A	B	C	D	E	F	G	H
Thickness Difference (mm)	+5	-15	+5	+20	-10	0	0	-5

Table 7-7: Difference between modelled plate thicknesses and final plate thicknesses.

CONCLUSIONS

The following conclusions are derived from the results of this analysis:

- The detailed finite element analysis of segment 6 suggests an actual capacity that is 5% greater than that calculated by EN 1993-1-5 Section 4, but this might be slightly reduced in segments with higher ratios of moment to axial force. This, in general, confirms that the selected design methods result in a sufficiently safe and economical structure.
- The part of the non-linearity due to plasticity will absorb some of the energy from the seismic loads that approach the section capacity.

7.3.3.4 Fatigue

The tower members and details are verified for the stress ranges resulting from the Fatigue Limit State. The direct fatigue stresses in the tower legs are primarily caused by rail and roadway loading. Wind tunnel testing has shown that vortex shedding induced oscillations of the tower leg occur at wind speeds of approximately 40 m/s and 65 m/s. Tower leg fatigue caused by vortex shedding is not a concern because both of these wind speeds will only occur rarely (refer to Section 7.4.3 for a discussion of the frequency distribution for wind speeds at the bridge site).

The tower legs are dominated by dead loads combined with seismic or wind loads and stress ranges due to live loading are a relatively small component of the total stresses. Therefore, the detail fatigue lives are verified using an approximate and simplified approach. The approach used is the same in concept as the simplified assessment specified in 1993-2 Section 9, however, an approximate Miner's summation is used in place of the damage equivalent factors, which are intended to account for Miner's summation. The maximum tower leg fatigue stress ranges can be approximately determined by a comparison of the design loading with the actual fatigue loading.

The design rail loading comprises 750 m long trains with a load intensity of 88 kN/m, a total weight of 66 MN and total mass of 6,728 tonnes. Two trains per track are considered with a minimum spacing of 750 m. The maximum rail loading in the tower results from these four design trains placed on the main span. The fatigue loading is based on RFI 44F, which states that the rail traffic should be taken as a "standard" traffic mix as defined in EN 1991-2 Table D.1, and shown in Table 7-8.

Considering the typical tower leg influence line length, the stress range due to rail loading will be primarily dependent on the total mass or weight of the train and is not sensitive to the axle configuration of the fatigue train. It is assumed that all fatigue trains have the mass of the heaviest train, type 5. Train type 5 has approximately one-third of the of the design train mass. Therefore, an approximate relationship between the design rail loading and the type 5 fatigue loading can be established.

Train Type	Trains/Day per Track	Train Mass (tonnes)	Train Weight (MN)	Traffic Volume
1	12	663	6.5	2.90
2	12	530	5.2	2.32
3	5	940	9.2	1.72
4	5	510	5.0	0.93
5	7	2,160	21.2	5.52
6	12	1,431	14.0	6.27
7	8	1,035	10.2	3.02
8	6	1,035	10.2	2.27
Total	**67**			**24.95**

Table 7-8: Standard railway traffic mix.

If the position and length of the trains were irrelevant, the stress range from one design train would be equal to one-quarter of the stress range from the total design rail loading. However, since a single train can be located at a more critical location on the influence line, it is conservatively assumed that the stress range due to one design train is equal to one-half of the stress range from the total design rail loading. Therefore, the stress range due to one type 5 fatigue train can be approximately determined as follows:

Stress range from one design train = one-half of the total design rail loading stress range (up to four trains)

Mass of one type 5 fatigue train = one-third of the single design train mass

Stress range from one type 5 fatigue train = 1/6 of the total design rail loading stress range

From the global IDBAS model, the maximum tower leg stress range due to the design rail loading is 50 MPa. Using the above comparison, the fatigue stress range due to the a single type 5 fatigue train would be 50/6 = 8.3 MPa

Assuming that one-half of all fatigue trains occur in groups of two and the other half of the trains occur in groups of four, the number of cycles for both train groups is:

Four-train group:

# of cycles = ½ * 67 trains/day * 2 tracks * ¼ * 365 days * 200 years = 1.24×10^6

Stress range = 8.3 MPa x 4 trains = 33 MPa

Two-train group:

# of cycles = ½ * 67 trains/day * 2 tracks * ½ * 365 days * 200 years = 2.41 x 10^6

Stress range = 8.3 MPa x 2 trains = 16.6 MPa

The fatigue life for a given stress range is determined from the fatigue strength curve, EN 1993-1-9 Figure 7.1. Assuming a very low fatigue detail category, $\Delta\sigma_c$ of 36 MPa, the fatigue endurance limits for each train loading type are calculated as follows:

Four-train group:

N_R = 2.644 x 10^6 cycles

Two-train group:

N_R = 5.34 x 10^7 cycles

The total fatigue damage, calculated using Miner's summation and multiplying by $\gamma_{mf} = 1.35$ is 0.7, which is well below the limit of 1.0. Therefore, fatigue is not a governing criterion for the tower legs.

7.3.3.5 Accidental Load Scenarios

As described in CG.10.00-P-RG-D-P-SV-T4-00-00-00-00-01 "General Design Principles," the Operational Risk Analysis determined probabilities of occurrence for the three accidental load scenarios specified in the Design Basis. Based on these probabilities of occurrence, fire loads are classified as Design Scenarios, for which the structure must be sufficiently protected or designed to resist, and the less probable impact and explosion loads are classified as Evaluation Scenarios, requiring only an assessment of the likely consequences.

DESIGN SCENARIOS - FIRE

Fire loads for tower leg plates B, C and D, which are adjacent to the roadway, are specified as maximum steel temperatures in Figure 7-42, Figure 7-43 and Figure 7-44, respectively. In each figure, steel temperature is plotted on the vertical axis and distance from the exposed plate surface is plotted on the horizontal axis. Steel temperature as a function of thickness is plotted for gas jet, radiation and pool fire scenarios, considering event durations between 500 and 4,000 seconds. The gaps in the steel temperature curves represent the gap between panels in the tower leg, and as such, the thickness measurements are valid only within a continuous line. For example, in Figure 7-44 for plate D, two continuous line segments are provided for each fire scenario; the first line segment between 0 mm and 40 mm represents the temperature variation through the thickness of the plate D directly adjacent to the roadway; the second line segment between 100 mm and 140 mm actually represents the temperature variation through the thickness of the plate D on the opposite side of the tower leg, and so 100 mm represents the surface closest to the fire on the second plate encountered. The derivation of these temperature curves is based on a one dimensional model that is described elsewhere.

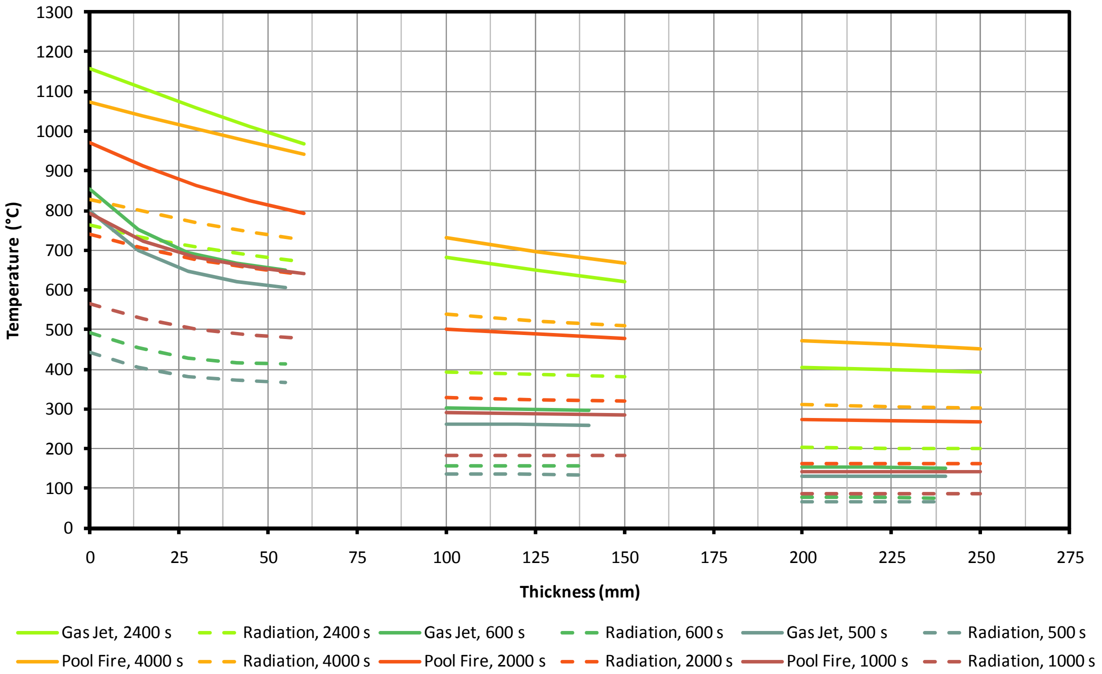

Figure 7-42: Plate B maximum steel temperatures.

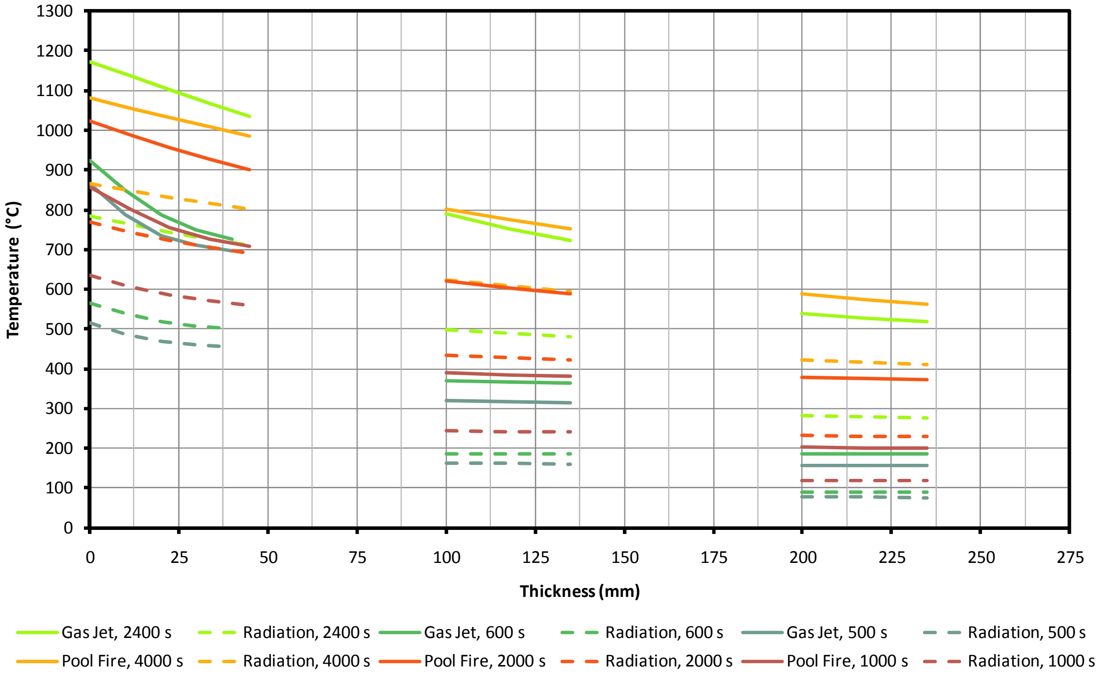

Figure 7-43: Plate C maximum steel temperatures.

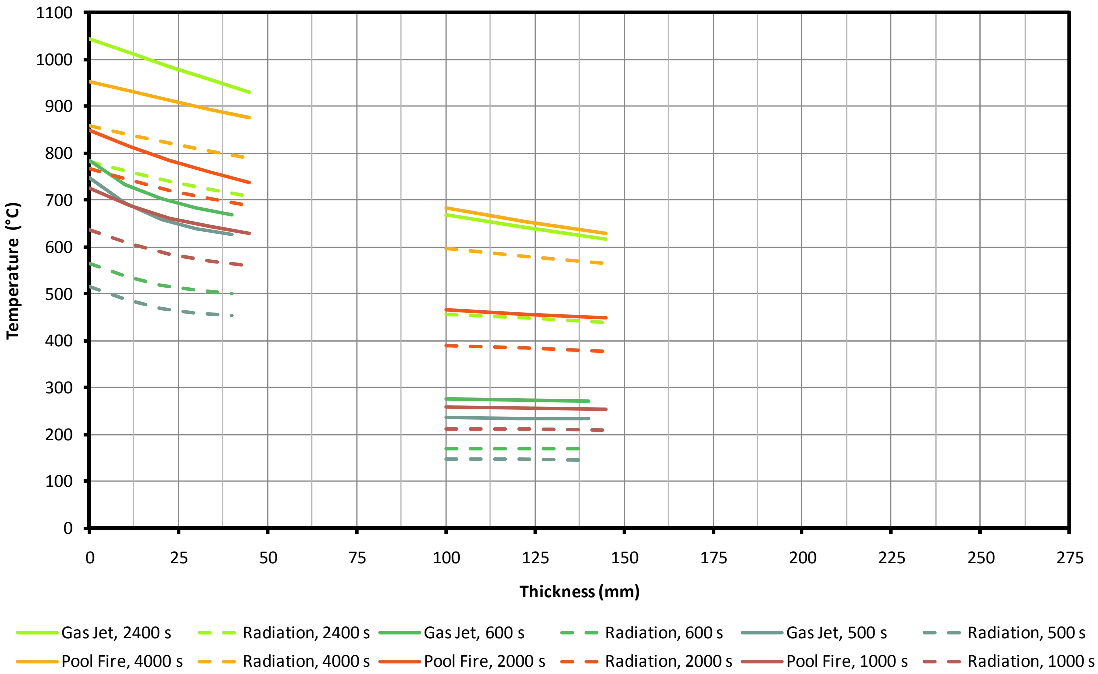

Figure 7-44: Plate D maximum steel temperatures.

For the most severe events considered, the mean temperature through the thickness of the plate closest to the fire is approximately 1000°C. For even the least severe events considered, the mean temperature through the thickness of the plates closest to the fire is approximately 500°C. The potential effects of these temperatures on the tower leg panels were assessed using the variation of steel properties with temperature described in EN 1993-1-2 Table 3.1. The steel panels begin to lose stiffness between 100°C and 200°C, begin to lose strength between 400°C and 500°C, and as the steel temperature rises, the coefficient of thermal expansion increases. The pool fire scenarios are considered to be the most likely of the events considered; for even the shortest 1000 s duration pool fire, the plate B, C and D surface temperatures are between approximately 700°C and 800°C. At these temperatures the steel has only 15% of its original strength and 11% of its original stiffness.

Because of the considerable bridge span, the towers require a substantial portion of their capacity just to support the bridge weight, and thus there is less reserve capacity to sustain accidental load scenarios (which are typically considered with reduced live loads) than there typically is in more conventional bridges.

The longitudinally and transversally stiffened steel panels comprising the tower leg are very sensitive to out-of-plane deformations. At a relatively low temperature of 300°C, the unstressed length of a typical 3,500 mm long panel will increase by 13 mm. The panel is unlikely to be able to achieve this elongation simply by stretching vertically, as it will be restrained by adjacent cooler panels and by the dominant compressive load. It will more likely achieve the elongation by buckling out-of-plane. A 13 mm elongation between fixed end points produces an outwards deformation of 130 mm (for a sinusoidal deformed shape). The panel will be unable to maintain its capacity in this, or even much less severe, buckled shapes. Because of the sensitivity of steel to high temperatures and the use of slender stiffened plates, the towers are extremely intolerant of high temperatures for even relatively short durations. As such, it would be impractical and uneconomical to design the towers maintain their capacity through the fire events considered, and the risk that fires on the bridge deck present to the towers must be mitigated through an appropriate combination of the following:

- Intumescent paint;
- Rigid-type insulating panels adjacent to the tower legs;
- Reduced fire brigade response times; and

- Automated sprinkler systems.

EVALUATION SCENARIOS

Impact

Design Basis Section 5.4.2 specified the impact loading as a 10,000 kg mass at a speed of 600 km/hour. In the absence of any specification, it was assumed that the area loaded by the impact is 7 m^2 or a circle of 3 m diameter.

Local Effects

The 8 m long plate D of the tower leg cross section is the most sensitive to impact, so the impact was assumed to occur on these panels. The analysis for "local" damage was made using a force derived from the loading, assuming a constant rate of momentum change, giving a force of 27.8 MN. Applying this force to plate D, centred on a transverse stiffener, results in utilization ratios between 5 and 10 for shear and moment in the stiffener, indicating that they are not strong enough to localise the damage.

As the transverse stiffeners fail, the plate D would deform as a membrane. However, the curvature of plate C, on either side of plate D, provides great in-plane flexibility for horizontal in-plane stresses, and so the membrane action is limited to vertical in-plane stresses. Therefore, the "local" resistance mechanism is a catenary spanning vertically. The load deflection characteristic of a catenary is highly non-linear, and so the use of an equivalent force is inappropriate and the analysis was made on the basis of finding a catenary such that the strain energy absorbed is equal to the initial kinetic energy of the impacting mass.

It is anticipated that the catenary action will develop over a length between 20 and 40 metres above and below the point of impact. This depends on several variables including:

- The capability of the segment splices to resist high strains and high strain rates without fracture;
- The capability of the transverse stiffeners connections to resist load at high deformations;
- The actual yield stress of the plate, which is commonly 15% higher than the nominal; and
- The increase in effective yield stress due to high strain rates.

The damage will likely comprise severe deformation of 10 or 20 transverse stiffeners, deformation of plate D into the tower leg by about 4 metres, bending of plates C, probable fracture of the welds between plate D and plates C, and crumpling of plates H on the side of the impact.

Global Effects

The global effects were considered for the case of the impact at mid-height between two cross beams. The section properties assumed were the gross properties of the leg less the entire plate D (including longitudinal stiffeners) on the side of the impact. The assumed axial compression in the leg was the factored dead load plus the axial compression force resulting from the catenary resisting local damage, which was calculated as 150% of the plate D yield-force, allowing for the increase in effective yield at high strain rate and the probability that the yield stress is above the nominal yield stress. The bending moment was calculated from the horizontal component of the catenary force applied at 40 metres above and below the point of impact. For the combined axial force, bending moment from major axis global buckling and lateral bending moment from the impact, the predicted tower leg utilization ratio is 0.93; and therefore, the tower might be expected to survive the specified impact.

This analysis is approximate, but has been made conservatively without any assumptions of redistribution of loads either around the tower leg section or up and down the tower leg.

<u>Explosion</u>

The explosion loading developed in the tender design was retained for the Progetto Definitivo. The specified loading is defined as a pressure pulse of 190 MN/m^2 with duration 0.0013 seconds, acting on a 10 m x 10 m area.

Local Effects

The specified pressure is much larger than the capacity of the skin plates and transverse stiffeners. Therefore, the effects of the loading were assessed by considering the potential movement of the skin plate and attached stiffeners as though they are free from restraint and the corresponding absorption of the kinetic energy that is required for this to be the case.

It is expected that such a high pressure would cause out-of-plane deflections exceeding 0.2 metres in the brief duration of the pulse which would generate high membrane stresses and fracture the skin plate and stiffeners, creating a hole in the side of the tower leg.

Global Effects

The applied pressure is very high, but the duration is short and the skin plate would not be able to resist the pressure, limiting the global effects on the tower. Given the large mass and inertia of the tower, the pulse does not affect the tower stability other than by the reduction of effective tower leg cross-section. Similar to the findings for impact, the leg section would be reduced by the removal of one of the skin plate panels. It is expected that the resistance of the damaged leg would be similar to that for the impact case, which gave an approximate utilization ratio of 0.93. The pulse would not produce a catenary of such length and with such membrane force as for the impact case, so the stability of the towers should be less affected. However, it is possible that parts of the wall adjacent to the explosion might detach and form projectiles that damage the opposite side of the leg. If this occurs, it is expected that the damage could be much more severe than that predicted for the impact case.

7.4 Cross Beams

Transverse cross beams connecting the two tower legs are located at approximately elevations +125 m, +250 m and +375 m. Each cross beam is 8 m wide and varies in depth from 11.5 m at the bridge centreline to approximately 22 m, 20 m and 18 m at the tower leg face, for cross beams 1, 2 and 3 respectively. A transverse elevation of cross beam 2 is shown in Figure 7-45. The cross beams comprise longitudinally and transversally stiffened steel panels for the webs and flanges. Similar to the tower legs, the tender design T-shaped longitudinal stiffeners have been replaced with flat plate stiffeners to simplify fabrication. The tender design moment resisting frame type transverse stiffeners have been replaced with braced frame transverse stiffeners to improve the resistance to sway type buckling modes of the webs. Typical cross beam cross sections are shown in Figure 7-46. Each cross beam will be fully shop fabricated and erected as a complete unit.

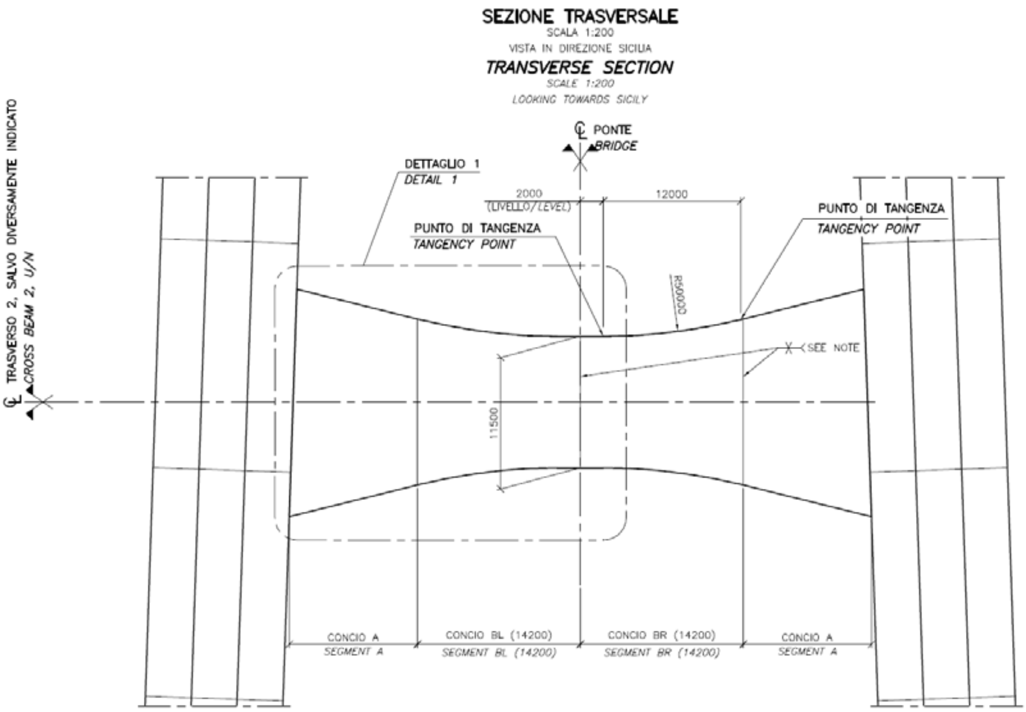

Figure 7-45: Cross beam 2 transverse elevation.

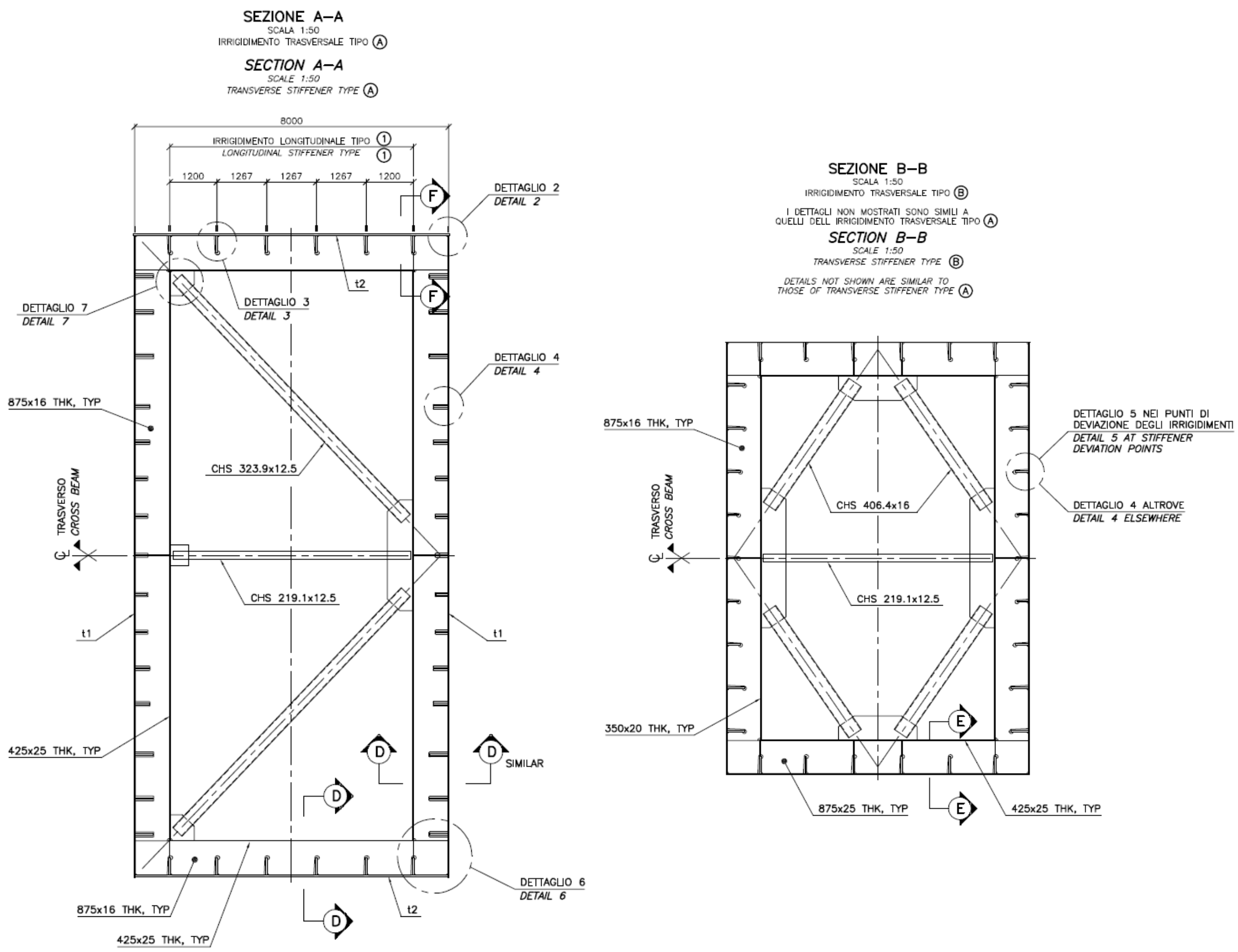

Figure 7-46: Typical cross beam cross-sections.

7.4.1 Longitudinal Elements

The cross beam longitudinal elements comprise web and flange plates and longitudinal plate stiffeners. Cross beam web and flange thicknesses are as shown in Table 7-9. Flange longitudinal stiffeners are 525x53 and web longitudinal stiffeners are 525x53, 400x40 or 300x30, and decrease in size from the flange to mid-depth, reflecting the relative decrease in flexural compression stresses. Web longitudinal stiffeners are fabricated straight and are kinked at transverse stiffeners to approximately follow the curving flange profile. As the cross beam depth decreases towards the bridge centreline, web longitudinal stiffeners are discontinued where they are no longer required.

Segment	Cross Beam 1		Cross Beam 2		Cross Beam 3	
	Web	Flange	Web	Flange	Web	Flange
A	30	25	40	35	35	40
B	35	25	45	25	40	30

Table 7-9: Cross beam plate thicknesses (mm).

Most cross beam elements are governed by von Mises stresses due to the significant shear forces that co-exist with the maximum moments. Similar to the tower legs, the cross beams were designed based on the efficiencies for each longitudinal stiffener and corner on the cross section. Efficiency is defined as the ratio of the compressive stress limit to the unfactored yield stress. Efficiencies were calculated for both longitudinal compressive stresses and shear. The shear capacity at each point was taken as the minimum of shear buckling capacity of the entire web panel or the sub-panel between the longitudinal stiffeners. For convenience, the cross section stress points were taken at the locations of the longitudinal stiffeners. The efficiencies for sub-panel buckling at stiffener locations were approximately taken as the minimum of the two adjacent sub-panels.

The cross beams have approximately constant shears and moments varying linearly from a maximum at the tower legs to approximately zero at the bridge centreline. The cross beam design, including the plate size distribution and stiffener spacing is optimized to suit the distribution of the forces and the variable cross beam depth. Therefore, web plate thicknesses in Segment B, located closest to the bridge centreline are larger than those in Segment A, located adjacent to the tower legs, because the shear forces are constant over the cross beam length and the web depth decreases towards the bridge centreline. The flange plate thickness generally decreases near the bridge centreline due to the rapidly decreasing moments. However, the section depth is also decreasing in the same fashion, limiting the possible reduction in the flange thickness.

The longitudinal stiffener spacing and size are optimized based on the distribution of shears and moments over the cross beam length. The design achieves a relatively constant utilization ratio over the web depth. The areas near the web mid-depth experience the highest shear stresses, but see relatively low longitudinal flexural stresses. Therefore, a low efficiency for longitudinal stresses is tolerated, as is indicated by the use of 300 x 30 longitudinal stiffeners. However, the longitudinal stiffener spacing in this region must be relatively small in order to prevent excess reductions for shear buckling of the sub-panels between stiffeners.

Similarly, for the portions of the web near the flange intersection, larger and more frequent longitudinal stiffeners are used, reflecting the higher longitudinal stresses in this area. The specified flange stiffeners are the same as those at the tops of the webs, as the longitudinal stresses in both locations are similar. The flange longitudinal stiffener spacing is also influenced by arrangement of the inspection/maintenance gantry wheels. Although, the gantry loading is relatively small, it is desirable for the wheels to run directly on top of the longitudinal stiffeners so as to not affect global design of the cross beam flange.

The governing cross beam design loads are ULS wind (static + dynamic) acting transverse to the bridge axis for cross beams 1 and 2 and ULS seismic and wind for cross beam 3. The cross beams stabilize the tower leg from transverse buckling, and so global buckling of the tower (effect of equivalent imperfections) causes significant additional cross beam moments and shears. These are determined as part of the tower leg analysis for the effects of equivalent imperfections, as described in Section 7.3.3.1. Governing ULS and SILS wind and seismic moments and shear forces in the Sicilia tower cross beams are plotted in Figure 7-47 and Figure 7-48 for cross beam 1, Figure 7-49 and Figure 7-50 for cross beam 2 and Figure 7-51 and Figure 7-52 for cross beam 3. The plotted moments act about a horizontal axis parallel to the bridge and the plotted shear forces act vertically. ULS and SILS seismic effects are very similar, differing in magnitude only by 10%, similar to relative increase in peak ground acceleration (6.3 / 5.8 = 9%). ULS and SILS wind effects differ by approximately 25%, which expectedly corresponds to the square of the 11.6% higher reference wind speed for SILS. Cross beam 2 is the most heavily loaded cross beam in shear and moment. Because of the difference in material partial factor considered for the ULS and SILS (1.1 versus 1.0), the largest force effects do not always produce the largest utilization ratios.

Figure 7-53 and Figure 7-54 show the cross beam strong axis moments and shear forces resulting from the transverse global buckling of the towers. The tower leg buckling induced cross beam force effects represent approximately one quarter to one third of the total design effect in the cross beams. For all loadings, the Calabria tower cross beam forces are similar.

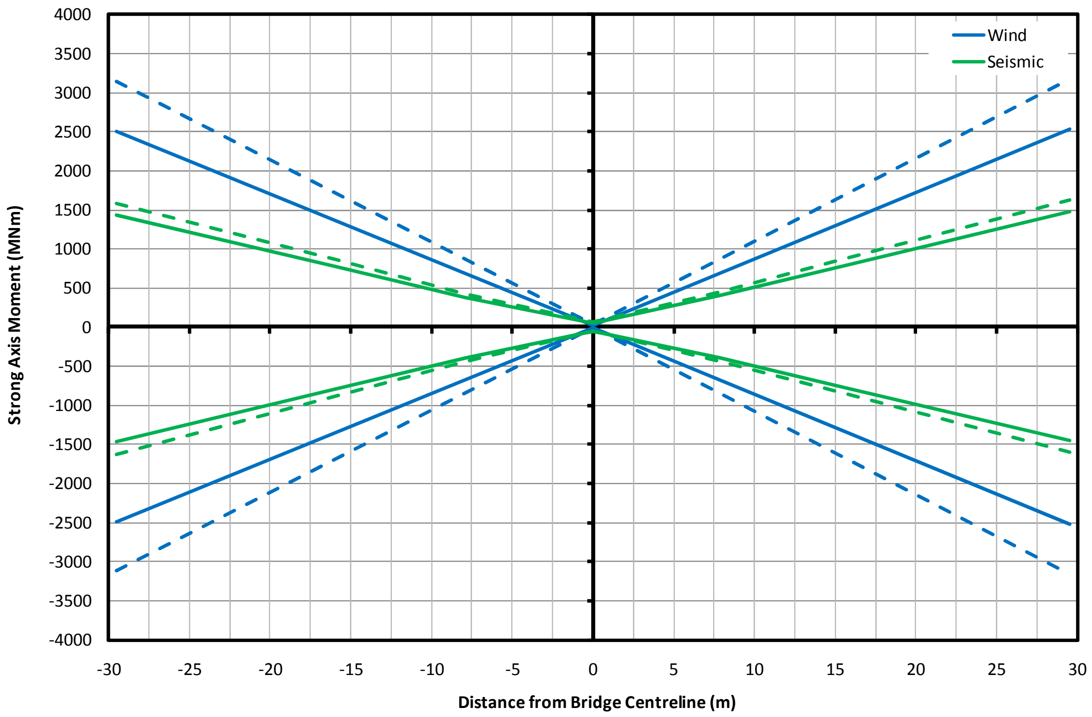

Figure 7-47: Sicilia cross beam 1 moments (ULS – solid lines, SILS – dashed lines).

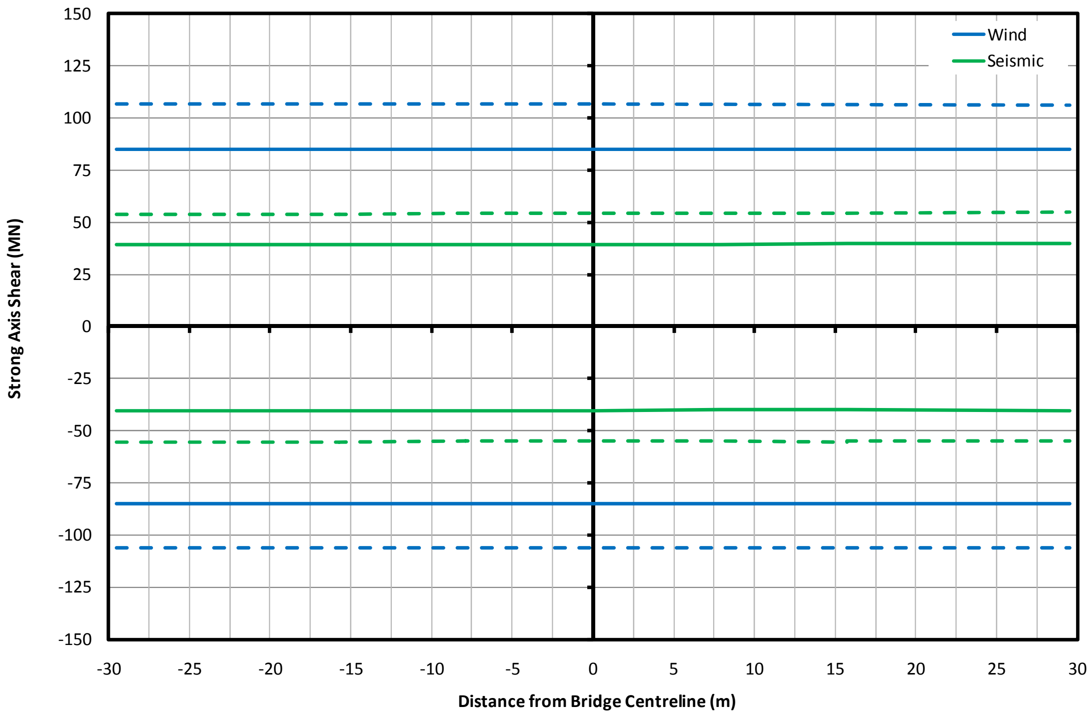

Figure 7-48: Sicilia cross beam 1 shear forces (ULS – solid lines, SILS – dashed lines).

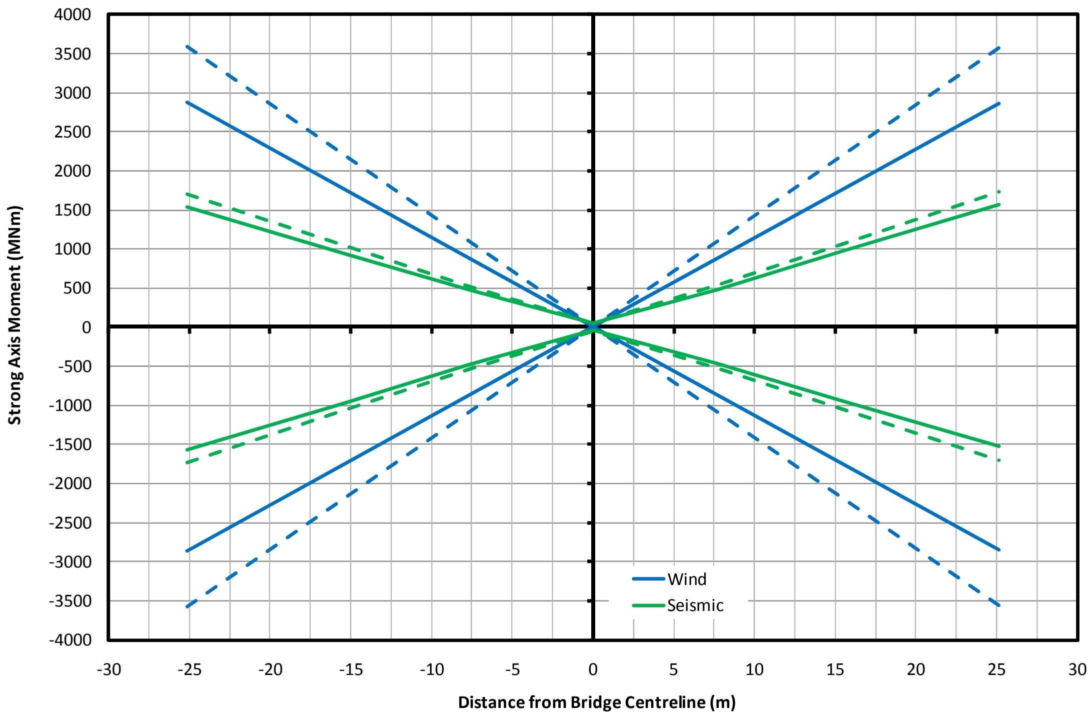

Figure 7-49: Sicilia cross beam 2 moments (ULS – solid lines, SILS – dashed lines).

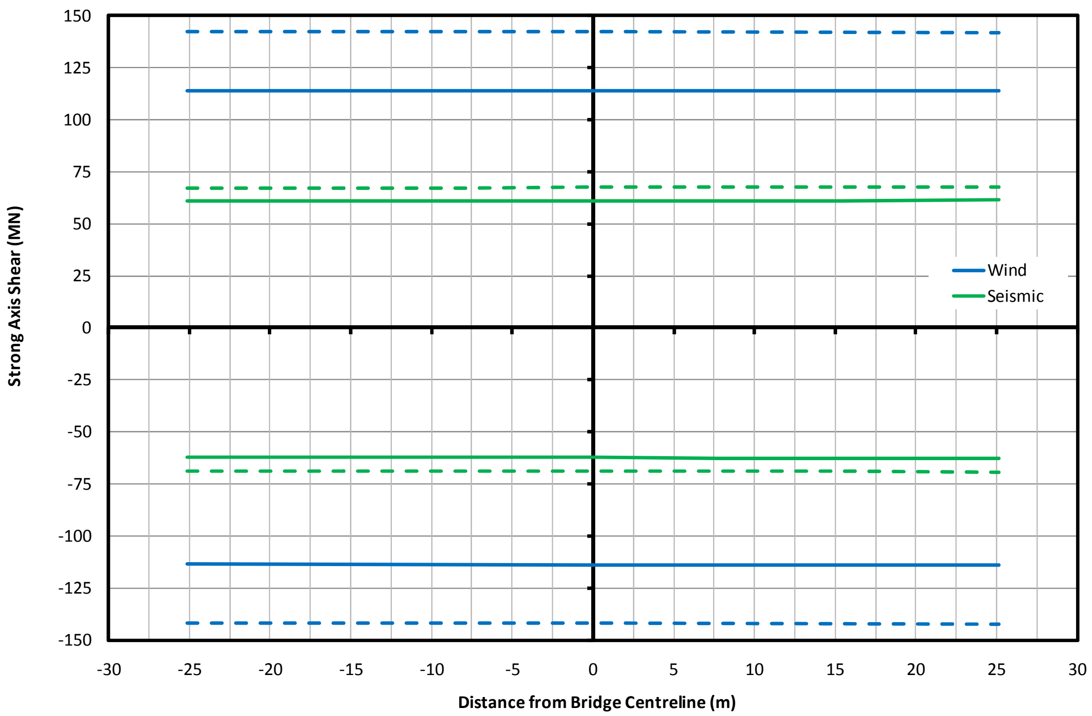

Figure 7-50: Sicilia cross beam 2 shear forces (ULS – solid lines, SILS – dashed lines).

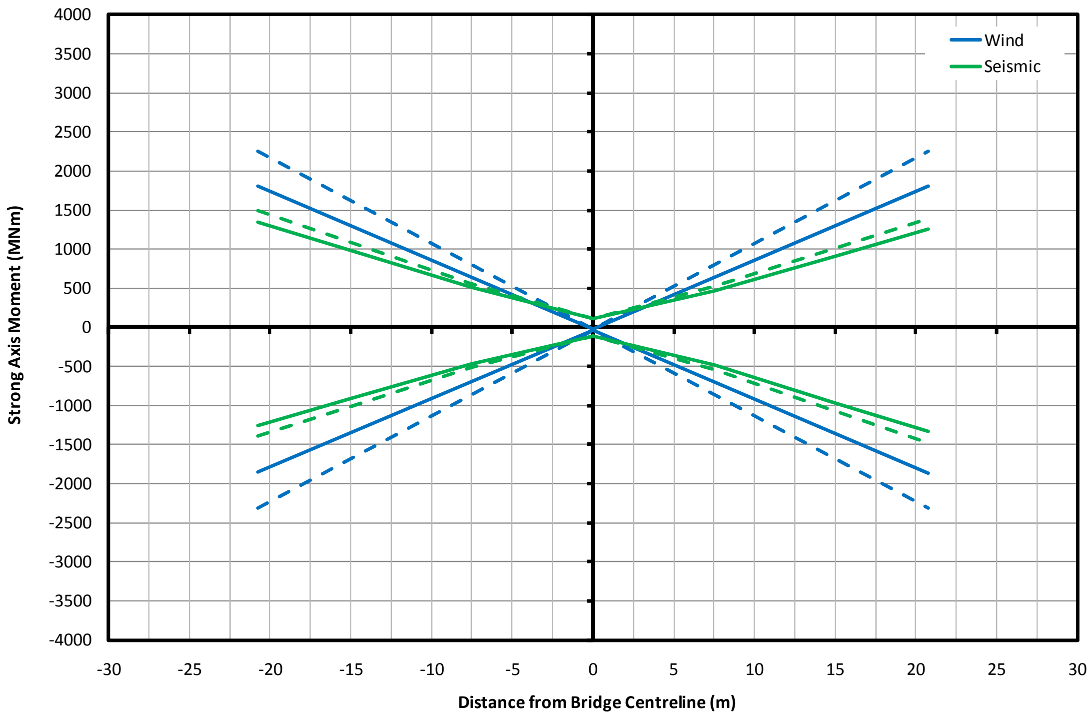

Figure 7-51: Sicilia cross beam 3 moments (ULS – solid lines, SILS – dashed lines).

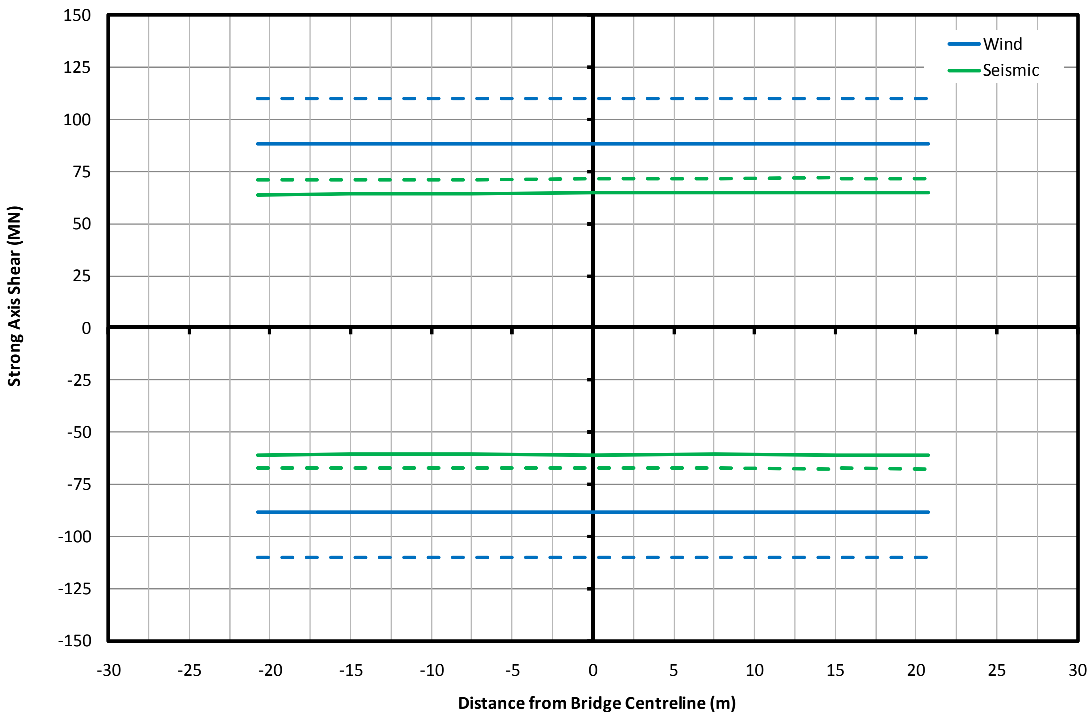

Figure 7-52: Sicilia cross beam 3 shear forces (ULS – solid lines, SILS – dashed lines).

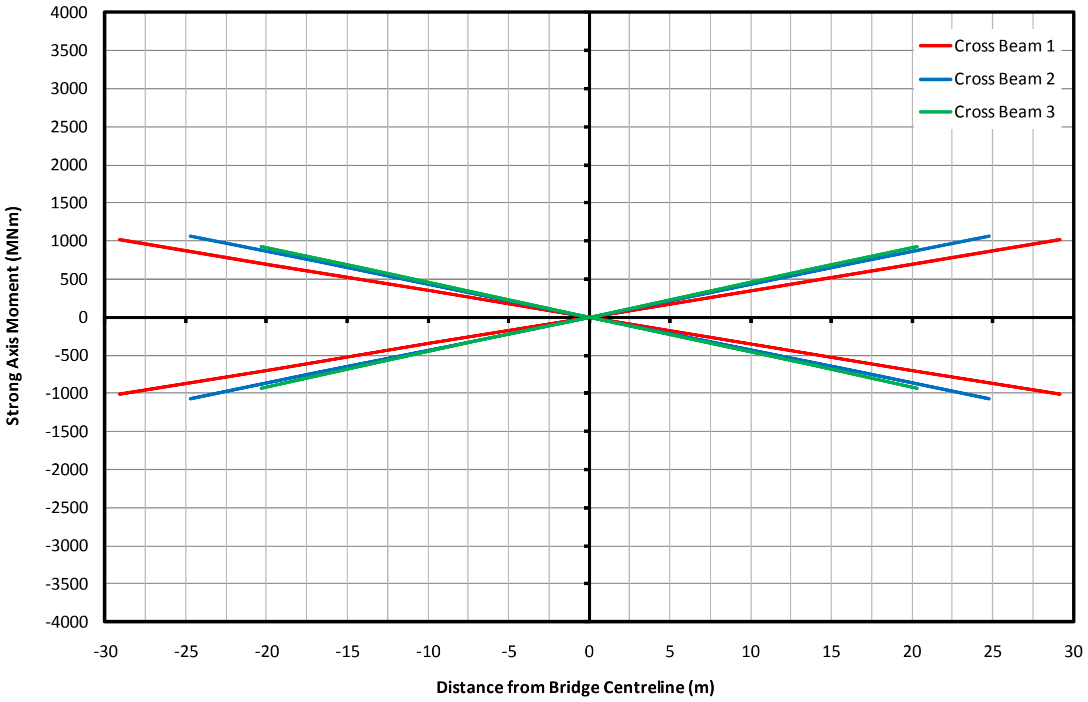

Figure 7-53: Cross beam moments due to tower leg equivalent imperfections.

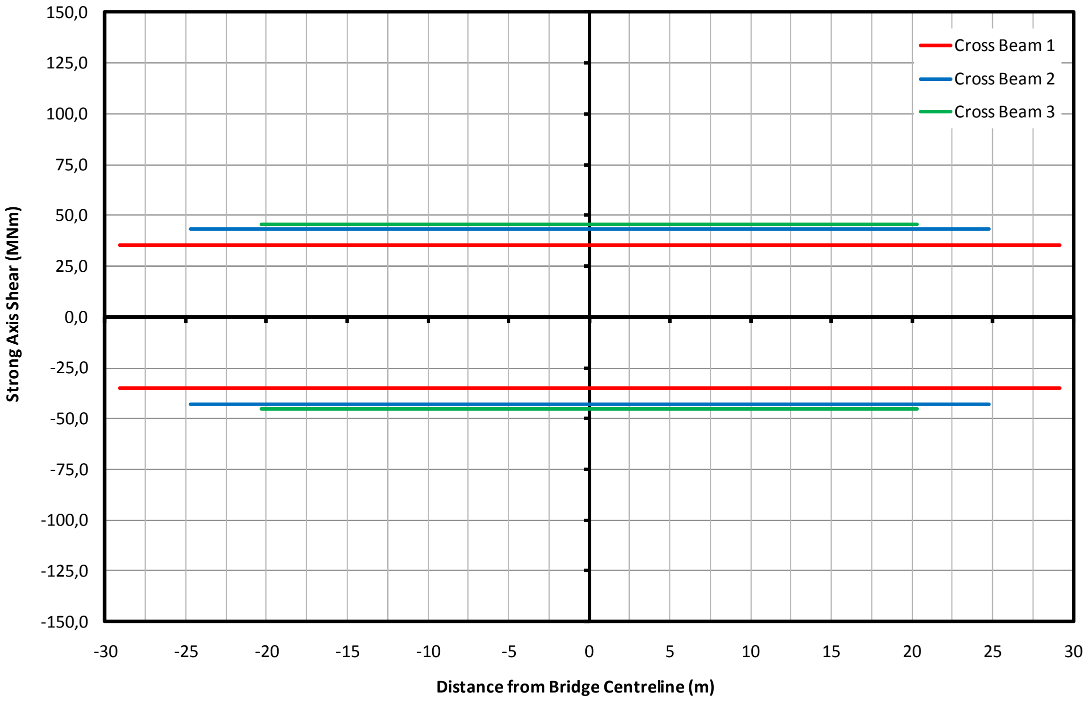

Figure 7-54: Cross beam shear forces due to tower leg equivalent imperfections.

Utilization ratios for von Mises stresses at all cross section points for cross beams 1, 2 and 3 are shown in Figure 7-55, Figure 7-56 and Figure 7-57, respectively. For clarity, only the utilization ratios for the governing ULS and SILS wind combinations and ULS seismic combination are shown. However, similar checks were performed for all relevant load combinations. The governing utilization ratios for the cross beam sections near the tower typically occur near the web-flange intersection because of coexisting high shear and moment. Near the bridge centreline, shear is the dominant effect and the governing utilization ratios occur near the mid-height of the web, where the maximum shear stresses exist. The maximum utilization ratios in each cross beam are between 0.8 and 0.9.

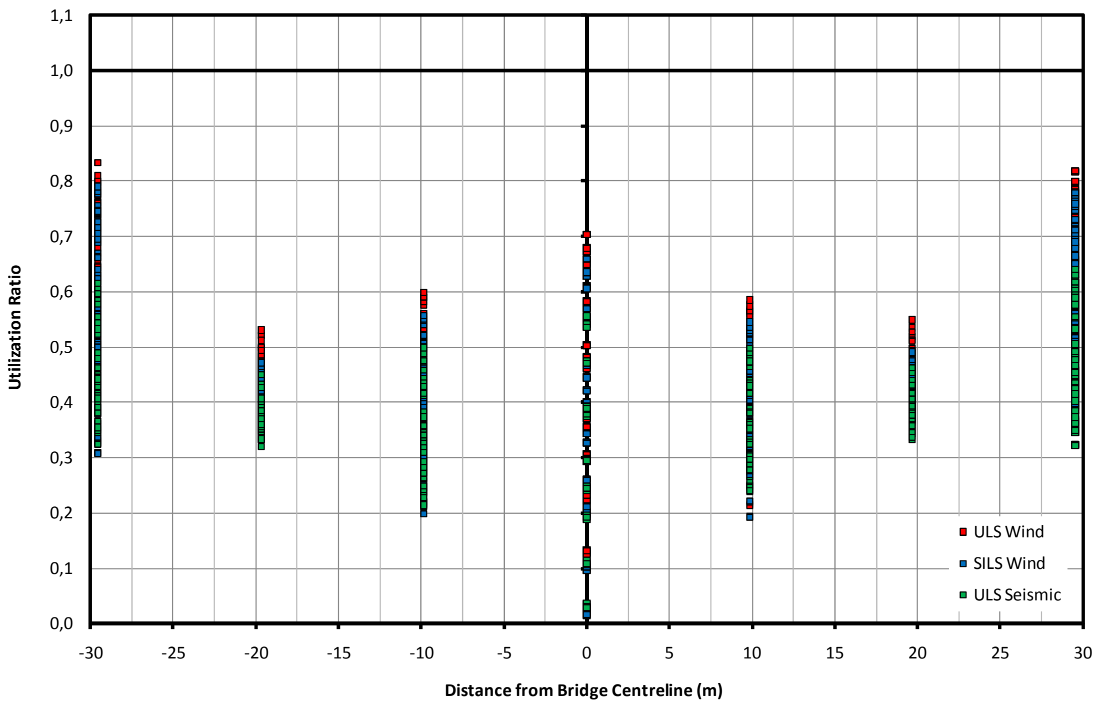

Figure 7-55: Sicilia cross beam 1 utilization ratios.

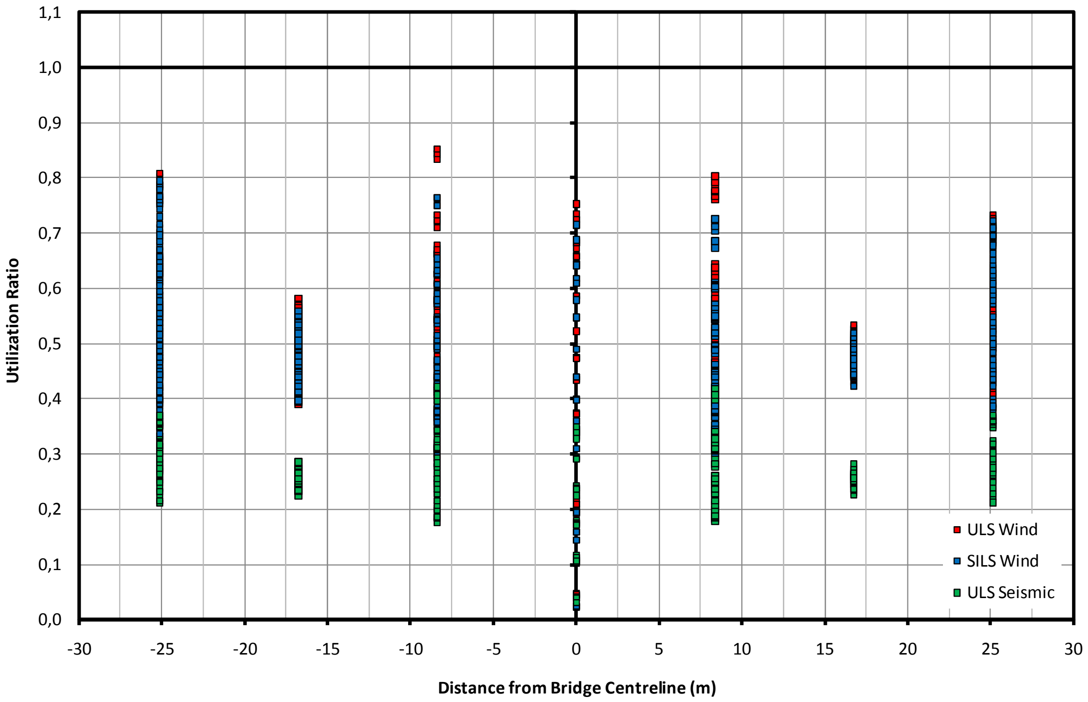

Figure 7-56: Sicilia cross beam 2 utilization ratios.

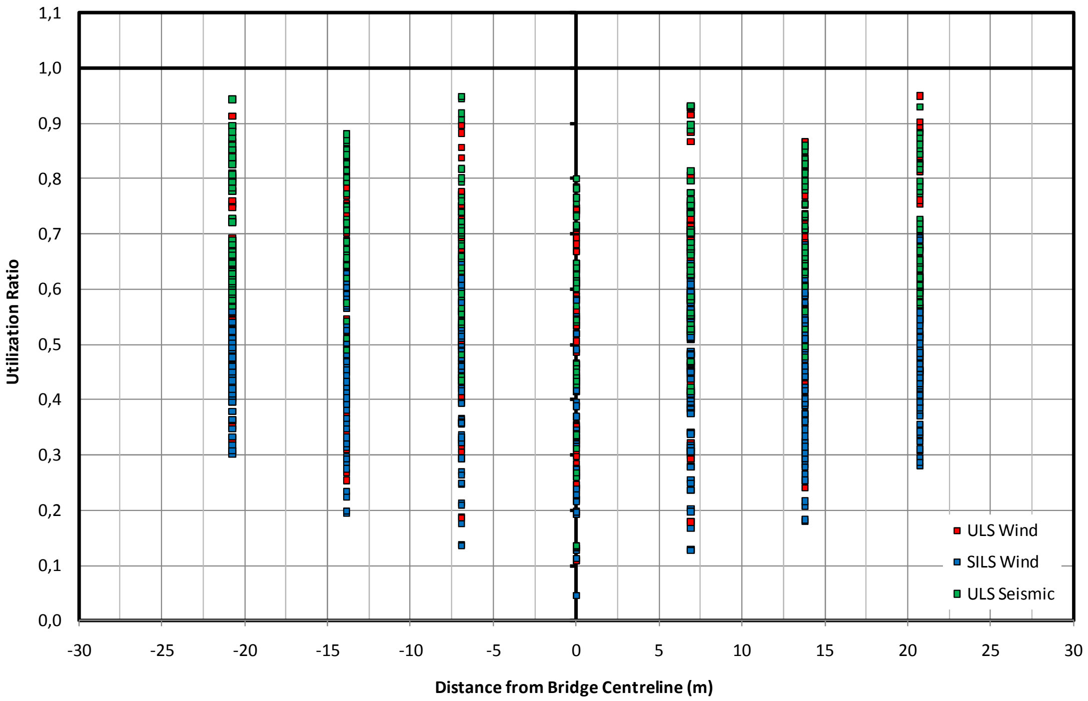

Figure 7-57: Sicilia cross beam 3 utilization ratios.

7.4.2 Transverse Elements

Similar to the tower legs, cross beam transverse stiffeners resist out-of-plane loading resulting from buckling of the longitudinal plates and stiffeners. For the cross beams, as described in CG.10.00-P-RG-D-P-SV-T4-00-00-00-00-01 “General Design Principles”, the following additional forces must also be considered:

- Deviation forces from the curved flange plates and stiffeners;
- Direct forces from gantry loading on the top flange;
- Axial forces from the reactions of adjacent transverse stiffeners; and
- Destabilizing effects of shear buckling of the webs.

As the design of the transverse stiffeners is essentially that of a simple span beam, the resulting forces are highly influenced by the transverse stiffener span length. Therefore, a cross bracing system, as shown in Figure 7-46, is used to reduce the transverse stiffener span lengths and limit stiffener demands. The bracing system comprises the following circular hollow sections: CHS 219.1x12.5, CHS 323.9x12.5 and CHS 406x16. The use of a braced system, as opposed to the frame system proposed in the tender design, has the additional benefit of more effectively resisting an overall sway-type buckling mode of the entire system.

Different transverse stiffeners and bracing arrangements are used in cross beam segments A and B due to the curved flange in segment B, which results in large deviation forces. In segment B, the braces are arranged to support the flange transverse stiffeners at the cross beam centreline, reducing the design shears by approximately 50% and the design moments by approximately 75%. In the absence of the additional brace point, the transverse stiffener would have to be approximately 1.8 m deep. Because of the large deviation forces, larger bracing members are also required.

The transverse stiffener bending capacity accounts for the lateral flange stability using methods similar to those described for the tower leg transverse stiffeners. To increase the lateral flange stability, small tab plates are also used at each end as there is no other restraint along the stiffener length that enables the flange warping stiffness to be developed. In addition, because of the larger deviation forces in the flange longitudinal stiffeners and the kinked profile in the web longitudinal stiffeners, the longitudinal stiffeners in these locations are welded directly to the transverse stiffener webs.

All transverse stiffeners were checked for both bending and minimum stiffness requirements. An additional check was performed for shear capacity of the gross and net sections at cut-out locations. Utilization ratios for each of the design checks for the segment A and B flange and web transverse stiffeners are shown in Table 7-10. For most locations, the transverse stiffeners are governed by stresses due to bending, referred to in the table as the "Minimum Inertia Required for Strength." This check is also heavily influenced by the lateral stability of the flanges, which limits the permissible flange stress. The type B transverse stiffeners on cross beam flanges are governed by shear, due to the short span length. This is reflected in the increased web thickness for these stiffeners.

Segment	A		B	
Element	**Flange**	**Web**	**Flange**	**Web**
Maximum Span Length (mm)	8000	10200	4000	7200
Stiffener Web	875 x 16	875 x 16	875 x 25	875 x 16
Stiffener Flange	425 x 25	425 x 25	425 x 25	350 x 20
UR for Minimum Inertia Required for Stiffness	0.48	0.48	0.27	0.20
UR for Minimum Inertia Required for Strength	0.94	0.91	0.73	0.98
UR for Shear on Gross Section	0.21	0.10	0.40	0.07
UR for Shear on Net Section	0.52	0.24	0.83	0.16

Table 7-10: Utilization ratios (UR) for cross beam transverse stiffeners.

The design forces in the bracing members were determined from the transverse stiffener design forces and end reactions. The braces are designed to work in tension and compression, and are therefore governed by the maximum compressive loads. The braces are standard sized hot-rolled circular hollow sections and have a yield strength of 355 MPa. Table 7-11 shows the maximum compressive loads and design capacity of each bracing member.

Transverse Stiffener Type	A		B	
Brace Element	Diagonal	Horizontal	Diagonal	Horizontal
Section Size	323.9 x12.5	219.1 x 12.5	406.4 x 16	219.1 x12.5
Maximum Compressive Force	1200 kN	700 kN	3450 kN	500 kN
Design Capacity, $N_{b,rd}$	1300 kN	950 kN	4150 kN	950 kN
UR for Axial Compression	0.92	0.73	0.83	0.52

Table 7-11: Utilization ratios (UR) for cross beam bracing members.

7.4.3 Fatigue

The cross beams are not subjected to direct stresses from live load on the bridge deck and so wind loads were considered to be the only reasonable source of fatigue loading. The cross beams are assessed for fatigue caused by regularly occurring wind loads using a simplified and conservative procedure. The frequency and cumulative frequency distributions of all wind speeds occurring at deck level of the Calabria tower are presented in Figure 7-58, with frequency plotted on the vertical axis and wind speed plotted on the horizontal axis. Wind speeds below 1 m/s, which represent 19% of the cumulative frequency, are not represented in the frequency distribution plot. The directional distribution of the winds is given by the wind rose in Figure 7-59, in which the vertical axis with the labels corresponds to North. The wind speed data is based on measurements taken at the Reggio Calabria airport and transformed to the bridge site considering the terrain between the two locations.

The regularly occurring winds are considerably smaller than the design wind speeds specified in the design basis. The design of the tower cross beams is governed by the SILS wind loads, which correspond to a wind speed of 60 m/s at 70 m above sea level. The root mean square structural response to time-varying winds is approximately proportional to $V^{2.8}$, where V is the wind speed. The cumulative wind speed distribution shows that 95% of all wind speeds occurring at the Calabria tower are less than 15 m/s. If it is assumed, very conservatively that:

- 15 m/s winds occur at the bridge site frequently enough that they represent an appropriate fatigue loading;
- all cross beam elements are stressed to the design yield stress, f_y/γ_{M0} under the governing SILS wind load combination;
- the wind always blows in the most critical direction; and

- the entire stress on all elements is attributable to the wind load,

then the maximum fatigue stress caused by the 15 m/s winds would be: $\left(\frac{15}{60}\right)^{2.8} \times \frac{f_y}{\gamma_{M0}} = 9\ \text{MPa}$

A 9 MPa stress is well below the constant amplitude stress threshold for even the worst of fatigue details, confirming that wind induced fatigue in the cross beams is not a concern.

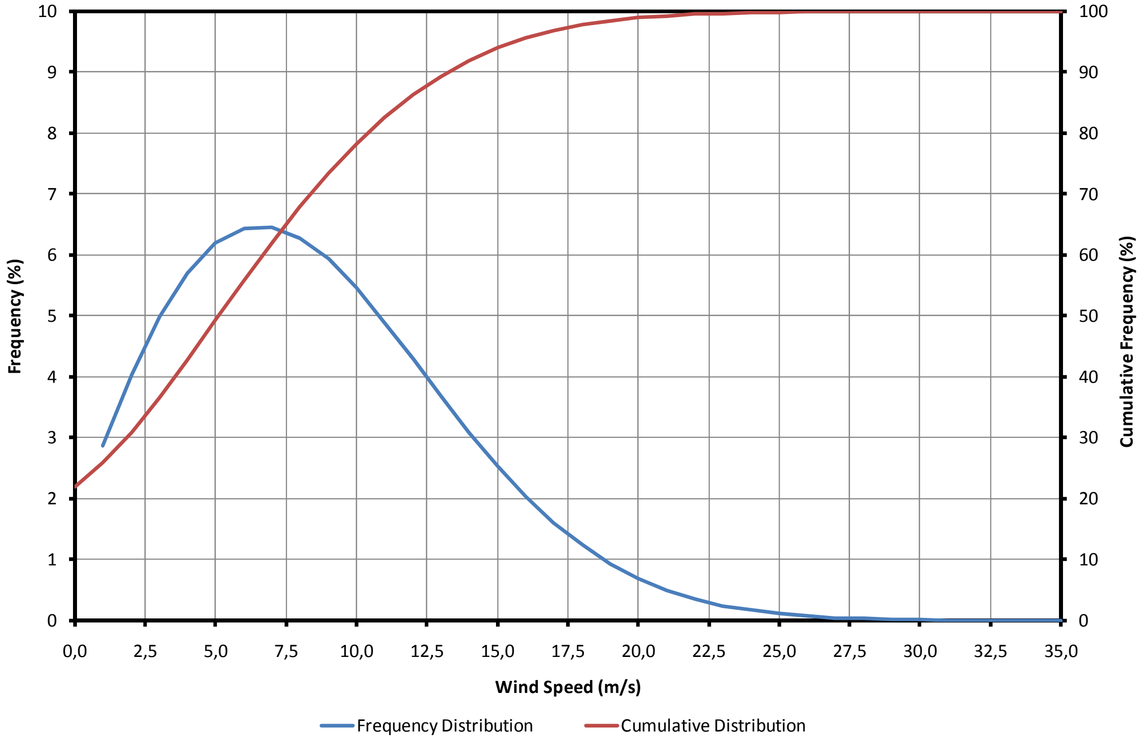

Figure 7-58: Frequency and cumulative frequency distributions of wind speeds at deck level of the Calabria tower.

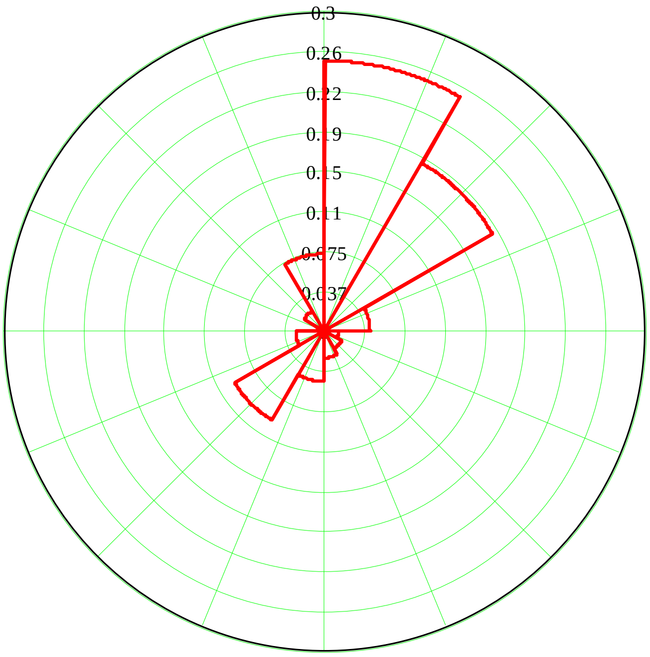

Figure 7-59: Wind rose for all wind speeds at deck level of the Calabria tower.

7.5 Base Anchorage

The tower base anchorage comprises the multi-strand post-tensioned anchorage tendons, the base plate and the local tower leg stiffening. The current tower base anchorage is similar in concept to that developed in the tender design except that the anchor bolts have been replaced by post-tensioning tendons to reduce the quantity of foundation reinforcement that was necessary to resist the transverse splitting forces being caused by the tower base reactions at the top of the foundation. A plan view of the tower base showing the locations of the tendon anchorages is shown in Figure 7-60; the local tower leg stiffening is not shown.

The tower base anchorage is proportioned to prevent decompression under the governing ULS/SILS loads during construction and in the completed bridge. The proportioning of the base anchorage components is described in this section.

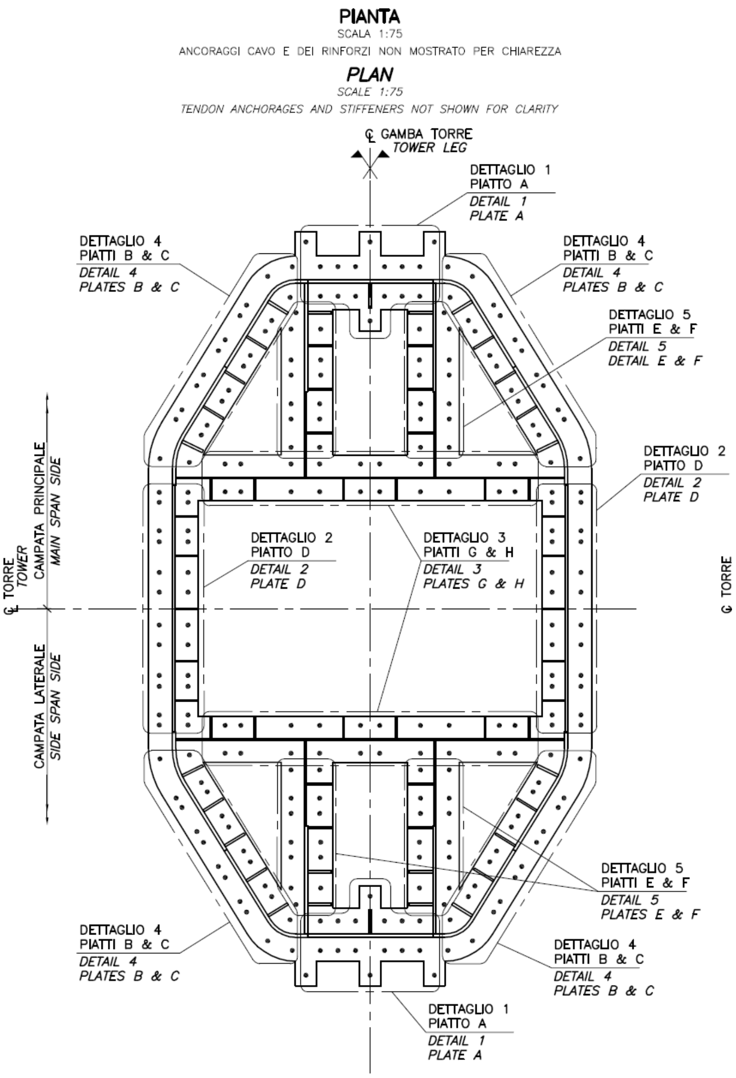

Figure 7-60: Tower base anchorage tendon arrangement.

7.5.1 Anchorage Tendons

Tensile demands at the tower base are resisted by multi-strand post-tensioned anchorage tendons. All tendons are looped through the tower foundation such that both end anchorages resist tensile demands at some point on the tower base. Tendons anchoring plates A, E, F, G and H on the main span side of the tower leg loop to the corresponding anchor points on the side span side of the tower leg. Tendons anchoring plates B, C and D on the east side of the tower leg loop to the corresponding anchor points on the west side of the tower leg. The only exceptions to this arrangement are the tendons anchoring the corner regions at the intersections of plates A, B and E, which are anchored to plate B, but loop between the main and side span sides of the tower leg. A typical tendon anchorage plan view and cross section are shown in Figure 7-61. The plan view shows the plate D anchorages on both the east and west sides of a tower leg together so that the tendon looping connections can be indicated. The tendon size required at each location is indicated by the 6-XX, for which the XX is the required number of strands. The lines connecting the strand size label to the anchorage locations indicates the pairs of anchorages that are part of the same tendon loop.

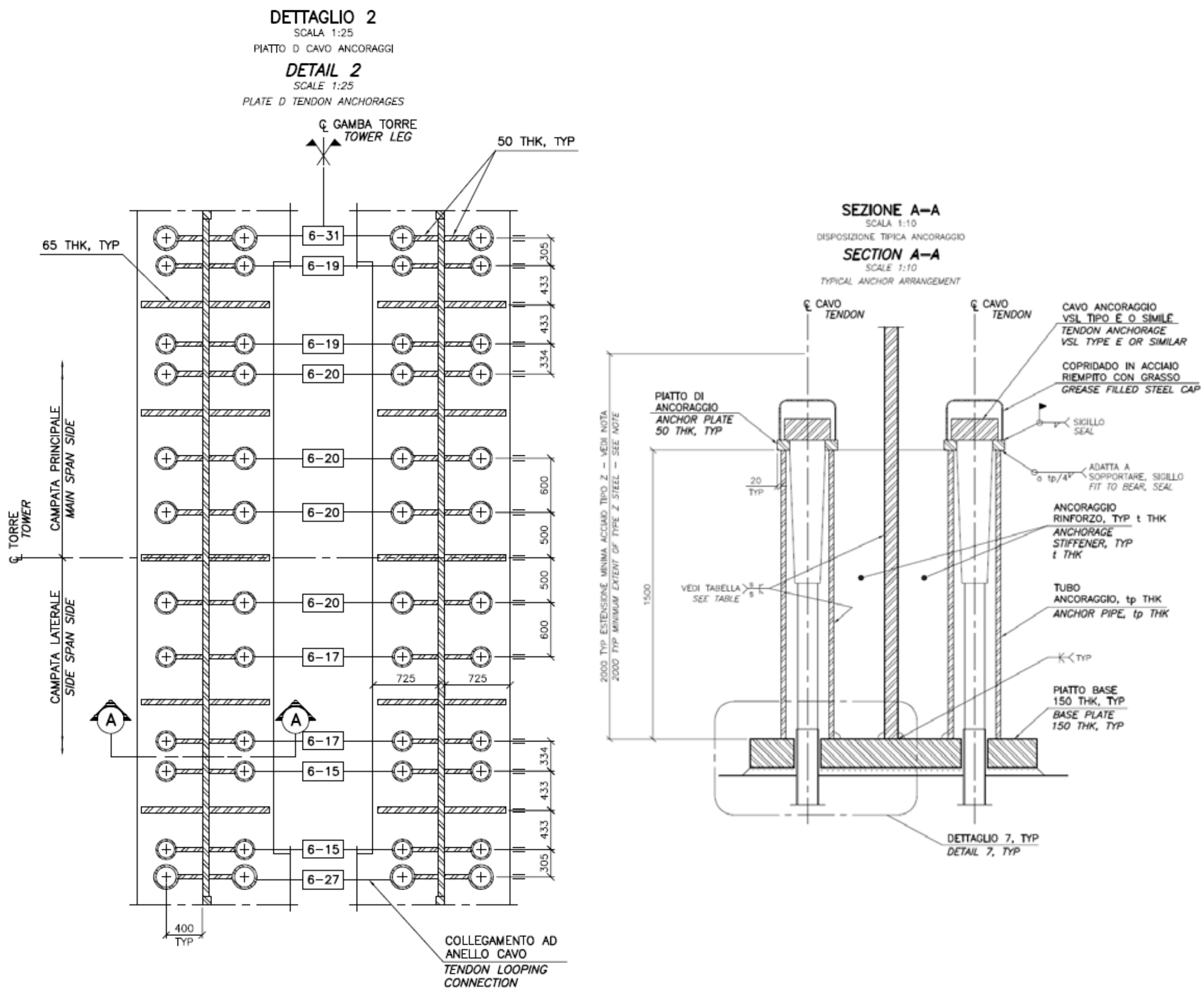

Figure 7-61: Plan view and cross section of plate D tendon anchorages.

The tendons comprise individually galvanized, greased and polyethylene sheathed strands, similar to those often used in parallel strand stay cables. The strands have an area of 150 mm^2 and an ultimate strength of 1860 MPa. The tendon ducts will be left ungrouted so that the tendons can be replaced. The tendons emerge from the tower foundation through holes in the tower base plate and extend through steel anchor pipes to the anchor head. The tendon ducts also pass through the base plate holes so as to prevent any contact between the tendon and grout beneath the base plate. The strand anchors are contained in grease filled steel caps that are welded to the top of the anchor plate. This arrangement results in fully encapsulated tendon with multiple corrosion barriers. The tendon ducts could also be dehumidified with relatively small additional effort and expense by connecting adjacent tendon anchor pipes with small diameter steel pipes so as to form a continuous duct through all of the tendons, through which dry air could be pumped.

The tendons vary in size from 9 to 55 strands, with the largest tendons generally being concentrated along plates A, B and E, where the tensile forces are the largest. The tendons have been designed considering VSL Type E anchorages and hardware dimensions, however, similar anchorages could be provided by other suppliers. Wherever possible, tendons are positioned a minimum of 400 mm from the nearest vertical tower leg/stiffener face to provide room for the initial stressing. The provided 400 mm clearance accommodates VSL's ZPE-1250 jack, which is capable of stressing a 6-55 tendon. As shown in Figure 7-62, the space available for anchoring the required tendons at the intersection of plates A, B and E is limited and 400 mm of clearance could not be provided for all tendons. It has been confirmed with VSL that the tendons as detailed can be installed and stressed using VSL's ZPE-23FJ monostrand jack, which requires only 90 mm of clearance. This jack can also be used for tendons located in areas of the tower cross section that may be more difficult to access with the large multistrand jack.

The tendons are proportioned to prevent the tower base from decompressing under any of the ULS/SILS load combinations during construction or in the completed bridge. Decompression of the tower base was selected as the design limit state to prevent the loss of rotational stiffness that would accompany the decompression. There is some potential to relax this criterion in a subsequent design phase if the non-linear moment-rotation stiffness relationship is incorporated into the global analysis model. It is expected that this might allow for a reduced number of anchorage tendons and reduced strand quantities.

The tendon anchors are connected to the main tower leg plates, about which they are in general symmetrically arranged. The stiffest and most direct load path for tensile tower base stresses to get from the tower leg and into the tendon anchors is through the main plates and anchorage stiffeners, rather than through the tower leg stiffening and subsequent bending and shear of the base plate. Therefore, it is assumed that all tensile tower base stresses are transferred to the tendon anchors through the main plates and anchorage stiffeners. The main tower leg plates provide sufficient area to carry all of the maximum tensile stresses without contribution from the stiffeners, and thus the assumed load path is viable.

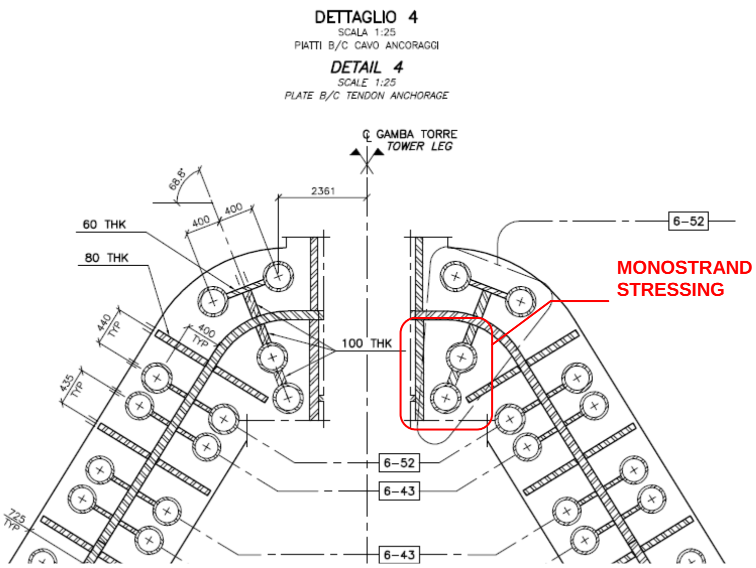

Figure 7-62: Tendon anchorages at the intersection of plates A, B and E.

Tendons are proportioned based on an effective tension force of:

$$F_{t,eff} = \frac{0.65 \cdot f_{pk}}{1.10} \cdot A_s$$

where f_{pk} is the ultimate tendon strength, 0.65 is the fraction of the ultimate strength that is effective after losses (friction, anchor set etc.), A_s is the tendon area and 1.10 is a safety factor that is considered so as to have additional confidence that the tower will not decompress and lose stiffness under the ultimate loads.

Maximum tensile tendon demands are calculated from the maximum design tensile stresses in the plate that they are anchoring, expressed as a tensile load per unit width of panel at each longitudinal stiffener. Maximum tensile demands in the completed bridge are computed for all of the governing ULS and SILS load combinations. Maximum tensile demands during construction (free standing tower or freestanding tower with tie-back) are computed at the ULS, considering the SLS2 level wind and seismic loads. Maximum tensile demands, governing conditions, required and provided number of tendons and strands are listed for each longitudinal stiffener of the Sicilia tower in Table 7-12. The locations of the longitudinal stiffeners on the tower leg cross section are indicated in Figure 7-10. The number of tendons required to anchor the corner regions at the intersections of the tower leg plates were computed separately. The demands for the Calabria tower are similar. Demands on the main and side span sides of the tower leg are listed separately.

Plate	Stiffener	Maximum Tensile Force (MN/m)	Governing Condition	No. of Tendons	Required Strands / Tendon	Provided Strands / Tendon
Main Span Side						
Plate A	LS1	25.2	ULS-Completed Bridge	6	52	52
Plate B	LS2	25.6	ULS-Completed Bridge	4	51	52
	LS3	22.4	Freestanding Tower with Tie-Back	4	43	43
Plate C	LS4	20.0	Freestanding Tower with Tie-Back	4	38	38
	LS5	18.1	Freestanding Tower with Tie-Back	4	35	35
	LS6	16.2	Freestanding Tower with Tie-Back	4	30	30
Plate D	LS7	10.3	SILS-Completed Bridge	4	19	19
	LS8	9.0	SILS-Completed Bridge	4	20	20
	LS9	7.6	SILS-Completed Bridge	4	19	20
Plate E	LS26	26.4	ULS-Completed Bridge	4	38	38
	LS27	21.4	Freestanding Tower with Tie-Back	4	38	38
	LS28	16.8	Freestanding Tower with Tie-Back	4	34	34
Plate F	LS29	9.1	Freestanding Tower with Tie-Back	4	19	19
Plate H	LS19	4.8	Freestanding Tower with Tie-Back	4	11	11
	LS20	5.6	Freestanding Tower with Tie-Back	4	11	11
Plate G	LS18	3.8	Freestanding Tower with Tie-Back	4	9	9
Side Span Side						
Plate A	LS1	12.8	Freestanding Tower	6	26	52
Plate B	LS2	14.2	Freestanding Tower	4	28	51
	LS3	12.7	Freestanding Tower	4	25	29
Plate C	LS4	11.2	Freestanding Tower	4	22	22
	LS5	9.7	Freestanding Tower	4	19	20
	LS6	8.2	Freestanding Tower	4	16	18
Plate D	LS7	7.0	SILS-Completed Bridge	4	13	15
	LS8	7.2	SILS-Completed Bridge	4	16	17
	LS9	7.6	SILS-Completed Bridge	4	19	20
Plate E	LS26	14.4	Freestanding Tower	4	22	38
	LS27	11.8	Freestanding Tower	4	21	38

	LS28	9.0	Freestanding Tower	4	19	34
Plate F	LS29	4.6	Freestanding Tower	4	10	19
Plate H	LS19	2.2	Freestanding Tower	4	5	11
	LS20	2.6	Freestanding Tower	4	5	11
Plate G	LS18	1.6	Freestanding Tower	4	4	9

Table 7-12: Tensile demand and required/provided tendons at the Sicilia tower base.

Tensile demands on the main span side of the tower leg are generally governed by the wind or seismic loads on the freestanding tower with tie-back; however, ULS seismic loads in the completed bridge govern the demands at the extreme longitudinal tower leg fibres on plates A, B and E and SILS wind loads in the completed bridge govern the demands on the extreme transverse tower leg fibres on plate D. Maximum tensile demands on the main span side of the tower leg are typically larger than those on the side span side because of the tower tie-back. For the tower leg plates governed by longitudinal loads, the main span tensile demands are approximately twice the corresponding side span loads. For the tower leg plates governed by transverse loads the difference is smaller.

Tensile demands on the side span side of the tower leg are generally governed by wind loads on the freestanding tower, except for the tensile demands on plate D, which are governed by SILS wind loads on the completed bridge.

At some locations on the tower leg cross section, such as corner regions and on plate E near plate A, there is not sufficient space available to anchor the combined number of tendons for the corner region itself and the adjacent longitudinal stiffeners. In these areas, the number of tendons was consolidated and the size of the provided tendons increased to allow the anchorages to be placed.

Looping of the tendons between the plate A and E main and side span anchorages results in some conservatism on the side span side, where the tensile demands are much lower. The increased strand quantities resulting from this conservatism can potentially be offset by stressing these tendons from only the main span anchorage. This optimization can be investigated further in a subsequent design phase.

The tendon anchor pipes are designed for the maximum tendon force, which occurs during the initial tendon stressing. The tendon stressing force is specified as $0.78 \cdot f_{pk}$, however, the pipes are conservatively designed, considering possible accidental overstressing, for $0.90 \cdot f_{pk}$. The pipes are short and stocky and so are proportioned based on their yield strength. The pipe sizes provided for each tendon size are list in Table 7-13.

Number of Strands	Pipe Outside Diameter (mm)	Pipe Thickness (mm)
0 - 12	200	15
13 - 19	225	20
20 - 22	250	20
23 - 27	275	25
28 - 31	275	25
32 - 37	300	30
38 - 43	325	30
44 - 55	350	35

Table 7-13: Anchor pipe sizes.

7.5.2 Plate Stiffening

The tower base plate stiffening comprises vertical base plate stiffeners and anchorage stiffeners. The base plate stiffeners are the fin shaped stiffeners that are welded to the tower leg plates opposite the tower leg longitudinal stiffeners, as shown in Figure 7-63, or between longitudinal stiffeners and anchorage stiffeners to reduce the base plate span. The bearing plate stiffeners carry the tributary base plate bearing pressures back to the tower leg plates. At the tower base the tower longitudinal stiffeners are deepened so that they bear within 50 mm of the base plate edge. The vertical anchorage stiffeners work similarly to the bearing plate stiffeners and connect the tendon anchor pipes to the tower leg plates.

The plate stiffening elements are designed for combined shear and bending stresses in accordance with EN 1993-1-5 Section 10, using the limit state equation:

$$\left(\frac{\sigma_{x,Ed}}{\rho_x \cdot f_y / \gamma_{M1}}\right)^2 + 3 \cdot \left(\frac{\tau_{Ed}}{\chi \cdot f_y / \gamma_{M1}}\right)^2 \leq 1.0$$

where $\sigma_{x,Ed}$ is the bending compressive stress, ρ_x is the compressive stress reduction factor for plate slenderness, f_y is the yield stress, τ_{Ed} is the shear stress, χ is the shear stress reduction factor for plate slenderness and γ_{M1} is the material partial factor. Stiffeners are 1500 mm deep and vary in thickness from 40 mm to 100 mm depending on the base plate area being supported. The corresponding compressive stress reduction factors vary between 0.53 and 1.0. For all stiffener thicknesses the shear stress reduction factor is 1.0.

The stiffeners are proportioned to carry only the tributary bearing pressures caused by externally applied loads. The bearing pressures caused by the tension forces in the anchorage tendons are equilibrated by the compressive force applied to the top of the anchor pipe and so those forces are not transmitted through the stiffeners back to the tower leg plates. It is assumed that bearing pressures within 150 mm of the tower leg plate faces are carried through the base plate thickness directly into the tower leg plates and do not cause shear or bending in the stiffeners. Bearing pressures outside of this zone must be transferred through the stiffeners. The anchorage stiffeners are also verified to have the shear capacity necessary to transmit the effective tensile force in the anchored tendon back to the tower leg plate, as required by the previously described load path.

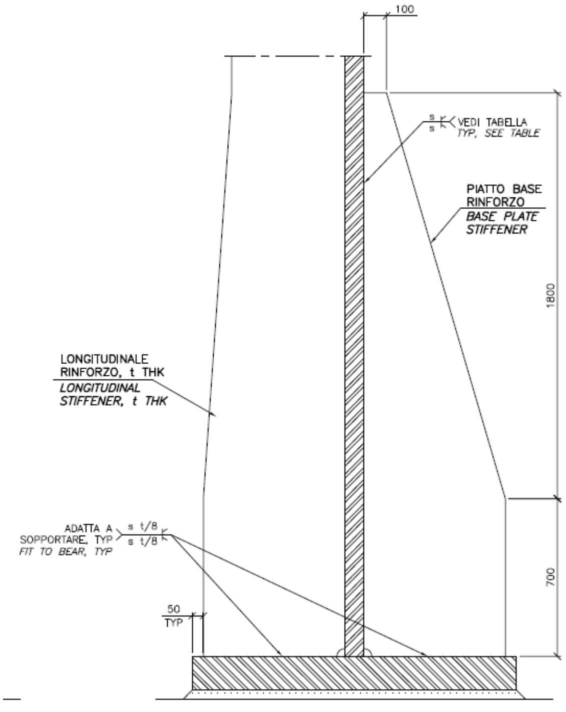

Figure 7-63: Tower base cross section showing longitudinal stiffener and base plate stiffener.

7.5.3 Base Plate

The base plate is a 150 mm thick steel plate that distributes the compressive forces in all of the tower leg plates and longitudinal stiffeners, and the pre-tensioning forces in the anchorage tendons approximately uniformly to the underlying 40 mm thick grout pad, which spreads the load further to the underlying concrete tower foundation. The base plate plan geometry is selected to support all of the longitudinal stiffeners and limit the bearing stress at the top of the concrete foundation to approximately 60 MPa. The base plate width is 725 mm outside of the tower leg skin plates and inside the tower leg it varies from a minimum of 675 mm along plates G and H to a maximum of 800 mm along plate A. The base plate width is increased locally around the isolated anchorage tendons along plate A, as shown in Figure 7-64 .

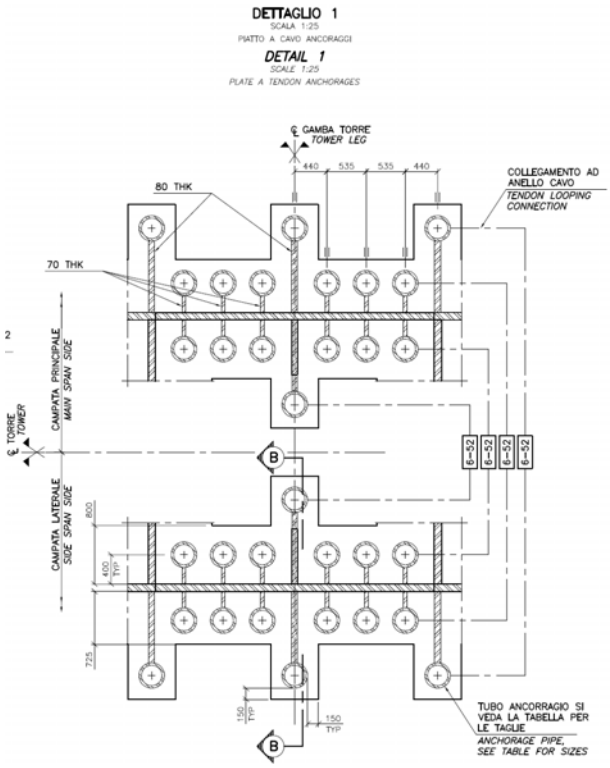

Figure 7-64: Local base plate widening along plate A.

The provided base plate has a design shear capacity of 29.3 MN/m and design plastic moment capacity of 1.90 MNm/m. Base plate demands are based on the maximum bearing pressures and the spans between adjacent stiffeners and the cantilever lengths beyond the tips of the stiffeners and anchorage pipes. On cantilever lengths the shear and moment demands are calculated as:

$V = P \cdot L$ per unit width

$M = V \cdot L/2$ per unit width

where P is the bearing pressure and L is the cantilever length. On continuous spans the shear and moment demands are calculated as:

$V = P \cdot L/2$ per unit width

$M = P \cdot L^2/10$ per unit width

The base plate is conservatively assumed to span in only one direction between tower leg stiffeners and given that the base is fully continuous across the stiffeners, both the hogging and sagging moments will be less than those assumed for design.

The maximum bearing pressures occur along plates A, B, C and E, for which the tower leg plate thicknesses and longitudinal stiffener sizes are largest. For the maximum bearing pressures, which are approximately 60 MPa, the base plate is able to span approximately 500 mm, which is greater than or equal to the maximum span along the most heavily loaded plates. The maximum base plate cantilever length is 225 mm, for which the bearing pressure resistance is approximately 65 MPa.

The base anchorage shear capacity is provided by friction between the base plate and the underlying grout pad. The maximum tower base shear force is 158 MN and is caused by the SILS longitudinal seismic combination. Conservatively assuming that the minimum tower leg axial compression force of approximately 1,000 MN acts concurrently with the maximum shear force, and ignoring the additional compression from the prestressing tendon forces, the shear resistance of the tower base anchorage is 500 MN, resulting in a maximum utilization ratio of 0.32. This low utilization ratio indicates that the design friction coefficient between the base plate and grout could be as low as 0.2 and still provide adequate shear capacity at the tower base.

7.6 Miscellaneous Design Considerations

7.6.1 Provision for Access

The tower legs and cross beams are provided with access systems that facilitate the inspection and maintenance of all tower components. The access systems comprises ladders in the four triangular cells, elevators and emergency ladders in both of the cells bounds by plates A, E, F and G and a staircase in the central cell. Access openings in the tower leg plates, allowing movement between the seven cells, are provided at one cross section per tower leg segment, and at additional locations as necessary to provide access to the cross beams, tower leg inspection gantries, suspended deck maintenance lanes, tower base and main cable saddles. Circular cut-outs of 1,000 mm diameter are provided in every triangular plate diaphragm to allow unrestricted movement vertically within those cells. The only cross beam access opening is the hatch in the cross beam 3 top flange that allows the main cable to be accessed. The typical arrangement of access openings provided in each tower leg segment is shown in Figure 7-65. All typical access openings are 800 mm wide and 2,000 mm tall.

The tower design has considered the presence of the required access openings in the main tower leg and cross beam plates. Because the access openings are located at only discrete elevations, it would be quite uneconomical to thicken all affected tower legs plates to compensate for the plate areas removed by the openings, therefore, the affected plates are reinforced around the access openings as shown in Figure 7-66. The reinforcing typically comprises a pair of 200 mm wide plates, with a thickness to match that of the affected plate, welded on both sides of the opening to replace the area that is removed. The reinforcing plates extend a sufficient distance above and below the opening to ensure that the load in the affected plate is able to transfer to the reinforcing plates before the opening. Transverse plate stiffeners spanning between the longitudinal stiffeners adjacent to the opening are provided above and below the opening. The reinforcing shown in Figure 7-66 is contained entirely within the space between adjacent tower leg transverse stiffeners, which is convenient for fabrication; however, the reinforcing for some of the openings in the thicker skin plates must extend beyond the adjacent transverse stiffeners so that enough weld length can be provided to transfer the required force to the reinforcing.

The proposed access opening elevations and reinforcing arrangement have been verified to the meet the typical structural requirements; however, the vertical positioning of the openings relative to the required access platforms and transverse stiffeners requires further consideration in the detailed design phase.

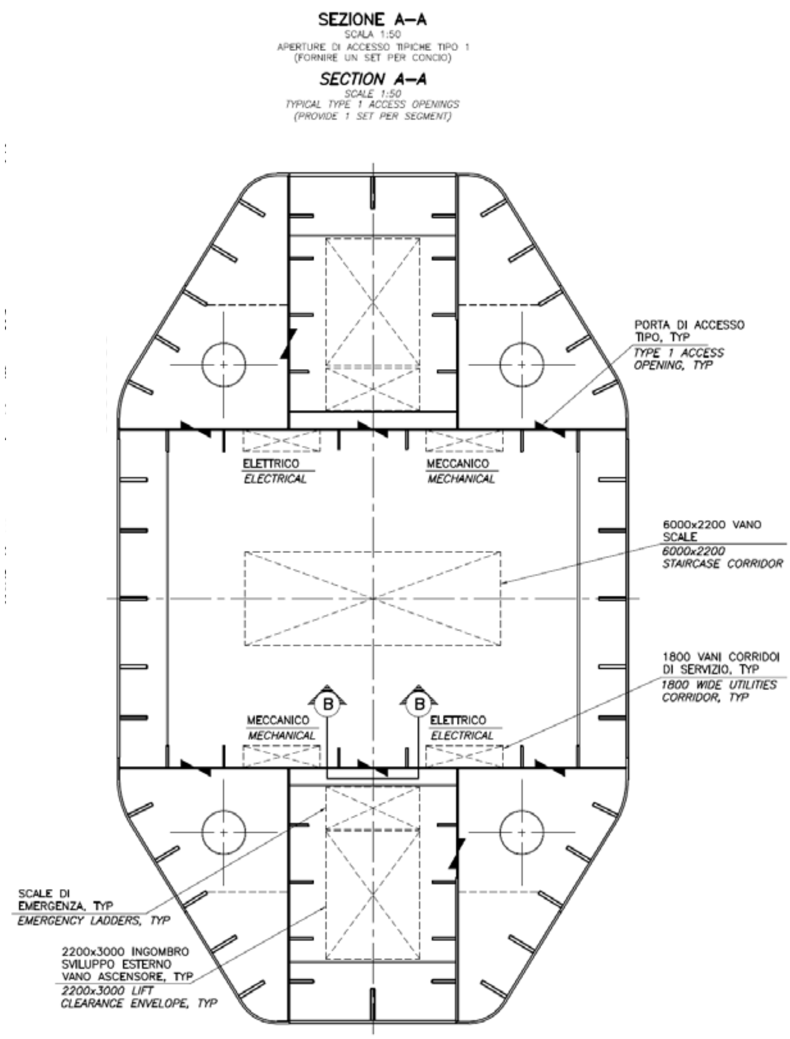

Figure 7-65: Typical access openings in tower leg cross section.

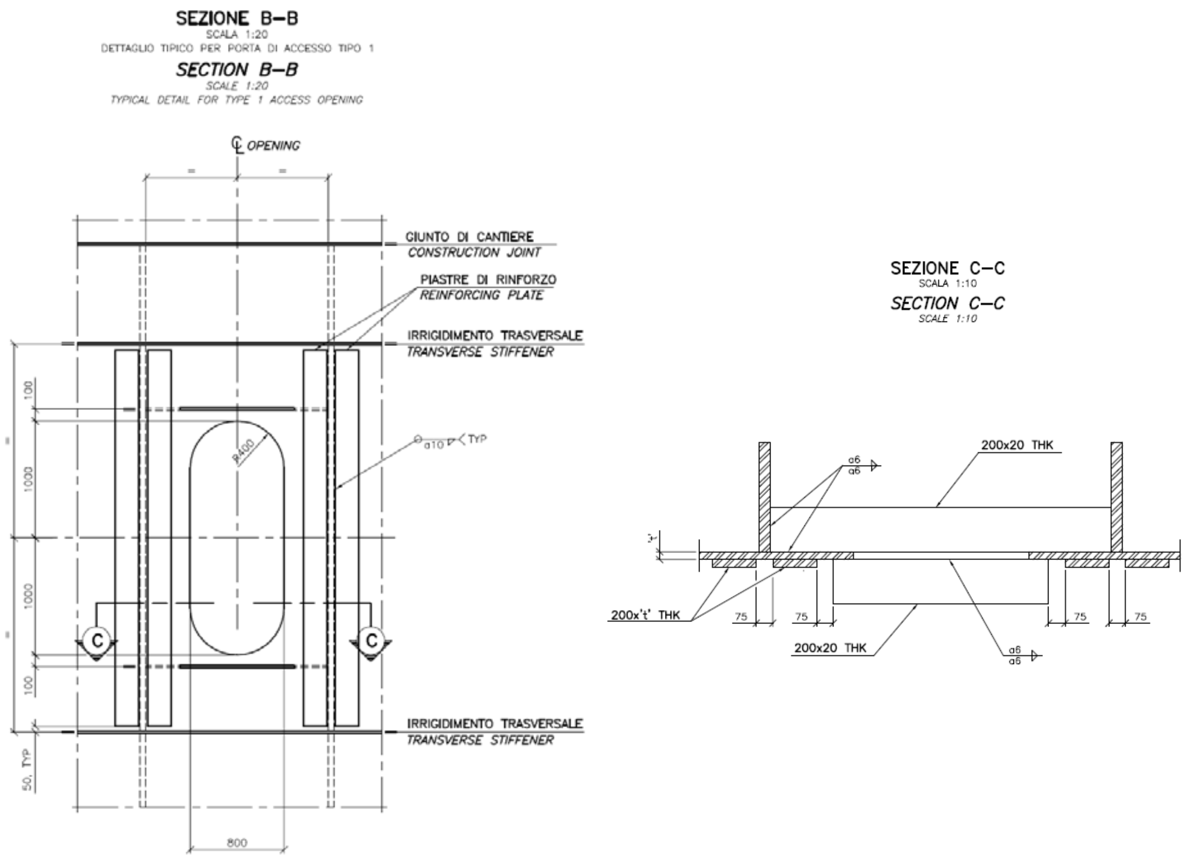

Figure 7-66: Typical reinforcing around access openings.

7.6.2 Connection of Non-Structural Components

Connections of non-structural components, such as access systems, electrical and mechanical infrastructure to the tower structure have not been proportioned in this design phase. However, it is anticipated that connections will be made through base plates welded to the tower structure. The base plates will have tapped holes or tab plates for attaching the non-structural components.

7.6.3 Electrical and Mechanical Interfaces

Electrical cables and mechanical piping enter the tower legs through a shaft in the concrete foundation. Once inside the tower legs the components are deviated to the dedicated corridors along plates G and H in the central 12 m x 8 m cell, as shown in Figure 7-65. The corridors are generally free from obstructions except for the type 2 diaphragms at the connection of the cross beam top and bottom flanges to the tower legs.

All structural tower plates through which pipes and electrical cables must pass will be reinforced locally to replace any steel area removed by the cut-out.

Drainage pipe inlets are provided at intermediate elevations in the tower as noted in the mechanical drawings and a catch basis and drain pipe will be embedded in the concrete foundation at the tower leg base to dispose of excess water resulting from pipe leakage, washing or fire fighting.

7.6.4 Dehumidification

The tower legs and cross beams are dehumidified by two independent dehumidification systems per tower. The first system dehumidifies one leg and cross beam 1 and the second system dehumidifies the other leg and cross beams 2 and 3. The dehumidification units are located in cross beams 1 and 2. The dehumidification system requires particular access openings to remain open or sealed as described on the dehumidification system drawings.

8 Summary

The tower legs and cross beams comprise longitudinally and transversally stiffened steel plate elements. The steel panels and stiffening elements are verified using the equivalent width method in accordance with the provisions of EN 1993-1-5. The tower leg and cross beam elements are verified at the ULS and SILS. SLS does not govern these elements and therefore SLS verifications are not performed. The tower leg design is governed by ULS seismic and SILS wind load combinations. The tower leg utilization ratios are generally between 0.95 and 1.0 for the governing load combination. The cross beam designs are governed by SILS transverse wind loads, with the critical stresses being a combination of shear and flexural compression. Maximum cross beam utilization ratios are approximately 0.9 for each cross beam, and vary more widely than for the tower leg because of the varying section depth and difference in the distributions of governing moments and shear forces.

The tower base anchorage comprises prestressed multi-strand tendons, local tower leg plate stiffening and a thick steel base plate. The base anchorage is verified to have sufficient pretension to prevent decompression under all SLS, ULS and SILS loads (tensile stresses beneath the base plate). Tendon sizes and other base anchorage components are generally governed by SLS2 loading during construction and ULS/SILS in the completed bridge.

Tower components are assessed for the FLS considering the effects of railway loading and fatigue level wind loading (cross beams only). Fatigue stresses are verified to be less than the stress limit for the detail category and the anticipated number of stress cycles.

The tower analysis and verification procedures are in general accordance with the design basis and NTC08, supplemented as necessary with the various Eurocodes.

Appendix A: Comparison of Time-History and Response Spectrum Seismic Force Effects

In this appendix detailed tower leg ULS time-history seismic analysis results from each time-history input are presented with the mean results used for design and the response spectrum seismic analysis (RSA) results.

Analysis results for the Sicilia tower are shown in Figure A-1 to Figure A-5. In each figure, the maximum positive and negative values for each time-history input are plotted in the same colour. The mean time-history force effects are represented by the solid black line and the RSA results are represented by the dashed black line. The plotted time-history results are the governing effects of the longitudinal or transverse dominant combination (based on (1.0 or 0.8) x Longitudinal + (0.8 or 1.0) x Transverse + 0.75 x Vertical). The plotted RSA results are the governing effects of the longitudinal, transverse or vertical dominant combinations (based on (1.0 or 0.3 or 0.3) x Longitudinal + (0.3 or 1.0 or 0.3) x Transverse + (0.3 or 0.3 or 1.0) x Vertical).

The agreement between the time-history force effects and RSA force effects is generally good with the RSA results generally within the range of time-history results. The apparent disagreement between the time-history and RSA axial forces reveals some of the limitations of the RSA method. The maximum RSA tower axial loads of approximately 600 MN (negative and most compressive) are caused by the vertical dominant combination; the maximum axial demand from the transverse dominant combination is approximately 450 MN and that from the longitudinal dominant combination is 385 MN, both of which are in much better agreement with the time-history results. The largest seismic axial loads in the tower legs are caused by vertical modes that in reality are heavily damped by soil-structure interaction. Although the RSA with a constant 5% damping sufficiently addresses the superstructure behaviour and provides reasonably representative damping for predicting shear and flexural loads in the tower legs, it underestimates the damping present for vertical tower modes. The tender design RSA considered composite modal damping, for which the damping of a particular mode was calculated as a weighted average of the damping values associated with the movements of particular structure components in the mode. This approach resulted in modal damping ratios of up to 18%, and much better agreement between the axial forces predicted by the time-history and RSA. Therefore, the time-history and RSA axial force results can not be expected to agree as well as they do for other force effects, and the results of the time-history analyses are more appropriate.

Coefficients of variation (COV) for the Sicilia tower leg time-history force effects are shown in Figure A-6. The raw output from the time-history analysis suggests COVs generally between 10% and 20% for each force effect over the tower height. Although these values are reasonable and expected for non-linear time-history analyses completed using partially artificial input motions, they must be considered in light of the dispersion of the input motions, as described in General Design Principles Section 5.2.4. Dispersion of the time-history inputs contributes to the variability in the time-history responses. This contribution must be considered when evaluating the statistical characteristics of the tower responses to the eight inputs. Considering the 6% COV in the input motions based on a 5% damped spectrum or the 12% COV based on the equivalent 2% damped spectrum, the COVs shown in Figure A-6 are limited and meet the requirements in GCG.F.05.03 Section 5.1 for using the mean results for design.

Analysis results for the Calabria tower are shown in Figure A-7 to Figure A-11. The comments on the output for the Sicilia tower apply equally to the Calabria tower output.

Coefficients of variation for the Calabria tower leg time-history force effects are shown in Figure A-12. The COVs are typically slightly larger than those shown for the Sicilia tower. However, similar to the Sicilia tower, when considered in light of the variability of the input motions the dispersion of the output is limited and reasonable for the type of analysis performed.

Also included at the end of this appendix in Figure A-13 to Figure A-36 are traces of the tower base and tower leg segment 17 axial forces, longitudinal moments and transverse moments for both towers as a function of time for each of the Sicilia and Calabria time-history inputs.

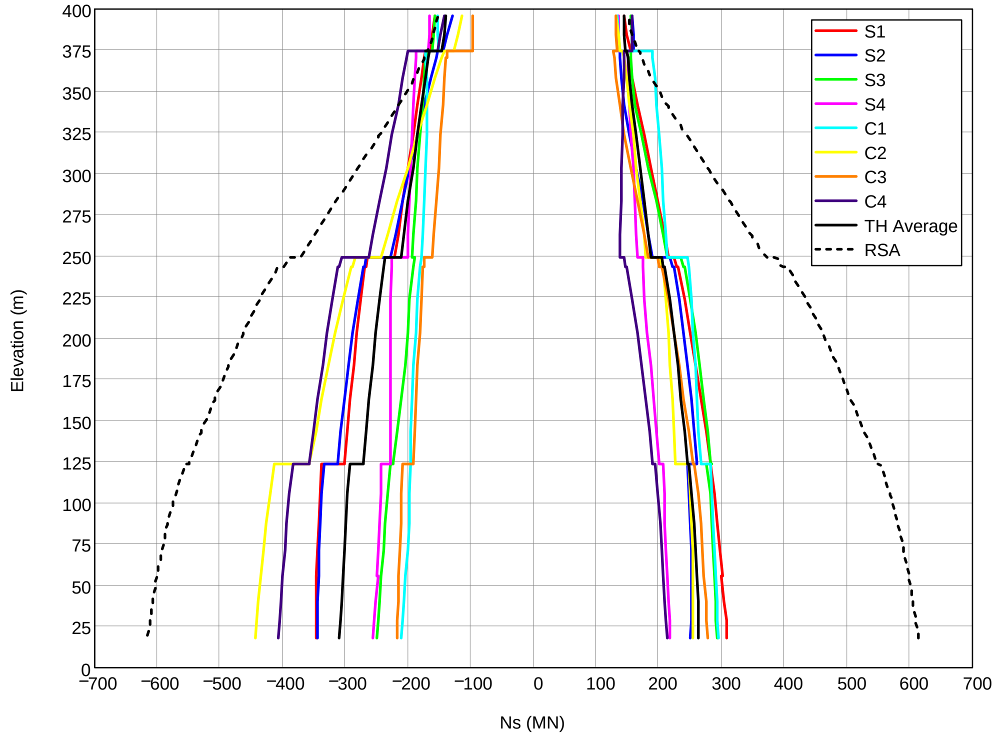

Figure A-1: Sicilia tower seismic axial loads.

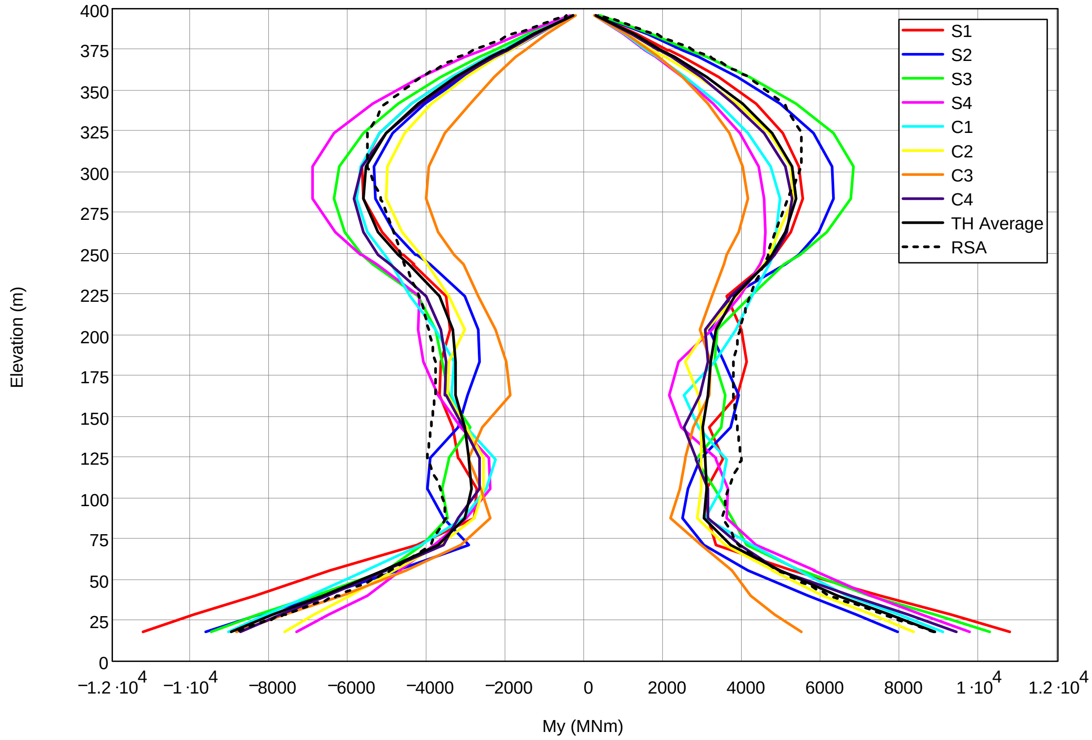

Figure A-2: Sicilia tower seismic longitudinal moments.

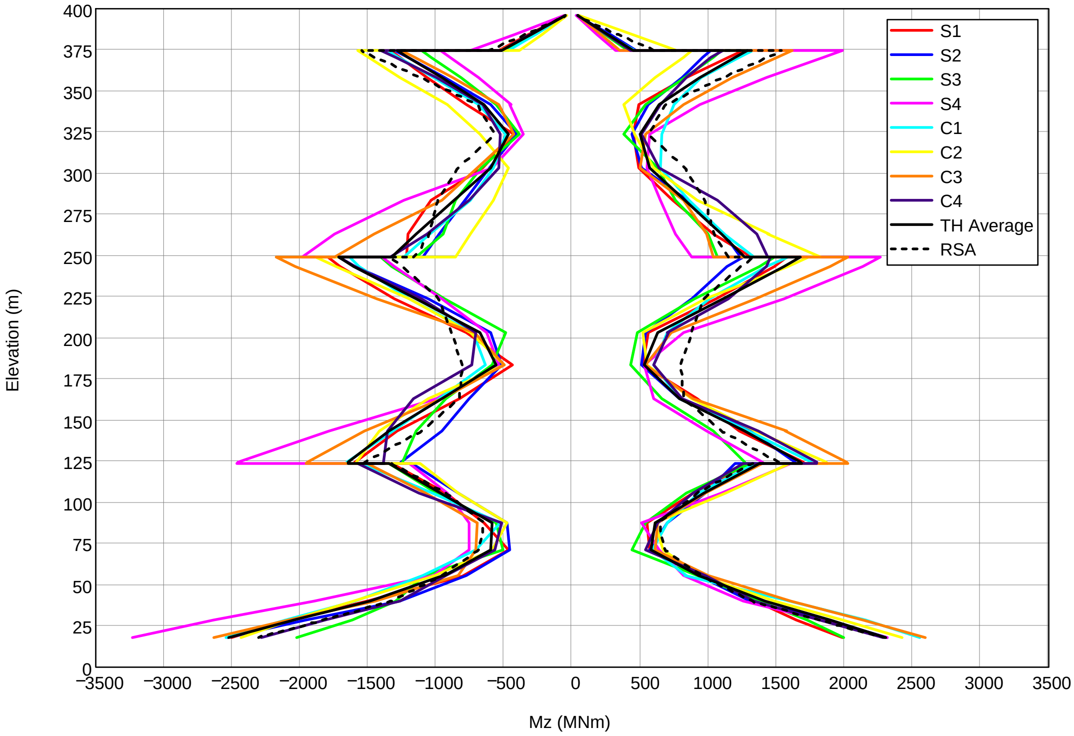

Figure A-3: Sicilia tower seismic transverse moments.

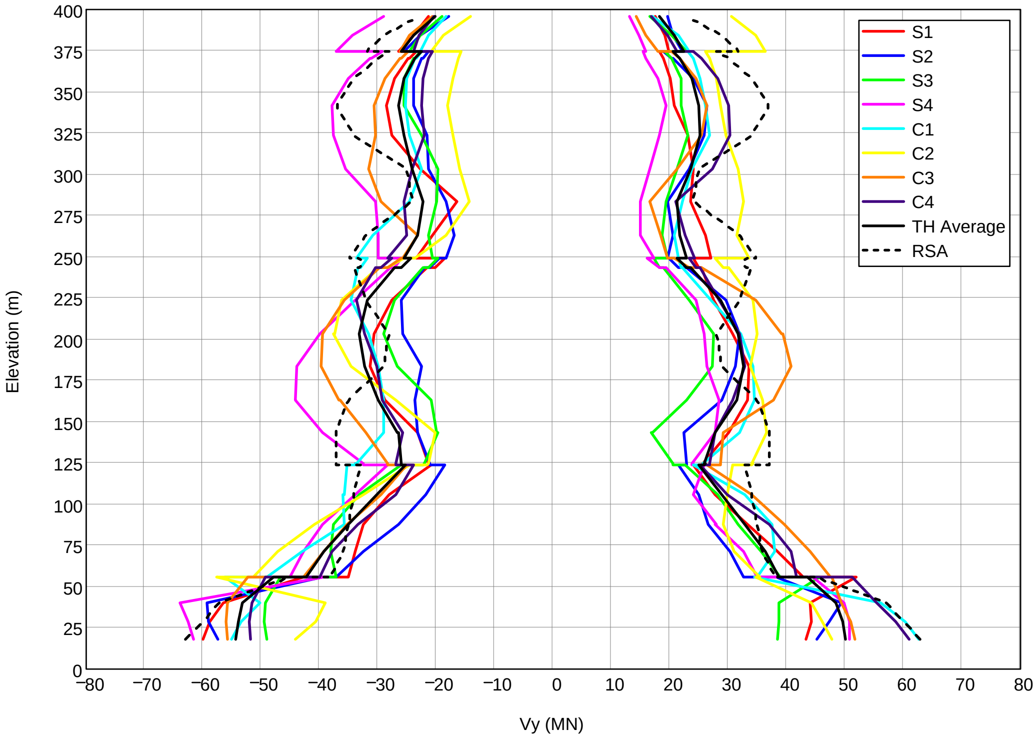

Figure A-4: Sicilia tower seismic transverse shear forces.

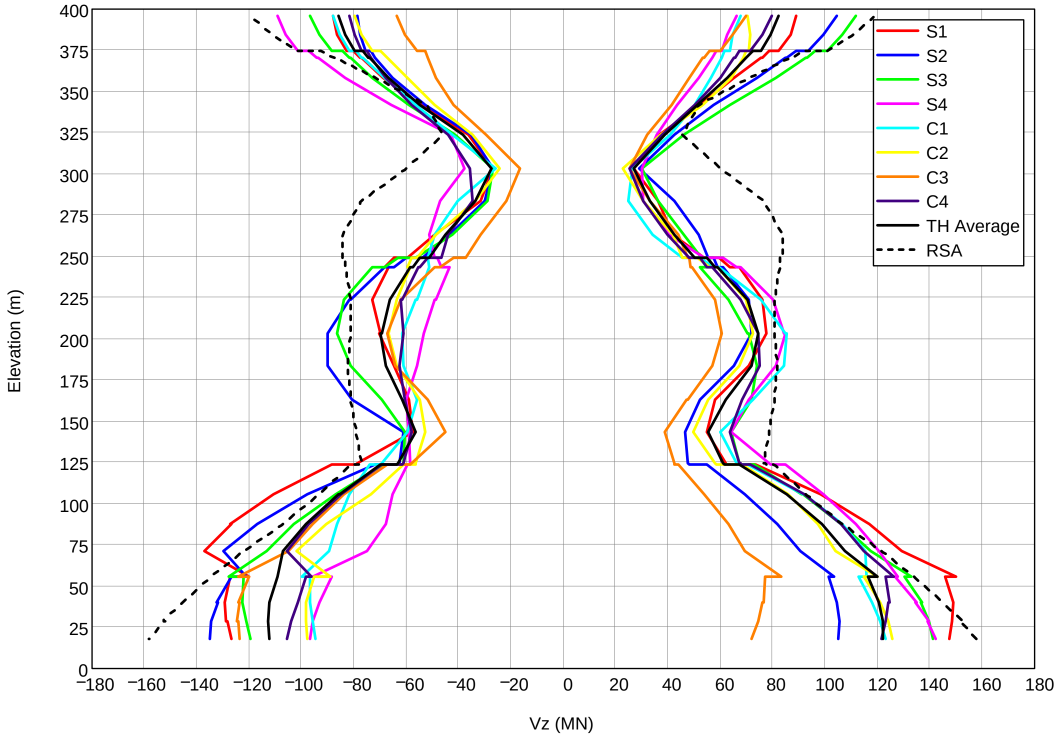

Figure A-5: Sicilia tower seismic longitudinal shear forces.

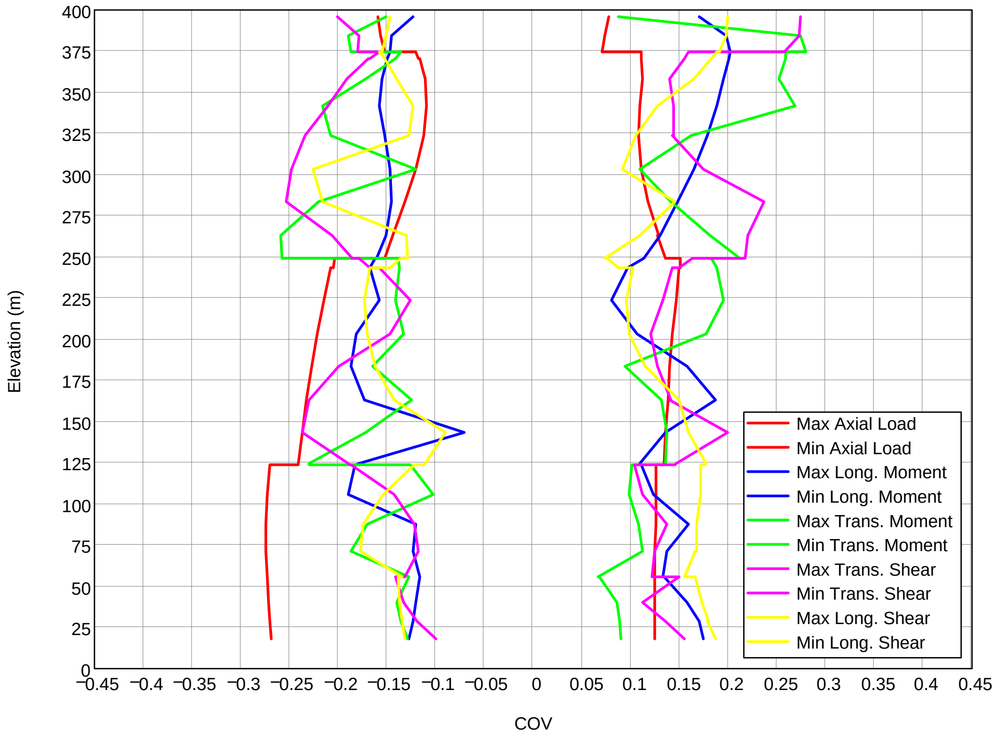

Figure A-6: Coefficients of variation for the Sicilia tower time-history output.

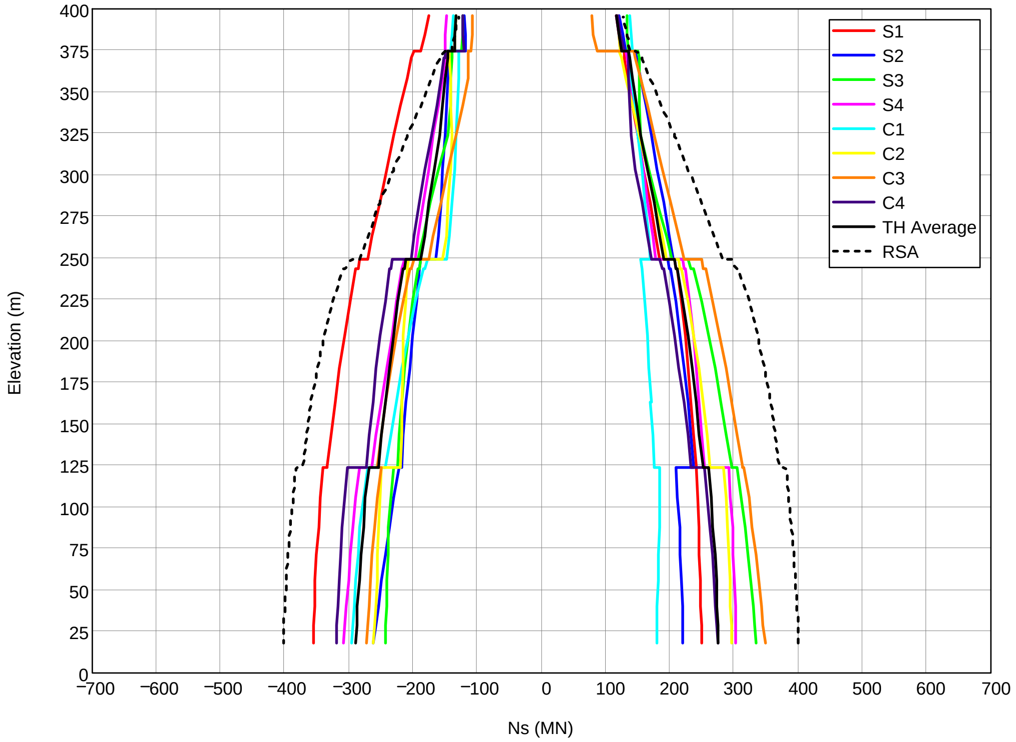

Figure A-7: Calabria tower seismic axial loads.

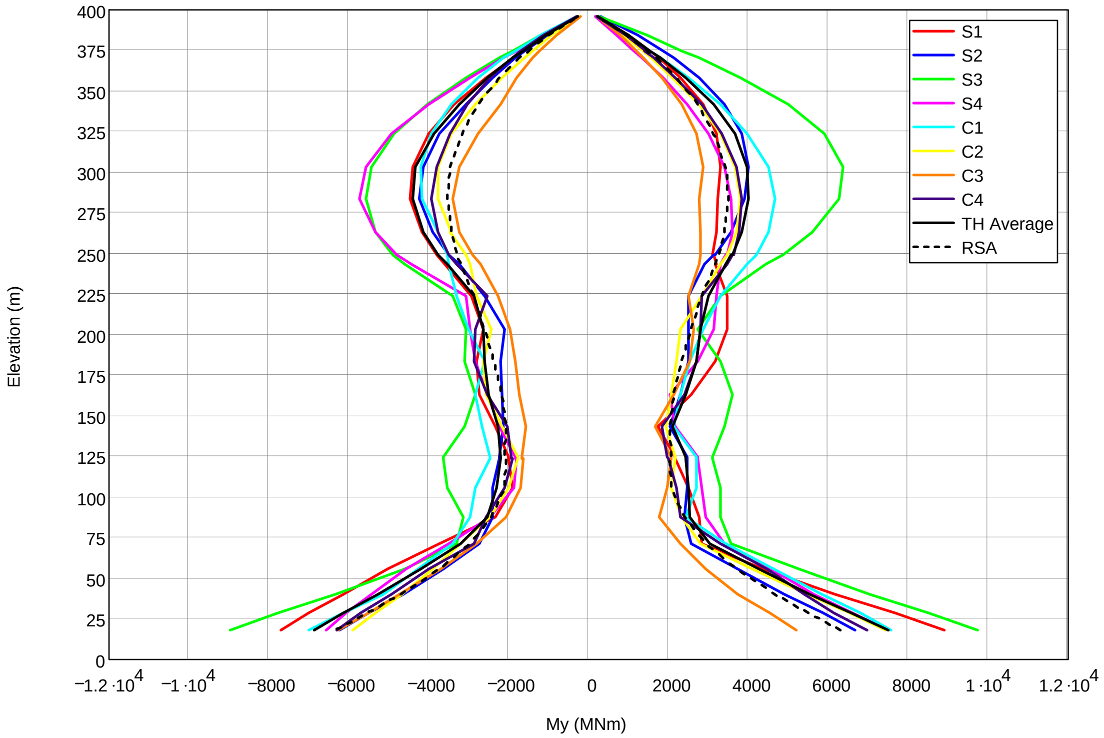

Figure A-8: Calabria tower seismic longitudinal moments.

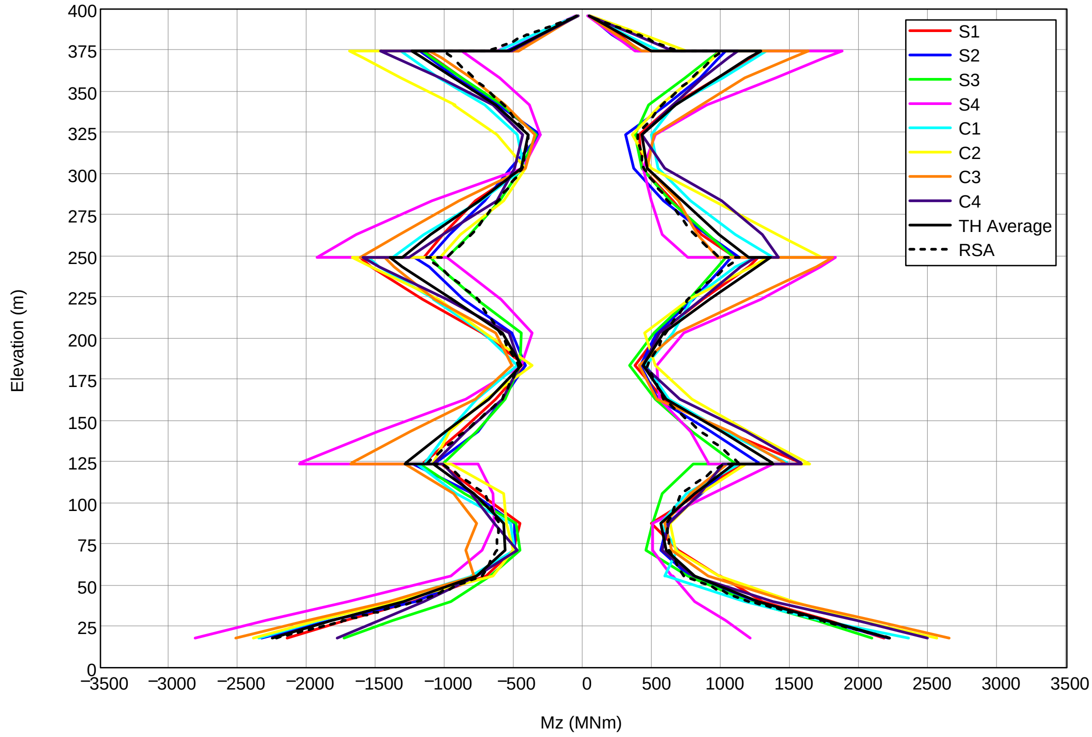

Figure A-9: Calabria tower seismic transverse moments.

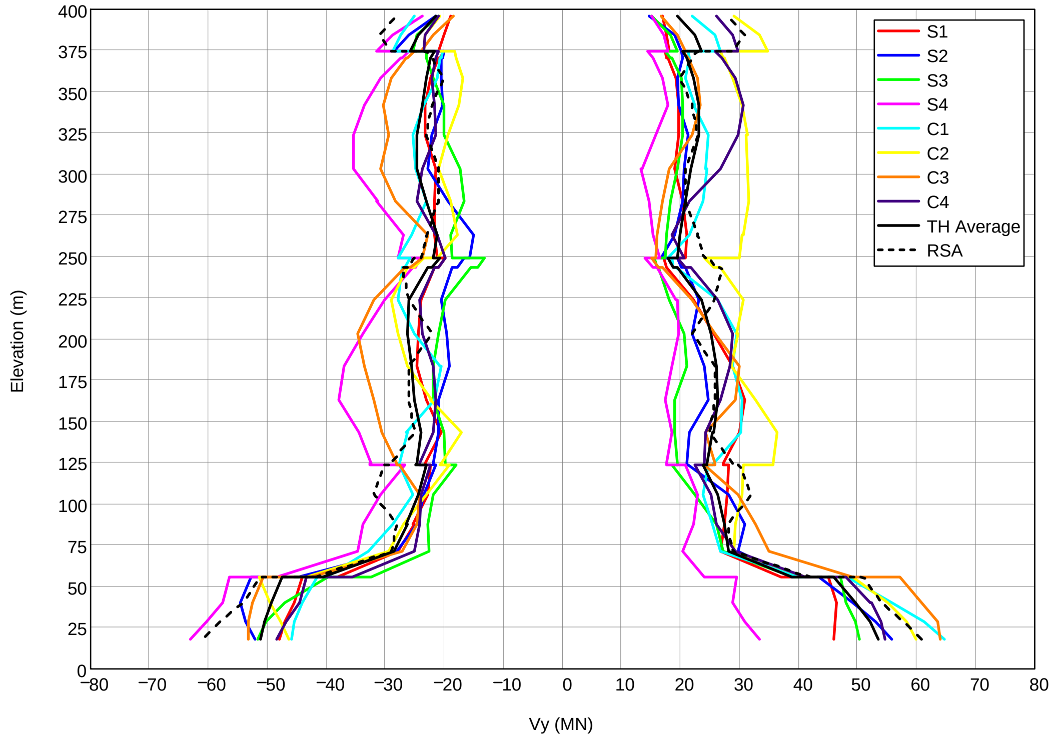

Figure A-10: Calabria tower seismic transverse shear forces.

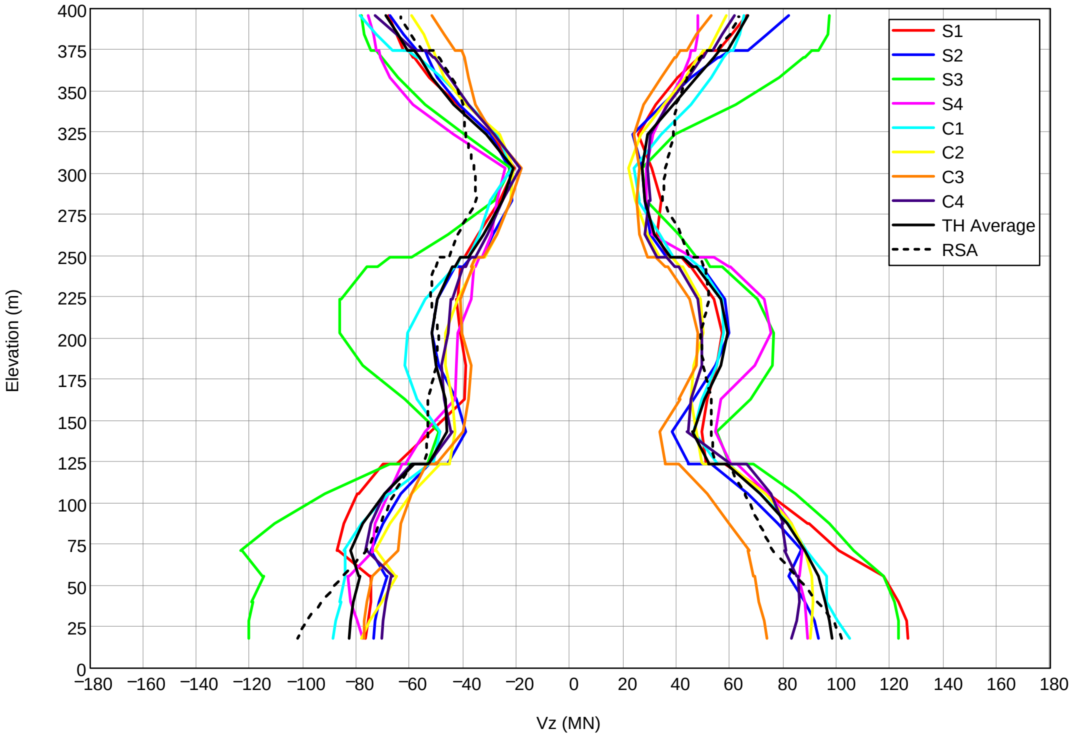

Figure A-11: Calabria tower seismic longitudinal shear forces.

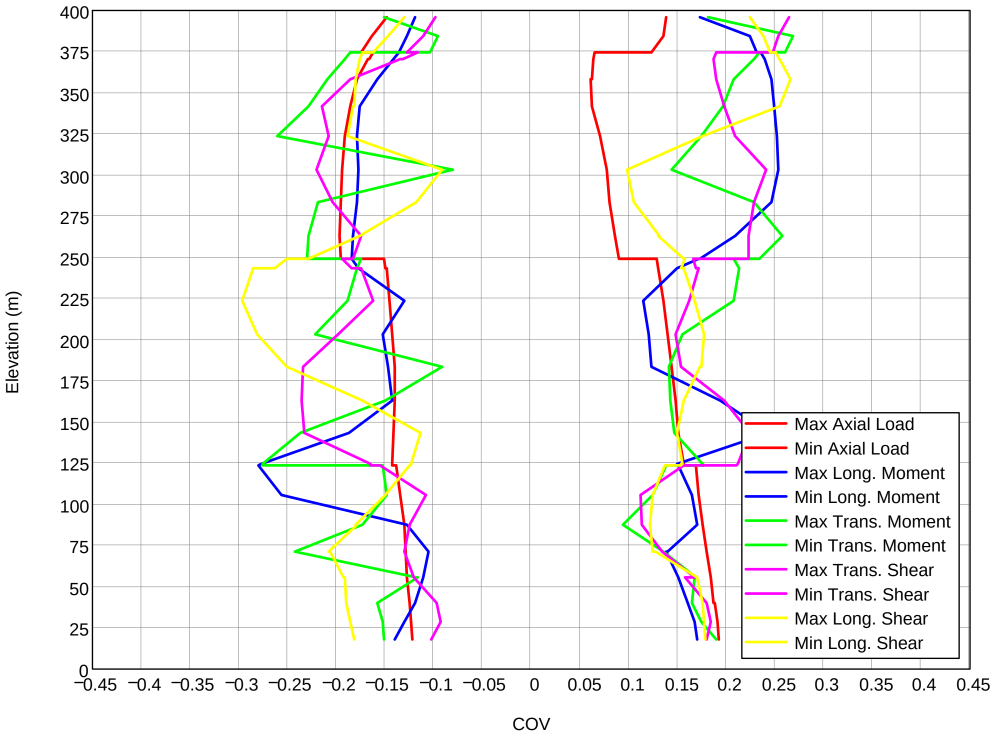

Figure A-12: Coefficients of variation for the Calabria tower time-history output.

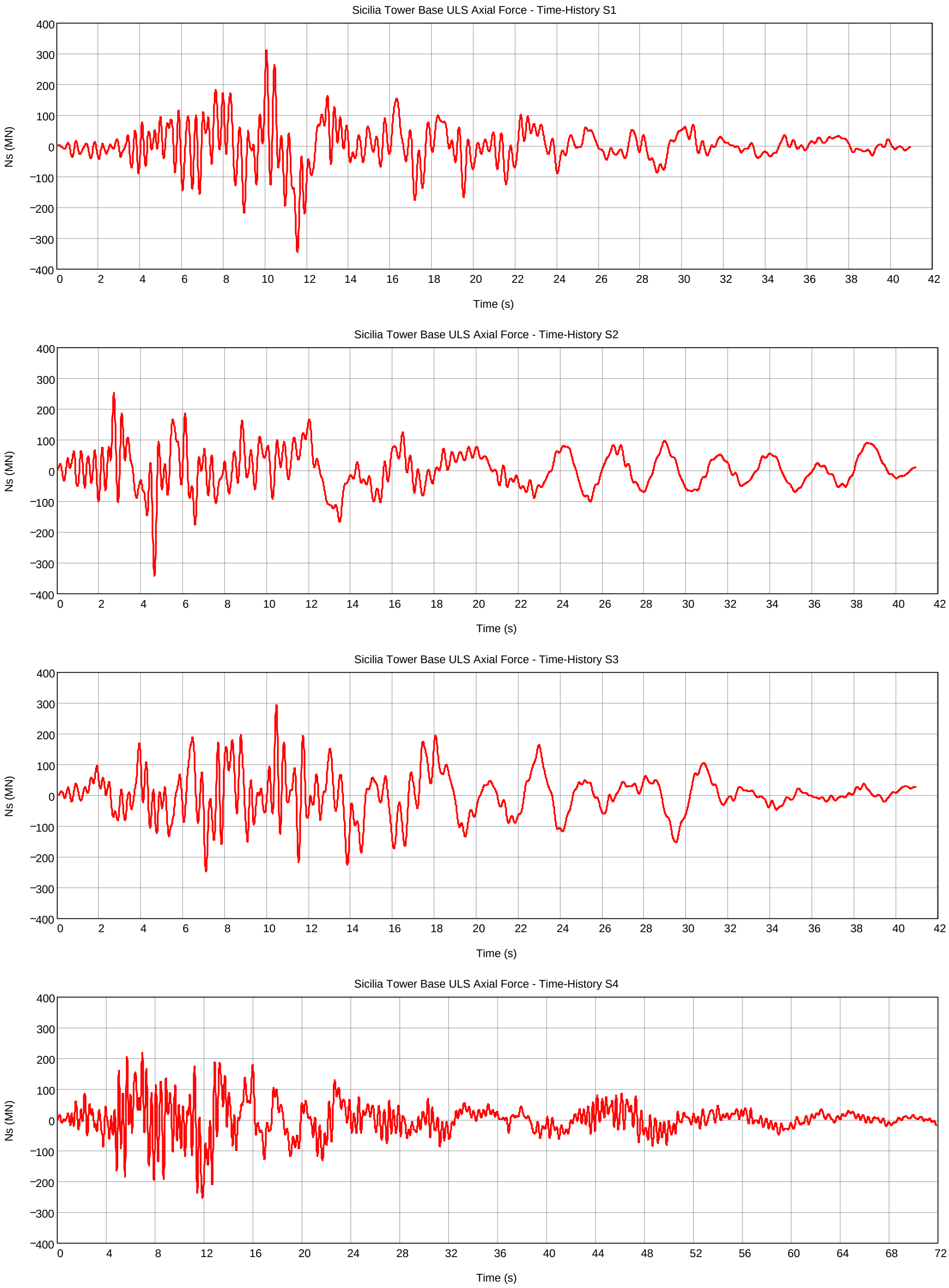

Figure A-13: Sicilia tower base ULS seismic axial loads as a function of time for Sicilia time-history inputs 1 to 4.

Figure A-14: Sicilia tower base ULS seismic axial loads as a function of time for Calabria time-history inputs 1 to 4.

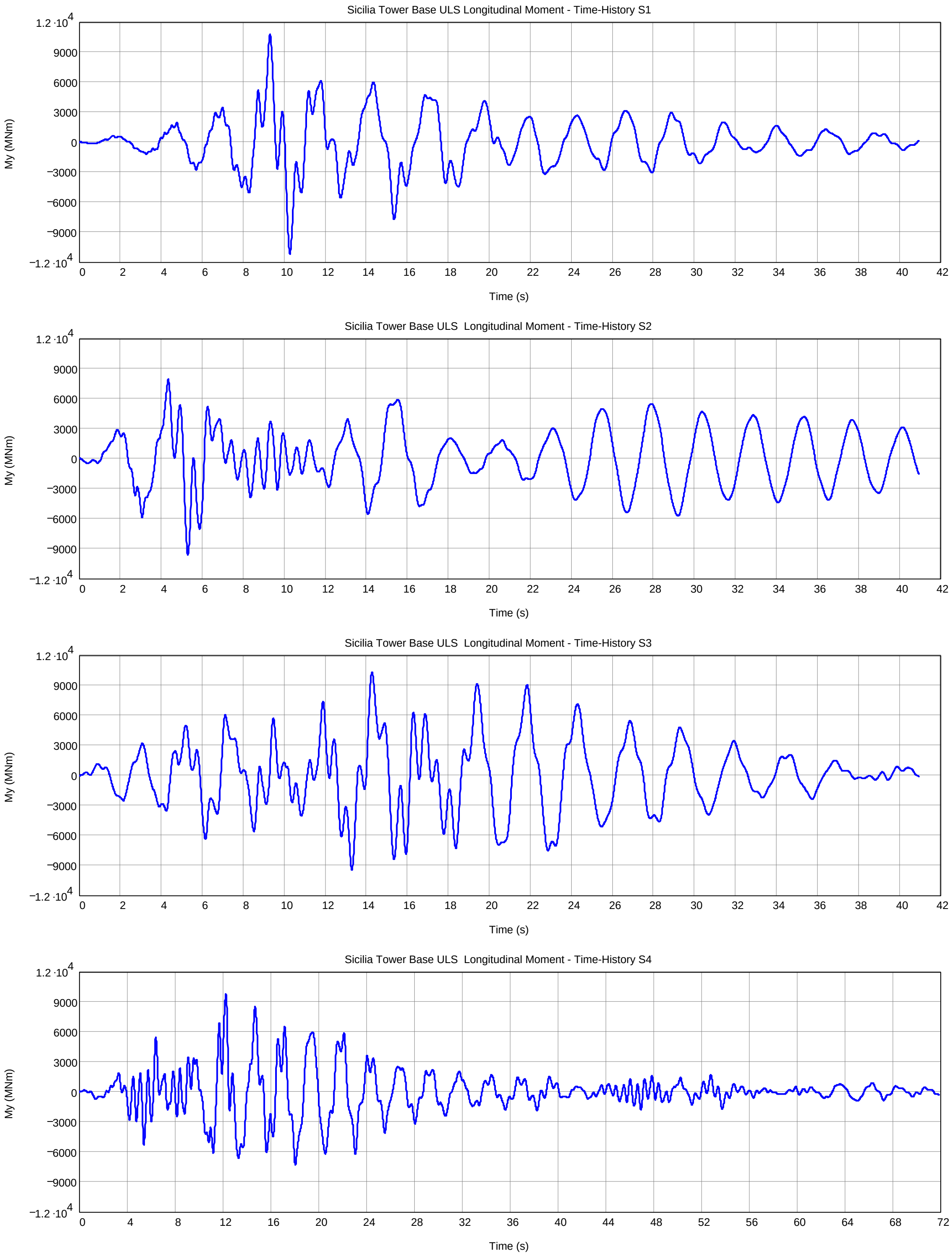

Figure A-15: Sicilia tower base ULS seismic longitudinal moments as a function of time for Sicilia time-history inputs 1 to 4.

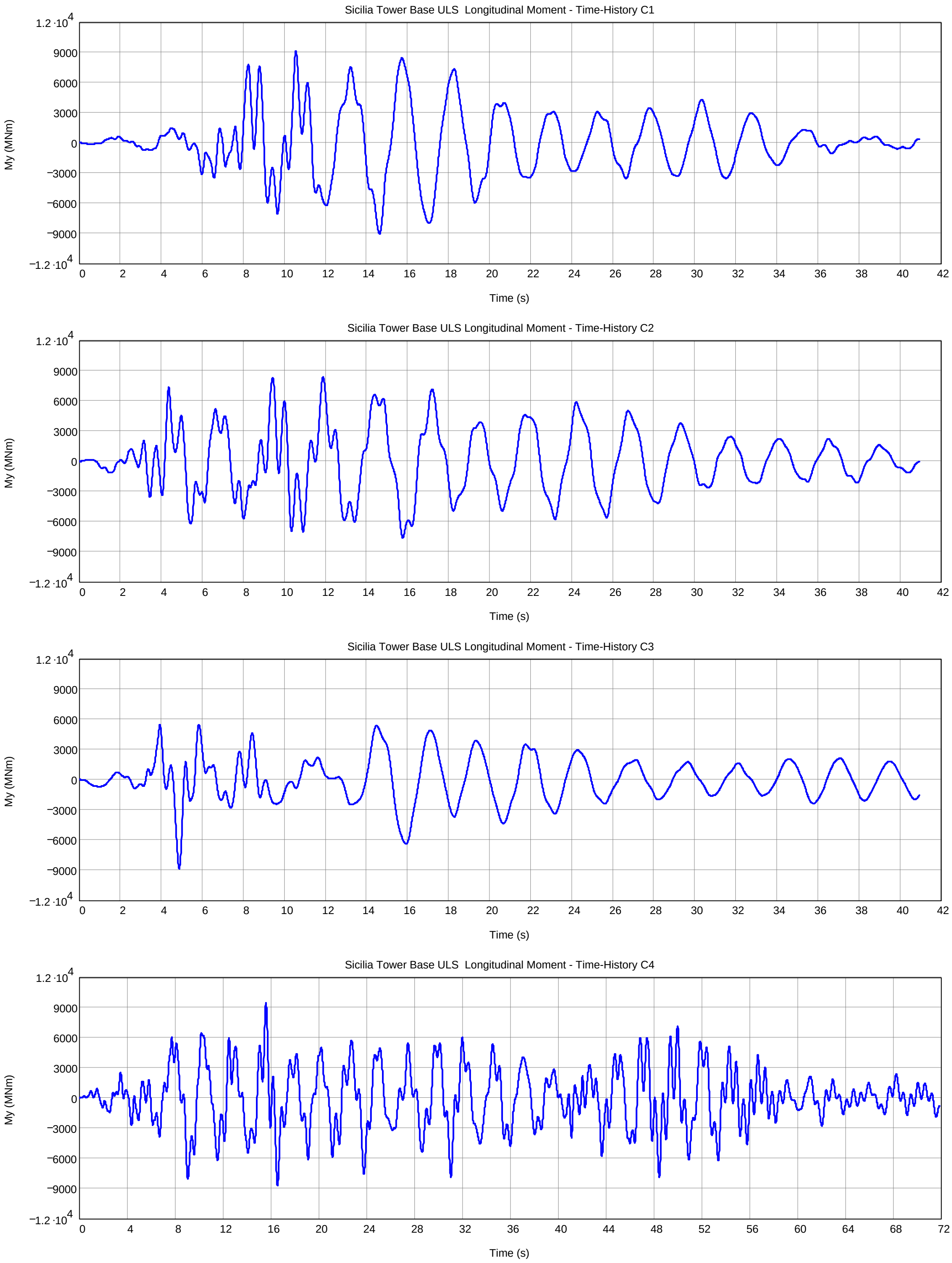

Figure A-16: Sicilia tower base ULS seismic longitudinal moments as a function of time for Calabria time-history inputs 1 to 4.

Figure A-17: Sicilia tower base ULS seismic transverse moments as a function of time for Sicilia time-history inputs 1 to 4.

Figure A-18: Sicilia tower base ULS seismic transverse moments as a function of time for Calabria time-history inputs 1 to 4.

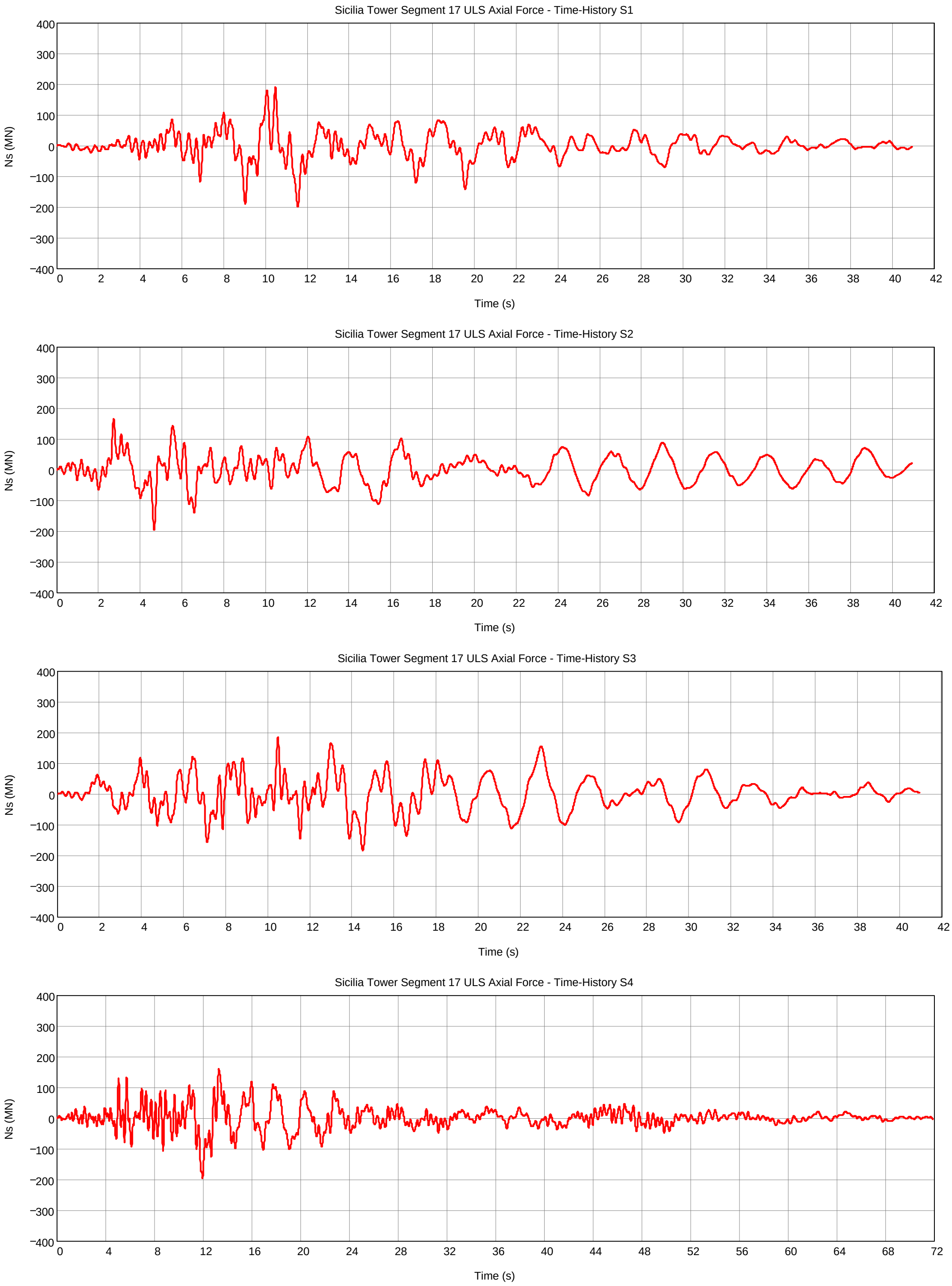

Figure A-19: Sicilia tower leg segment 17 ULS seismic axial loads as a function of time for Sicilia time-history inputs 1 to 4.

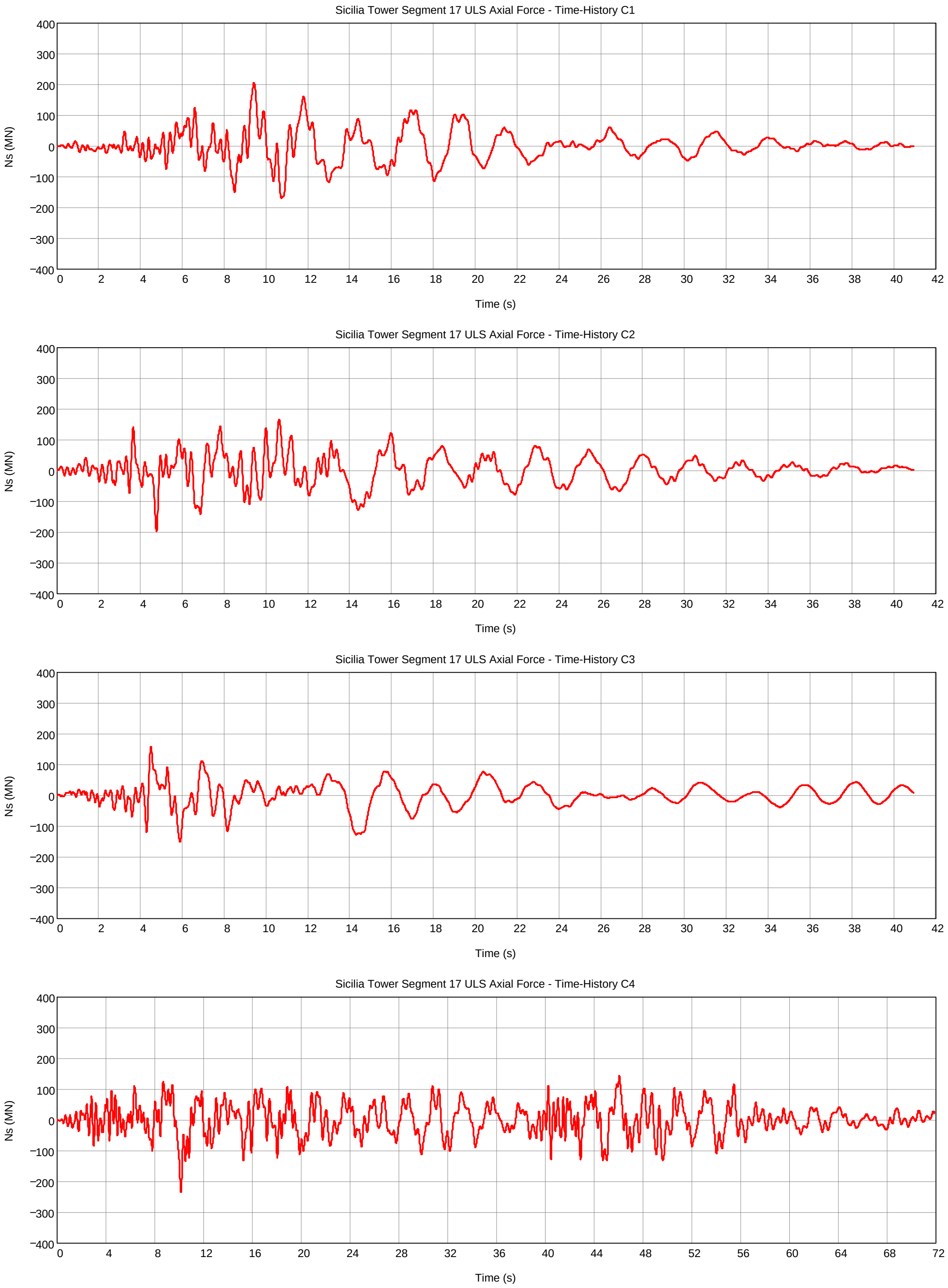

Figure A-20: Sicilia tower leg segment 17 ULS seismic axial loads as a function of time for Calabria time-history inputs 1 to 4.

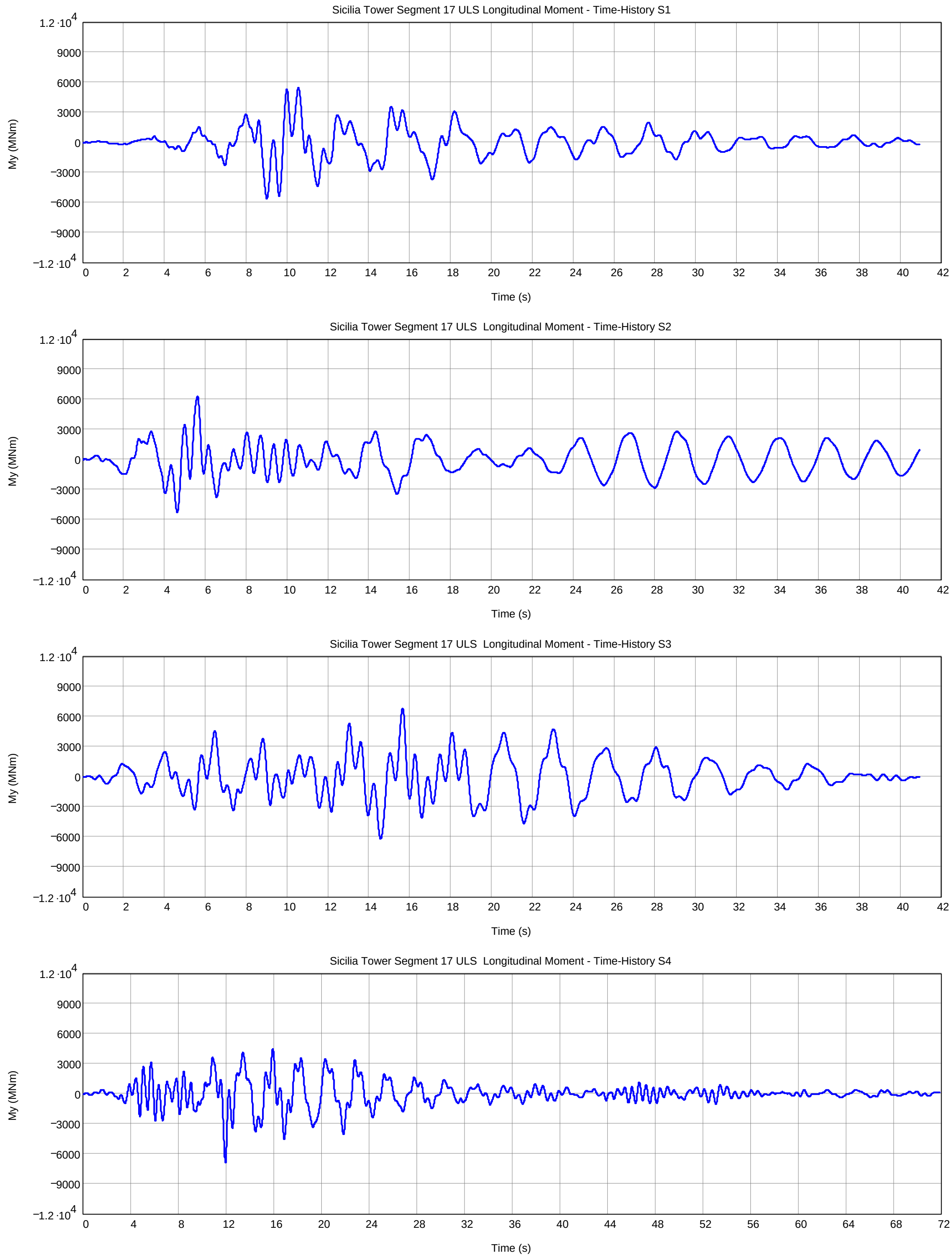

Figure A-21: Sicilia tower leg segment 17 ULS seismic longitudinal moments as a function of time for Sicilia time-history inputs 1 to 4.

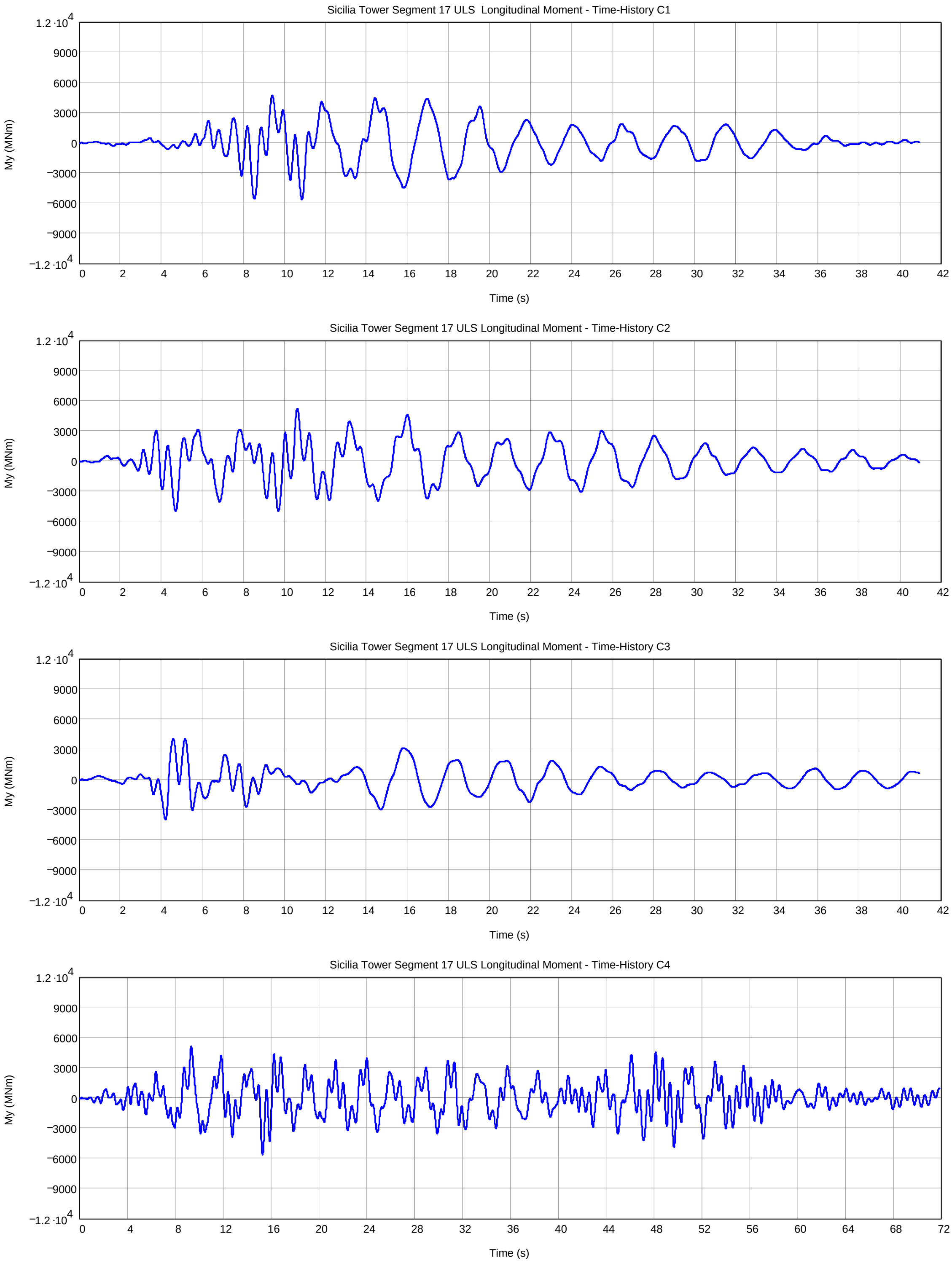

Figure A-22: Sicilia tower leg segment 17 ULS seismic longitudinal moments as a function of time for Calabria time-history inputs 1 to 4.

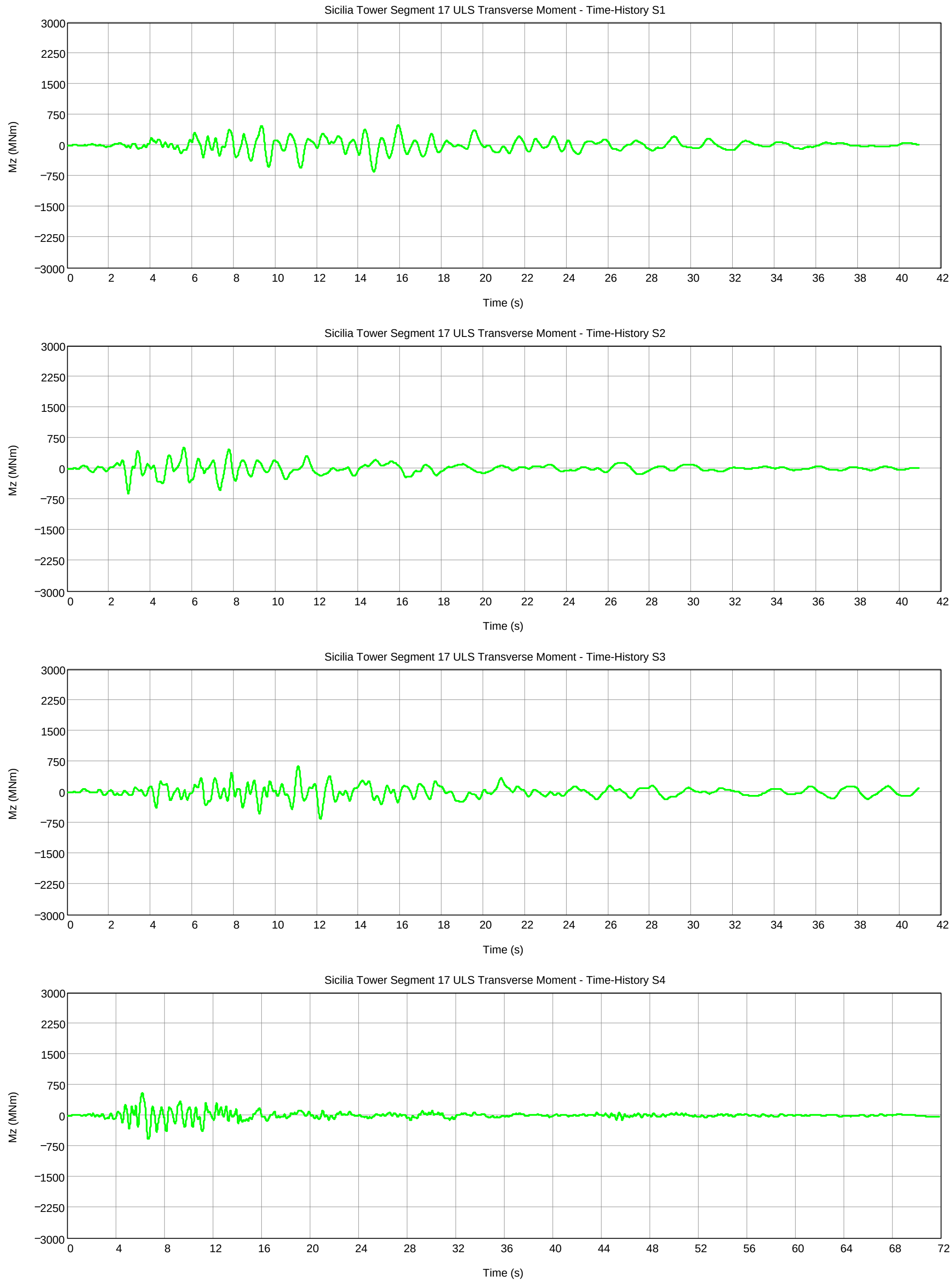

Figure A-23: Sicilia tower leg segment 17 ULS seismic transverse moments as a function of time for Sicilia time-history inputs 1 to 4.

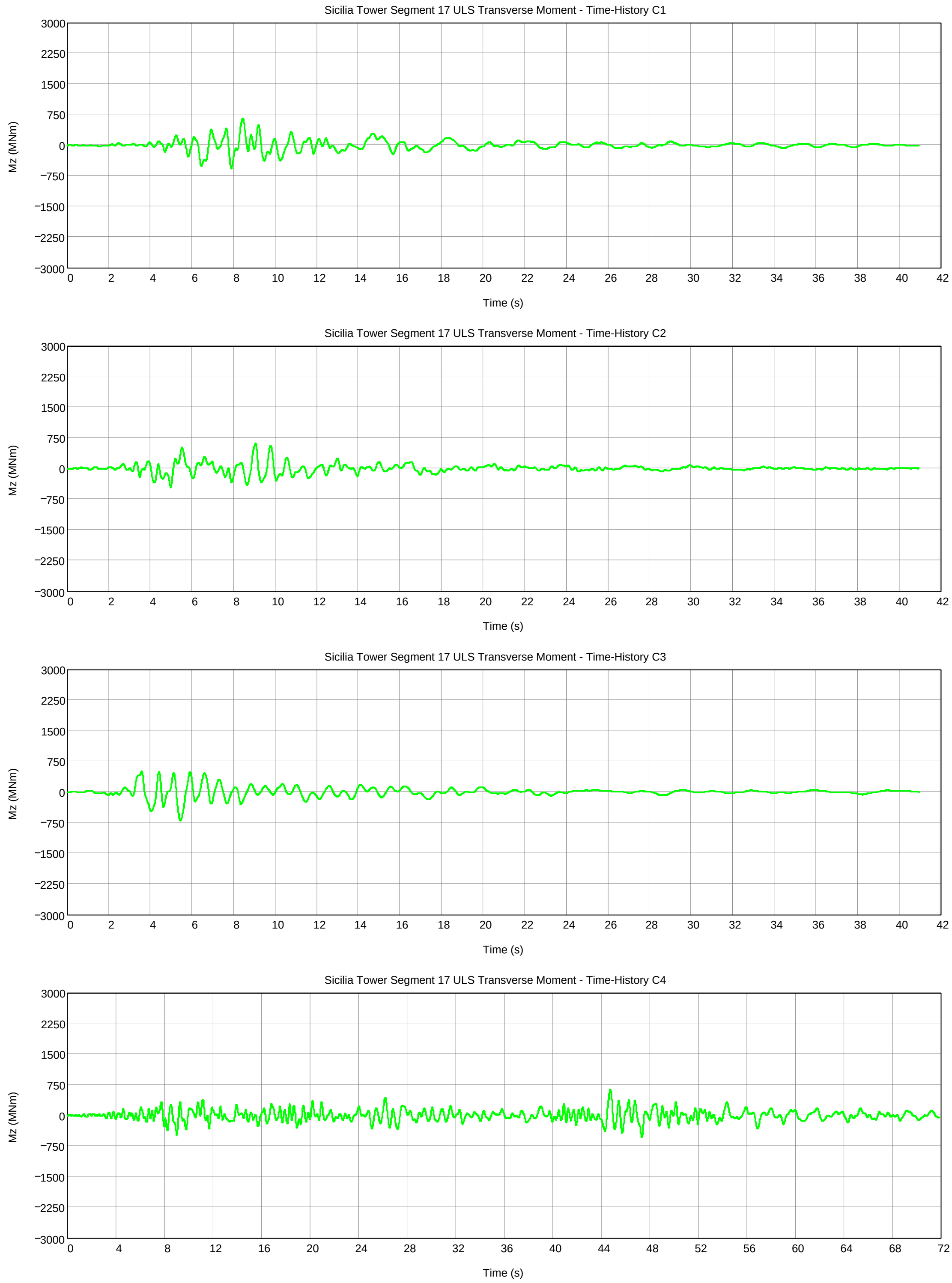

Figure A-24: Sicilia tower leg segment 17 ULS seismic transverse moments as a function of time for Calabria time-history inputs 1 to 4.

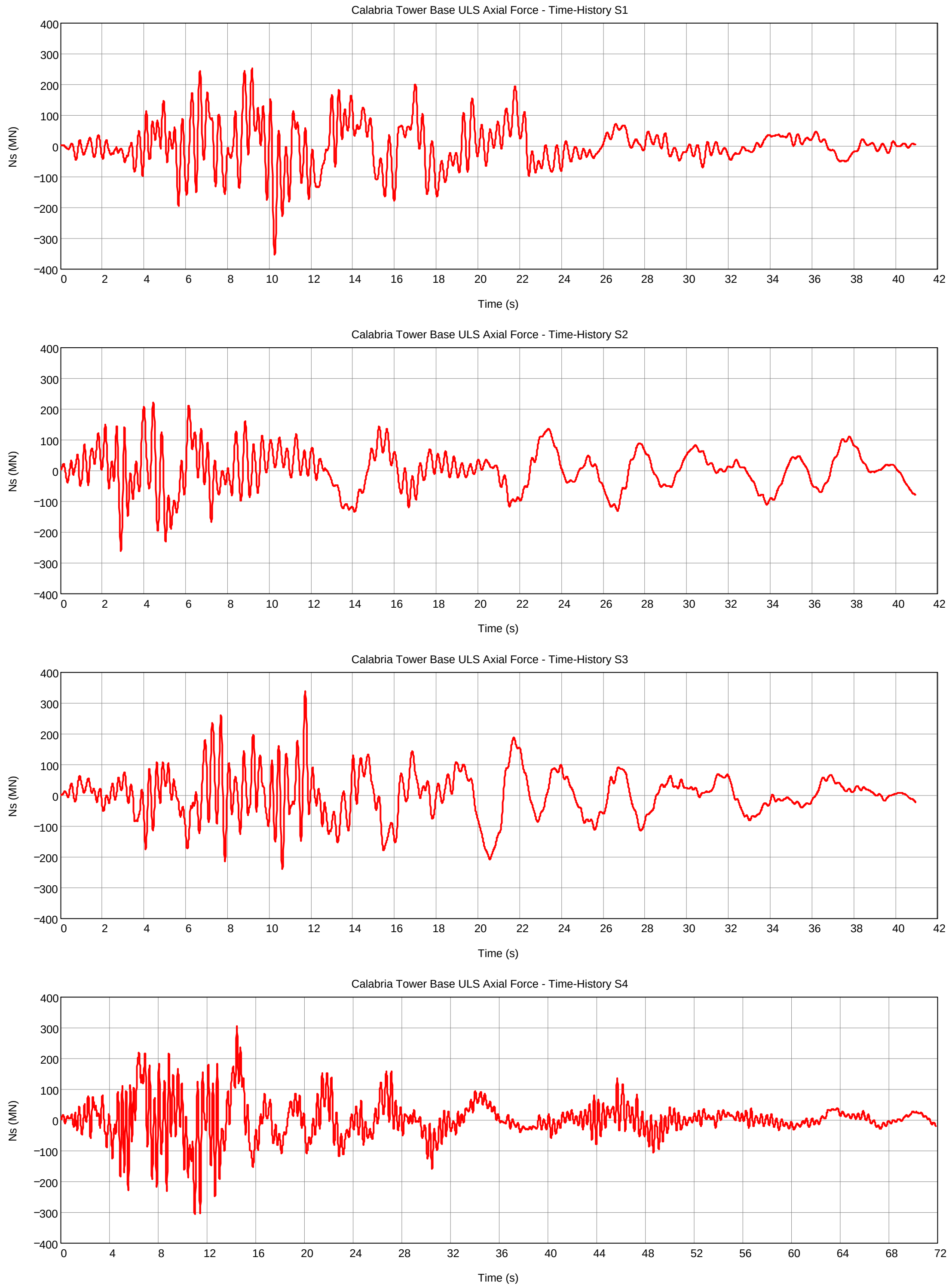

Figure A-25: Calabria tower base ULS seismic axial loads as a function of time for Sicilia time-history inputs 1 to 4.

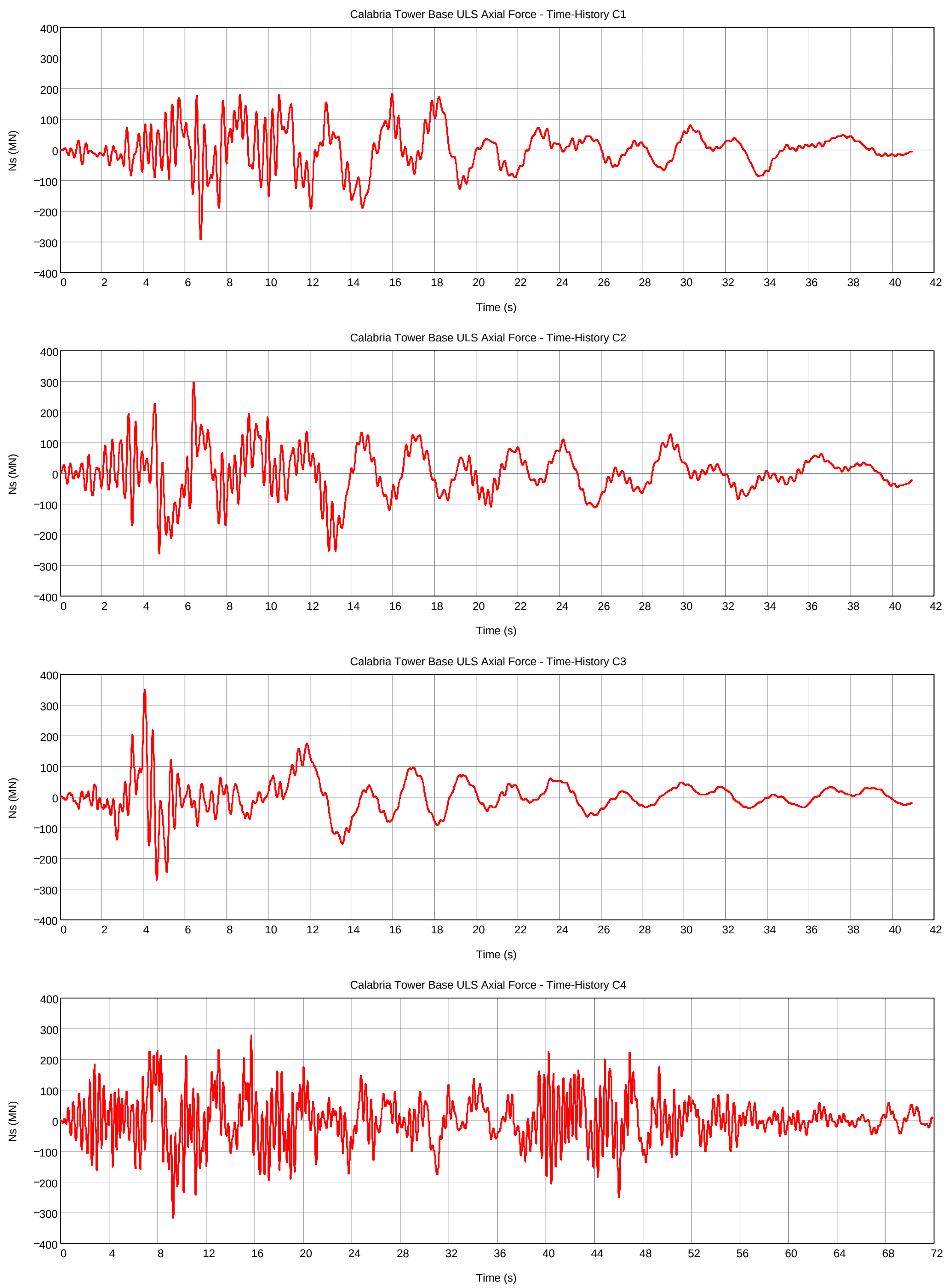

Figure A-26: Calabria tower base ULS seismic axial loads as a function of time for Calabria time-history inputs 1 to 4.

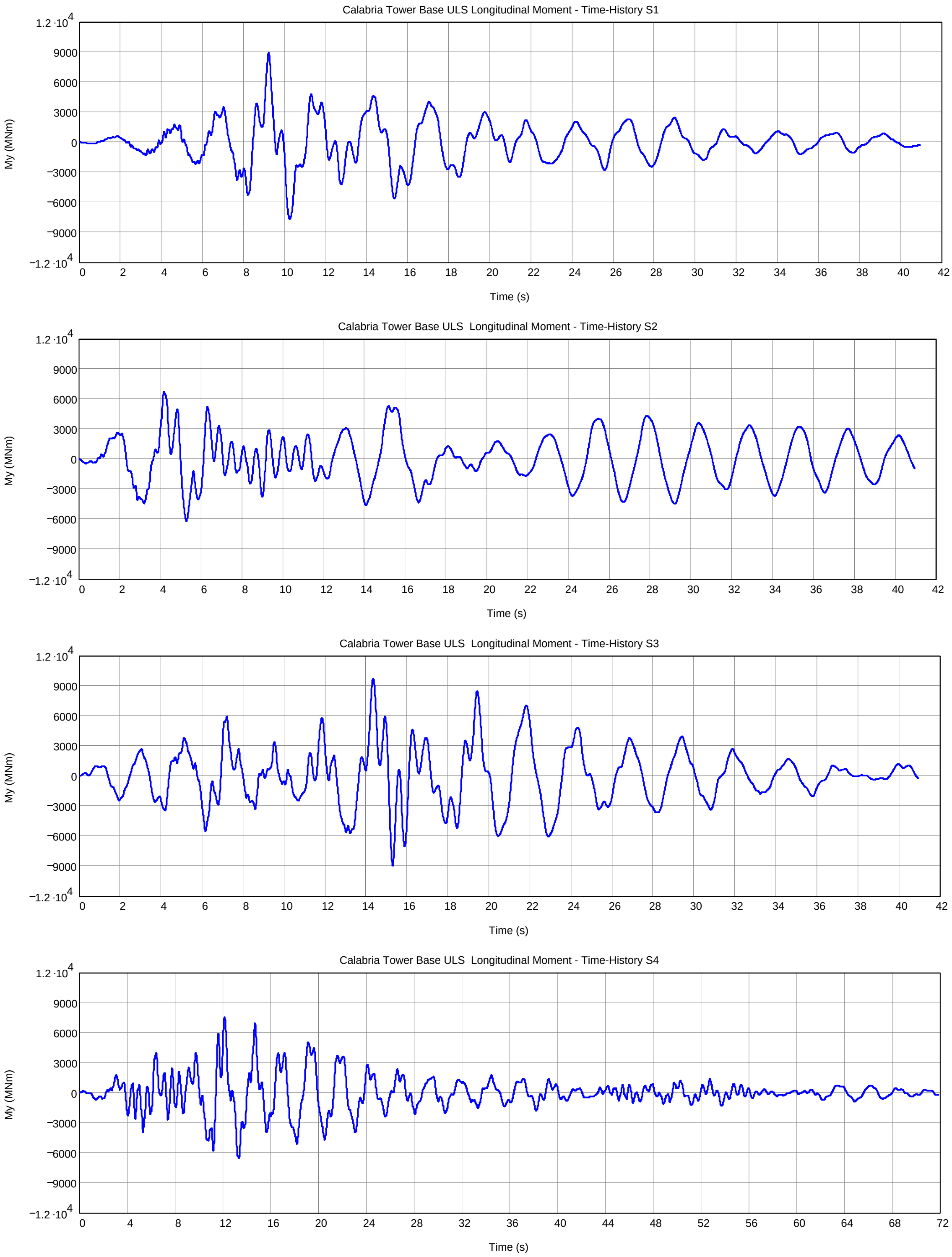

Figure A-27: Calabria tower base ULS seismic longitudinal moments as a function of time for Sicilia time-history inputs 1 to 4.

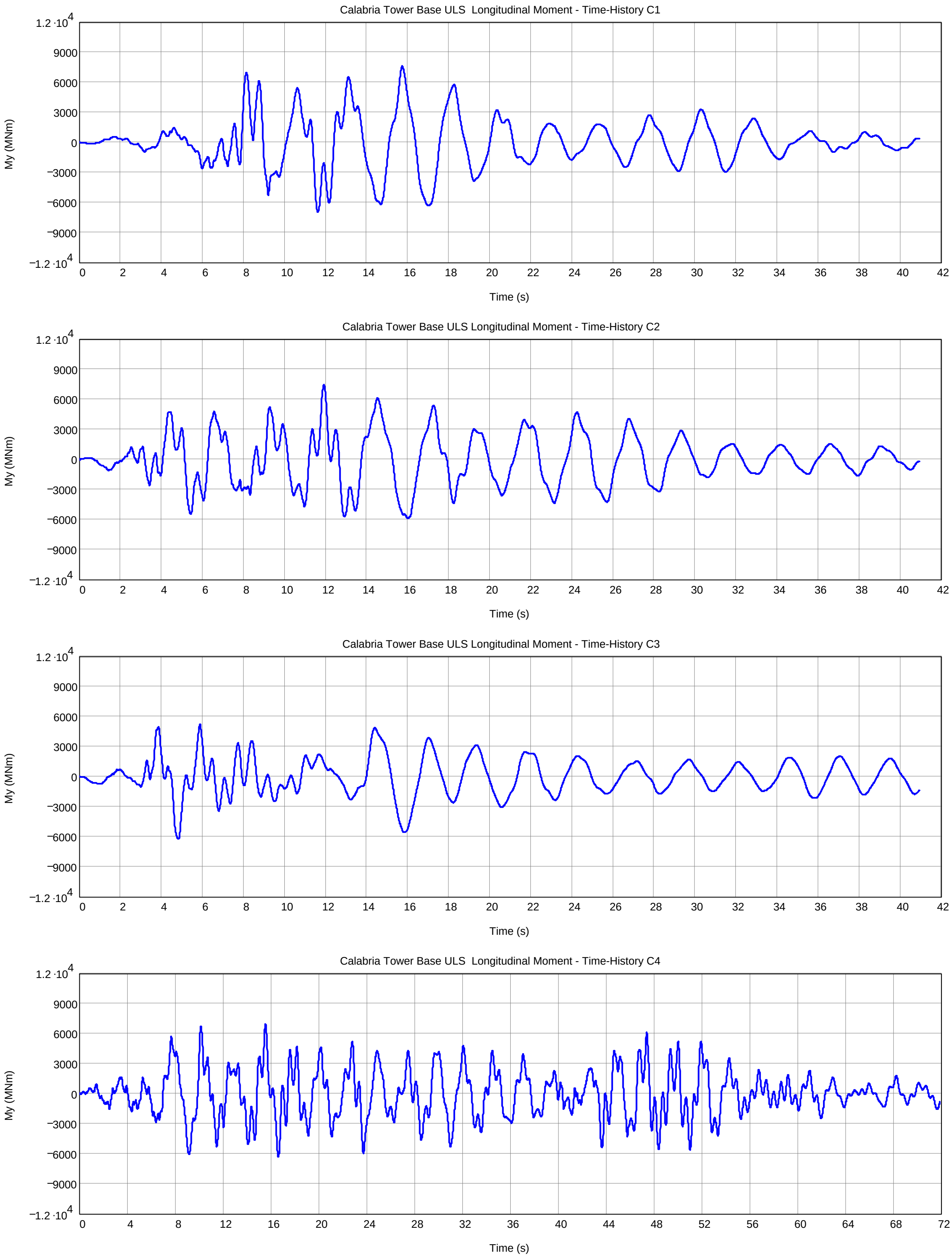

Figure A-28: Calabria tower base ULS seismic longitudinal moments as a function of time for Calabria time-history inputs 1 to 4.

Figure A-29: Calabria tower base ULS seismic transverse moments as a function of time for Sicilia time-history inputs 1 to 4.

Figure A-30: Calabria tower base ULS seismic transverse moments as a function of time for Calabria time-history inputs 1 to 4.

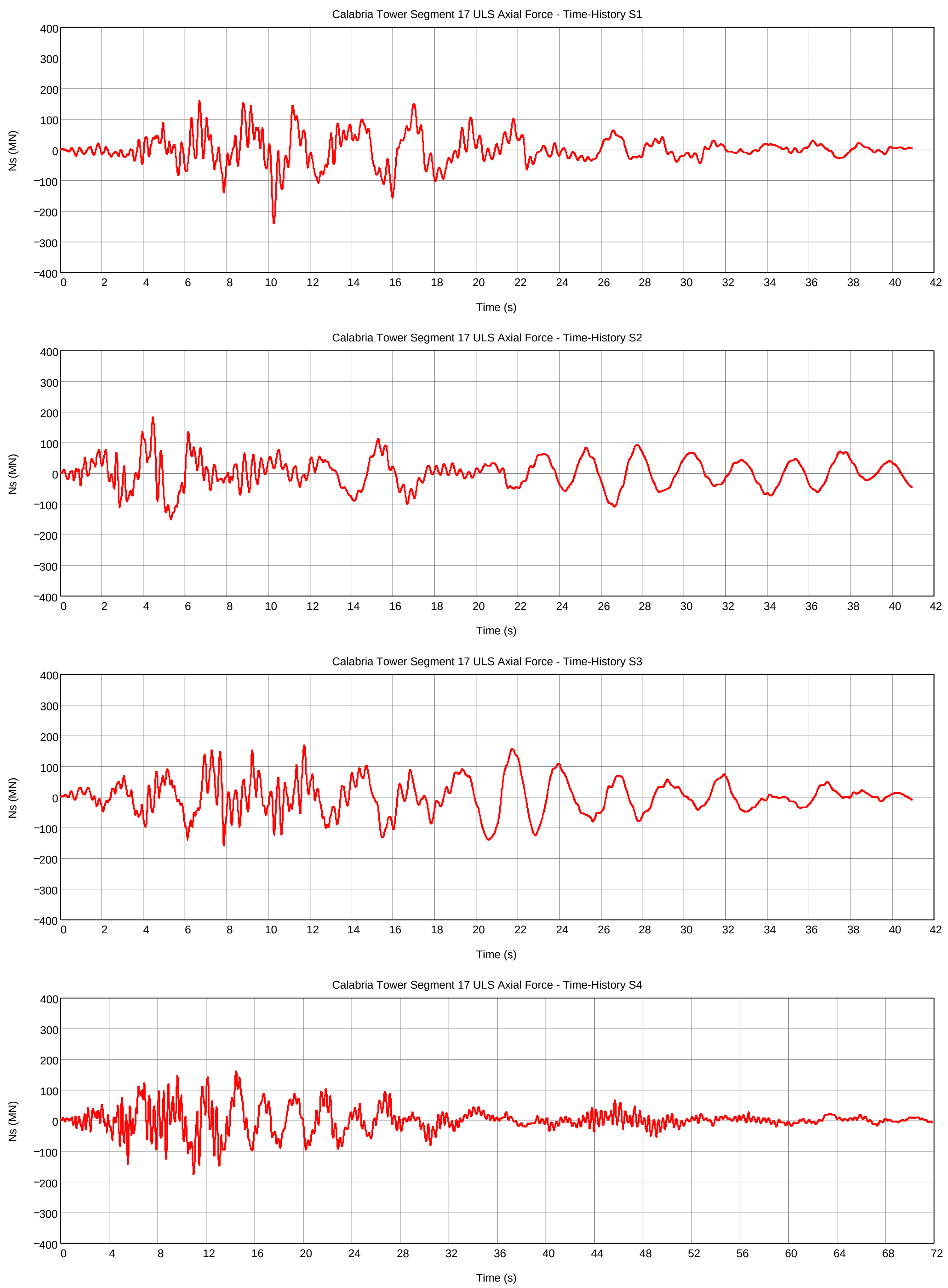

Figure A-31: Calabria tower leg segment 17 ULS seismic axial loads as a function of time for Sicilia time-history inputs 1 to 4.

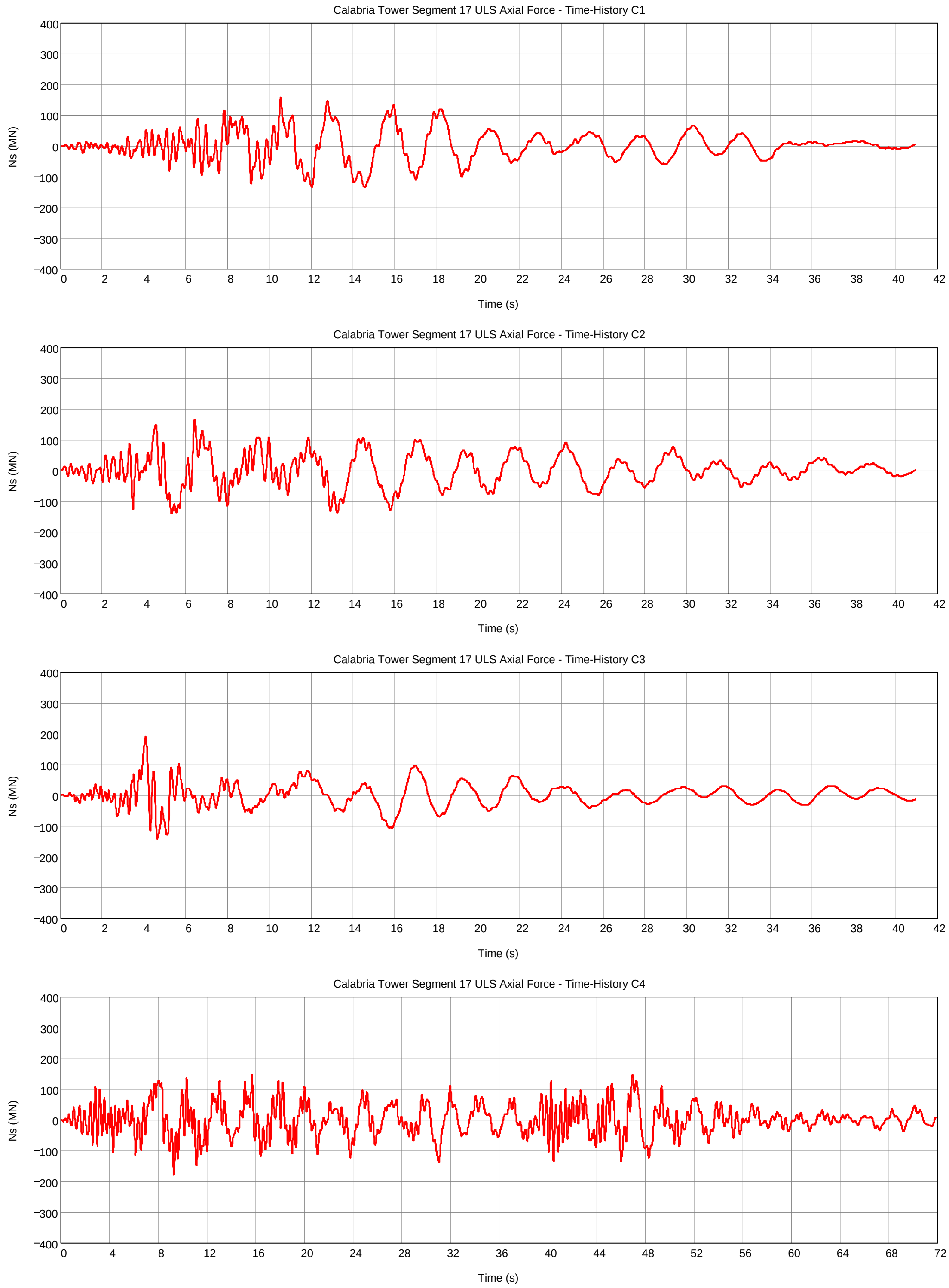

Figure A-32: Calabria tower leg segment 17 ULS seismic axial loads as a function of time for Calabria time-history inputs 1 to 4.

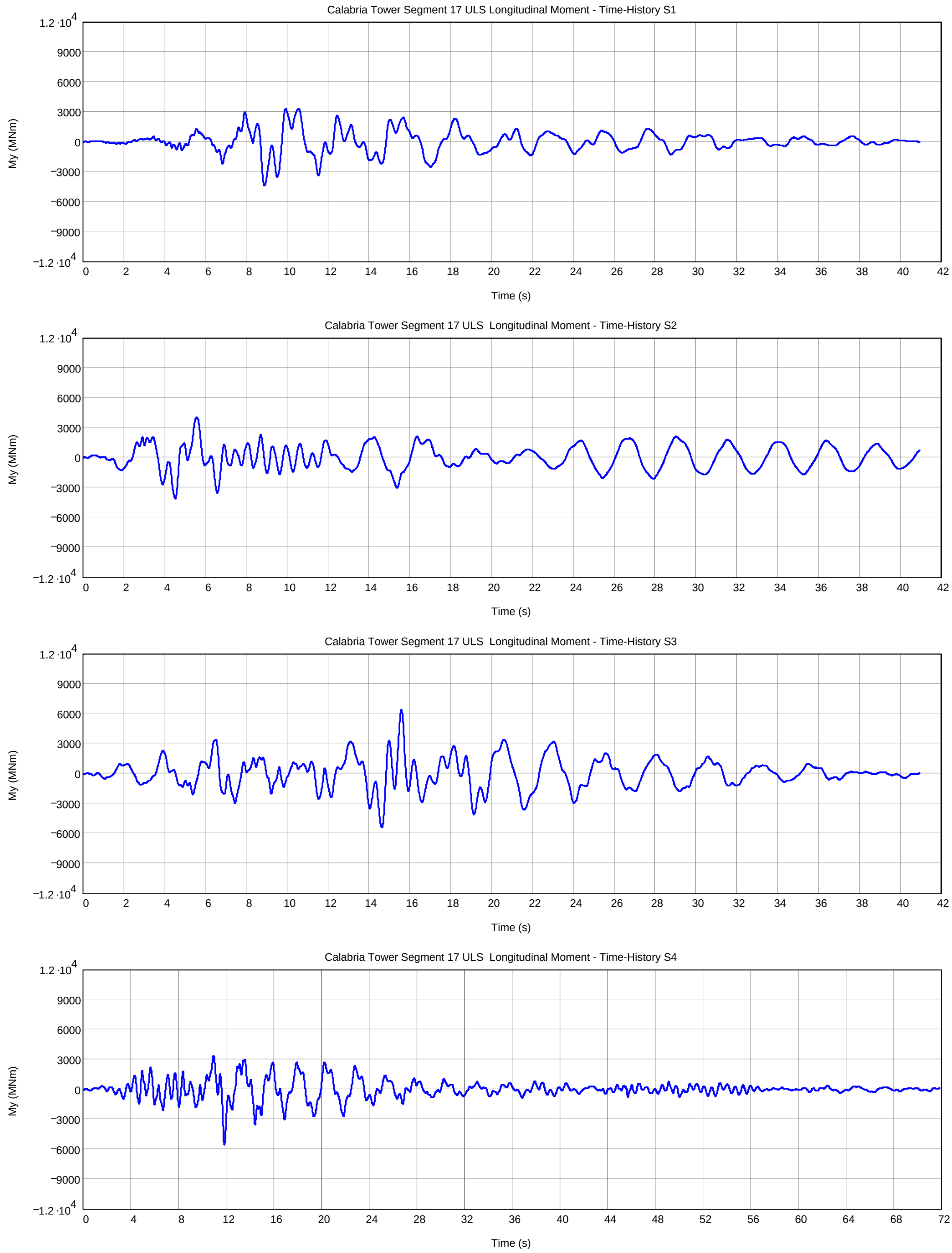

Figure A-33: Calabria tower leg segment 17 ULS seismic longitudinal moments as a function of time for Sicilia time-history inputs 1 to 4.

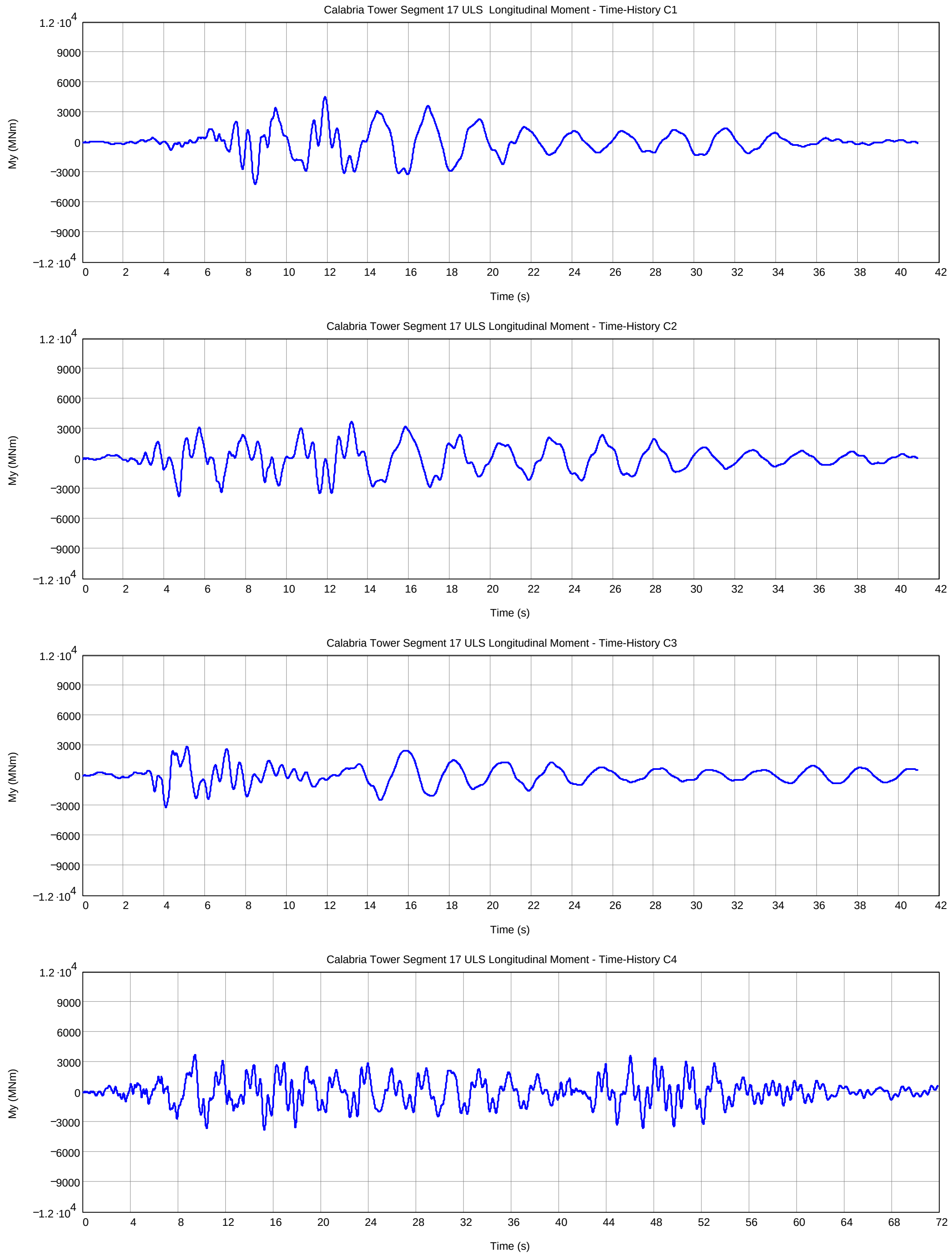

Figure A-34: Calabria tower leg segment 17 ULS seismic longitudinal moments as a function of time for Calabria time-history inputs 1 to 4.

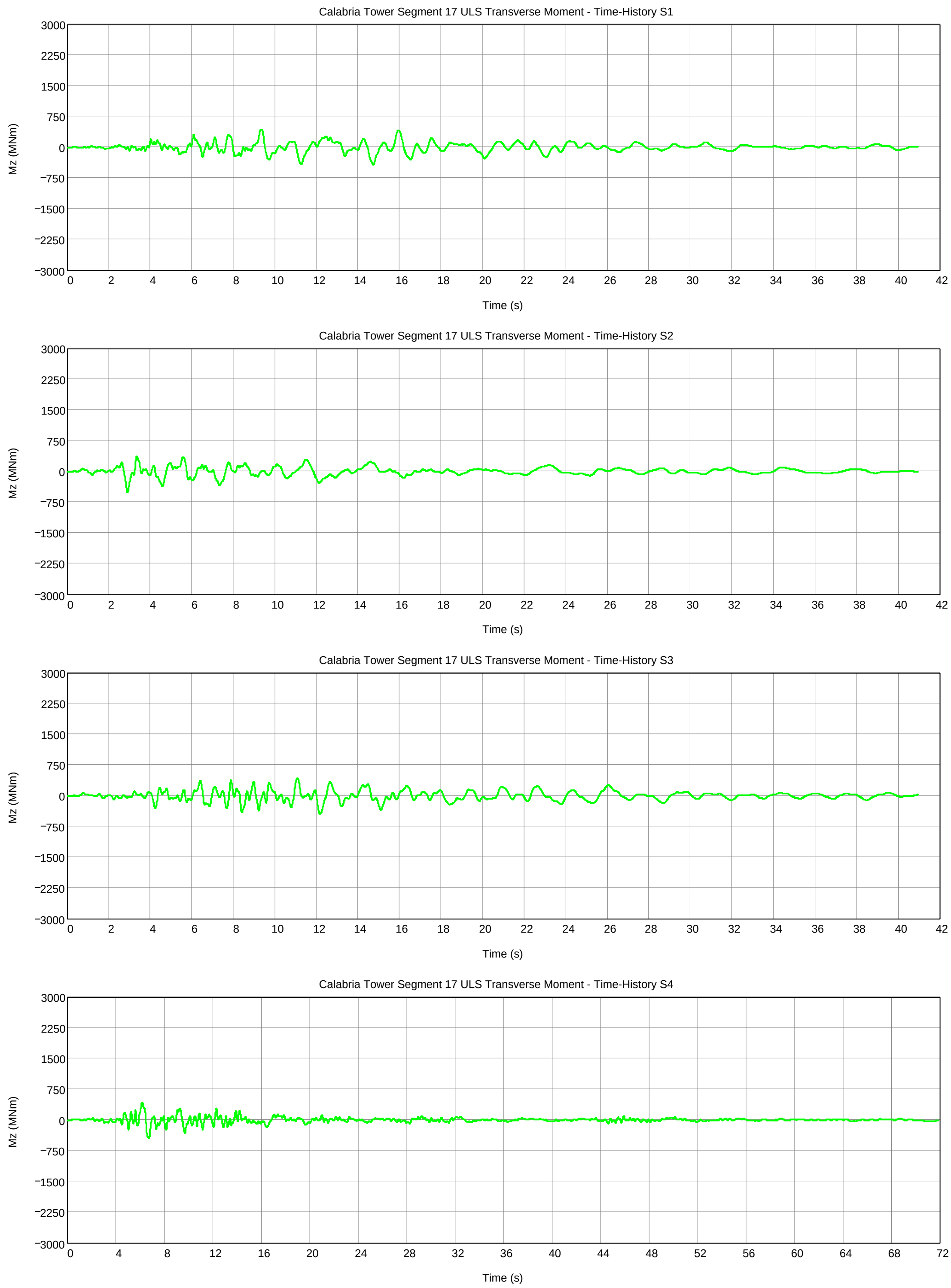

Figure A-35: Calabria tower leg segment 17 ULS seismic transverse moments as a function of time for Sicilia time-history inputs 1 to 4.

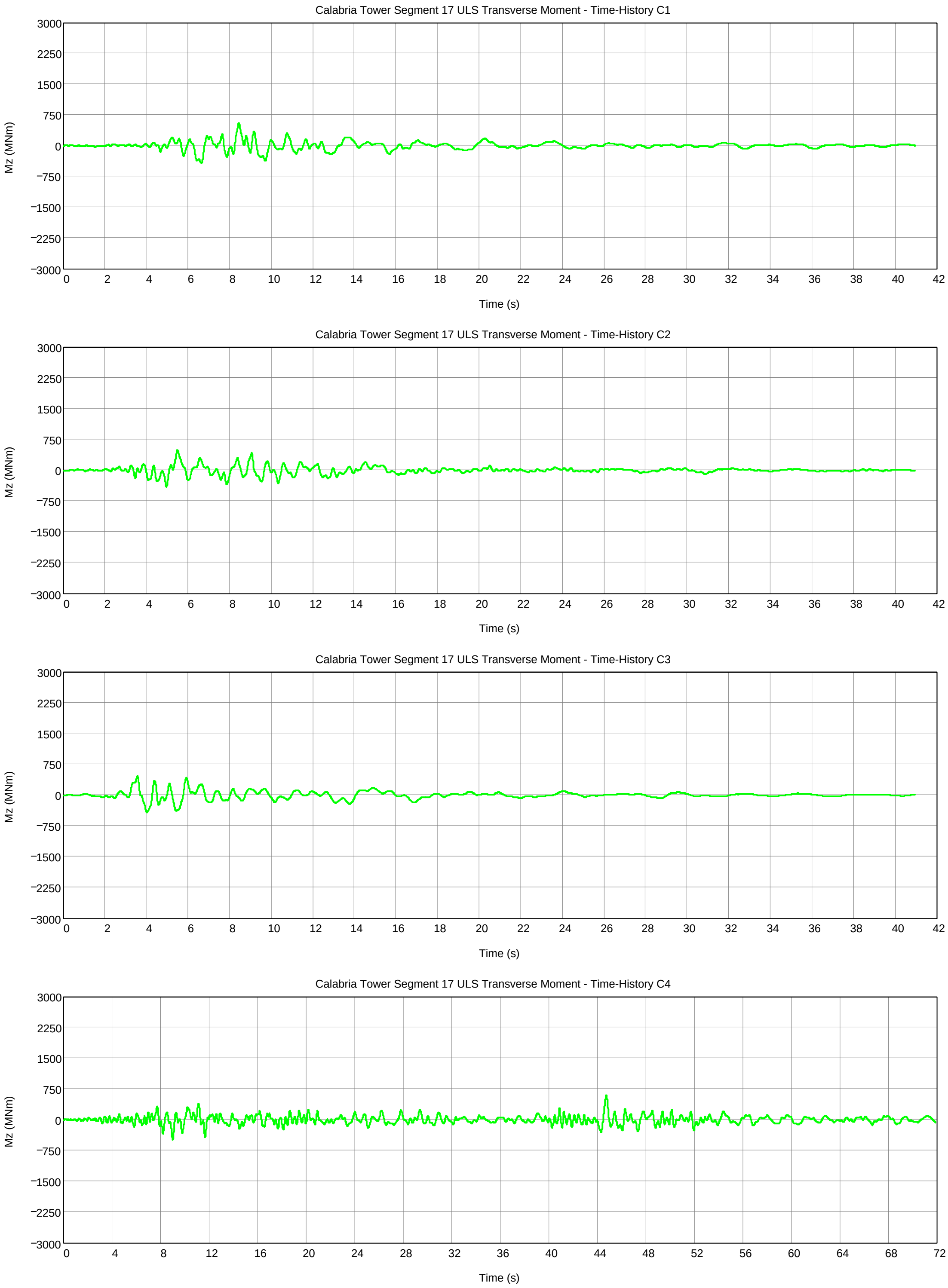

Figure A-36: Calabria tower leg segment 17 ULS seismic transverse moments as a function of time for Calabria time-history inputs 1 to 4.

Appendix B: Calabria Tower Leg Force Effects

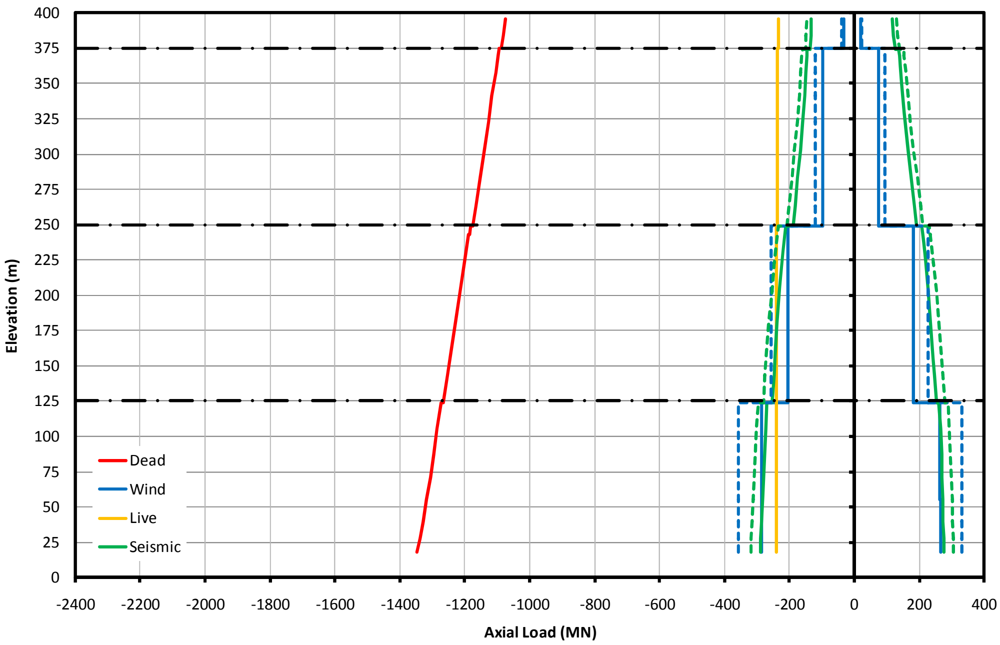

Figure B-1: Calabria tower leg unfactored axial loads (ULS – solid lines, SILS – dashed lines).

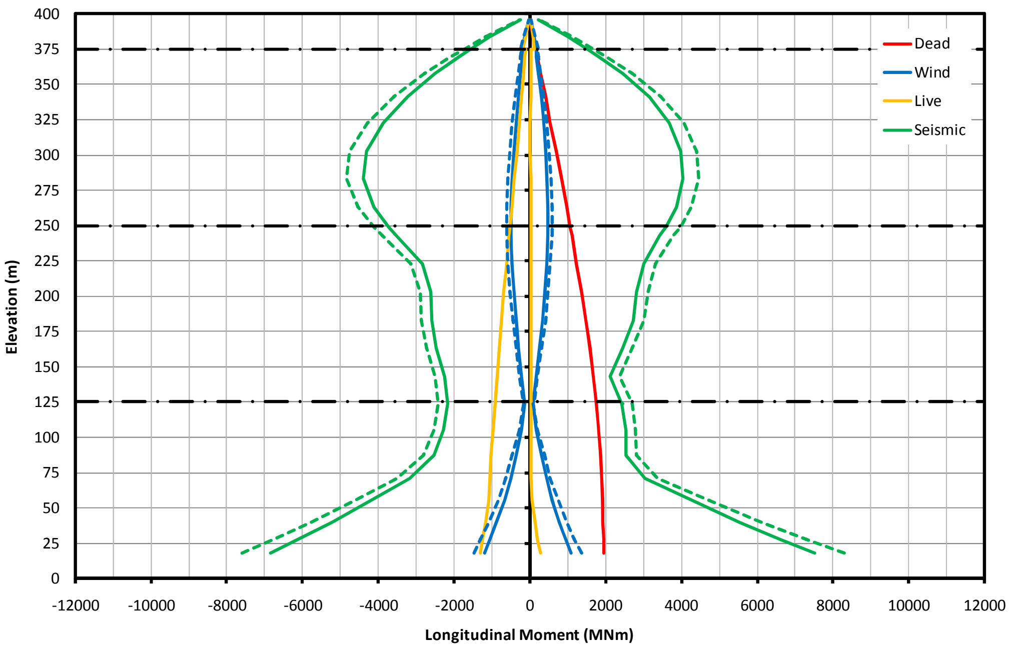

Figure B-2: Calabria tower leg unfactored longitudinal moments (ULS – solid lines, SILS – dashed lines).

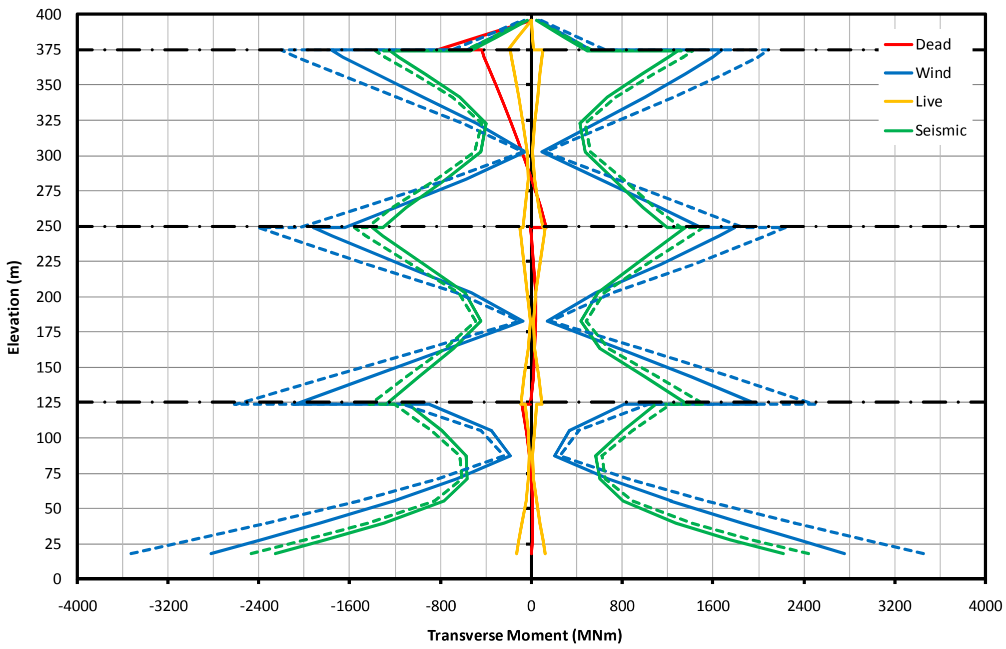

Figure B-3: Calabria tower leg unfactored transverse moments (ULS – solid lines, SILS – dashed lines).

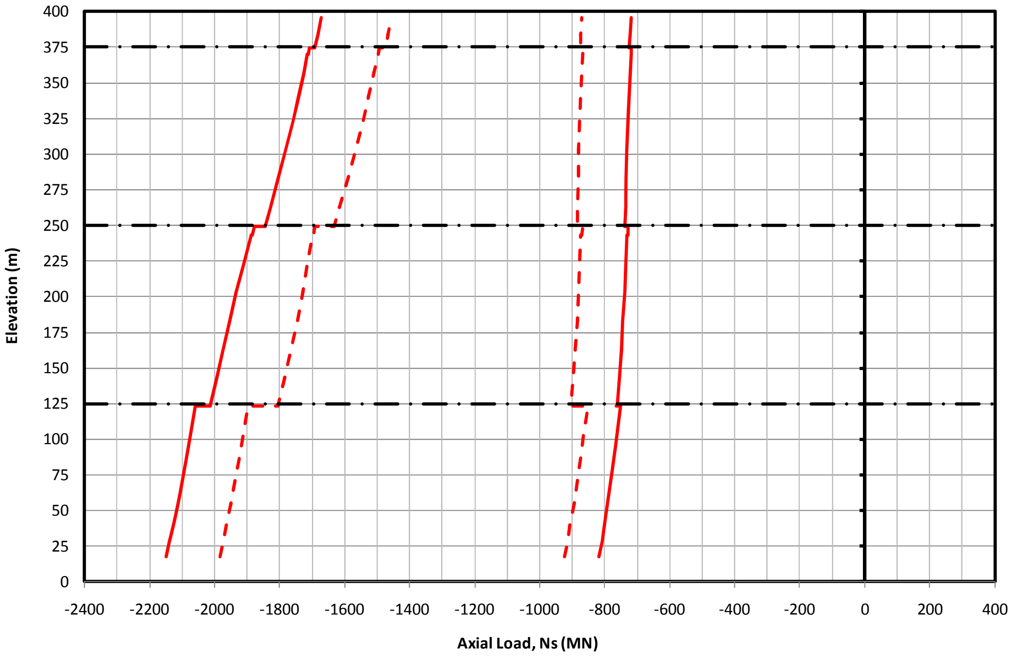

Figure B-4: Calabria tower leg factored axial force envelope (ULS – solid lines, SILS – dashed lines).

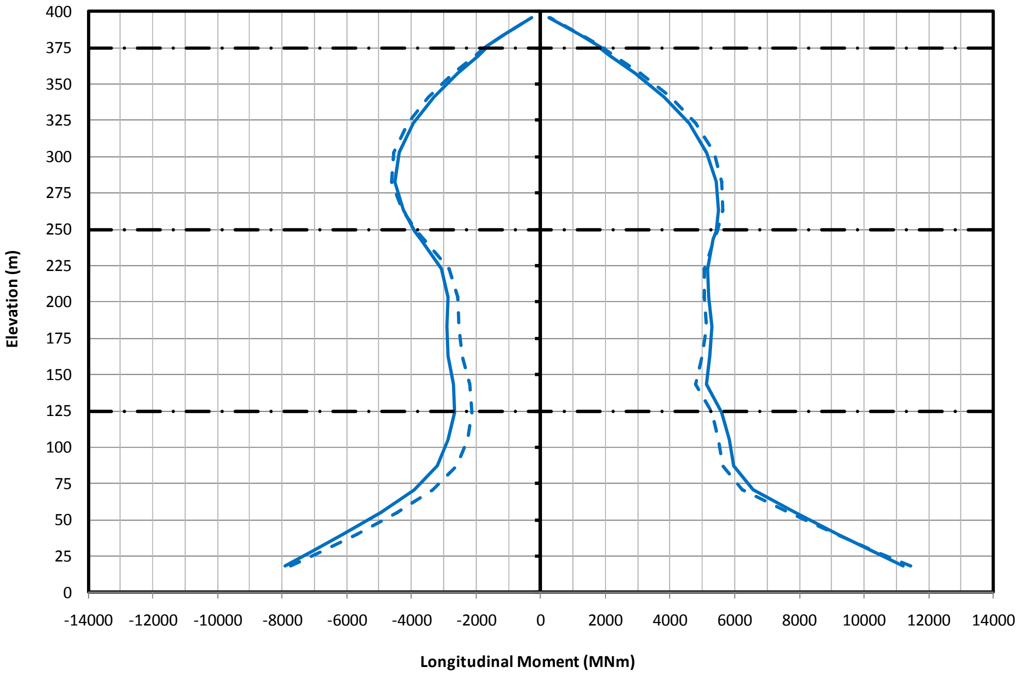

Figure B-5: Calabria tower leg factored longitudinal moment envelope (ULS – solid lines, SILS – dashed lines).

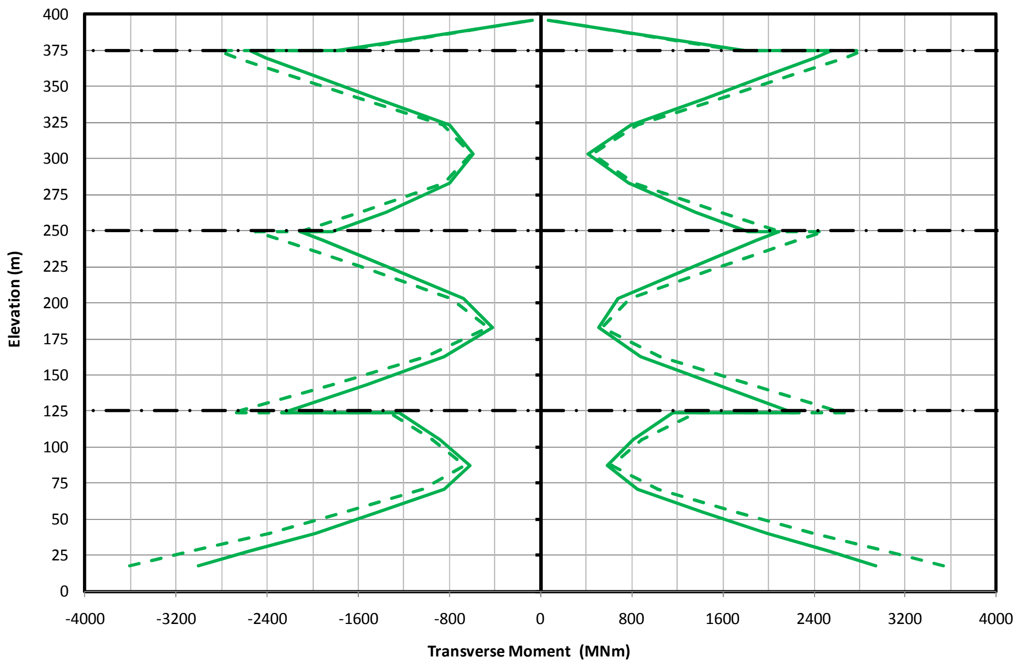

Figure B-6: Calabria tower leg factored transverse moment envelope (ULS – solid lines, SILS – dashed lines).

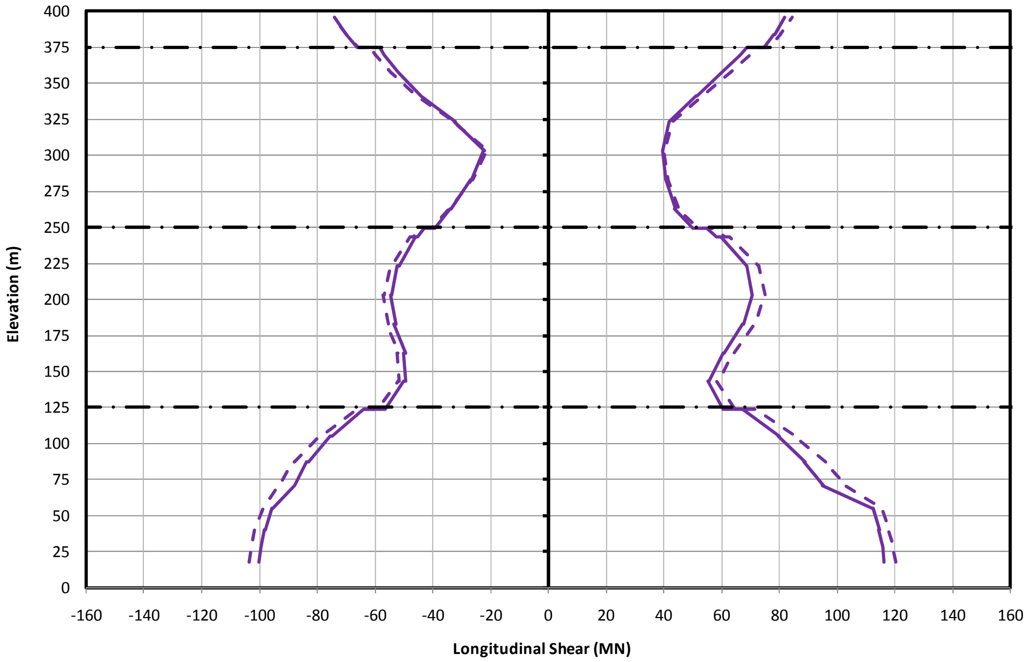

Figure B-7: Calabria tower leg factored longitudinal shear force envelope (ULS – solid lines, SILS – dashed lines).

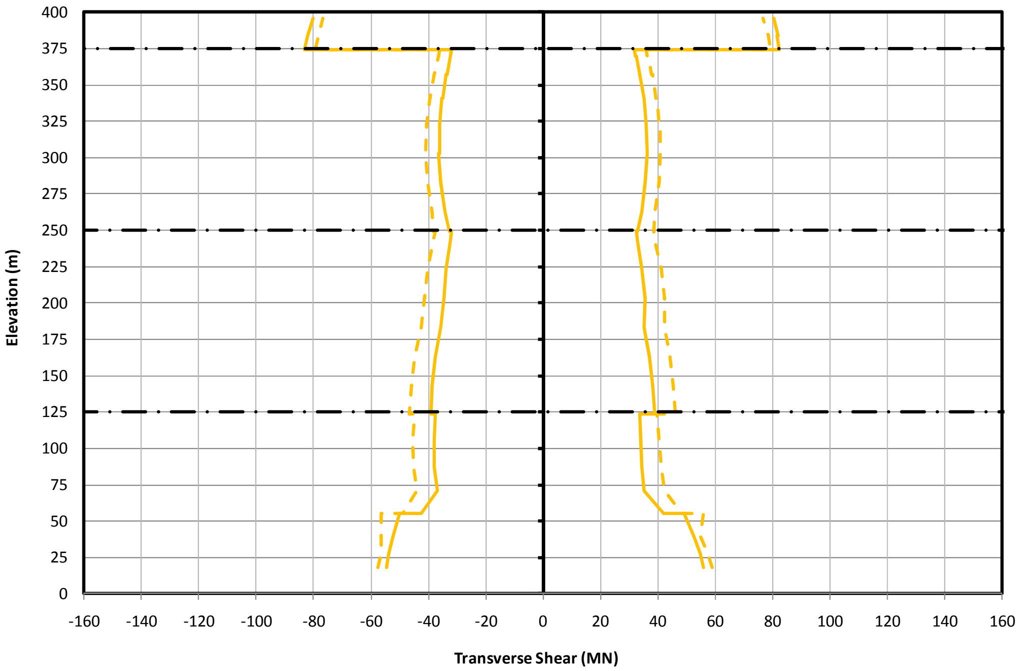

Figure B-8: Calabria tower leg factored transverse shear force envelope (ULS – solid lines, SILS – dashed lines).

Appendix C: Assessment for the Envelope of Seismic Time-History Analysis Force Effects

On account of the exceptional importance of the bridge, the tower legs were also assessed for the envelope of the seismic time-history analysis force effects at the ultimate limit state. The objective of this assessment was to evaluate the potential extent of damage that might result from a larger than expected seismic event. The design verifications were therefore completed considering all partial safety factors equal to 1.0, so that actual stress levels in the tower legs could be determined. The maximum ULS utilization ratios determined for the Sicilia and Calabria towers are shown in Figure C-1 and Figure C-2, respectively, for each time-history input for the longitudinal and transverse dominant combinations. In each figure, the time history inputs are denoted by the abbreviation S1L, in which S represents Sicilia (or C for Calabria) inputs, 1 represents the input number (1, 2, 3 or 4) and L represents the dominant direction (L for longitudinal or T for transverse). Utilization ratios are represented by solid squares for longitudinal combinations and by hollow squares for transverse combinations.

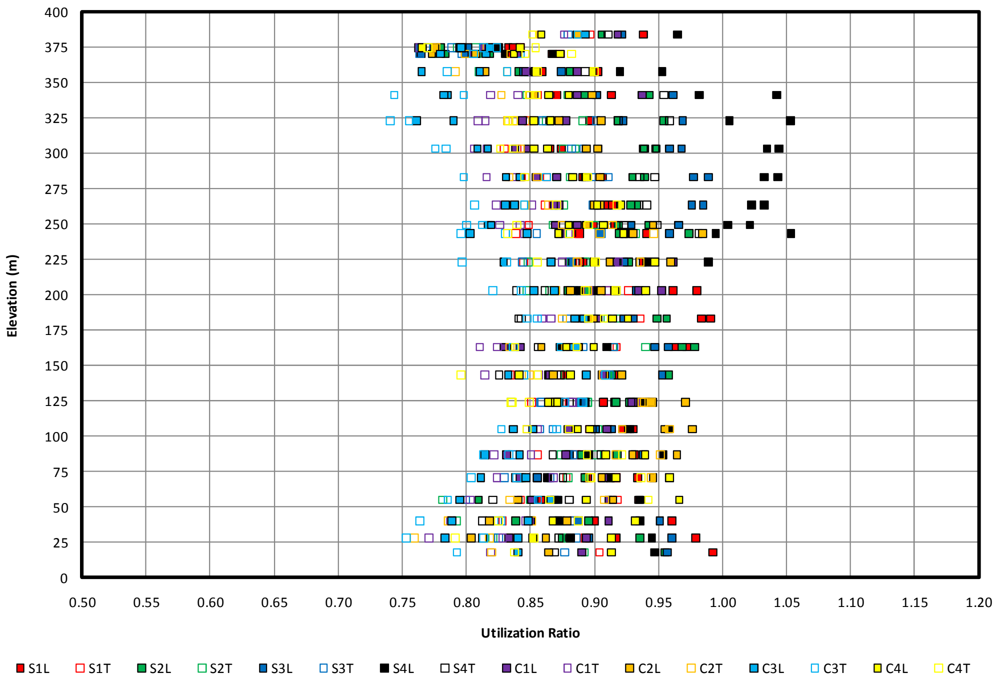

Figure C-1: Sicilia tower leg utilization ratios for each time-history input for longitudinal and transverse dominant combinations (all partial safety factors = 1.0).

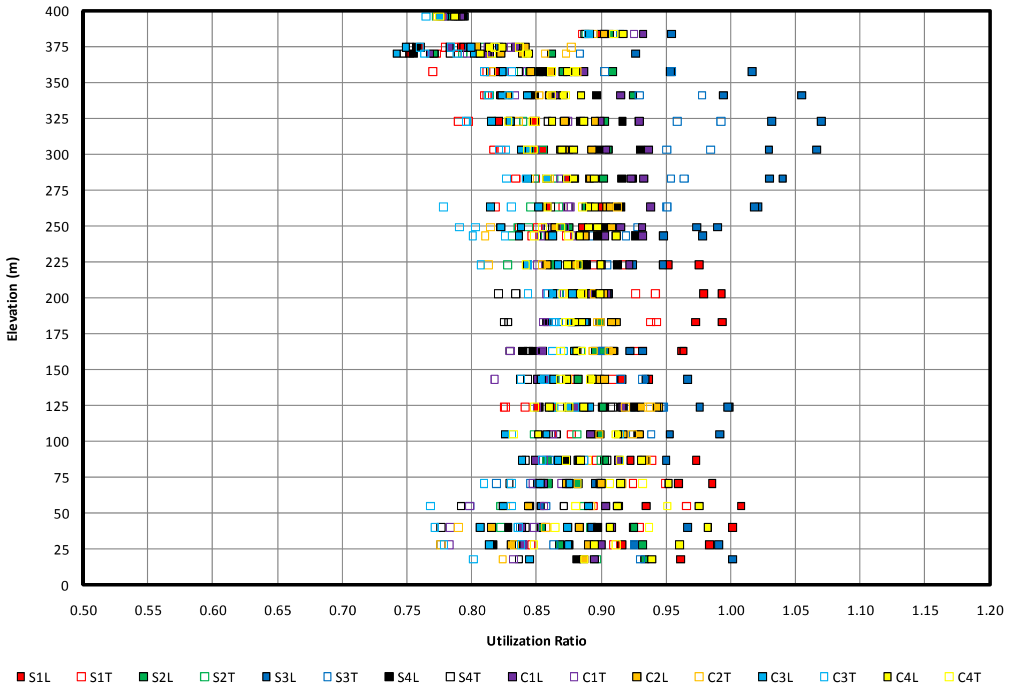

Figure C-2: Calabria tower leg utilization ratios for each time-history input for longitudinal and transverse dominant combinations (all partial safety factors = 1.0).

For both towers the governing utilization ratios result from the longitudinal dominant combinations. The maximum utilization ratios are caused by input S3 for the Sicilia tower and input S4 for the Calabria tower. Based on the design verification methods with the partial safety factors equal to 1.0, the maximum utilization ratios are greater than 1.0 only between elevations 250 m and 350 m, with a maximum value of 1.07 for Calabria tower leg segment 17 and 1.05 for Sicilia tower leg segment 18. As is shown in Appendix A, the different time-history inputs cause the greatest variation of longitudinal moment in this portion of the tower height.

A detailed finite element model of Calabria tower leg segment 17 was used to more accurately assess stress levels in the various parts of the segment under the governing load combination. The model was created using the same criteria and material models as described in Section 7.3.3.3 for the similar model used to confirm the appropriateness of the design verification methods. The critical load combination comprised the following factored load components at the bottom of the segment (most heavily stressed cross-section): axial load, Ns = 1730 MN, longitudinal moment, My = 7865 MNm, transverse moment, Mz = 160 MNm, transverse shear, Vy = 16 MN, longitudinal shear, Vz = 14 MN. The load-deformation response of the model (for axial shortening and longitudinal and transverse rotations) is shown in Figure C-3, in which the load factor plotted on the vertical axis is the fraction of the specified loads that are applied in a particular load increment and the shortening and end rotation relative to theoretical elastic response at the specified loads is plotted on the horizontal axis. The black solid line at a load factor of 1.0 represents the load increment at which the specified loads are applied to the model. The diagonal black dashed lines represent increasing levels of flexibility from fully elastic (Secant 1X) to highly inelastic (Secant 3X).

The deviations of the load-deformation curves from the line representing the fully elastic response is due to the effects of residual stresses and geometric imperfections. At the specified loads, the axial shortening is approximately 20% larger and the rotations are approximately 30% larger than the theoretical elastic response. The analysis indicates that the ultimate capacity of the segment is approximately 14% higher than the specified loads; however, when allowing for the second order effects of the decreased secant stiffness of the segment, the predicted lower bound ultimate capacity is 11% larger than the specified loads. The analysis indicates that the section can carry the maximum seismic demands that the design verifications had suggested were in excess of the section capacity.

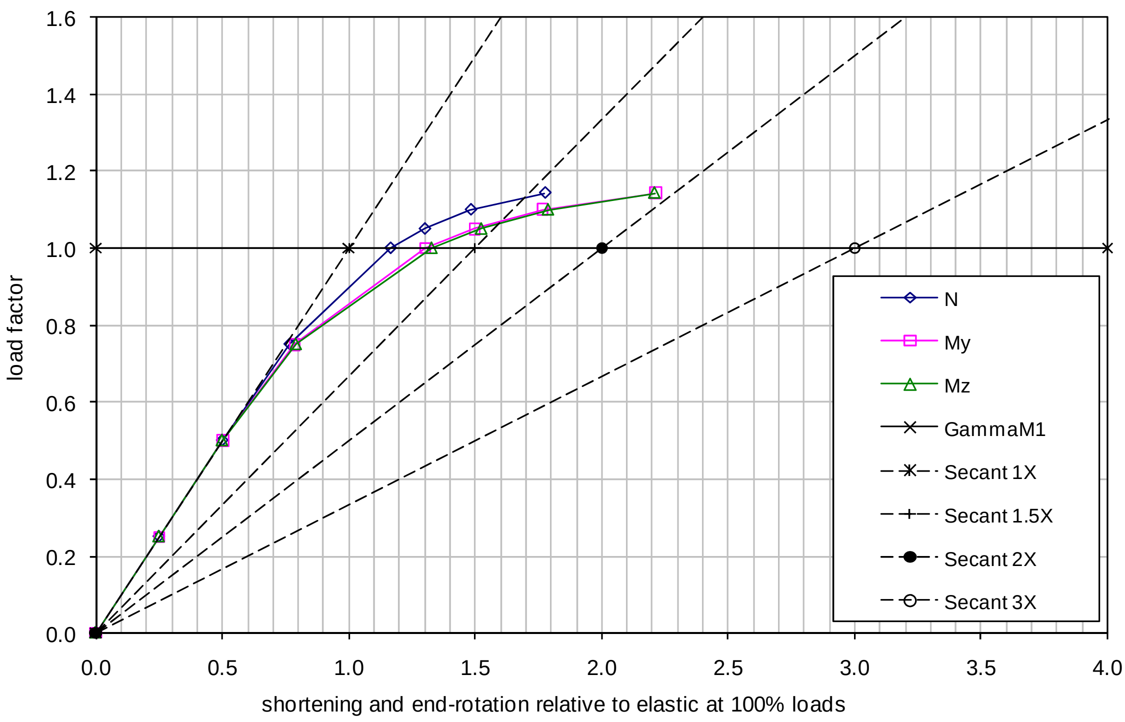

Figure C-3: Load-deformation response of Calabria tower leg segment 17 under the maximum seismic time-history load combination.

The extent of damage that might be expected in the segment at the specified loads was evaluated considering the induced stresses and strains. Longitudinal stresses (axial) on the most compressed side of the segment are shown in Figure C-4. All compressive stresses less than 350 MPa are plotted in the same colour so as to reduce the size and increase the number of stress intervals plotted close to the yield strength of the steel. The maximum reported compressive stress is 520 MPa and is shown to occur very locally at the intersection of plates A and B at the base of the segment on the right side of the figure. This stress is unreasonably high and not believed to be representative of the actual stress that would exist at this point, as the defined stress-strain curve is essentially perfectly plastic beyond the yield stress of 460 MPa, as shown in Figure C-5 (see section 7.3.3.3 for additional comments on the stress-strain curve used), and because the transverse moment causes higher compressive stresses at the opposite intersection of plates A and B. This higher than reasonable stress is likely a result of the boundary conditions at the connection of the rigid spider element through which load is applied to the model. Away from this point and at similar point on the other side of plate A the maximum compressive stresses are between 450 MPa and 475 MPa. Stresses of this magnitude occur in the lower panels on plates B and C and intermittently along the curved portion of plate B near its connection to plate A. Away from these areas, the maximum stresses are clearly below yield.

Because the steel was modelled as essentially perfectly plastic beyond the yield stress, stresses can not provide as effective an assessment of damage potential as can strains. Longitudinal strains (axial) on the most compressed face of the segment under the specified loads are shown in Figure C-6. Strains less than 0.002 are plotted in the same colour so as to reduce the size and increase the number of strain intervals plotted close to the yield strain. The maximum reported compressive strain of 0.003827 occurs near the bottom of the section on the curved portion of plate B is and very localized. Away from this point, the maximum strains are generally between 0.003 and 0.00325. As indicated in Figure C-5, these strains are all less than that corresponding to full yield (based on the 0.2% proof stress, which would give a full yield strain of 0.00419) and therefore, this tower leg segment achieves the requirement of repairable damage, as specified for the towers at the ULS in GCG.F.04.01 Table 6 and defined in Table 5 as "Occurrence of localised inelastic behaviour…"

Given that this is the most heavily stressed tower leg segment under the envelope of the time-history analysis results, the behaviour of the adjacent tower leg segments for which design verifications also indicate utilization ratios greater than 1.0, are expected to be similar but less severe.

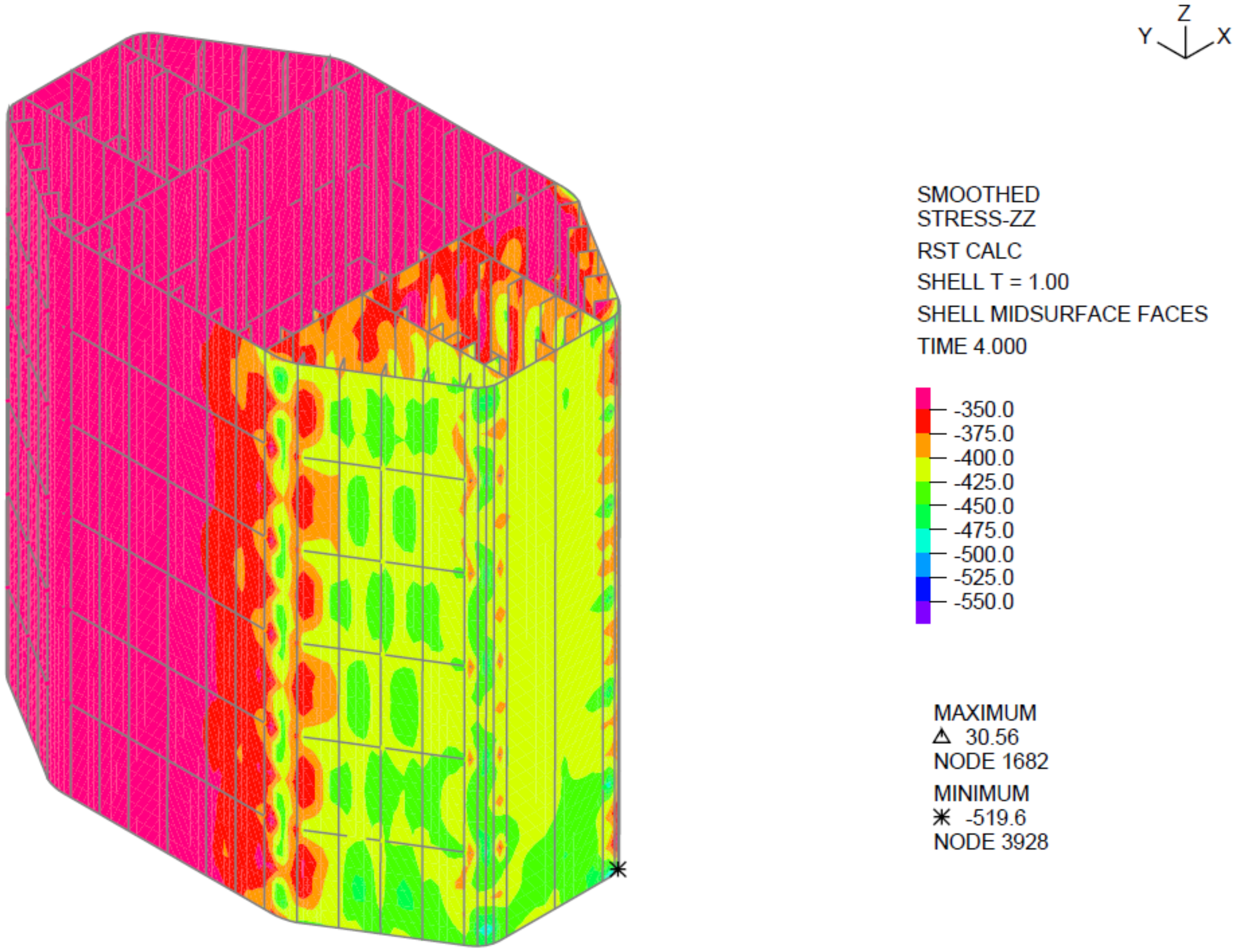

Figure C-4: Calabria tower leg segment 17 longitudinal stresses due to maximum seismic force effects.

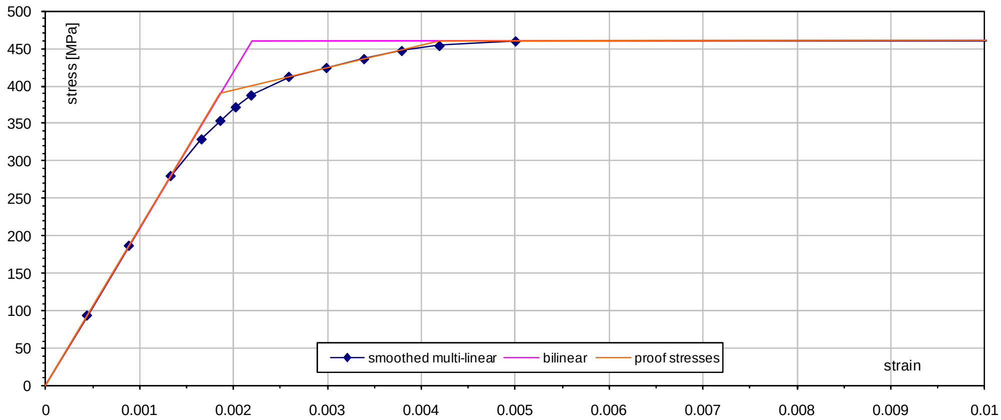

Figure C-5: Modelled stress-strain curve.

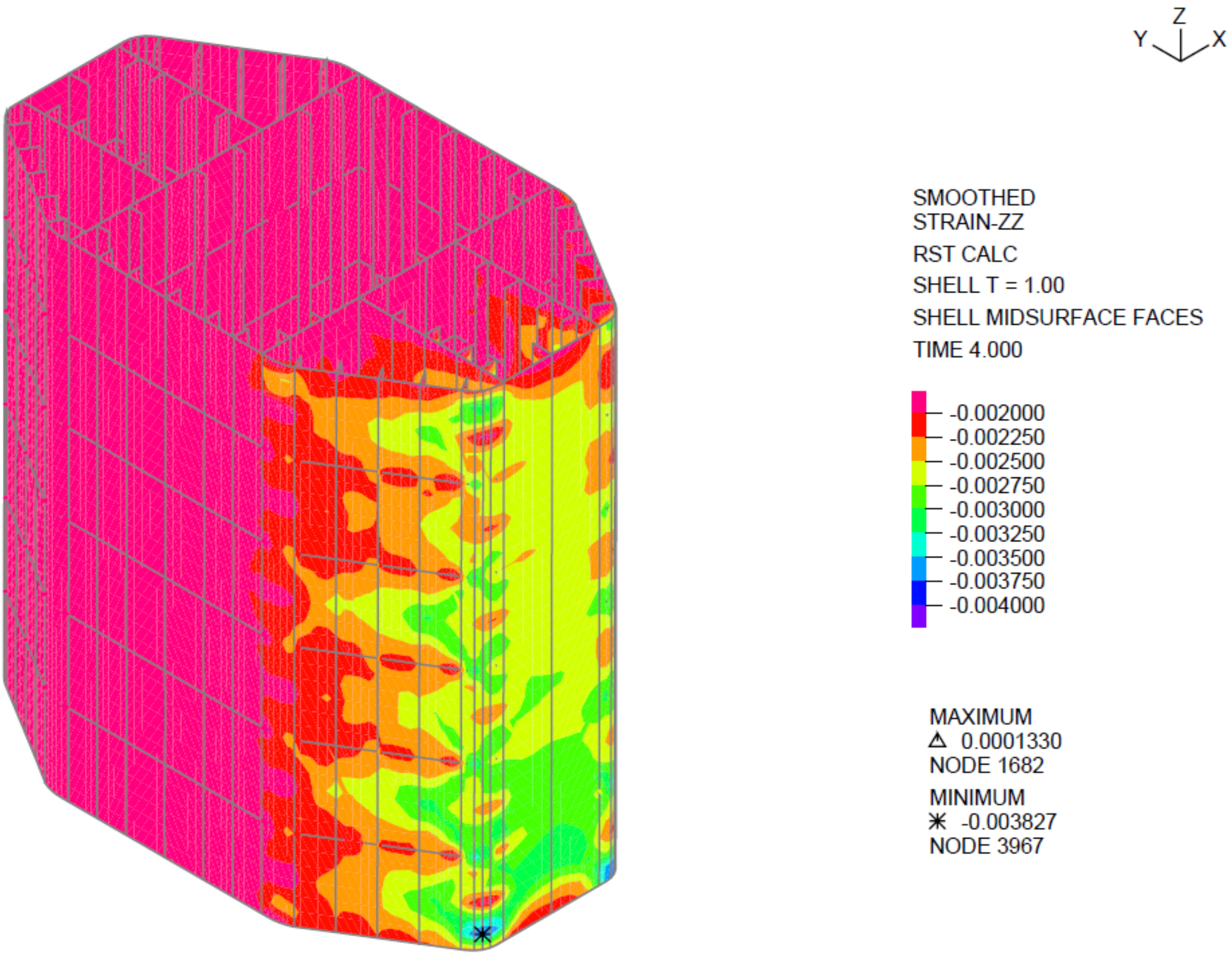

Figure C-6: Calabria tower leg segment 17 longitudinal strains due to envelope seismic force effects.